INL/EXT-17-42891
PNNL-27386

GeoVision Analysis Supporting Task Force Report: Geothermal Hybrid Systems

D. S. Wendt, G. Neupane
Idaho National Laboratory

C. L. Davidson, R. Zheng, M. A. Bearden
Pacific Northwest National Laboratory

June 2018

The INL is a U.S. Department of Energy National Laboratory operated by Battelle Energy Alliance under contract DE-AC07-05ID14517

PNNL is operated by Battelle for the U.S. Department of Energy under contract DE-AC05-76RL01830

INL/EXT-17-42891
PNNL-27386

GeoVision Analysis Supporting Task Force Report: Geothermal Hybrid Systems

D. S. Wendt, G. Neupane
Idaho National Laboratory

C. L. Davidson, R. Zheng, M. A. Bearden
Pacific Northwest National Laboratory

June 2018

Idaho National Laboratory
Idaho Falls, Idaho 83415

http://www.inl.gov

Prepared for the
U.S. Department of Energy
Geothermal Technologies Office
Under DOE Idaho Operations Office
Contract DE-AC07-05ID14517

CONTENTS

FIGURES

TABLES

1.0 Introduction

Hybrid systems combine two or more energy types and/or produce two or more products to overcome limitations inherent in the respective stand-alone systems, addressing limitations on energy resource flexibility, efficiency, reliability, emissions, and/or economics. In general, for a hybrid system to be preferable to a stand-alone system, it must provide additional value in a way that cannot be accomplished by the hybridized technologies implemented as separate stand-alone systems.

Geothermal hybrid systems can provide power output more closely matched with the electrical load profile, offset the impacts of resource productivity decline, or enhance the capabilities of a given power generation project through the addition of ancillary or value-added operations (e.g. energy for CO_2 capture operations, or raw material for brine mining). The GeoVision hybrids systems evaluation focuses on aspects of hybrid technology that can increase the utilization of geothermal energy. Important aspects of the hybrid systems analysis therefore include evaluating conditions where hybrid technologies could decrease the costs of geothermal power generation and/or increase the viability of low temperature geothermal resources.

The GeoVision Study hybrid systems analysis evaluates geothermal hybrid technologies that are likely to play a role in the future of the geothermal energy industry. This includes hybrid thermo-electric power generation technologies in which geothermal energy is coupled with solar and fossil energy sources; applications where geothermal energy is used for process heat applications such as CO_2 capture and thermal desalination; analysis of compressed air energy storage augmented with geothermal energy; as well as an assessment of geothermal brines for mineral recovery applications.

1.1 General Approach

The GeoVision study market penetration analysis uses the Geothermal Electricity Technology Evaluation Model (GETEM) and Regional Energy Deployment System (ReEDS) models to evaluate stand-alone geothermal power generation, and the dGeo model to evaluate geothermal direct use applications. Unfortunately, neither of these modeling approaches support evaluation of hybrid systems. Since many of the hybrid systems evaluated are thermo-electric power generation technologies, the initial approach for determining hybrid system market penetration focused on integrating the hybrid systems analysis into the ReEDS model. Ultimately it was determined that hybrid systems could not be integrated into the ReEDS model without impacting the GeoVision project schedule.

It was therefore not possible to include hybrid thermo-electric power generation technologies in the overall GeoVision Study market penetration analysis. The alternate approach selected was to perform case study analyses, in which the performance and costs of hybrid geothermal systems are compared with stand-alone geothermal systems, to provide insight as to the potential benefits that can be provided through the use of geothermal hybrid technologies.

In the case study analyses, as in the P2P market penetration analysis, the GETEM model was used to evaluate geothermal resource cost and performance. The case study analyses were able to incorporate the GETEM inputs corresponding to the reference scenario (Business-As-Usual) and improved scenarios (Tech Transfer and Exploration De-Risk improved scenarios were used in various hybrid system case studies). A listing of the GETEM input variables that differentiate the improved scenarios from the reference scenario is included in Appendix A. Where possible, the case study analyses leveraged prior hybrid system analyses, models, and literature as appropriate. In general, there are few industrial deployments of geothermal hybrid technologies, so much of the analysis presented in this report is original and is based on modeling and simulation of the specified hybrid systems. A summary of the hybrid systems evaluated and the general attributes of each system is presented below in Table 1.

Table 1. Summary of hybrid systems evaluated in GeoVision study.

Hybrid System	Prior Research	Previous Deployment	Configuration Evaluated in GeoVision analysis	Geothermal Resource T Evaluated	Geothermal Resource Characteristics Best Suited for Hybrid Application	Advantages Compared to Stand-Alone Applications	Disadvantages Relative To Stand-Alone Applications	Cost Range and Drivers
Solar thermo-electric power generation	refs [1-26]	Enel Green Power Stillwater hybrid geo-solar power plant: brine pre-heating retrofit	Supercritical ORC with solar heating of working fluid	150°C – 200°C	Greatest LCOE improvement relative to stand-alone plants for low T geothermal resources	Improved temporal correlation with electrical load; increased capacity; decreased LCOE for projects with high geothermal resource development costs	Additional cost and complexity	Threshold cost varies with scenario, resource type, and electricity pricing schedule
Coal thermo-electric power generation	refs [27-42]	N/A	NETL Case 11 (supercritical coal plant) with geothermal preheating of boiler feedwater	150°C – 250°C	Applicable across the range of temperatures; Higher temperature applications yield improved LCOE and net power generation	Replacement of higher value steam with geothermal heat for preheating results in higher overall system efficiency, power generation and LCOE compared to standalone. Additional power generation enabled by geothermal integration is zero-emissions, reducing overall plant emissions intensity (per kWh)	Added siting and operational complexity (geothermal resource, coal plant)	Varies with resource and hybrid system design
Natural Gas thermo-electric power generation	refs [43-46]	N/A	NETL Case 12 (combined cycle natural gas) with inlet air precooling via geothermal driven LiBr chiller	150°C	Excellent potential use for low-temperature resources in areas with high seasonal ambient temperature variability	Facilitates increased summer nameplate capacity for existing gas plants in areas with high ambient summer temperatures. Leverages existing baseload gas generation stock to increase peak generation capacity without greenfield capital investment	Added siting and operational complexity (geothermal resource, gas plant, gas supply); additional emissions associated with use of additional gas enabled by precooling	Varies with resource and hybrid system design
CO_2 capture from fossil thermo-electric power plants	[NEED REFS]	N/A	NETL Case B31A (supercritical coal plant with CO2 capture) with geothermal preheating of boiler feedwater	150°C – 250°C	Applicable across the range of temperatures; higher temperature applications yield improved efficiency and lower capture costs.	Offsets a portion of the parasitic load associated with CO2 capture, resulting in higher net power sales. CO2 capture can be turned down or bypassed entirely during peak demand, implementing the system as in the non-capturing (NETL Case 9) scenario described above	Added siting and operational complexity (geothermal resource, coal plant, CO2 storage)	Varies with resource, hybrid system design and capture rate

Hybrid System	Prior Research	Previous Deployment	Configuration Evaluated in GeoVision analysis	Geothermal Resource T Evaluated	Geothermal Resource Characteristics Best Suited for Hybrid Application	Advantages Compared to Stand-Alone Applications	Disadvantages Relative To Stand-Alone Applications	Cost Range and Drivers
Biomass combustion, drying, biofuels	refs [47-51]	N/A	Multiple	150°C – 250°C	Not attractive in any of the bioenergy configurations evaluated	None of the configurations evaluated provided an attractive alternative to use of the geothermal resource for stand-alone power generation	Limited need for geothermal heat within bioenergy processes evaluated	Cost of GT heat is higher than existing process sources; few opportunities for economies of scale
Compressed air energy storage	refs [52-54]	N/A	Compressed air energy storage using geothermal preheating of air prior to turboexpansion	150°C – 250°C	Applicable across the range of temperatures; higher temp applications yield better LCOEs	Renewable-enabled grid-scale balancing resource offers a zero-emissions alternative to gas combustion turbines for balancing	Siting complexity is compounded by the need for both a suitable CAES reservoir and a good geothermal resource, as well as access to a sufficient market for balancing resources	Varies with resource, CAES reservoir performance, power market dynamics and system design
Thermal desalination	refs [55-77]	Salton Sea/Imperial Valley USA MED pilot plant; Kimolos Island (Greece) MED plant	Multiple Effect Distillation (MED)	100°C – 200°C	Lowest geothermal LCOH and purified water LCOW achieved with high T geothermal resources	Stand-alone application evaluated, but desalination could be coupled with geothermal power generation to improve economics and geothermal energy utilization in electrical load-following applications	Co-location of geothermal resource, feed water source, and water market is a barrier to significant technology deployment	LCOW targets of $\$1.50/m^3$ for reference scenario and $\$1.00/m^3$ for improved scenario
Mineral Recovery from geothermal brine	refs [78-103]	Simbol Materials Inc. pilot-scale Li extraction plant at the Salton Sea; LLNL project pilot-scale geothermal silica recovery at Mammoth Lakes	N/A	N/A	Basin and Range geographic province determined to have geothermal brines with compositions best suited for mineral recovery	Mineral recovery can provide an additional source of revenue to improve the economics of geothermal power generation	Possibly complex recovery process must handle large volume of brine and recover low concentration of target compounds	Processing costs will vary with recovery technology and are largely unknown

2.0 Geothermal-Solar: Hybrid Geo-Solar Binary Power Plant Supply Curve Analysis

Highlights

- This analysis evaluated a hybrid geo-solar air-cooled supercritical binary cycle power plant configuration for the GeoVision scenarios
- General benefits of hybrid geo-solar technology include the ability to decrease the risks and mitigate impacts associated with geothermal resource productivity decline
- Hybrid geo-solar power plants improve the temporal correlation between generation and load. Use of geo-solar hybrid plants could therefore largely defend against the economic penalties that would otherwise be associated with air-cooled geothermal power generation in a time-of-delivery electricity pricing market.

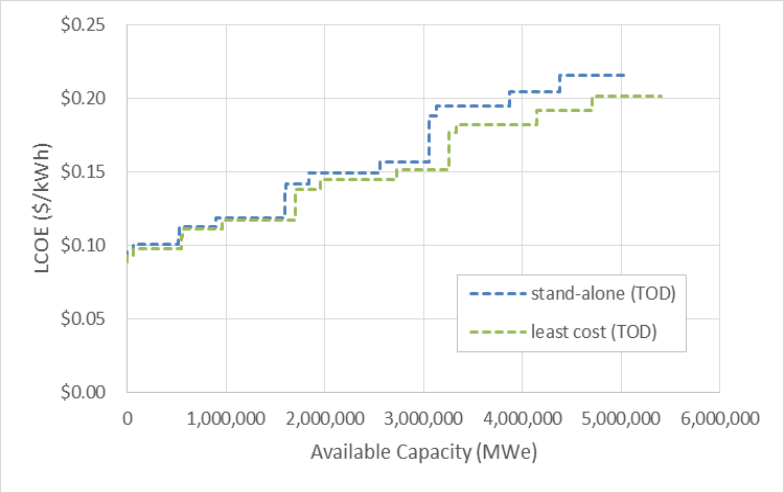

Comparison of stand-alone geothermal plant and least cost (hybrid or stand-alone) Technology Transfer Scenario supply curves (Deep EGS resource with TOD pricing)

- If the costs of solar collectors can be reduced to the targets set by DOE and the concentrating solar power industry, hybrid geo-solar technology will allow LCOE reductions in locations with good solar resource and where stand-alone geothermal power generation costs are moderate (~$0.10/kWh) to high (≫$0.15/kWh).
- This analysis indicates that hybrid geo-solar technology generally provides the greatest reductions in LCOE when paired with low-temperature geothermal resources (where costs of stand-alone geothermal power generation tend to be highest).
- For all geothermal resource types evaluated, there is a threshold LCOE where a geothermal industry that utilizes hybrid geo-solar plants would be able to provide increased capacity at an equal or lower LCOE than a geothermal industry comprised solely of stand-alone geothermal plants (see table).

LCOE of hybrid geo-solar relative to stand-alone geothermal (reported as a capacity-weighted average) and threshold LCOE above which hybrid geo-solar provides lower cost and higher capacity electrical power generation ($/kWh)

	Business-as-Usual				Technology Transfer			
	Level Pricing		TOD Pricing		Level Pricing		TOD Pricing	
Identified hydro	104.8%	$0.159	102.1%	$0.136	101.8%	$0.133	99.1%	$0.087
Undiscovered hydro	103.9%	All hybrid > stand-alone	101.2%	$0.145	100.6%	$0.129	98.0%	All hybrid < stand-alone
Near-Field EGS	85.9%	All hybrid < stand-alone	81.9%	All hybrid < stand-alone	100.2%	$0.111	97.5%	$0.068
Deep EGS	89.5%	All hybrid < stand-alone	86.2%	All hybrid < stand-alone	98.4%	$0.138	96.0%	$0.089

2.1 Introduction and Overview

2.1.1 General Background

Geothermal and solar are renewable energy resources that can provide thermal energy for electrical power generation or other thermal applications. Geothermal and solar resources have attributes that differ considerably, but can be combined to obtain a hybrid heat source with superior characteristics to the individual resources.

Geothermal energy is steady and reliable, but is subject to resource productivity declines over long time periods. Additionally, air-cooled geothermal power plant performance suffers during mid-day periods when the ambient temperature is elevated. Since geothermal heat is supplied at a relatively low temperature, stand-alone geothermal power plants operate with relatively low thermal efficiency. Another consequence of the relatively low temperature of geothermal resources is that variations in the geothermal resource productivity (temperature or flow rate) and the ambient temperature can have significant negative impacts on power plant performance.

Solar energy is an intermittent renewable energy source. While long term solar resource performance can be accurately predicted for a given location, short term performance can be highly variable. Solar energy is only available during the day time, with additional variability introduced by the presence or absence of cloud cover at a given geographic location. Solar energy can be directly converted to electricity via photovoltaic (PV) technology, or heat via concentrating solar collectors. Solar heat can be converted to electricity in a thermoelectric power plant. Concentrating solar technology can supply heat at temperatures of 500°C or greater, which allows concentrating solar power (CSP) plants to operate with greater efficiency than stand-alone geothermal plants. However, the intermittent nature of solar heat requires use of thermal storage for reliable plant operations.

Solar thermal energy can be combined with geothermal energy in a thermo-electric power plant. A hybrid geothermal solar-thermal power plant can synergistically combine the attributes of both heat sources to produce a power plant with superior performance. Solar heat input to an air-cooled geothermal power plant can increase power generation during the mid-day hours when stand-alone geothermal plant performance is typically lowest. The hybrid plant can continue to operate during periods when solar energy is unavailable without use of thermal storage. Shared use of a common power block can reduce capital costs relative to separate stand-alone geothermal and solar-thermal plants. Additionally, the solar field can be resized in the event of long term geothermal resource productivity decline to mitigate risks associated with underutilization of the power block.

Commercial geo-solar hybrid plant deployment is currently limited to Enel Green Power's Stillwater plant. The Stillwater geothermal solar hybrid plant is a retrofit configuration in which the solar heat supplements the geothermal heat input to the ORC power block. The Stillwater hybrid plant uses a "brine preheating" configuration in which the solar heat is added to the geothermal production fluid en route to the power block. The solar field operates as a closed-loop with a pressurized water heat transfer fluid (HTF). Heat from the solar field HTF is transferred to the production fluid from the site's coolest production wells via a heat exchanger. The solar heat addition increases the production fluid temperature. The power block then utilizes the greater energy content of the solar-heated production fluid to increase net power generation.

CSP deployment in stand-alone and hybrid applications is currently limited by the costs of the solar collectors. Hybrid geo-solar applications where the elevated temperature of the solar heat is not effectively utilized suffer an efficiency penalty that exacerbates the relatively high costs of solar heat. Future hybrid plant configurations that can take full advantage of the high temperature solar heat while maintaining the ability to reduce capital costs through elimination of thermal storage and/or use of a common power block will increase the economic competitiveness of geothermal solar hybrid power

plants. Possible next generation geothermal solar hybrid plant configurations include ORC cycles with solar heat input to the ORC working fluid; dual pressure level or dual fluid power cycles with high temperature solar heat and intermediate temperature geothermal heat utilization/integration; and concentrating solar power plants utilizing geothermal heat for boiler feedwater heating (see Chapter 3.0 for a case study analysis of the latter hybrid plant configuration).

2.1.2 GeoVision Analysis

The GeoVision hybrid systems analysis focused on aspects of hybrid technology that can increase the utilization of geothermal energy. Important aspects of the hybrid systems analysis therefore include evaluating conditions where hybrid technologies could decrease the costs of geothermal power generation and/or increase the viability of low temperature geothermal resources.

As previously mentioned, the brine-preheating configuration is currently utilized in the single commercially deployed hybrid geo-solar power plant. A next-generation implementation of hybrid geo-solar binary power plants could realize performance benefits from heating the working fluid in an air-cooled supercritical binary power plant (Figure 1); this next-generation hybrid power plant configuration is examined in this analysis.

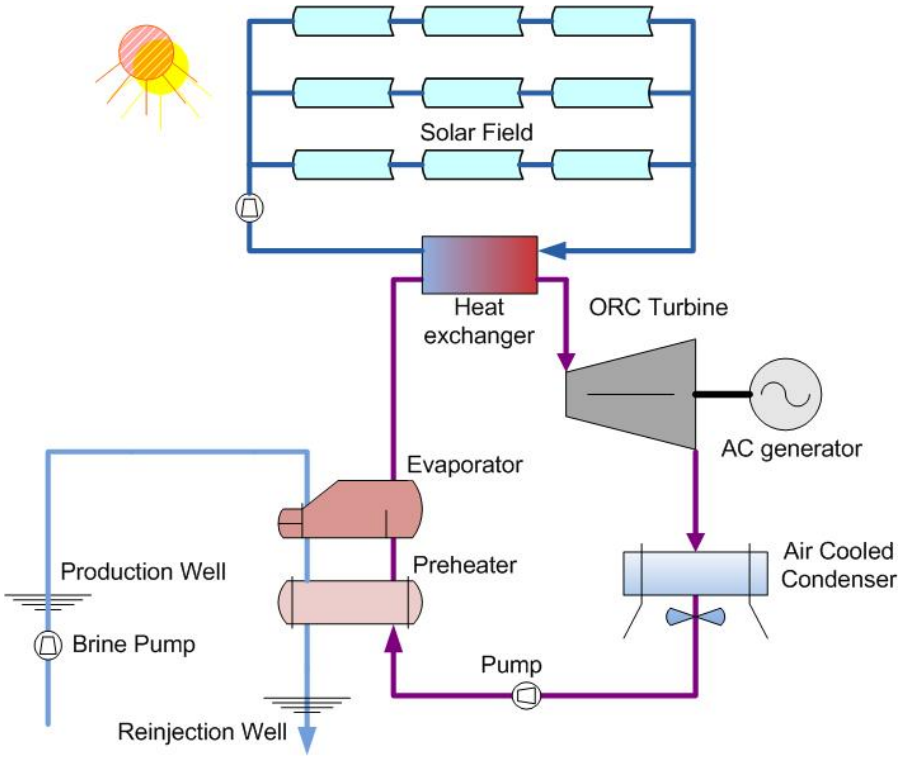

Figure 1. ORC working fluid hybrid plant configuration [22].

2.2 Hybrid Geo-Solar Power Plant Supply Curve Analysis

A number of scenarios have been investigated as part of the GeoVision Study market penetration analysis performed by the Potential to Penetration (P2P) task force. Each of these scenarios is defined by a set of technical, economic, and market conditions that may be representative of the future energy market. The GeoVision Study market penetration analysis predicts the quantity of geothermal power that would deploy in each of the selected scenarios. The market penetration analysis uses the ReEDS model to predict deployment of geothermal power plants. The ReEDS model is currently unable to evaluate hybrid

power plants, and it was therefore not possible to evaluate the potential market penetration from hybrid geo-solar power plants in the current GeoVision analysis.

This analysis of hybrid geo-solar power plants attempts to emulate many of the important aspects of the stand-alone geothermal plant market penetration analysis. These include the development of a model to evaluate the performance and cost of hybrid geo-solar power plants under various geothermal and solar resource conditions, the use of a geothermal and solar resource dataset to establish supply curves that characterize the quantity of electrical power that could be deployed at various costs, and the analysis of scenarios under which hybrid geo-solar power plants may provide advantages relative to stand-alone geothermal plants.

Although the stand-alone geothermal supply curves generated for each scenario of the GeoVision market penetration analysis present capital costs (in terms of $/kW of capacity) as a function of total available capacity, the hybrid geo-solar supply curves were presented as LCOE as a function of total available capacity. Whereas the stand-alone geothermal supply curves are an intermediate market penetration analysis result and are used as input to the ReEDS model, the hybrid geo-solar market analysis cannot currently be performed in ReEDS and the supply curves are one of the final results of the analysis. Since the capital costs do not represent all costs associated with deployment of a hybrid power plant, LCOE (which includes CAPEX, OPEX, and financial contributions) was used to designate the cost associated with deployment of various quantities of hybrid geo-solar power.

Of the GeoVision Scenarios, the hybrid geo-solar analysis was performed for the Business-As-Usual and Technology Transfer Scenarios. The Business-As-Usual Scenario represents conditions corresponding to the status quo, i.e. the geothermal industry continues to operate under present baseline conditions. The Technology Transfer Scenario is an improvement scenario in which exploration & well development incorporate improvements from other industry technology transfers. A listing of the GETEM input variables that differentiate the improved scenarios from the reference scenario is included in Appendix A. The hybrid geo-solar analysis is consistent with the GeoVision market analysis Technology Transfer Scenario but also includes an assumed reduction in the capital cost of the solar collectors as described below.

The hybrid geo-solar analysis includes the evaluation of two electricity pricing schedules. The first is a level pricing schedule in which the price of electricity is constant with time. The second is a time-of-delivery (TOD) pricing schedule in which the price of electricity varies throughout the day. In the TOD pricing schedule, electricity pricing is generally higher when demand (or load) is greater such that consumers have an incentive to shift usage to times of off-peak demand. The power output from hybrid geo-solar plants is generally known to correspond more closely to the periods of greater power demand and hybrid plants are expected to offer economic advantages in a TOD electricity pricing market. This analysis utilizes the SAM/CSP Physical Trough TES Dispatch/Generic Summer Peak TOD pricing schedule [104] in calculating the LCOE of stand-alone and hybrid plants operating in a TOC pricing power market.

As previously noted, major advantages of solar resources include that they can be easily characterized and have consistent long-term performance. These characteristics effectively reduce the risk associated with solar resource development, which should ultimately have the impact of reducing discount rates for developing power plants utilizing these resources. Despite the potential for solar resource utilization to reduce discount rates associated with hybrid plant development, this analysis assumes identical WACC for stand-alone and hybrid geo-solar plants (as well as geothermal resource and solar resource infrastructure). If a decreased WACC were implemented for solar hardware the LCOE for hybrid geo-solar power generation would decrease from the values reported in this analysis.

2.2.1 Geothermal and Solar Resource Data

Analysis of hybrid geo-solar power plants requires a dataset that includes geothermal and solar resource data at each geographic location to be evaluated. The P2P Task Force supplied the Hybrid Systems Task Force with a dataset that includes geothermal resource data for four geothermal resource types (identified hydrothermal, undiscovered hydrothermal, near-field EGS, and deep EGS). By using the geothermal resource dataset used by the P2P Task Force, the geothermal resource data used by the Hybrid Systems Task Force is consistent with that used to construct the GeoVision Study market penetration analysis supply curves.

The Hybrid Systems Task Force developed a combined geothermal-solar resource dataset by augmenting the P2P Task Force geothermal resource dataset with solar resource data from the National Solar Radiation Database (NSRDB) [105]. Solar data was coupled with the geothermal resource data for each of the geothermal resource types as detailed below.

The geothermal resource database characterizes Identified Hydrothermal and Near-Field EGS resources at specific geographic sites by reservoir temperature and reservoir depth. Identified Hydrothermal and Near-Field EGS resource site latitude/longitude coordinates were entered into the NSRDB Viewer "find location" query tool to obtain the corresponding average solar DNI data.

The geothermal resource database characterizes Deep EGS resources by temperature and depth (data not provided in a geographic site-specific format that can be further parsed to include solar resource data). The Deep EGS hybrid geo-solar plant analysis therefore includes a general analysis in which all Deep EGS sites are evaluated using a solar resource value of 6.0 kWh/m^2/day (a value assumed to represent the lower end of solar resources for which hybrid geo-solar plants would be viable).

A supply curve analysis of hybrid geo-solar power plants was not performed for undiscovered hydrothermal resources due to the limited number of sites with geothermal resource temperature in the range modeled for the hybrid plant analysis. Additionally, the undiscovered hydrothermal resource capacity was characterized by state, which provides too broad of a geographic area for accurate solar resource characterization. A simplified evaluation of hybrid plant LCOE relative to stand-alone plant LCOE was performed for the sites in the applicable geothermal resource temperature range using the average solar resource data from the identified hydrothermal sites in each state.

2.2.2 Solar Field Model

The solar field was modeled using the System Advisor Model (SAM) with a solar field configuration similar to that used in the EGP Stillwater hybrid geo-solar power plant. The Stillwater solar field is constructed of SkyFuel SkyTrough parabolic trough solar concentrators and uses pressurized water as the heat transfer fluid [23]. The solar field size and thermal output of this reference configuration were scaled as required to meet the hybrid plant requirements at each site evaluated. The maximum solar field size evaluated for each site corresponded to that resulting in solar heat input equal to 25% of the stand-alone geothermal plant operating from an equivalent geothermal resource.

A breakdown of the solar hybridization capital costs used in this analysis is presented in Table 2. Full projects costs also include heat exchanger, contingency, and indirect costs [22]. Solar field O&M costs are estimated as 30% of total CSP plant O&M from the SAM CSP Parabolic Trough Model [104].

Table 2. Solar field capital costs assumed in GeoVision hybrid geo-solar analysis.

Cost Item	BAU Scenario CAPEX	Tech Transfer Scenario CAPEX	Reference or Comment
Site preparation	$10/m²	$10/m²	Assuming an existing plant site [106]
Solar collector field	$150/m²	$75/m²	SAM default CSP parabolic trough (physical) model solar field cost [104]; SunShot CSP trough target cost [107]
HTF system	$33/m²	$33/m²	Based on water-HTF solar field as in SAM's linear Fresnel model [104]

2.2.3 Power Block Model

Geo-solar air-cooled binary plant performance is impacted by changes in solar heat input and ambient temperature. In order to accurately characterize geo-solar plant performance relative to stand-alone geothermal plants, an evaluation technique that can account for time-dependent variations in power plant output as a function of changing resource and ambient conditions is required. This approach required simulation of power plant performance at on- and off-design conditions. Power plant "design" models developed in Aspen Plus were used to establish representative equipment specifications for three geothermal resource design conditions (150, 175, and 200°C). Aspen Plus-based power plant "rating" models were subsequently used to establish a map of plant performance as a function of geothermal resource temperature, solar heat input, and ambient temperature. These performance maps were established for each of the three plant designs corresponding to the three geothermal resource temperatures evaluated.

The power block evaluated in this analysis is a supercritical basic (non-recuperated) air-cooled binary cycle. The working fluid selection was dependent on the geothermal resource design temperature (R-134a, iC4, and R-245fa were selected for geothermal resource temperatures of 150°C, 175°C, and 200°C, respectively). In all cases a power plant ambient design temperature of 10°C was selected.

Hybrid plant power block capital costs were set equal to those of a stand-alone plant with equal geothermal heat input (assumes no major equipment configuration changes relative to stand-alone geothermal plant power block). Significant changes to the base power block configuration would negatively impact plant performance during periods without solar heat input while introducing additional capital costs. In order to ensure the model does not predict performance that would require equipment performance ratings be exceeded, the hybrid plant gross power generation is limited to 125% of design point gross power generation in the hybrid plant rating model (comparable to the max output of the stand-alone plant). Since the maximum hybrid plant output generally coincides with periods when stand-alone plant output would typically be lowest (mid-day periods when ambient temperature is high), this constraint does not in practice limit the hybrid plant performance.

The total hybridization costs include the costs of the solar field listed in the previous section (site preparation, solar collectors, and HTF system) and the heat exchanger used to transfer heat from the solar field HTF to the binary cycle working fluid. The HTF-to-WF heat exchanger is assumed to have an overall heat transfer coefficient equal to 1000 $W/m^2/K$ and a log-mean temperature difference (LMTD) of 30 K. The HTF-to-WF HX was costed using a shell & tube heat exchanger installed capital cost correlation [108] and updated to reference year dollars using the Producer Price Index (PPI) heat exchanger table included in GETEM.

2.2.4 Hybrid GETEM Model

A Microsoft Excel spreadsheet-based model was developed to couple power plant performance maps with geographic location-specific typical meteorological year (TMY) data sets in order to estimate plant

performance at one hour time intervals. TMY data sets were obtained for four representative geographic sites with average daily solar direct normal irradiance (DNI) values ranging from 4.5 to 7.5 kWh/m^2/day. The coupling of the plant performance maps with the TMY data allows estimation of geo-solar hybrid plant for any combination of geothermal resource temperature and average solar DNI in the ranges evaluated.

A spreadsheet-based model infrastructure was utilized to maximize compatibility and interoperability with GETEM (the model used in for techno-economic evaluation of stand-alone geothermal power plant projects for the various scenarios evaluated in the GeoVision study). In the hybrid plant analyses, GETEM was used to estimate geothermal resource performance and cost for each site evaluated, while the hybrid spreadsheet model was used to evaluate power plant performance and cost (using GETEM-derived power plant capital and operating cost calculations as applicable). GeoVision scenario-specific GETEM input parameters compiled by the P2P task force were used in evaluating each site.

As previously described, the geothermal resource database supplied by the P2P task force was modified to include solar resource data at each site. A VBA macro was utilized to evaluate geo-solar hybrid plants at all sites designated for each of the geothermal resource types in this database (identified hydrothermal, undiscovered hydrothermal, near-field EGS, and deep EGS). Geothermal and solar resource parameters for each site are passed by the macro to the linked GETEM and Hybrid GETEM spreadsheet models, where GETEM calculates geothermal reservoir performance and cost, and the Hybrid GETEM spreadsheet pairs the geothermal and solar resource conditions with the corresponding power plant performance map (based on geothermal resource temperature) and geographic site TMY data (based on average solar DNI). The model then adjusts plant performance for project size and brine effectiveness (as optimized by GETEM) and outputs hourly power generation, capital costs and O&M costs of the stand-alone and hybrid plants.

A sample plot of estimated hourly power generation for the stand-alone and hybrid plants is included below in Figure 2. The power generation profiles shown are calculated for stand-alone and hybrid power plants operating from a 175°C geothermal resource located in Reno, Nevada during a TMY week in early June. The geothermal resource in these simulations is specified to provide the thermal energy necessary to operate a 30 MW_e (design) stand-alone geothermal power plant, while the hybrid plant solar field is sized to provide thermal input equal to 25% of the design point geothermal heat input.

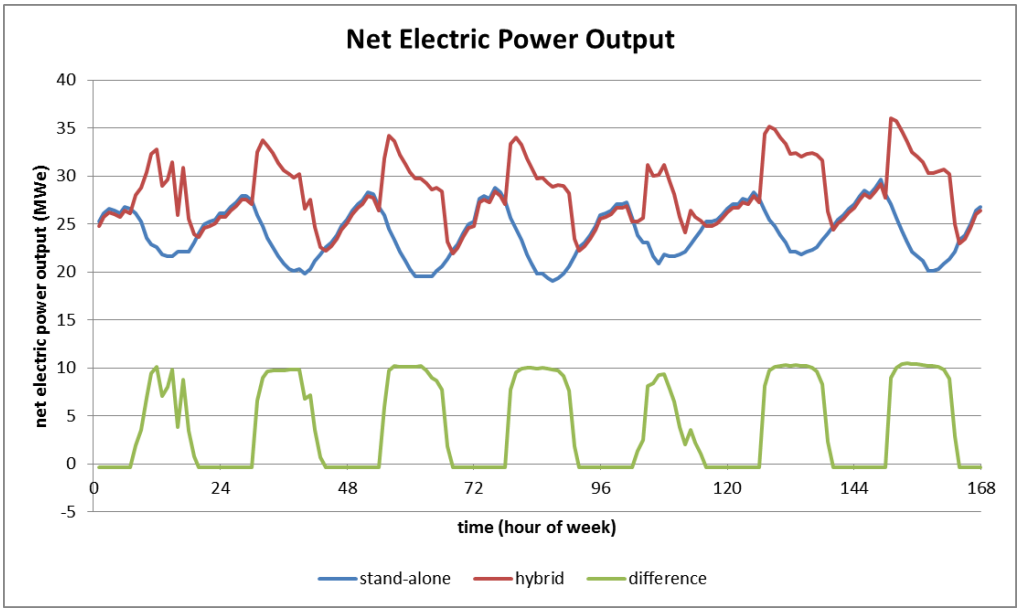

Figure 2. Sample comparison of stand-alone geothermal and hybrid geo-solar hourly power generation.

2.3 Results

In this analysis, hybrid and stand-alone geothermal plant supply curves are presented for the subset of geothermal resources in the P2P supply curve dataset with temperatures in the range of 150°C < T < 225°C and solar resources with average annual DNI > 4.8 kWh/m^2/day. While it would be possible to operate hybrid geo-solar plants with resources outside of these ranges, power plant performance models have not yet been developed for resource conditions outside of the specified ranges. However, the majority of the geothermal resources included in the P2P supply curve dataset fall within the range of conditions for which hybrid plant performance models do exist, so the results and conclusions presented in this analysis are generally representative and applicable, although the supply curves in this analysis will differ from those generated by the P2P task force where geothermal resources of all temperatures are considered.

Whereas the P2P supply curves are presented in terms of installed capital cost versus available capacity, in this analysis supply curves are plotted in terms of LCOE versus available capacity. This alteration was made in order to evaluate the resource types and scenarios for which hybrid geo-solar plant economics are favorable relative to stand-alone geothermal plants using a metric that incorporates capital costs, operating costs, and electric power generation over the specified power plant operating life (these inputs would normally be incorporated into the ReEDS market penetration modeling, which is not currently able to evaluate hybrid systems).

Due to the difference in the way P2P and Hybrid Systems task force supply curves are generated for stand-alone and hybrid plants, respectively, the supply curves generated in this analysis cannot be directly compared against P2P supply curves. Nonetheless, the P2P ReEDS analysis predicts significant deployment of certain geothermal resource types in the improved scenarios evaluated; when the hybrid geo-solar analysis predicts LCOE reductions relative to stand-alone geothermal plants over a significant range of the available capacity for these resource types, it is expected that hybrid plants would increase deployment (by providing power at lower cost and/or providing increased capacity at the same cost).

It is also important to note that in the supply curves presented in this analysis, stand-alone and hybrid plant capacity is calculated as the average value during the first year of operation. Since the power output of both air-cooled stand-alone plants and hybrid plants is highly variable, use of the annual average capacity is considered more representative than the design point capacity for this analysis. The stand-alone and hybrid plant capacities presented in the supply curves are referenced to the plant sales value listed for each site in the stand-alone geothermal resource database, which appropriately scales the calculated stand-alone and hybrid plant results to match the available geothermal resource at each site considered.

2.3.1 Identified Hydrothermal

There are no significant LCOE drivers that favor the use of hybrid geo-solar technology relative to stand-alone geothermal for the Business-As-Usual Scenario (Figure 3). The primary motivation for using hybrid geo-solar technology in this scenario would be to increase the temporal correlation between electrical power generation and electrical load, to decrease the risks associated with the development of a stand-alone geothermal reservoir (solar resource can be characterized with more certainty), and/or to decrease the negative impacts associated with geothermal resource productivity decline.

Hybrid geo-solar electricity generation costs are similar to those for stand-alone geothermal technology in the Technology Transfer Scenario. Figure 4 provides a comparison of the Technology Transfer Scenario supply curves for two discrete cases; a resource base comprised completely of stand-alone geothermal plants versus a resource base comprised completely of hybrid geo-solar plants. In reality, if both stand-alone and hybrid geo-solar technology were available at all sites, each site would deploy using the technology that resulted in the lowest LCOE. Merged supply curves that utilize the least cost option

(stand-alone or hybrid geo-solar) for each site are presented in Figure 5 (level pricing) and Figure 6 (TOD pricing).

The incremental capacity provided by hybrid geo-solar technology becomes more economical than stand-alone geothermal at an LCOE threshold value of $0.133/kWh for the Technology Transfer level pricing scenario (Figure 5) and $0.087/kWh for the Technology Transfer TOD pricing scenario (Figure 6). Greater than 1600 MW (level pricing market) or 880 MW (TOD pricing market) of identified hydrothermal deployment would be required to include capacity from hybrid geo-solar power plants.

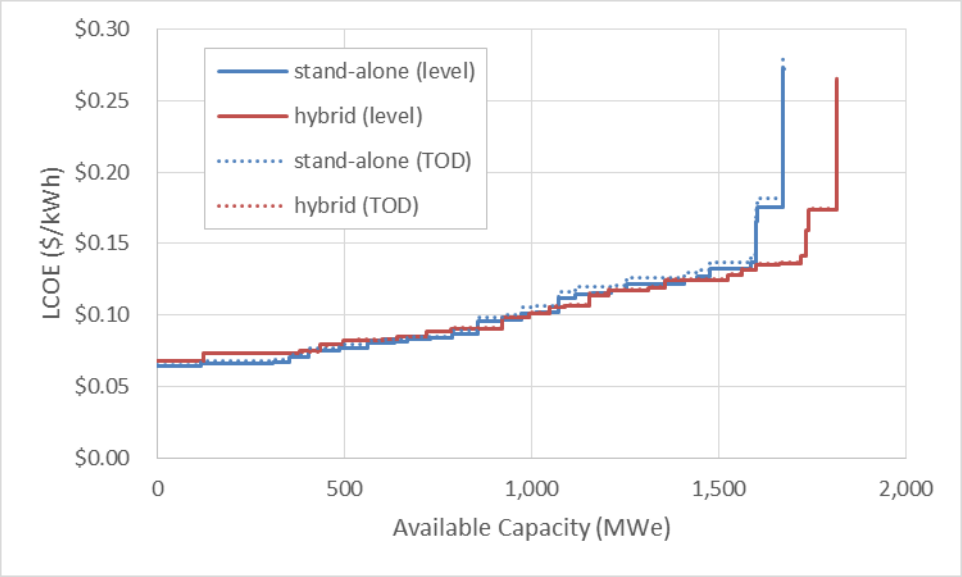

Figure 3. Identified Hydrothermal supply curve (BAU scenario).

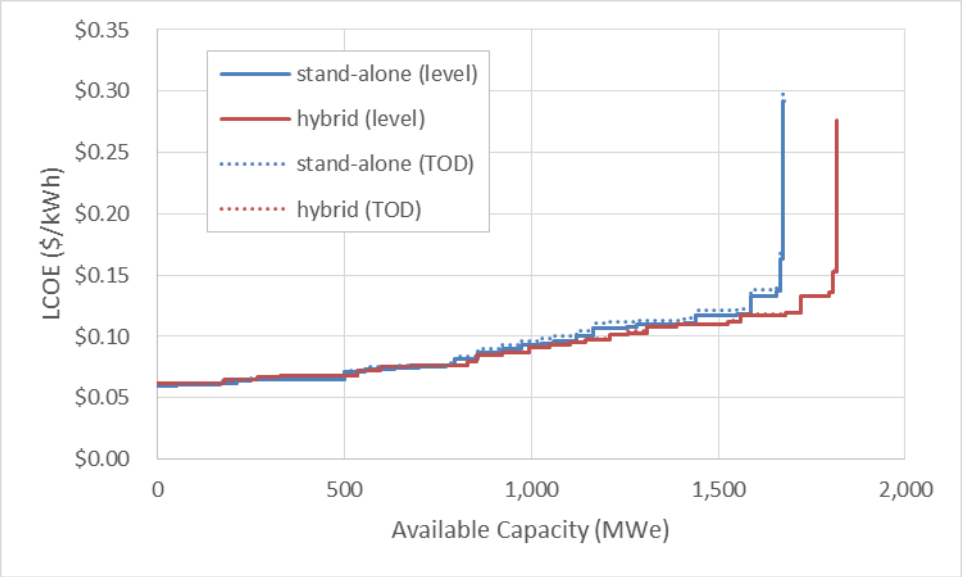

Figure 4. Identified Hydrothermal supply curve (Tech Transfer scenario).

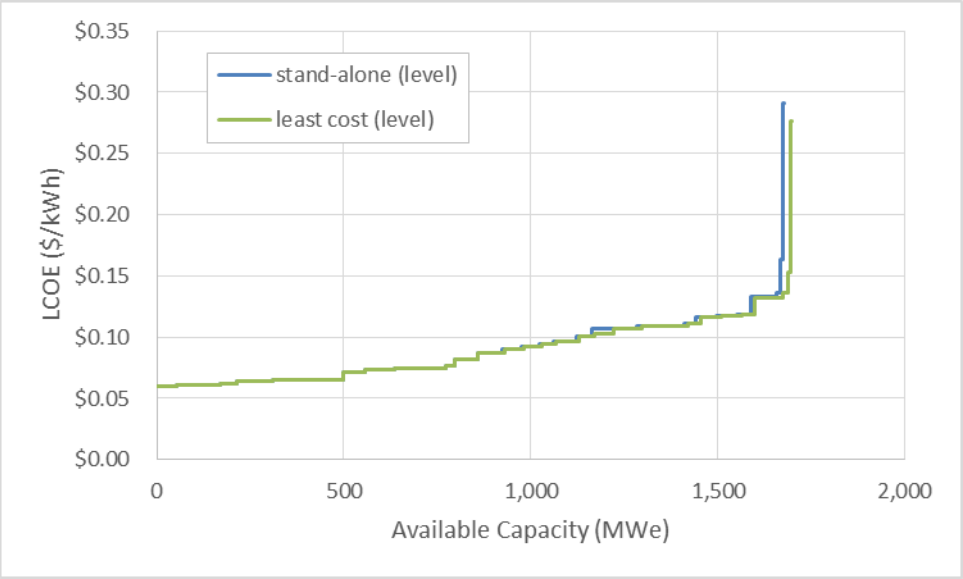

Figure 5. Merged stand-alone and hybrid geo-solar Identified Hydrothermal supply curve (Technology Transfer Scenario, level pricing).

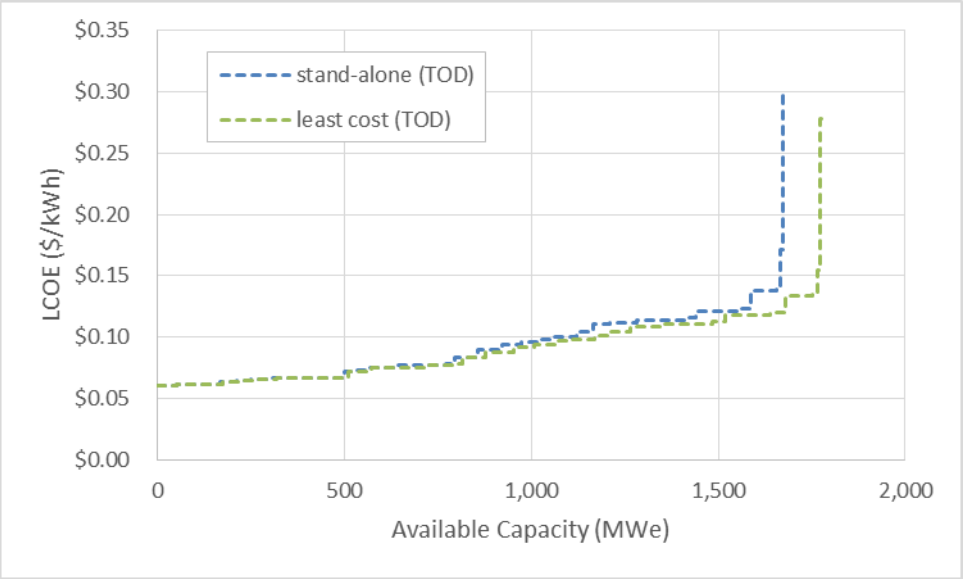

Figure 6. Merged stand-alone and hybrid geo-solar Identified Hydrothermal supply curve (Technology Transfer Scenario, TOD pricing).

2.3.2 Undiscovered Hydrothermal

Undiscovered hydrothermal resource capacity is reported at the state level in the P2P supply curve database, which results in large uncertainties regarding the TMY specific data (i.e., solar radiation and ambient temperature). Also, undiscovered hydrothermal supply curve dataset entries with temperatures within the range modeled for hybrid geo-solar power plants in this analysis (150-200°C) represent less than 25% of the plant sales (available capacity) in the undiscovered hydrothermal supply curve dataset. Therefore, the undiscovered hydrothermal resource assessment data does not include sufficient data to establish supply curves for the comparison of stand-alone geothermal and hybrid geo-solar power plants.

Although the combined geothermal and solar resource data was insufficient to develop undiscovered hydrothermal hybrid plant supply curves, the LCOE for hybrid and stand-alone plants were calculated for sites in the dataset that fall into the geothermal resource temperature range for which hybrid plants were evaluated (150-200°C) using solar resource data corresponding to the average of all identified hydrothermal sites in the same state. While hybrid plants did not generally result in LCOE improvements in the BAU Scenario, the hybrid LCOE was lower at all undiscovered hydrothermal sites evaluated in the Tech Transfer Scenario with TOD pricing. The capacity weighted average LCOE reduction from use of hybrid plants at sites for which the minimal resource data was available is summarized in Table 3 along with the results for other geothermal resource types.

2.3.3 Near Field EGS

Hybrid geo-solar technology reduces LCOE for all sites evaluated in the Near Field EGS Business-As-Usual Scenario. The hybrid geo-solar capacity-weighted average LCOE is 85.9% of that for stand-alone geothermal with level pricing, and 81.9% of that for stand-alone geothermal with TOD pricing. However, as can be seen from Figure 7, a substantial fraction of both the hybrid geo-solar and stand-alone geothermal Near Field EGS sites have LCOE greater than $0.50/kWh and are considered unlikely to deploy in a deregulated electricity market where other less expensive electricity sources (e.g., wind, solar PV, fossil, etc.) are likely to be available. Nonetheless, hybrid geo-solar technology significantly increases the available capacity of electrical power with LCOE < $0.50/kWh in the BAU Scenario to (730 MW of hybrid geo-solar capacity versus 510 MW of stand-alone geothermal capacity).

The Technology Transfer Scenario supply curve (Figure 9) indicates less available capacity for the hybrid geo-solar plant than in the BAU Scenario supply curve (Figure 7). This is due to the difference in geofluid pumping parasitic losses between the two scenarios. Parasitic losses are much higher in BAU Scenario than in the Technology Transfer Scenario, which causes GETEM to select a power plant design with higher brine efficiency. Therefore, the power plant efficiency used in the BAU Scenario is greater than that used in the Technology Transfer Scenario, which results more electrical power generation from the available solar heat in the BAU Scenario.

The Technology Transfer Scenario results in a significant decrease in LCOE relative to the Business-As-Usual Scenario for both stand-alone geothermal and hybrid geo-solar power plants using Near Field EGS resources. Figure 9 provides a comparison of the Technology Transfer Scenario supply curves for two discrete cases; a resource base comprised completely of stand-alone geothermal plants versus a resource base comprised completely of hybrid geo-solar plants. In reality, if both stand-alone and hybrid geo-solar technology were available at all sites, each site would deploy using the technology that resulted in the lowest LCOE. Merged supply curves that utilize the least cost option (stand-alone or hybrid geo-solar) for each site are presented in Figure 10 (level pricing) and Figure 11 (TOD pricing).

The availability of hybrid geo-solar technology would result in LCOE reductions at Near Field EGS sites where the stand-alone geothermal LCOE would be approximately $0.111/kWh or greater for a level pricing market (Figure 10). Greater than 585 MW of Near Field EGS deployment would be required to include capacity from hybrid geo-solar power plants in a level pricing market. However, in a TOD pricing market, hybrid geo-solar technology results in a lower LCOE than stand-alone plants at all sites evaluated (Figure 11). The deployment of predominantly hybrid plants would therefore be expected in the Technology Transfer Scenario with TOD pricing.

Hybrid geo-solar technology provides the greatest LCOE reduction for Near Field EGS sites with lower geothermal reservoir temperatures. This is illustrated in plots of the hybrid geo-solar LCOE as a percentage of the stand-alone plant LCOE for the Near Field EGS sites evaluated in the BAU and Tech Transfer Scenarios presented as Figure 8 and Figure 12, respectively. The economic advantages of combining geothermal and solar heat are most significant when geothermal heat costs are high (as is the

case for the lower temperature Near Field EGS sites) such that the addition of solar heat can reduce the overall cost of the heat input to the power block.

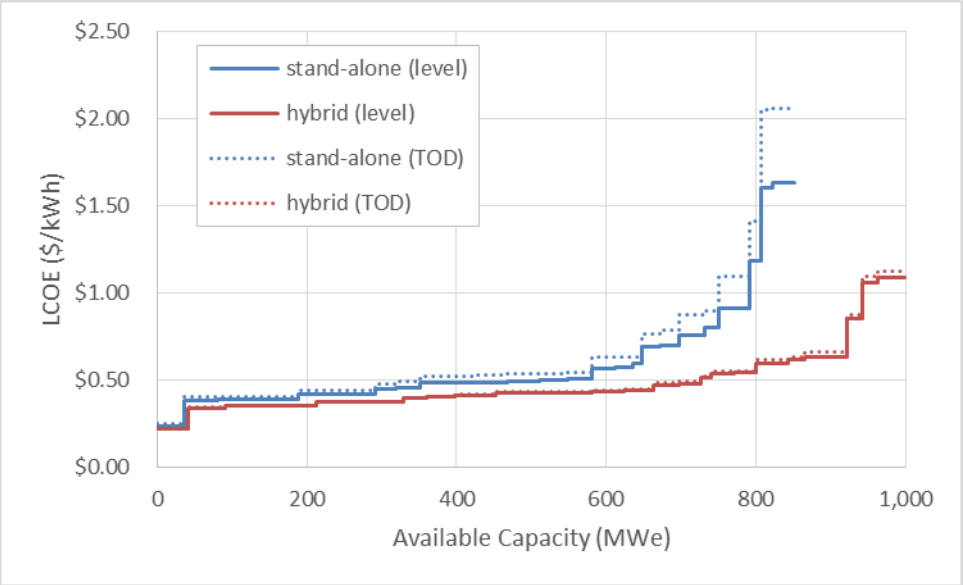

Figure 7. Near Field EGS supply curve (BAU scenario)

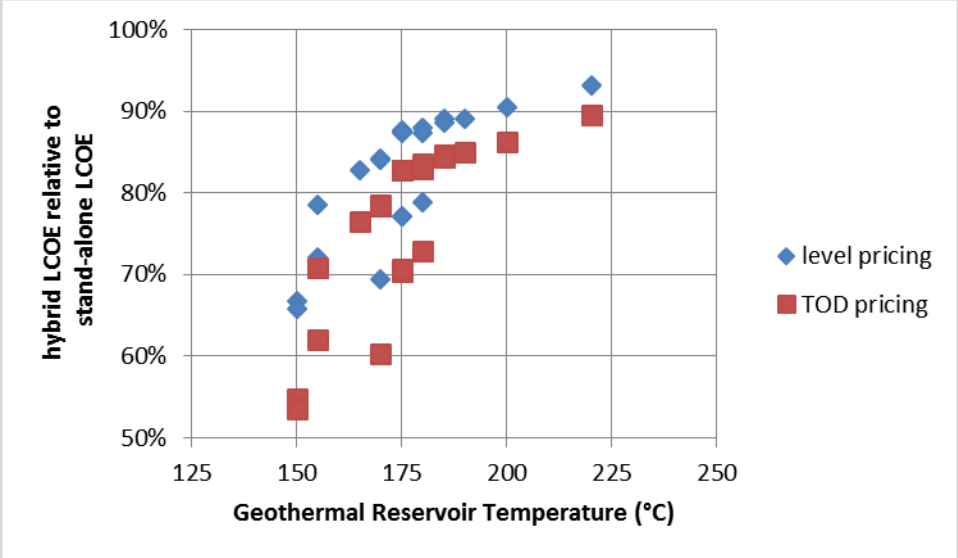

Figure 8. Near Field EGS hybrid geo-solar LCOE as percentage of stand-alone geothermal LCOE for Business-As-Usual scenario.

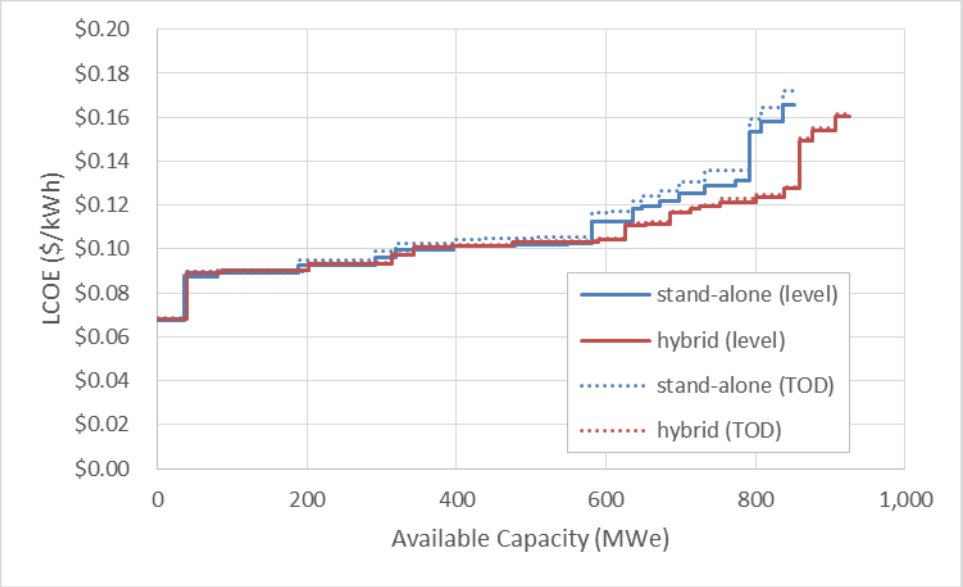

Figure 9. Near Field EGS supply curve (Tech Transfer scenario).

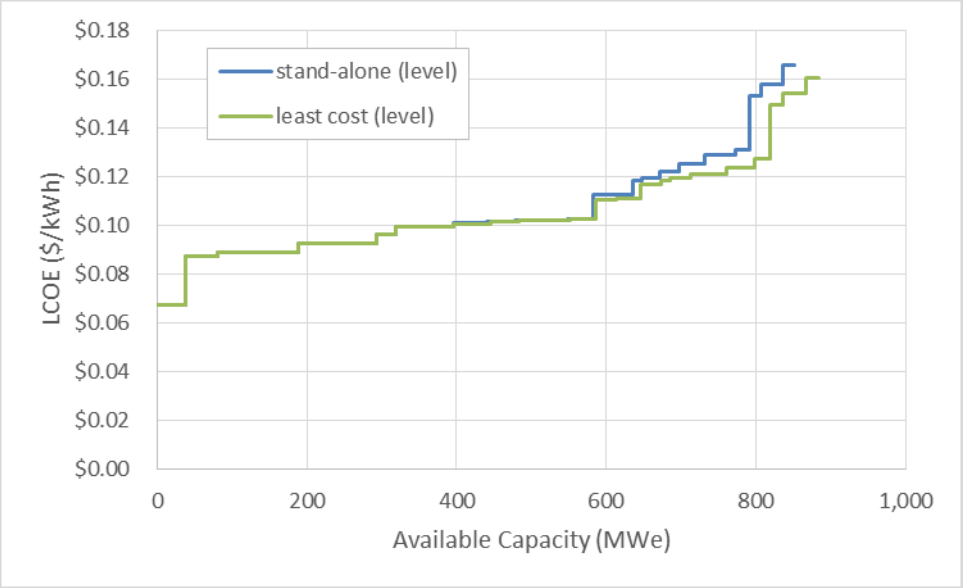

Figure 10. Merged stand-alone and hybrid geo-solar Near Field EGS supply curve (Technology Transfer scenario, level pricing).

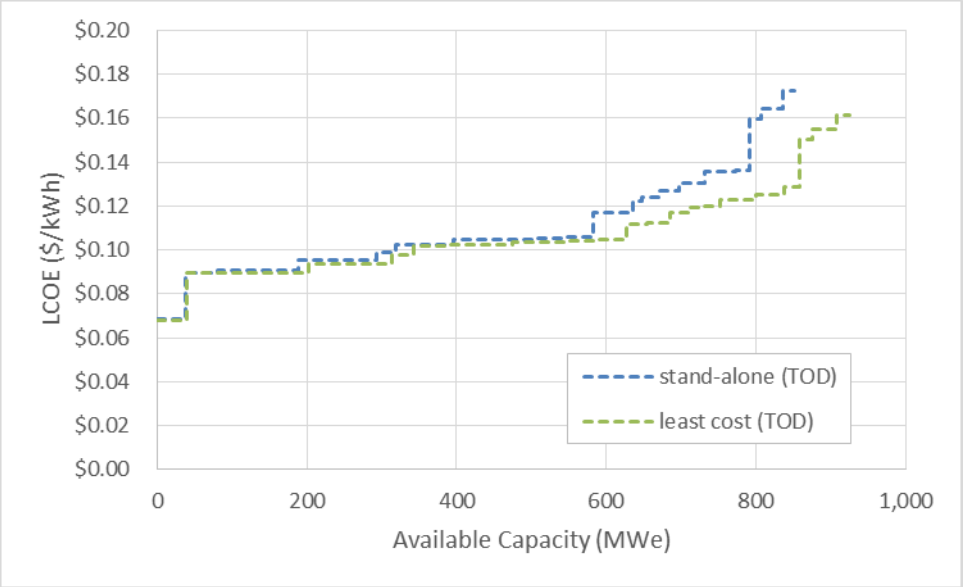

Figure 11. Merged stand-alone and hybrid geo-solar Near Field EGS supply curve (Technology Transfer scenario, TOD pricing).

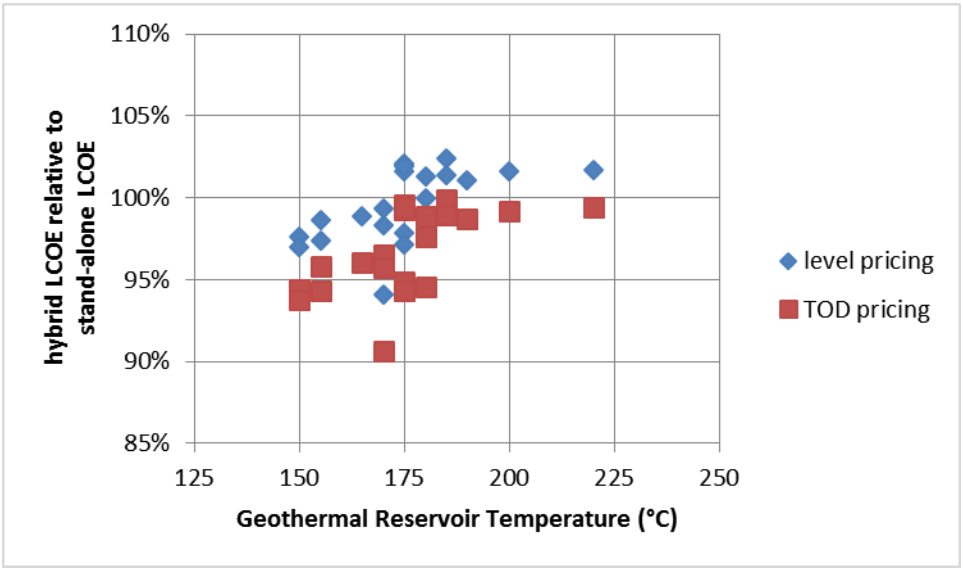

Figure 12. Near Field EGS hybrid geo-solar LCOE as percentage of stand-alone geothermal LCOE for Technology Transfer scenario.

2.3.4 Deep EGS

A geothermal resource data set that categorized the availability of Deep EGS heat not only by temperature and depth but also by solar resource was not available for this analysis. Therefore, Deep EGS hybrid geo-solar supply curves are constructed assuming a 6.0 kWh/m^2/day solar resource is available at all sites. Since the average solar resource for the continental U.S. is ~3.5 kWh/m^2/day and it is presumed that hybrid geo-solar technology will only be deployed in areas with above average solar resource, the Deep EGS hybrid geo-solar supply curves generated in this analysis are only approximate. These approximate

supply curves are nonetheless instructive for comparing the relative costs of hybrid geo-solar and stand-alone geothermal at locations with solar resource of at least 6.0 kWh/m^2/day. The states of Arizona, California, Colorado, New Mexico, Nevada, and Utah have average annual DNI > 6.0 kWh/m^2/day [109]. These states represent approximately 22% of the land area of the 48 contiguous US states.

As with the Near Field EGS resource, hybrid geo-solar technology reduces LCOE for all sites evaluated in the Deep EGS Business-As-Usual Scenario. The hybrid geo-solar capacity-weighted average LCOE is 89.5% of that for stand-alone geothermal with level pricing, and 86.2% of that for stand-alone geothermal with TOD pricing. However, as can be seen from Figure 13, the majority of this capacity has an LCOE > $1.00/kWh which is expected to significantly limit deployment (the capacity-weighted average LCOE reductions described in the previous sentence only consider sites with LCOE < $1.00/kWh). As illustrated in Figure 14, the largest improvements in LCOE result from the use of hybrid geo-solar technology with lower temperature geothermal resources.

The P2P market penetration analysis does not predict any deployment of Deep EGS resources in the BAU Scenario. While the use of hybrid geo-solar plants would lower the LCOE of Deep EGS power generation, the costs are likely still too high for significant deployment in this scenario.

The Technology Transfer Scenario results in an order of magnitude reduction in electricity costs for both Deep EGS stand-alone geothermal and hybrid geo-solar power generation. As was the case for Near Field EGS resources, the Deep EGS Technology Transfer Scenario supply curve (Figure 15) indicates less available capacity for the hybrid geo-solar plant than in the BAU Scenario supply curve (Figure 13). Again this is due to the higher geofluid pumping parasitic losses driving the BAU Scenario toward higher brine efficiency to minimize LCOE, which results in higher plant efficiency and increased power generation from the available solar heat in the BAU Scenario.

Figure 15 provides a comparison of the Technology Transfer Scenario supply curves for two discrete cases; a resource base comprised completely of stand-alone geothermal plants versus a resource base comprised completely of hybrid geo-solar plants. In reality, if both stand-alone and hybrid geo-solar technology were available at all sites, each site would deploy using the technology that resulted in the lowest LCOE. Merged supply curves that utilize the least cost option (stand-alone or hybrid geo-solar) for each site are presented in Figure 16 (level pricing) and Figure 17 (TOD pricing).

Figure 16 indicates that the availability of hybrid geo-solar technology in an electricity market with level pricing would result in LCOE reductions at Deep EGS sites where the stand-alone geothermal LCOE would be approximately $0.138/kWh or greater. Figure 17 indicates that in a TOD pricing market hybrid geo-solar technology results in a lower LCOE than stand-alone plants at all sites evaluated. The deployment of predominantly hybrid plants would therefore be expected at deep EGS sites in the Technology Transfer Scenario with TOD pricing.

Figure 18 indicates that hybrid geo-solar technology tends to be more cost-effective when paired with lower temperature geothermal resources. From a technical and logistical perspective, these would likely be the most readily accessible EGS resources and may therefore be the EGS resources that would be most likely to come online. These results suggest that the use of hybrid geo-solar technology may be desirable in the initial deployment of EGS technology in scenarios resembling both the Business-As-Usual and Technology Transfer Scenarios.

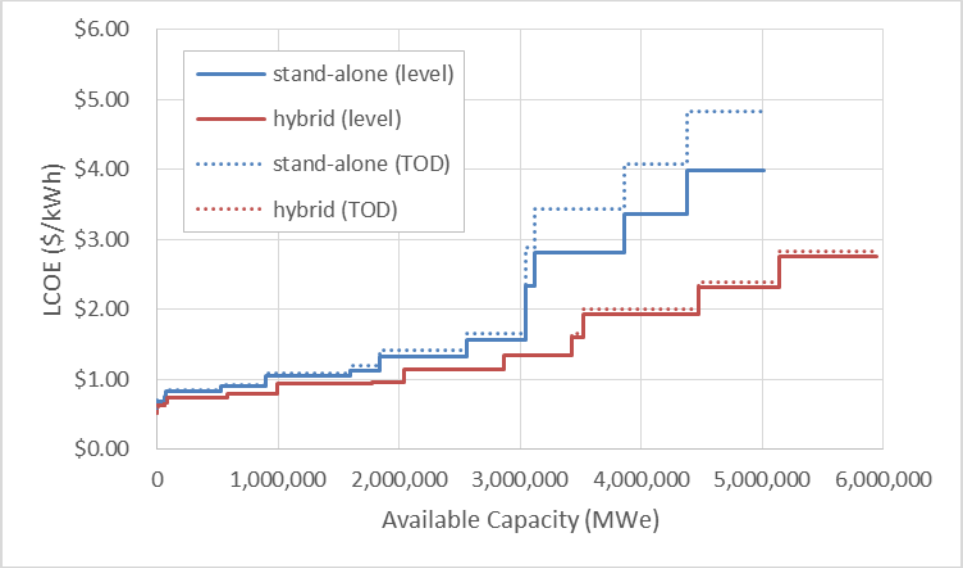

Figure 13. Deep EGS supply curve (BAU scenario).

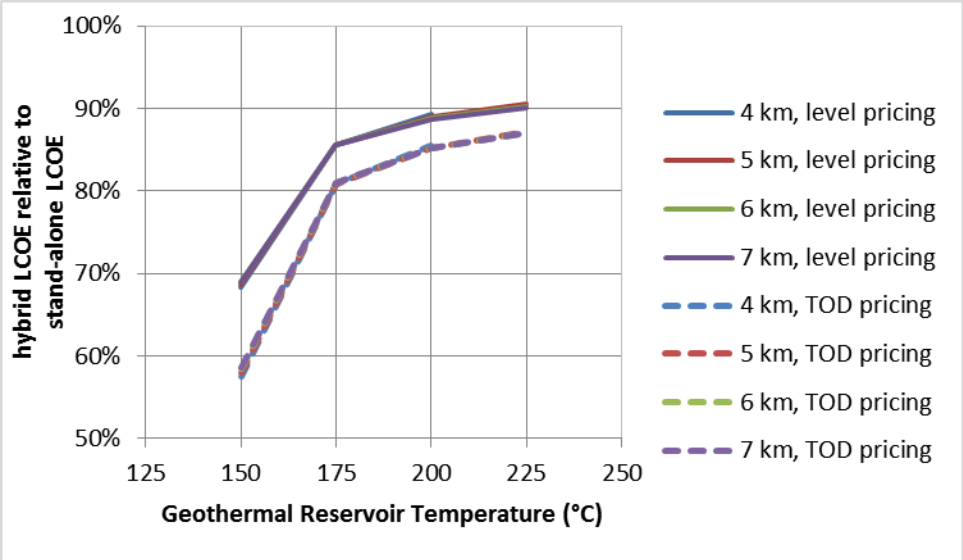

Figure 14. Deep EGS hybrid geo-solar LCOE as percentage of stand-alone geothermal LCOE for Business-As-Usual Scenario. Largest LCOE reductions result from using hybrid geo-solar technology with lower temperature geothermal resources.

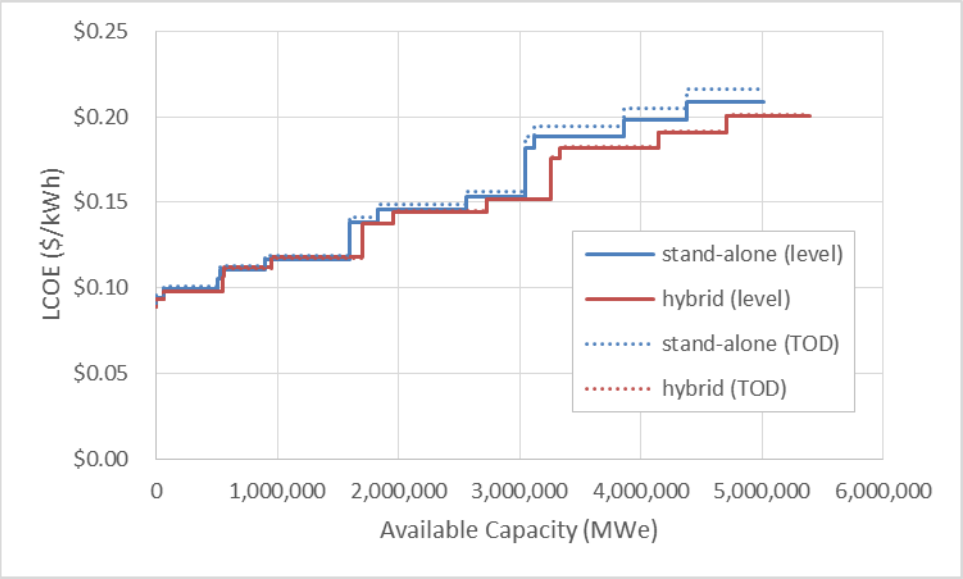

Figure 15. Deep EGS supply curve (Technology Transfer scenario).

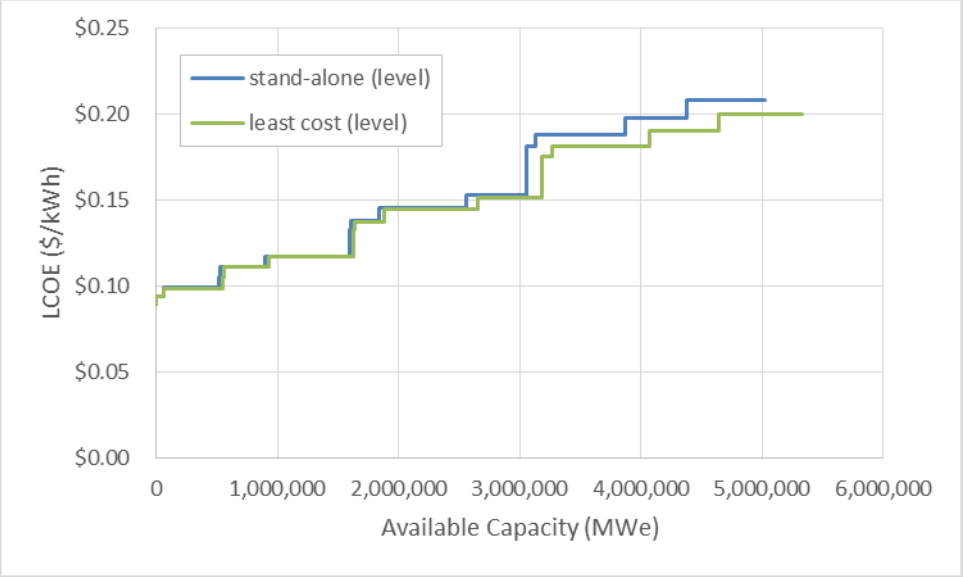

Figure 16. Merged stand-alone and hybrid geo-solar Deep EGS supply curve (Technology Transfer scenario, level pricing).

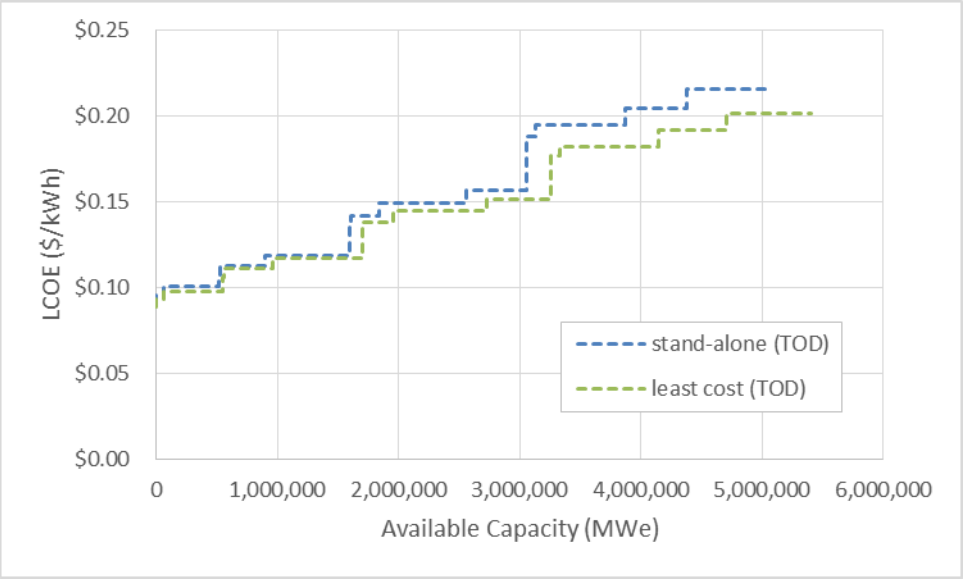

Figure 17. Merged stand-alone and hybrid geo-solar Deep EGS supply curve (Technology Transfer scenario, TOD pricing).

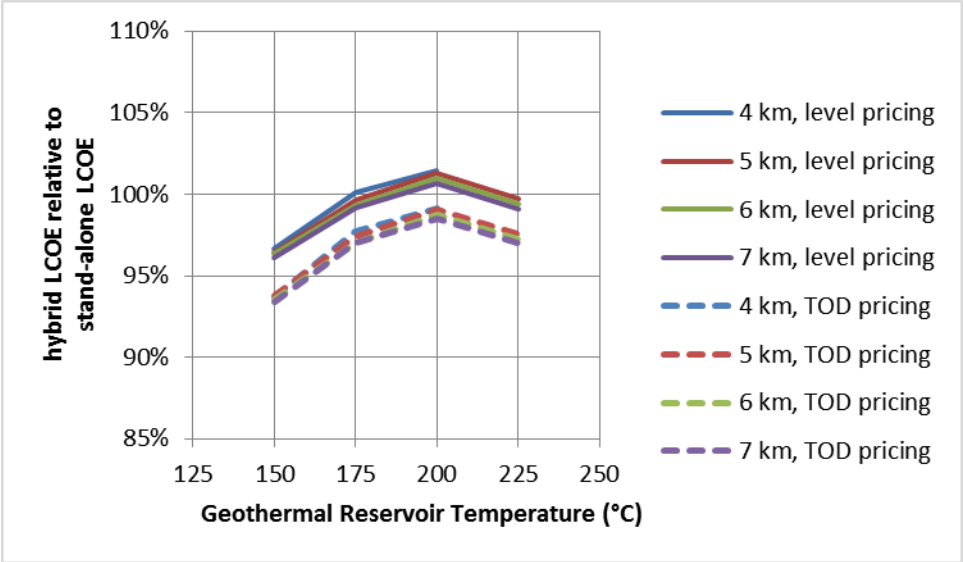

Figure 18. Deep EGS hybrid geo-solar LCOE as percentage of stand-alone geothermal LCOE for Technology Transfer scenario.

2.4 Summary

The performance characteristics of hybrid geo-solar power plants are generally considered superior to those of stand-alone air-cooled geothermal power plants (i.e. the hybrid plant power generation profile is more closely matched to the electrical grid load). Evidence for the improved correlation between hybrid geo-solar plant output with the electrical load is provided through evaluation of a TOD electrical pricing scenario (where greater electricity sales prices are assigned to times when electrical demand is greatest). In the TOD pricing scenario, greater LCOE reductions are realized through use of the hybrid geo-solar plant due to the hybrid plant being able to provide increased revenues during periods when more revenue is available from increased electrical sales pricing.

Table 3. LCOE of hybrid geo-solar relative to stand-alone geothermal (hybrid plant LCOE as percentage of stand-alone LCOE, reported as a capacity-weighted average).

	Business-as-Usual		Technology Transfer	
	Level Pricing	TOD Pricing	Level Pricing	TOD Pricing
Identified hydro	104.8%	102.1%	101.8%	99.1%
Undiscovered hydro	103.9%	101.2%	100.6%	98.0%
Near-Field EGS	85.9%[a]	81.9%[a]	100.2%	97.5%
Deep EGS	89.5%[a]	86.2%[a]	98.4%	96.0%

(a) Sites with stand-alone geothermal plant LCOE > $1.00/kWh excluded from calculation.

The reduction in LCOE provided by hybrid ORC plants is generally smaller in magnitude for the Tech Transfer Scenario than for the BAU Scenario. This is primarily due to the significant reduction in geothermal resource development costs associated with the Tech Transfer Scenario. While decreased solar hardware costs are also used in the evaluation of the Tech Transfer Scenarios, the hybrid plant LCOE is driven mainly by the geothermal costs (the majority of the heat input in the hybrid ORC configuration comes from geothermal energy) such that there is less opportunity for LCOE reduction from incorporating low cost solar energy. Nonetheless, several significant opportunities for hybrid technology to lower LCOE and increase the deployment of plants that utilize geothermal energy were identified. Applicable conditions for each resource type and scenario are summarized below:

Business-As-Usual (level and TOD pricing)

In the Business-As-Usual Scenario with level pricing identified hydrothermal stand-alone and hybrid plant LCOE are similar; variability in geothermal resource development costs results in a site-by-site determination as to which plant type will result in the lower LCOE. In this scenario, hybrid technology may be deployed on a site-by-site basis and be utilized primarily for mitigating geothermal resource development risks or impacts associated with geothermal resource productivity decline.

Insufficient resource data were available for rigorous site-by-site evaluation of hybrid plants at undiscovered hydrothermal sites; this analysis does not suggest that hybrid plants would significantly reduce LCOE at undiscovered hydrothermal sites, but as with identified hydrothermal sites this determination would likely be made based on site-specific considerations.

In the BAU Scenario with level pricing significant reductions in LCOE result from the use of hybrid geo-solar technology with near-field EGS and deep EGS resource types. Near-field EGS hybrid plant LCOE is lower than stand-alone plant LCOE at every site evaluated. Deep EGS hybrid plant LCOE is lower than stand-alone plant LCOE at every temperature and depth combination evaluated (assuming a minimum average solar resource of 6.0 kWh/m^2/day). However, the LCOE associated with hybrid plant power generation are likely still too high to realize significant deployment.

Technology Transfer Scenario (level pricing)

Technology Transfer Scenario (level pricing) results are similar to those from the BAU Scenario for the identified hydrothermal and undiscovered hydrothermal resource type, i.e. variability in geothermal resource development costs and other site-specific considerations result in a site-by-site determination of whether to utilize hybrid technology.

The near field EGS supply curve for the Technology Transfer Scenario with level pricing (Figure 10) indicates that hybrid technology provides the least-cost LCOE option for deployment of capacity greater than 585 MW from the sites evaluated (geothermal resource 150°C < T < 225°C; solar resource > 4.8 kWh/m^2/day), which corresponds to LCOE values of $0.111/kWh or greater.

The deep EGS supply curve for the Technology Transfer Scenario with level pricing (Figure 16) indicates that hybrid technology provides the least-cost LCOE option for deployment of capacity greater than

1,600,000 MW from deep EGS resources in the temperature range of 150°C to 225°C with a minimum average solar resource of 6.0 kWh/m^2/day, which corresponds to LCOE values of $0.138/kWh or greater.

Technology Transfer Scenario (TOD pricing)

Hybrid plant configurations are predicted to provide a lower capacity-weighted average LCOE (the average LCOE of all available capacity; see Table 3) than stand-alone geothermal plants for all resource types (identified hydrothermal, undiscovered hydrothermal, and near-field EGS with geothermal resource 150°C < T < 225°C and solar resource > 4.8 kWh/m^2/day; deep EGS with geothermal resource 150°C < T < 225°C, depth of 4 km to 7 km, and solar resource of 6.0 kWh/m^2/day) in the Technology Transfer Scenario with TOD pricing. Therefore, a geothermal power industry comprised completely of hybrid plants would, on average, result in lower pricing than a market comprised completely of stand-alone geothermal plants in the Technology Transfer Scenario with TOD pricing.

The identified hydrothermal supply curve for the Technology Transfer Scenario with TOD pricing (Figure 6) indicates that hybrid technology provides the least-cost LCOE option for deployment of capacity greater than 880 MW from the sites evaluated (geothermal resource 150°C < T < 225°C; solar resource >4.8 kWh/m^2/day), which corresponds to LCOE values of $0.087/kWh or greater. Utilization of hybrid technology increases the available capacity from the identified hydrothermal resource sites evaluated from 1680 MW to 1775 MW.

Near-field EGS hybrid plant LCOE is lower than stand-alone plant LCOE at all sites evaluated (geothermal resource 150°C < T < 225°C; solar resource >4.8 kWh/m^2/day). Deep EGS hybrid plant LCOE is lower than stand-alone plant LCOE for all temperature and depth combinations evaluated (geothermal resource 150°C < T < 225°C; depth of 4 km to 7 km; solar resource of 6.0 kWh/m^2/day). The deployment of predominantly hybrid plants would therefore be expected at near field EGS and deep EGS sites in the Technology Transfer Scenario with TOD pricing.

2.5 Conclusion

This analysis evaluated a hybrid geo-solar air-cooled supercritical binary cycle power plant configuration. Other hybrid geo-solar plant configurations, including geothermal boiler feedwater heating, flash plant configurations, and/or combined cycle configurations were not included in the supply curve analysis; however, a case study analysis of hybrid CSP power plants using geothermal boiler feedwater heating is included in Chapter 3.0.

General benefits of hybrid geo-solar technology include the ability to decrease the risks and mitigate impacts associated with geothermal resource productivity decline. The hybrid plant therefore will better utilize the power block equipment (a “sunk cost”) as a function of time and decreasing geothermal resource. Although this analysis does not incorporate the use of a lower discount rate for the hardware associated with the solar resource, hybrid geo-solar power generation costs would improve relative to stand-alone geothermal if lower discount rates were used for these components.

Hybrid geo-solar power plants also improve the temporal correlation between generation and load (as demonstrated through the increased favorability of hybrid geo-solar LCOE relative to stand-alone geothermal power in a time-of-delivery pricing scenario). Use of geo-solar hybrid plants could therefore largely defend against the economic penalties that would otherwise be associated with air-cooled geothermal power generation in a time-of-delivery electricity pricing market.

This analysis suggests that if the costs of solar collectors can be reduced to the targets set by DOE and the concentrating solar power industry, hybrid geo-solar technology will allow LCOE reductions in locations with good solar resource and where stand-alone geothermal power generation costs are moderate (~$0.10/kWh) to high (≫$0.15/kWh), i.e. when the cost of solar heat is low, hybrid geo-solar technology provides a means by which to reduce the LCOE of geothermal power generation. This analysis indicates

that hybrid geo-solar technology generally provides the greatest reductions in LCOE when paired with low-temperature geothermal resources (where costs of stand-alone geothermal power generation tend to be highest).

Although the ReEDS market analysis model is not currently able to evaluate market penetration for hybrid technologies, the supply curves generated in this analysis suggest that for all geothermal resource types evaluated, there exists a threshold LCOE where a geothermal industry that utilizes hybrid geo-solar plants would be able to provide increased capacity at an equal or lower LCOE than a geothermal industry comprised solely of stand-alone geothermal plants. The supply curve capacity ranges where hybrid plants provide increased capacity at equal or lower LCOE to stand-alone plants represent the market conditions where the use of hybrid plants could significantly impact the deployment of power plants that utilize geothermal energy. Further analysis using ReEDS is necessary to quantify the impact of hybrid geo-solar plant availability on the utilization of geothermal energy as a source of power generation.

3.0 Geothermal-Solar: Case Study Analysis of CSP power plant with geothermal boiler feedwater heating

Highlights

- A case study analysis of hybrid CSP power plants using geothermal boiler feedwater heating plant configuration was performed. The hybrid GT-CSP plant converts geothermal energy to electricity at a higher efficiency than a stand-alone geothermal plant. Additionally, the hybrid GT-CSP plant operates with a higher capacity factor than a stand-alone CSP plant.
- In general, the hybrid CSP plant is able to provide decreases in LCOE relative to stand-alone geothermal, especially when considering lower geothermal resource temperatures. However, the LCOE for stand-alone CSP tends to be lower than for the hybrid plant at the lowest geothermal resource temperatures evaluated, and the LCOE for stand-alone geothermal is lower than that of the hybrid plant at the highest geothermal resource temperatures evaluated. The hybrid CSP configuration therefore tends to be the lowest LCOE option for an intermediate range of geothermal resource temperatures, which will vary on a site-by-site basis.

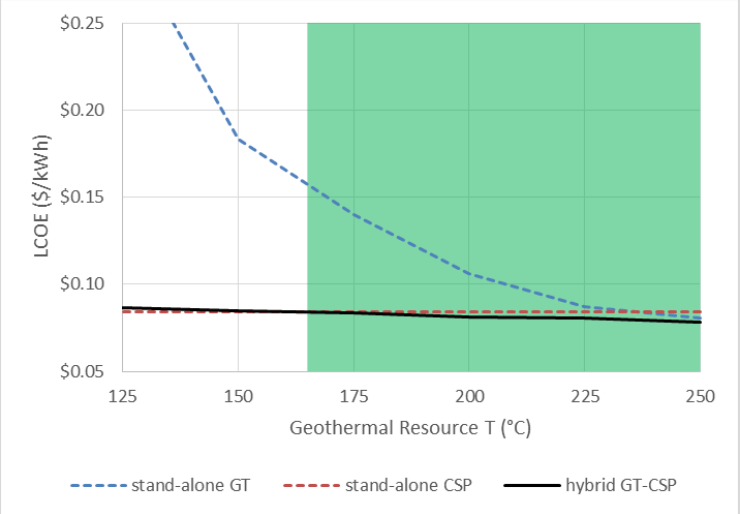

Deep EGS LCOE for stand-alone GT, stand-alone CSP, and hybrid CSP-GT power plants in Exploration De-Risk Scenario. The LCOE for the hybrid plant is lower than the LCOE for both stand-alone GT and CSP plants in the range of geothermal resource temperatures designated by the shaded plot area.

3.1 Introduction

Stand-alone concentrated solar power (CSP) plants are able to operate at higher temperatures, and consequently higher efficiencies, than geothermal (GT) power plants. This analysis evaluates the cost and performance of a hybrid CSP-GT plant configuration in which geothermal heat is used to provide boiler feedwater heating in a steam Rankine cycle CSP plant (Figure 19). Using geothermal heat for the boiler feedwater heating reduces the extraction of low pressure steam for this purpose, such that a greater fraction of the steam can be used to drive the turbines for electrical power generation.

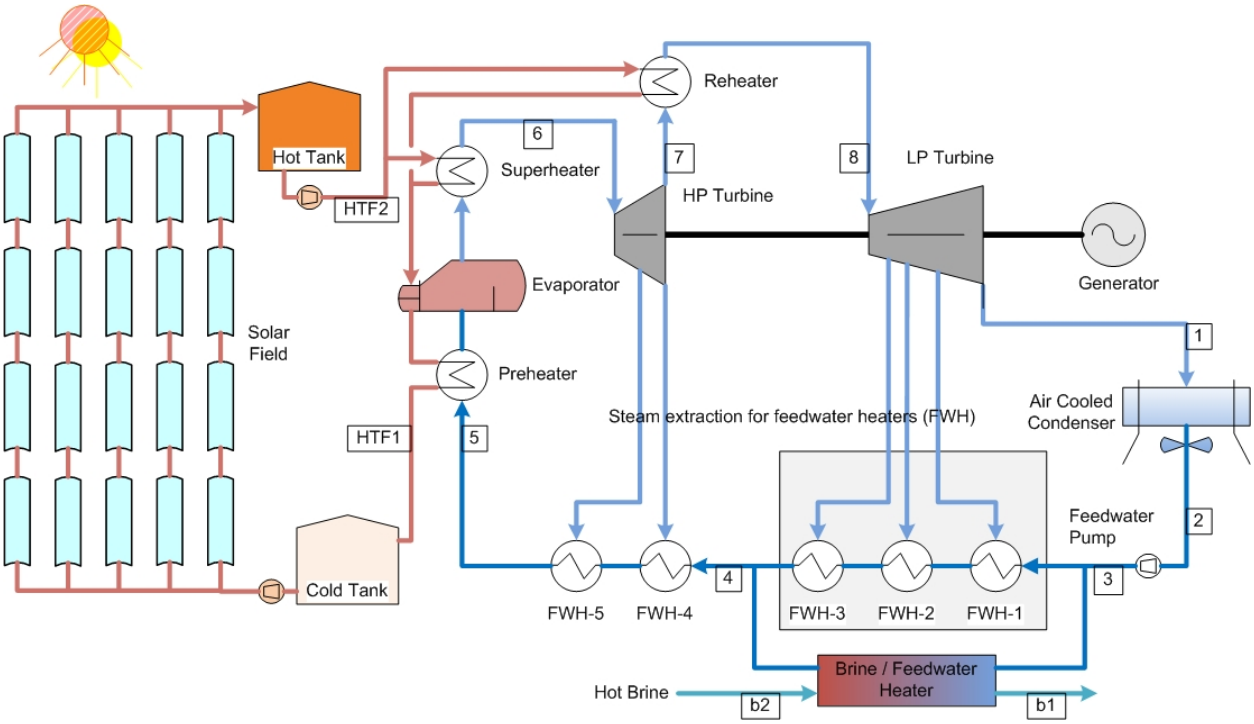

Figure 19. Schematic of a representative CSP plant showing energy from geothermal brine replacing the three low-temperature feedwater heaters (FWH-1, FWH-2, and FWH-3), thereby eliminating steam extractions from the low-pressure turbine. Open, hot (direct contact) FWHs are shown for simplicity, although the model uses closed FWHs [21].

This analysis investigated stand-alone and hybrid CSP plant configurations in which the solar field size and thermal energy storage capacity were modified to provide an increased capacity factor relative to the default System Advisor Model (SAM) CSP plant configuration. A CSP plant with higher capacity factor is better able to utilize geothermal energy by minimizing the amount of time the plant is offline and the geothermal energy cannot be used.

3.2 Methods

This analysis compares the cost and performance of hybrid CSP-GT plants against the cost and performance of stand-alone GT and stand-alone CSP plants. These plant configurations were evaluated in two case studies: (1) an undiscovered hydrothermal geothermal resource type with GeoVision Business-As-Usual Scenario (reference scenario) GETEM input values and reference solar hardware costs, and (2) a deep Enhanced Geothermal System (EGS) geothermal resource type with GeoVision Exploration De-Risk Scenario (improved scenario) GETEM input values and improved solar hardware costs. In both of these case studies, stand-alone and hybrid plant performance was evaluated for specified geothermal resource temperature and depth combinations using Daggett, CA solar insolation and ambient temperature TMY data. A listing of the GETEM input variables that differentiate the improved scenarios from the reference scenario is included in Appendix A.

The cost and performance of the stand-alone GT plants was estimated using the GeoVision 2016 version of the Geothermal Electricity Technology Evaluation Model (GETEM), which is the standard modeling tool utilized in the GeoVision study for evaluating geothermal power plant performance. GETEM was also used to compute the well field performance and capital and operating costs for the geothermal resources utilized in the hybrid CSP-GT power plants.

The cost and performance of the stand-alone CSP plants was estimated using version 2017.1.17 rev1 of SAM [104]. SAM was also used to compute the hourly solar field and thermal energy storage performance (thermal output and parasitic loads) and provide typical meteorological year (TMY) data for the hybrid CSP-GT plant analysis.

The solar field size was adjusted to provide an increased CSP plant capacity factor by increasing the solar multiple (SM) and the thermal energy storage (TES) capacity as specified in Table 4. With the exception of the modifications listed in Table 4, the SAM default CSP parabolic trough (physical) model solar field specifications were used for both stand-alone and hybrid CSP plant evaluation. The reference costs listed in Table 4 are used for evaluating the GeoVision Business-As-Usual (BAU) Scenario. The improved costs listed in Table 4 are used for evaluating the GeoVision Exploration De-Risk Scenario.

The performance of the stand-alone CSP and hybrid CSP-GT power plants were simulated using Aspen Plus based models. The design parameters for the stand-alone and hybrid CSP power cycles used in the Aspen Plus power cycle models are listed in Table 5. The Aspen Plus stand-alone and hybrid CSP power cycle models utilized the WILS-LR property method to compute Therminol VP-1 solar field heat transfer fluid (HTF) properties, the STEAMNBS property method to compute the water and steam properties (geofluid and steam Rankine cycle working fluid), and the IDEAL property method to compute air properties. Hybrid CSP-GT plant performance was evaluated for selected geothermal resource design point temperatures of 125°C, 150°C, 175°C, 200°C, 225°C, and 250°C.

The Aspen Plus models were also used to simulate the off-design performance of the hybrid CSP-GT power plants over a range of operating conditions. The power plant models calculated off-design performance using an approach similar to that used by Patnode [110] and Padilla [111]: The pressure drop of each turbine stage was calculated using Stodola Law [112], the efficiency of each turbine stage was calculated using an efficiency reduction factor [113], and the heat exchanger performance was calculated using the effectiveness-NTU method [114].

Independent variables that were varied to characterize the hybrid plant off-design performance included (1) solar field thermal output, (2) geothermal resource temperature [analysis assumes 0.5%/yr temperature decline], and (3) dry bulb ambient temperature. A unique regression function was established to predict hybrid plant performance as a function of these independent variables for each geothermal resource design temperature investigated (125°C, 150°C, 175°C, 200°C, 225°C, and 250°C). The regression functions were then used in combination with SAM TMY hourly data to estimate power plant performance. The power plant performance, capital costs, and operating and maintenance (O&M) costs were then used to compute levelized cost of electricity (LCOE) using the DOE Energy Efficiency and Renewable Energy (EERE) approach as implemented in GETEM.

Table 4. Reference and improved scenario solar field configuration and costs

	reference	improved	Reference or comment
Hybrid Plant Configuration			
Solar multiple	4	4	SAM default SM = 2 [104]
Thermal energy storage (hr)	16	16	SAM default TES = 6 hr [104]
Turbine inlet pressure control	Sliding	Sliding	SAM default is fixed turbine inlet pressure control [104]
Condenser type	Air-cooled	Air-cooled	Consistent with SAM default [104]
Geographic location	Daggett, CA	Daggett, CA	SAM TMY solar resource and ambient temperature data used for hourly calculation of plant performance [104]
Hybrid Plant Economic Analysis Parameters			
Site improvements ($/m^2)	20	10	CSP trough roadmap and target values [107]
Solar field ($/m^2)	150	75	SAM default CSP parabolic trough (physical) model solar field cost [104]; SunShot CSP trough target cost [107]
Heat transfer fluid system ($/m^2)	50	50	CSP trough roadmap [107];
Storage ($/kWh$_t$)	25	15	CSP trough roadmap and target values [107]
Plant/project life	25 years	25 years	GeoVision Scenario GETEM input value
Annual rate of GT resource temperature decline	0.5%/yr	0.5%/yr	GeoVision Scenario GETEM input value
Contingency	15%	15%	GeoVision Scenario GETEM input value
Indirect costs	12%	12%	GeoVision Scenario GETEM input value
Discount rate during operation	7%	7%	GeoVision Scenario GETEM input value
Taxes	39.2%	39.2%	GeoVision Scenario GETEM input value

Table 5. CSP Steam Rankine cycle design parameters

Variable	Value	Reference or Comment
Heat Exchangers		
HTF inlet temperature	393.3°C	Appendix B in Turchi [106]
HTF flow rate	5,017,440 kg/hr	Appendix B in Turchi [106]
Evaporator pressure	91.4 bar	Appendix B in Turchi [106]
Evaporator minimum internal temperature approach	5°C	steam mass flow rate varied to achieve design specification
Reheat steam conditions	371°C 25 bar	Appendix B in Turchi [106]
geofluid mass flow rate	500,000 kg/hr	
geofluid heat exchanger minimum internal temperature approach	5°C	cold side heat duty varied to achieve design specification
Steam Turbines		
turbine inlet conditions	371°C 91.4 bar	Appendix B in Turchi [106]
number of stages	2 HP 5 LP	Patnode [110], Padilla [111], Montes, et al. [115]
turbine isentropic efficiencies (all stages)	0.90	adjusted to match SAM simulation gross power output results
HP turbine steam extraction pressures	49.85 bar 25 bar	HP steam extraction pressures set to achieve equal Δh_s w.r.t. steam extraction saturation pressures [116, 117]
LP turbine steam extraction pressures	12.44 bar 5.43 bar 1.99 bar 0.63 bar	LP steam extraction pressures set to achieve equal Δh_s w.r.t. steam extraction saturation pressures [116, 117]
Air-Cooled Condenser		
ambient temperature	42.2°C	Appendix B in Turchi [106]
condensing pressure	0.166 bar	Appendix B in Turchi [106]
hot side ΔT	3°C	Table 16 in Wagner and Gilman [118]
condenser air pressure ratio	1.0028	Table 16 in Wagner and Gilman [118]
fan isentropic efficiency	0.80	Table 16 in Wagner and Gilman [118]
fan mechanical efficiency	0.94	Table 16 in Wagner and Gilman [118]
Feedwater Heaters		
LP steam FW heater configuration	3 closed FW heaters; 1 deaerator	Patnode [110], Padilla [111], Montes, et al. [115]
HP steam FW heater configuration	2 closed FW heaters	Patnode [110], Padilla [111], Montes, et al. [115]
terminal temperature difference	2.8°C	Padilla [111], Drbal, et al. [119]
Boiler Feed Pumps		
pump isentropic efficiencies (all)	0.695	Table 12 in Wagner and Gilman [118]

3.3 Results and Discussion

A stand-alone CSP plant with the default SM and TES capacity located in Daggett, CA (solar resource of 7.6 kWh/m^2/day) is calculated to have a LCOE of $0.133/kWh and $0.093/kWh with the reference and improved scenario solar hardware costs, respectively. The stand-alone CSP plant with the modified SM

and TES capacity in the same location has LCOE values of $0.126/kWh and $0.084/kWh for the reference and improved scenario solar hardware costs, respectively.

The modified configuration (high capacity factor) stand-alone CSP plant LCOE was used as the basis for comparing stand-alone and hybrid CSP plant economics. Since the modified CSP plant configuration has a lower LCOE than the SAM default CSP plant configuration when using the solar field costs specified in this analysis, cases in which the hybrid plant LCOE is lower than the stand-alone plant LCOE will be applicable for both the default and modified stand-alone CSP plant configurations (i.e., if the hybrid geo-solar plant LCOE is lower than the stand-alone CSP plant LCOE, it will be lower regardless of whether the CSP plant configuration resembles the SAM default configuration or the GeoVision modified configuration).

3.3.1 Business-As-Usual Scenario with Undiscovered Hydrothermal Resource

The case study analysis of the Business-As-Usual Scenario with an undiscovered hydrothermal resource utilized the reference solar hardware costs listed in Table 4 and the resource and hybrid plant specifications listed in Table 6.

Table 6. Resource and hybrid plant specifications for case study analysis based on Business-As-Usual Scenario

Plant type	Hybrid geo-solar (solar CSP with GT boiler feedwater heating)					
TMY data	Daggett, CA (7.6 kWh/m^2/day annual average DNI)					
Solar resource	Parabolic trough solar field @ 1,892,453 m^2 (SM=4)					
Geothermal resource	Greenfield hydrothermal @ 138.8 kg/s (2 production wells)					
T (°C)	250	225	200	175	150	125
depth (m)	2,000	2,000	2,000	2,000	2,000	2,000
geofluid pumping parasitic load (kW)	864.6	598.1	463.6	517.2	582.2	658.9
Plant capacity (MWe)	120.1	115.1	111.8	107.8	104.4	101.9
Net efficiency	29.0%	29.0%	29.0%	29.2%	29.5%	30.0%
Capacity factor	81.2%	81.2%	81.6%	81.5%	81.4%	81.1%

A stand-alone CSP plant using the solar resource specified in Table 6 has a capacity of 100 MW and a net efficiency of 32.0% with a calculated capacity factor of 45.7% (SM=2) or 80.1% (SM=4). Stand-alone geothermal binary cycle plants (geothermal flash plants were not considered in this analysis) using the geothermal resource flow rate and temperatures specified in Table 6 have capacity ranging from 4.9 MW (125°C) to 15.4 MW (250°C) with a GETEM specified capacity factor of 95%.

The hybrid plant generally operates with a higher capacity factor than the stand-alone solar plant and with greater output and efficiency than the stand-alone geothermal plant. The hybrid plant efficiency is slightly lower than the stand-alone CSP plant as a result of the lower average heat source temperature (geothermal heat input is supplied at a lower temperature than the solar heat). The hybrid plant efficiency increases with decreasing GT resource T due to the corresponding decrease in GT heat input (a greater fraction of the hybrid plant heat input is from solar heat supplied at temperatures approaching 400°C).

The LCOE of the stand-alone geothermal, stand-alone CSP, and hybrid geo-solar power plants are shown as a function of geothermal resource temperature in Figure 20. The results plotted in Figure 20 are based on the use of a binary power cycle for all stand-alone geothermal plants, independent of resource temperature. While the LCOE for a stand-alone CSP plant is plotted in Figure 20, this value does not change with geothermal resource temperature. The range of geothermal resource temperatures where the

hybrid plant LCOE is lower than the stand-alone GT and stand-alone CSP plant LCOE is designated by green shading.

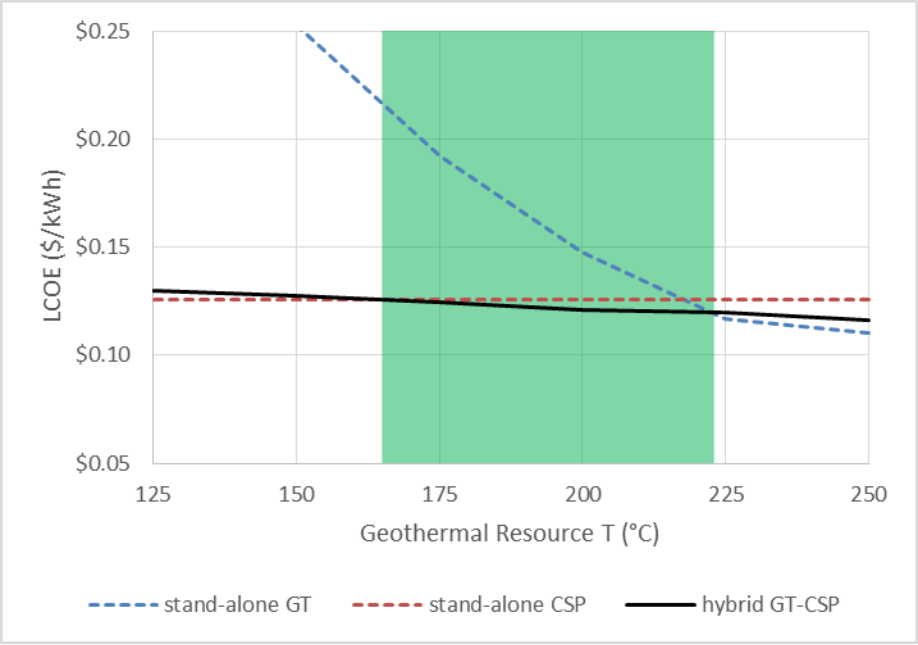

Figure 20. Undiscovered Hydrothermal LCOE for stand-alone binary GT, stand-alone CSP, and hybrid CSP-GT power plants in Business-As-Usual Scenario. The LCOE for the hybrid plant is lower than the LCOE for both stand-alone GT and CSP plants in the range of geothermal resource temperatures designated by the shaded plot area.

3.3.2 Exploration De-Risk Scenario with Deep EGS Resource

The case study analysis of the Exploration De-Risk Scenario with a deep EGS resource utilized the reference solar hardware costs listed in Table 4 and the resource and hybrid plant specifications listed in Table 7.

Table 7. Resource and hybrid plant specifications for case study analysis based on Exploration De-Risk Scenario

Plant type	Hybrid geo-solar (solar CSP with GT boiler feedwater heating)					
TMY data	Daggett, CA (7.6 kWh/m^2/day annual average DNI)					
Solar resource	Parabolic trough solar field @ 1,892,453 m^2 (SM=4)					
Geothermal resource	Greenfield EGS @ 138.8 kg/s (2 production wells)					
T (°C)	250	225	200	175	150	125
depth (m)	6,000	6,000	5,000	5,000	4,000	4,000
geofluid pumping parasitic load (kW)	1.6	1.6	123.4	313.3	625.7	786.6
Plant capacity (MWe)	121.0	115.7	112.2	108.0	104.3	101.8
Net efficiency	29.2%	29.2%	29.1%	29.3%	29.5%	29.9%
Capacity factor	81.3%	81.3%	81.6%	81.5%	81.4%	81.1%

The stand-alone CSP plant performance is unchanged between the BAU and Exploration De-Risk Scenarios with a capacity of 100 MW, a net efficiency of 32.0%, and a calculated capacity factor of

45.7% (SM=2) or 80.1% (SM=4). Stand-alone geothermal binary cycle plants using the geothermal resource flow rate and temperatures specified in Table 7 have capacity ranging from 3.9 MW (125°C) to 16.0 MW (250°C) with a GETEM specified capacity factor of 95%. The discrepancies in hybrid plant capacity between the BAU and Exploration De-Risk Scenarios are due to the differences in geofluid pumping requirements associated with the different resource types utilized in each scenario.

The same general conclusions from the BAU scenario analysis hold for the Exploration De-Risk scenario regarding hybrid plant efficiency and capacity factor relative to the stand-alone GT and CSP plants. Figure 21 presents the LCOE of the stand-alone geothermal, stand-alone CSP, and hybrid geo-solar plants as a function of geothermal resource temperature. As in Figure 20, the range of geothermal resource temperatures where the hybrid plant LCOE is lower than the stand-alone GT plant LCOE and stand-alone CSP plant LCOE is designated by green shading.

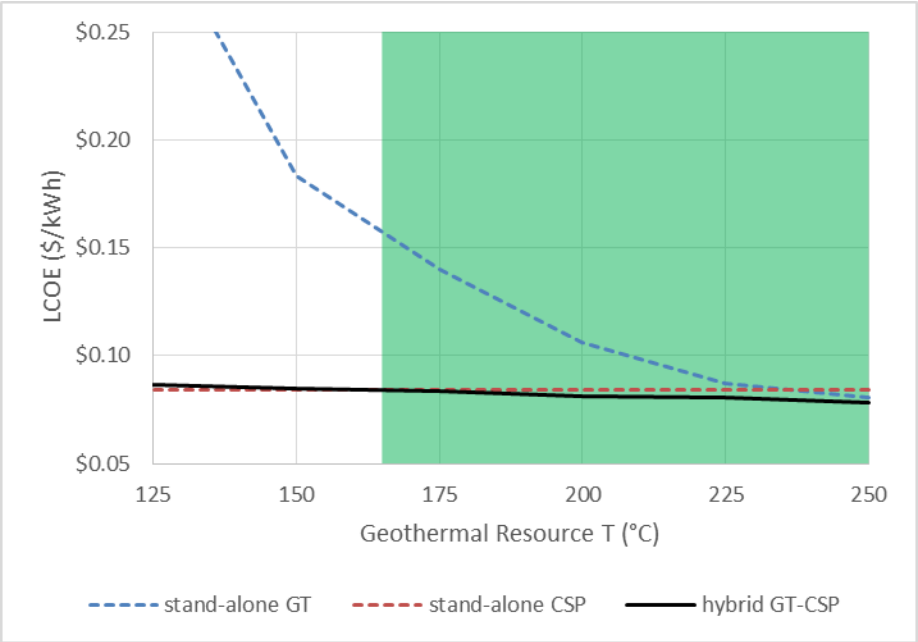

Figure 21. Deep EGS LCOE for stand-alone GT, stand-alone CSP, and hybrid CSP-GT power plants in Exploration De-Risk Scenario. The LCOE for the hybrid plant is lower than the LCOE for both stand-alone GT and CSP plants in the range of geothermal resource temperatures designated by the shaded plot area.

In both scenarios evaluated, the boiler feedwater heating hybrid plant LCOE is lower than both the stand-alone GT LCOE and stand-alone CSP LCOE for a significant range of geothermal resource temperatures. This temperature range generally corresponds to the conditions where stand-alone geothermal plant LCOE and stand-alone CSP plant LCOE are similar, i.e. the hybrid plant outperforms both stand-alone plants in situations where the stand-alone plants are cost-competitive with each other. When one of the stand-alone power plants has a significantly lower LCOE than the other, hybridization does not overcome this cost differential and use of the least-cost stand-alone plant would result in the lowest LCOE.

Another way of viewing this result is that the hybrid plant significantly extends the range of geothermal resource temperatures over which a power plant that utilizes geothermal heat is cost-competitive with stand-alone CSP (e.g., in both cases evaluated a stand-alone CSP plant has lower LCOE than a stand-alone GT plant using a 200°C geothermal resource, but the hybrid plant LCOE is lower than either stand-alone option resulting in the theoretical deployment of a power plant that uses geothermal energy instead of one that does not).

In addition to the results presented in Figure 20 and Figure 21, numerous other geothermal resource temperature and depth combinations, geographic locations with lower average DNI solar resource, as well as the GeoVision Technology Transfer improved scenario were investigated. For nearly all of the alternate conditions evaluated, there was a subset of geothermal resource temperatures where the hybrid plant LCOE was lower than both stand-alone plants. This suggests that in scenarios where stand-alone geothermal and stand-alone CSP LCOE is similar, use of hybrid CSP-GT technology could provide performance and economic benefits.

It is important to note that the geothermal resources considered in this case study analysis were of intermediate size (total production fluid flow rate of approximately 140 kg/s). The geothermal levelized cost of heat (LCOH) would decrease at sites where larger volumes of production fluid are available, which would shift the stand-alone GT and hybrid plant LCOE curves in Figure 20 and Figure 21 downward having the net effect of narrowing the range of geothermal resource temperatures at which the LCOE of the hybrid plant is lower than both of the stand-alone plants.

3.4 Conclusions

The hybrid CSP-GT plant offers several performance advantages relative to stand-alone GT and stand-alone CSP plants. The hybrid CSP-GT plant converts geothermal energy to electricity at a higher efficiency than a stand-alone geothermal plant. Additionally, the hybrid CSP-GT plant operates with a higher capacity factor than a stand-alone CSP plant.

In general, the hybrid CSP-GT plant is able to provide significant decreases in LCOE relative to stand-alone geothermal, especially when considering lower geothermal resource temperatures. However, the LCOE for stand-alone CSP tends to be lower than for the hybrid plant at the lowest geothermal resource temperatures evaluated. The hybrid CSP-GT configuration therefore tends to be the lowest LCOE option for an intermediate range of geothermal resource temperatures, which will vary on a site-by-site basis.

In the cases evaluated, the geothermal resource temperatures for which the hybrid plant lowers LCOE are in the range of approximately 175°C to 225°C, for which there is a significant quantity of geothermal resource availability (these cases considered a location with a solar resource greater than 7 kWh/m^2/day, although unpublished results from this analysis indicates that these general conclusions are also applicable in cases with a solar resource between 5 and 7 kWh/m^2/day). The hybrid plant could therefore be widely applicable, deploying before stand-alone GT and stand-alone CSP at locations (and in scenarios) where the LCOE of the stand-alone plants are comparable such that the hybrid plant could provide the lowest LCOE alternative.

4.0 Geothermal Hybrid Coal-Fired Thermoelectric Power Generation

Highlights

- This analysis evaluated the use of geothermal fluid for boiler feedwater preheating in coal-fired power plants.
- Coal plants were represented using NETL Baseline Case 11 (supercritical pulverized coal).
- ASPEN design cases were created and modeled for 150, 200, and 250 °C geothermal resources.
- Integration of ASPEN results with GETEM allowed comparison of resource utilization under hybrid and standalone geothermal generation cases.
- Using geothermal resources to improve efficiency in a coal-fired power plant can generate significantly more net power at lower levelized costs of electricity (LCOEs), compared to standalone geothermal power generation via flash or ORC.
- Benefits of this hybrid approach are most notable for higher-temperature resources, with power sales converging for stand-alone and hybrid configurations in the 150 °C case.
- Low-productivity resources are unlikely to be attractive for coal plants, which require high, sustained production rates to displace significant heat duty.

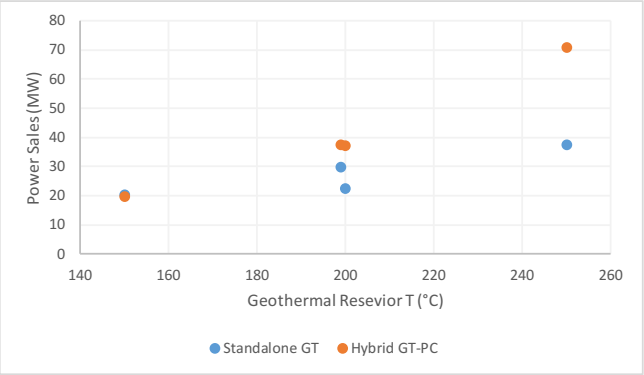

Comparison of power sales from GT-coal hybrid and standalone geothermal generation analyses, by resource temperature (hydrothermal case).

Component costs, power sales, and levelized costs of electricity for the GT-coal hybrid and standalone geothermal generation analyses, by resource temperature. The 199 and 200 °C cases were used in GETEM to evaluate binary and flash configurations, respectively.

Geothermal Reservoir Temperature	150 °C		199 °C		200 °C		250 °C	
Plant Type	Standalone GT	Hybrid GT-PC	Standalone GT	Hybrid GT-PC	Standalone GT	Hybrid GT-PC	Standalone GT	Hybrid GT-PC
LCOE - EERE Methodology								
LCOE, with Royalties ($/kWh)	0.2548	0.1709	0.1545	0.0885	0.1616	0.0674	0.1008	0.0716
Power Sales (MW)	20.29	19.75	29.70	37.48	22.47	37.28	37.37	70.97
Capital Costs ($/kWh)	0.2033	0.1379	0.1225	0.0706	0.1254	0.0525	0.0766	0.0552
Exploration	0.0518	0.0543	0.0346	0.0282	0.0358	0.0215	0.0211	0.0111
Drilling	0.0694	0.0727	0.0445	0.0362	0.0410	0.0246	0.0239	0.0126
Field Gathering System	0.0060	0.0063	0.0039	0.0032	0.0056	0.0034	0.0035	0.0018
Stimulation	0.0000	0.0000	0.0000	0.0000	0.0000	0.0000	0.0000	0.0000
Power Plant	0.0728	0.0011	0.0373	0.0012	0.0401	0.0013	0.0265	0.0288
Permitting	0.0033	0.0035	0.0022	0.0018	0.0028	0.0017	0.0017	0.0009
Makeup Drilling Costs	0.0000	0.0000	0.0000	0.0000	0.0000	0.0000	0.0000	0.0000
Operating Costs ($/kWh)	0.0516	0.0329	0.0321	0.0179	0.0362	0.0150	0.0242	0.0164
O&M - Labor	0.0065	0.0068	0.0054	0.0044	0.0060	0.0036	0.0048	0.0025
Maintenance - Plant	0.0123	0.0002	0.0063	0.0002	0.0074	0.0002	0.0049	0.0047
Maintenance- Wells/Reservoir	0.0120	0.0126	0.0078	0.0064	0.0095	0.0057	0.0056	0.0029
Maintenance- Gathering System	0.0006	0.0006	0.0004	0.0003	0.0006	0.0004	0.0004	0.0002
Water Makeup Costs	0.0000	0.0000	0.0000	0.0000	0.0000	0.0000	0.0000	0.0000
Production Pump Maintenance	0.0015	0.0016	0.0011	0.0009	0.0013	0.0008	0.0015	0.0008
Taxes & Insurance	0.0125	0.0070	0.0073	0.0036	0.0075	0.0027	0.0047	0.0036
Royalties	0.0062	0.0041	0.0037	0.0021	0.0039	0.0016	0.0024	0.0017

4.1 Overview

Hybridization concepts with geothermal feedwater preheating in conventional steam power plants are evaluated based on power generation performance and LCOE. Both hydrothermal resources and enhanced geothermal systems (EGS) at 150, 200, 250 °C are considered. For each geothermal resource scenario, a boiler feedwater preheating process is configured by modifying a baseline supercritical pulverized coal plant [120]. Geothermal fluid is used to replace extraction steam to preheat the feedwater at different stages of the baseline preheater train based on geofluid temperature. As a result, more steam is available to generate electricity in the coal power plant turbines, which can achieve a higher thermodynamic efficiency than typical organic Rankine cycle or flash steam power plants used in standalone geothermal systems. Thus, a hybrid steam power plant configured with geothermal feedwater preheating can either *produce more power* than the conventional coal plant or *consume less fuel* to produce the same power as the conventional plant. The results from this study show that, in general, the additional power generation from such hybridization is more than power generation from a standalone geothermal power plant at a lower LCOE, except for cases of low-enthalpy geothermal resources.

4.2 Methodology

4.2.1 Approach

A set of greenfield geothermal resource scenarios is selected to match a portion of the baseline coal steam plant's feedwater preheating duty. For simplicity at the stage of this first-cut evaluation, only the geothermal resource temperature is allowed to vary from 150 to 250 °C with 50 °C intervals, while all other characteristics such as geofluid well count and production rate are fixed. Production rate is based on a study presented by Heldebrant (201x), which evaluated a similar concept for the North Valmy plant in Nevada using production rates taken from the Beowawe geothermal field. The key attributes of the geothermal resource scenarios evaluated for the GeoVision study are summarized in Table 8.

Table 8. Geothermal resource scenario key assumptions.

Resource Type	Greenfield Hydrothermal or EGS
Resource Temperature	150, 200, 250 °C
Resource Depth	10,000 ft
Conversion System	Binary or flash (resource type and temperature dependent)
Project Life	30 or 25 years (resource type and temperature dependent)
Production Well Flow Rate	375,000 lb/hr
Number of Production Wells	8
Production Wells Pumping	Yes

This study relies on the Geothermal Electricity Technology Evaluation Model (GETEM), developed by Idaho National Laboratory for the DOE Geothermal Technologies Office, to provide a full geothermal resource scenario. Besides Table 8, all other parameters needed to describe a geothermal power generation project are taken as the GETEM default values.

For each distinct geothermal resource temperature, an Aspen Plus-based process model is developed from a baseline coal plant model to implement a geothermal heat exchanger train to replace, strategically, a section of the convention feedwater heater system. The position of the geothermal heat exchanger is selected based on the best match between the inlet and outlet temperatures of both the feedwater and the geofluid streams. The ASPEN Plus plant model is optimized so that temperature cross is avoided even as the geothermal well head temperature declines over the lifetime of the production wells. Because coal plants are designed to operate at full steam capacity during periods of high demand—though at an efficiency penalty caused by bypassing the feedwater preheating system—this study assumes that the baseline coal power plant has sufficient reserve capacity in steam turbines, condenser, and cooling tower to handle the additional amount of steam made available by the reduction in steam extraction for feedwater preheating due to geothermal integration.

The integration of the hybrid plant Aspen Plus model with the GETEM model was implemented at stream level through the geofluid stream from the production wellhead for each unique resource scenario (see Section 4.2.3 for a full list). Stream properties of the wellhead geofluids are calculated using the GETEM model and used to specify the inlet stream to the geothermal heat exchanger in the hybrid plant Aspen Plus model.

The main output parameters are the net power sales and the LCOE for the geothermal integration. This study assumes that the coal steam plant is already paid for, and thus it is excluded from the geothermal integration LCOE calculation. For the hybrid plant, net power sales is defined as the net increase in power output from the hybrid plant compared to the baseline coal plant, minus the geothermal pumping power demand. The decline in power output due to geothermal degradation is discounted over the plant lifetime in the LCOE calculation. The capital cost of the geothermal heat exchanger is estimated using the Aspen Exchanger Design & Rating tool and Aspen Process Economic Analyzer. All other cost elements are estimated using a modified GETEM model that allows evaluation of both standalone and hybrid geothermal plants.

4.2.2 Reference Case

4.2.2.1 *Standalone geothermal (GETEM)*

Both hydrothermal and EGS geothermal resources are evaluated. For each resource type, three different temperatures are selected: 150, 200, 250 °C, to represent low, medium, and high enthalpy grades, respectively. The conversion system is selected following GETEM default criteria, i.e. air-cooled binary (organic Rankine cycle) plants for below 200 °C and flash steam plants for geothermal resource temperatures of 200 °C and higher. The specific GETEM version used is the 2016 revision, provided by the National Renewable Energy Laboratory for the GeoVision Study [121].

For this study, several minor adjustments were made to the GETEM model:

- To evaluate the impact of the technology used by the standalone geothermal at the 200 °C break where GETEM switches generation technology, additional cases at 199 °C are also included to capture both flash and binary options.
- For the EGS cases, the injectivity parameter is adjusted slightly, depending resource temperature, to avoid GETEM error check related to well hydrostatic pressure.
- Phased addition of wells to replenish declining geothermal production is not considered in this preliminary evaluation. Instead, a simple thermal degradation profile was used to account for productivity decline in LCOE calculations.

4.2.2.2 *Baseline coal steam plant (ASPEN)*

The baseline coal steam plant evaluated in this study is a supercritical pulverized coal power plant, specified by Case 11 in the NETL report *Cost and Performance Baseline for Fossil Energy Plants Volume 1: Bituminous Coal and Natural Gas to Electricity (Revision 2, 2010)* [120]. The plant has 550 MWe nominal net output and uses a single reheat 24.1 MPa/593 °C/593 °C (3,500 psig/ 1,100 °F/1,100 °F) cycle without CO_2 capture. An Aspen Plus model to match the NETL Case 10 (subcritical steam cycle) baseline case was created in prior work at PNNL and modified and validated to match the specifications documented in the NETL Case 11 report.

4.2.3 Hybrid Plant Design Cases

In the baseline coal plant, the condensate pump delivers condensate from the condenser to the deaerator through a series of low-pressure heaters (LP-FWHs). The turbine-driven boiler feedwater pump (BFW) delivers the feedwater from the deaerator tank to the economizer through a series of high-pressure heaters (HP-FWHs). In the NETL Case 11, there are four LP-FWHs and three HP-FWHs. The design strategy for the hybrid plant is to find a lower section of the FWH train with the combined heat duty matching the enthalpy content of the geothermal fluid. The heat duties can be calculated from the NETL Case 11 heat and mass balance data (included here for reference, Figure 22). The calculated FWH duties are listed in Table 9. The enthalpy content of the geothermal fluids can be estimated from the well head temperature and flow rate and an assumed temperature approach at the geothermal FWH. Thus, with a minimum temperature approach of 5 °C and a condensate stream at about 40 °C, the geofluid can be assumed to exit the hybrid plant FWH at 45 °C. With the geothermal resource scenarios considered in this study (Table 8), the enthalpy content of the 150, 200, and 250 °C resources at the 3 million lb/hr total production flow are estimated to 166, 246, and 330 MW, respectively. Comparing the above numbers with the FWH duties in Table 9, the 150 °C geothermal resource scenario is a good match for the combined duties of four LP-FWHs: 159 MW. Similarly, the 200 and 250 °C scenarios can be matched to the combined duties of FWHs 1 to 6 and 1 to 7, respectively. Based on the above analysis, the NETL Case 11 flowsheet is modified for each of the geothermal resource scenarios, with the addition of a geothermal FWH, bypass of the selected original FWHs, and adjustment of extraction steam flow accordingly. For the 200 and 250 °C cases, the original deaerator is also bypassed. Deaeration occurs in the condenser for these cases [122]. The resulting flowsheets are presented in Figure 22 through Figure 25. The hybrid plant Aspen models constructed this way are then manually adjusted by small changes to the remaining extraction steam flows to ensure that no temperature cross occurs in the active FWHs and that the overall flowsheet converges. For each geothermal resource scenario, the hybrid plant model is run a number of times at different geofluid temperatures representing different times during the plant life as the reservoir temperature gradually declines.

Table 9. Heat duties of the coal plant feedwater heaters (NETL Baseline Case 11).

Heat Exchanger	FW Outlet T (°C)	Duty (MW)
Condenser	39.2	
FWH1	60.8	31.4
FWH2	81.3	30.0
FWH3	103.3	32.3
FWH4	147.2	65.2
Deaerator	176.3	73.8
FWH6	215.3	67.4
FWH7	266.4	95.5
FWH8	291.4	68.4

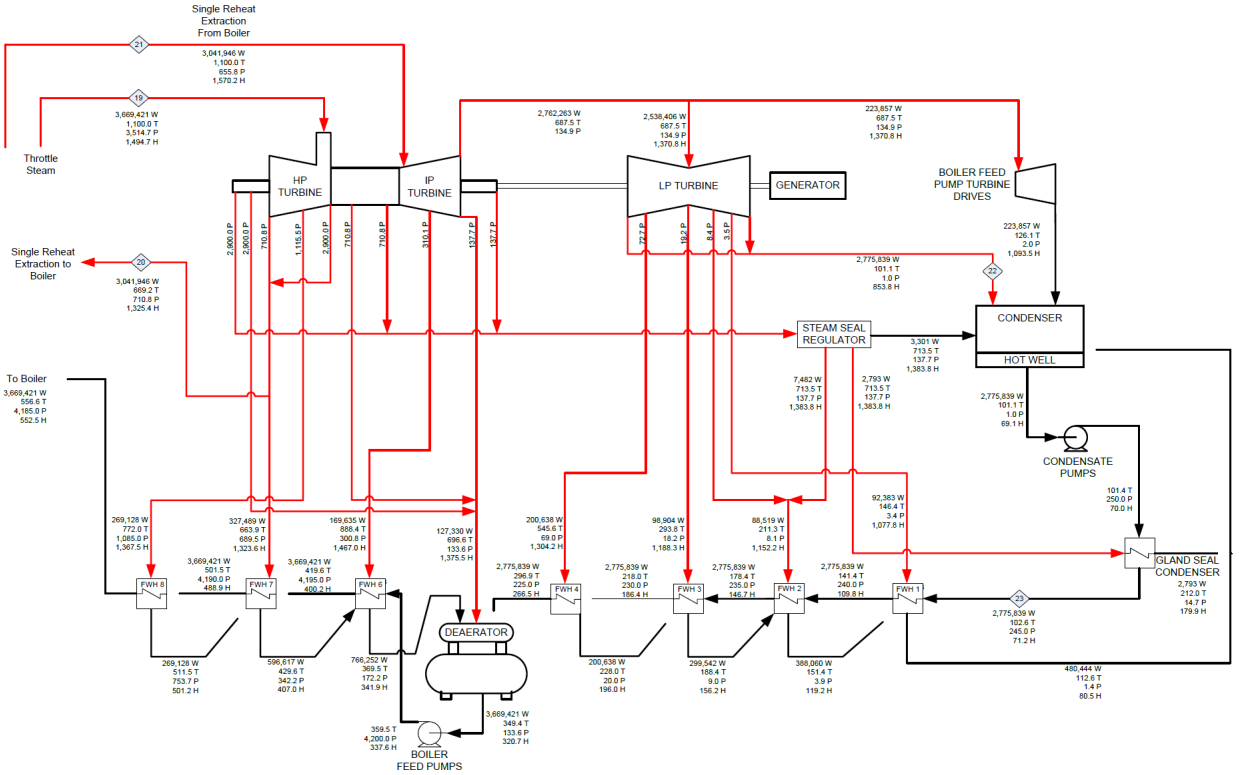

Figure 22. NETL Case 11 heat and mass balance, supercritical steam cycle.

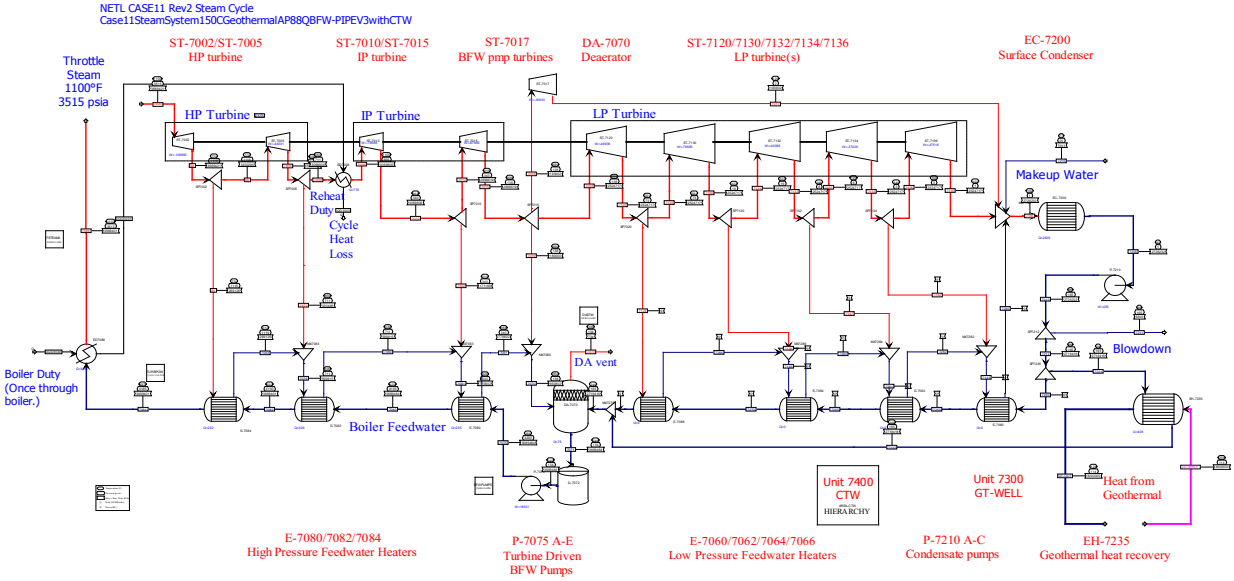

Figure 23. Aspen Plus flow diagram of the hybrid power plant with 150 °C geothermal fluid.

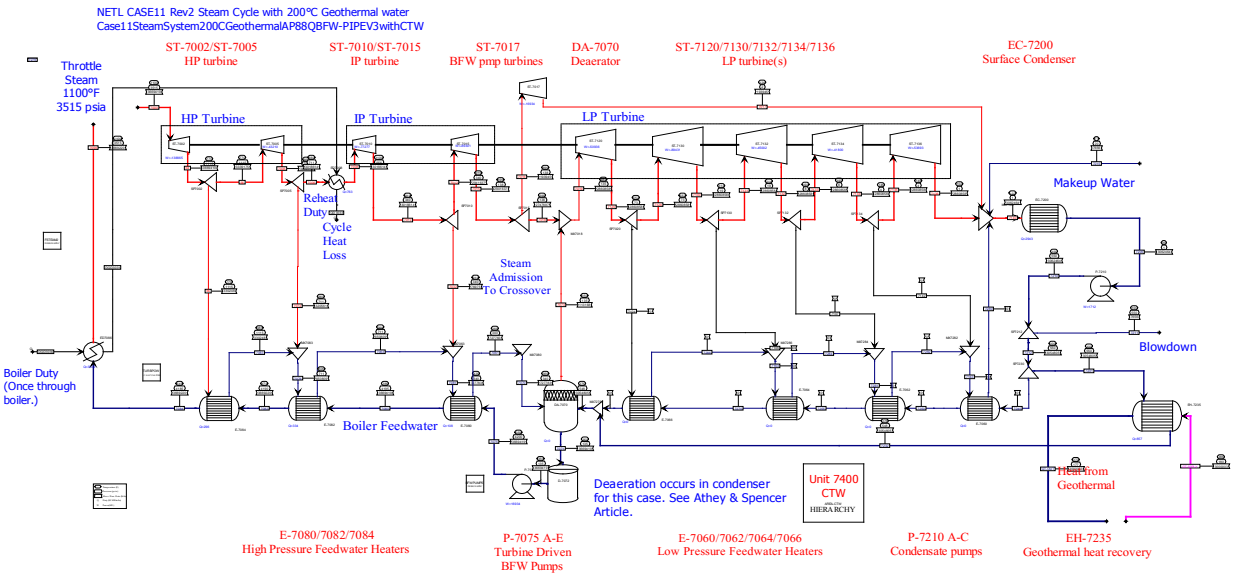

Figure 24. Aspen Plus flow diagram of the hybrid power plant with 200 °C geothermal fluid.

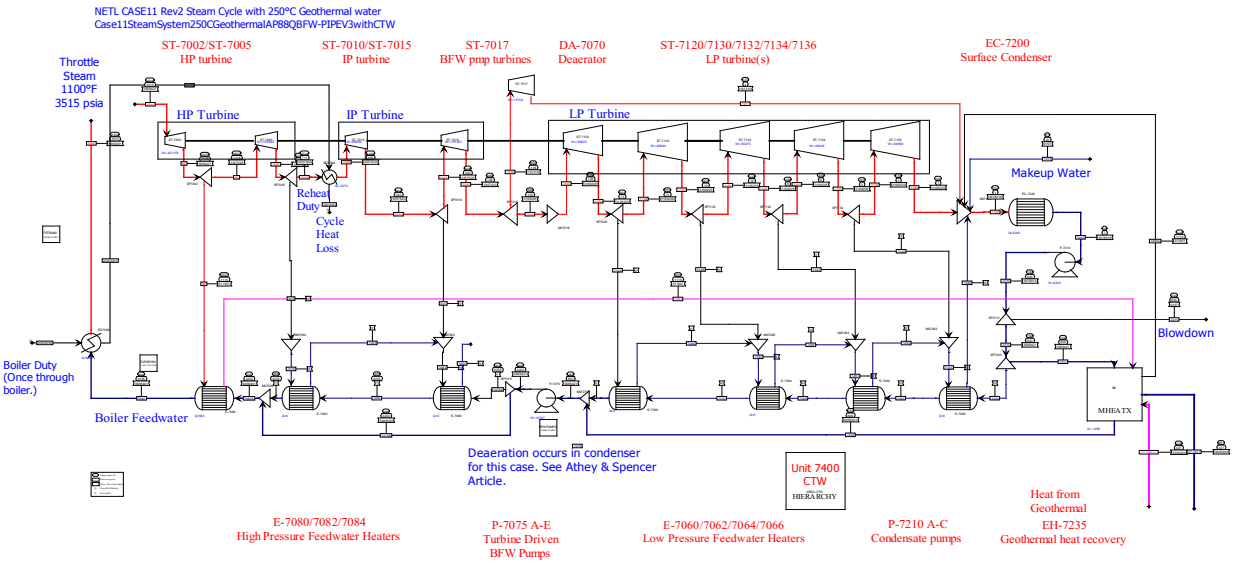

Figure 25. Aspen Plus flow diagram of the hybrid power plant with 250 °C geothermal fluid.

4.2.4 GETEM Integration

The Excel spreadsheet-based GETEM model is used to estimate geofluid pumping power requirements. It is assumed that the pumping power for production and injection is the same for geofluid delivery to both the standalone and the hybrid plants. The net power output of the hybrid plant is obtained from the turbine power generation and auxiliary loads given by the Aspen model. The hybrid plant power sales are then calculated by subtracting the GETEM-generated geo-pumping power from the net power output.

The hybrid plant LCOE calculation is carried out on a separate spreadsheet developed for this study. This spreadsheet contains a modified copy of the GETEM LCOE calculation sheet. Input and output parameters on the GETEM workbook are linked to the hybrid plant spreadsheet. When the scenario input is changed within the GETEM model, the hybrid plant spreadsheet recalculates the LCOE using the

appropriate hybrid plant performance data. This approach avoids direct modifications of the GETEM model itself.

The actual LCOE calculation is based on the present value of the hybrid plant power output and the costs associated with the geothermal integration. The plant output at quarter plant life intervals is obtained directly from the Aspen models. These data allow estimation of the power output at intermediate plant years by interpolation. The GETEM model approximates the decline in plant power output with an exponential decay function, and gives a satisfactory fit to the Aspen hybrid plant output data. Therefore, the GETEM method is adopted and only the power output at plant start and at reservoir life are needed to calculate a capacity degradation factor.

The costs of the geothermal well field are also obtained directly from the GETEM model. The costs associated with the conversion system for the standalone geothermal plant are ignored. The costs of the geothermal FWH are calculated from an equipment procurement cost using the same multipliers and rates as the GETEM model. The procurement cost is obtained by first a detailed sizing the geothermal FWH using Aspen Exchanger Sizing & Rating tool and then exporting the design data to Aspen Process Economy Analyzer to generate an equipment cost. For the 150 °C resource scenario, a low-cost plant-and-frame exchanger is adequate, though at higher geothermal temperatures, shell and tube exchangers are selected to handle the higher pressure load. Stainless steel is selected for all exchangers as a conservative choice. The GETEM model does not give a list of materials for geofluid exchangers, but carbon steel is listed in some cost tables. Without further analysis, stainless steel is deemed a reasonable choice for this study, with the understanding that if low-cost carbon steel is adequate, the LCOE results of this study can be updated accordingly and the current values will provide an upper bound.

4.3 Results

4.3.1 Hybrid Plant Performance

The hybrid plant performance is summarized in Table 10 and Table 11. Geothermal integration with the coal steam plant increases power sales at each geothermal resource temperature, except the lowest (150 °C). In fact, because the low-temperature geothermal fluid displaces so little process steam, the net power sales for the hybrid case decrease relative to the standalone case at 150 °C.

Table 10. Hybrid plant performance using hydrothermal resources.

GT Reservoir Temperature	150 °C	199 °C	200 °C	250 °C
GT Standalone Plant				
Power Plant Type	Binary	Binary	Flash	Flash
Power Sales (MW)	20.29	29.70	22.47	33.31
Net Power (MW)	20.83	30.11	23.69	35.30
GT Pump Power (MW)	0.54	0.41	1.22	2.00
Brine Effectiveness (W-hr/lb)	6.76	9.90	7.49	11.10
GT Integration				
Power Sales (MW)	19.75	37.48	37.28	70.97
Net Power (MW)	20.29	37.89	38.50	72.96
Brine Effectiveness (W-hr/lb)	6.58	12.49	12.43	23.66
Power Sales at Plant Life (MW)	11.07	22.27	22.34	46.29
Power Sales Boost	-3%	26%	66%	113%

Table 11. Hybrid plant performance using EGS resources.

GT Reservoir Temperature	150 °C	199 °C	200 °C	250 °C
GT Standalone Plant				
Power Plant Type	Binary	Binary	Flash	Flash
Power Sales (MW)	8.51	19.71	8.19	22.54
Net Power (MW)	22.45	33.32	23.72	39.42
GT Pump Power (MW)	13.94	13.61	15.53	16.88
Brine Effectiveness (W-hr/lb)	2.84	6.57	2.73	7.51
GT Integration				
Power Sales (MW)	6.37	24.31	23.07	56.15
Net Power (MW)	20.30	37.92	38.60	73.03
Brine Effectiveness (W-hr/lb)	2.12	8.10	7.69	18.72
Power Sales at Plant Life (MW)	0.74	12.27	14.71	35.18
Power Sales Boost	-25%	23%	182%	149%

Although a detailed second-law analysis is beyond the scope of the current study, it is useful to compare the plant power output to the exergy content in the geofluids, which puts a limit on the maximum amount of work that can be extracted. The hydrothermal resource cases (Figure 27) are selected as an example because the exergy content of the reservoir fluid is more simply defined than that of a body of hot, dry rock. Because electrical energy is essentially pure exergy, the hybrid plant *is* clearly more efficient in transferring the exergy content of geofluids into electricity. This is possible because the coal power plant operates at a greater efficiency than the binary and flash steam plants due to its higher working fluid temperature. The displacement of extraction steam with geothermal heat for feedwater heating makes more steam available for generation in the coal plant's turbines, at temperatures much higher than those possible in standalone geothermal power plants.

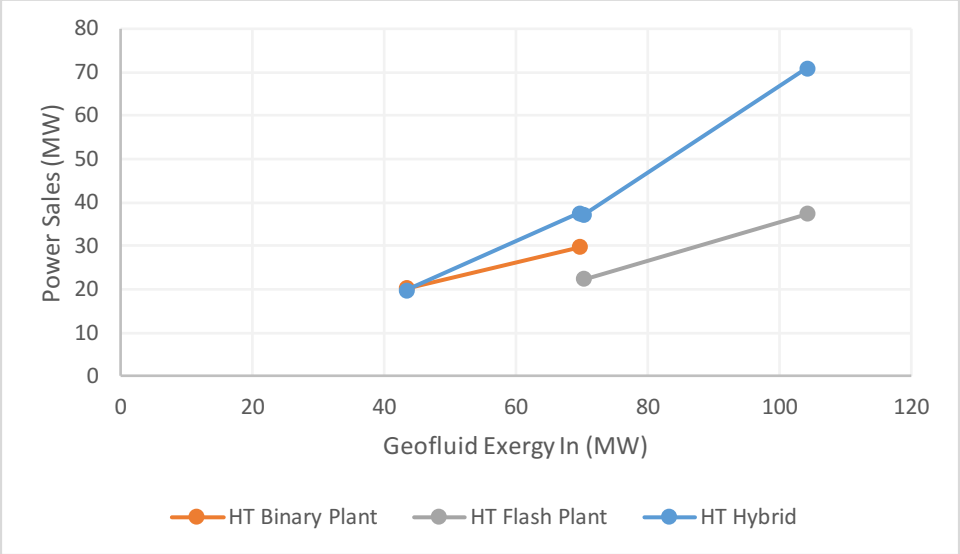

Figure 26. Efficiency comparison of standalone and hybrid plant with hydrothermal (HT) resources.

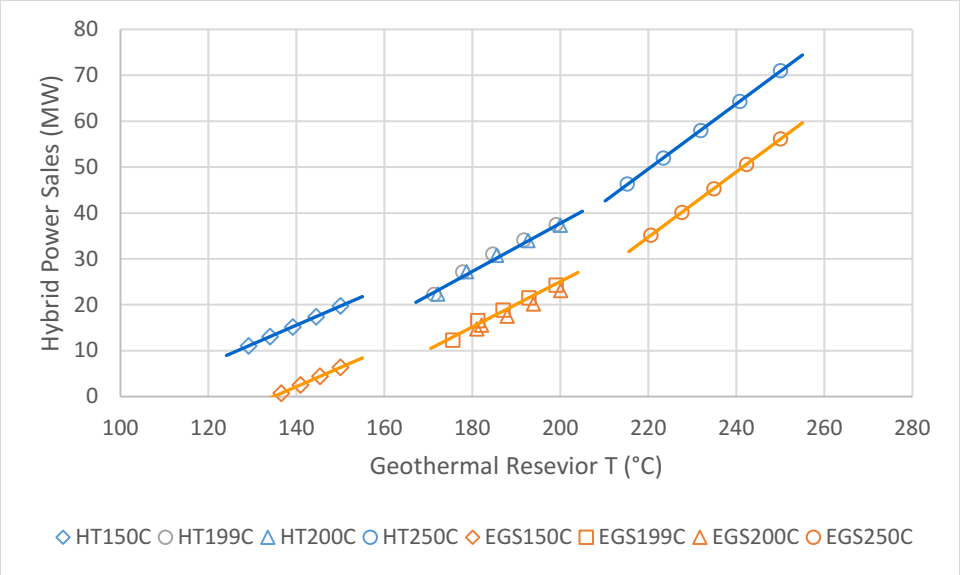

Figure 27. Effects of thermal degradation on hybrid plant performance for hydrothermal (HT) and engineered geothermal (EGS) resources, at each resource temperature evaluated.

It is interesting to compare the effects of reservoir thermal degradation on power sales to the effects of initial reservoir temperature. Plots of these effects are presented in Figure 27, which includes both hydrothermal and EGS resource scenarios. In terms of power sales, hydrothermal hybrid plants clearly outperform the EGS hybrid plants by a relatively consistent margin, reflecting the increased pumping power required for production from EGS fields.

4.3.2 Levelized Costs of Electricity

LCOEs for each resource temperature case, as well as the capital and operating cost components upon which they are based, are shown in Table 12 and Table 13. Note that, because all costs are denominated in dollars per kilowatt-hour, the higher power sales associated with nearly all of the hybrid configurations result in an amortization of capital and operating costs over more kilowatt-hours, resulting in a lower cost per-kilowatt-hour for geothermal resource acquisition, even though each case uses the same flow rate. Beyond the higher net power sales, the hybrid configurations include savings on the power plant capital and maintenance costs, because the project significantly leverages existing capital and economies of scale for other costs. Thus, even for the 150 °C case, where the standalone configuration outperforms the hybrid on net power sales (20.29 vs. 19.75 MW), the hybrid outperforms on LCOE ($0.17 vs $0.25/kWh). LCOEs improve as a function of increasing temperature, though at uneven rates. At 250 °C, a higher-cost shell-and-tube heat exchanger is required for the hybrid system, resulting in an increase in LCOE relative to the hybrid case at 200 °C.

Table 12. LCOE of hybrid plant with hydrothermal resources.

Geothermal Reservoir Temperature	150 °C		199 °C		200 °C		250 °C	
Plant Type	Standalone GT	Hybrid GT-PC	Standalone GT	Hybrid GT-PC	Standalone GT	Hybrid GT-PC	Standalone GT	Hybrid GT-PC
LCOE - EERE Methodology								
LCOE, with Royalties ($/kWh)	0.2548	0.1709	0.1545	0.0885	0.1616	0.0674	0.1008	0.0716
Power Sales (MW)	20.29	19.75	29.70	37.48	22.47	37.28	37.37	70.97
Capital Costs ($/kWh)	0.2033	0.1379	0.1225	0.0706	0.1254	0.0525	0.0766	0.0552
Exploration	0.0518	0.0543	0.0346	0.0282	0.0358	0.0215	0.0211	0.0111
Drilling	0.0694	0.0727	0.0445	0.0362	0.0410	0.0246	0.0239	0.0126
Field Gathering System	0.0060	0.0063	0.0039	0.0032	0.0056	0.0034	0.0035	0.0018
Stimulation	0.0000	0.0000	0.0000	0.0000	0.0000	0.0000	0.0000	0.0000
Power Plant	0.0728	0.0011	0.0373	0.0012	0.0401	0.0013	0.0265	0.0288
Permitting	0.0033	0.0035	0.0022	0.0018	0.0028	0.0017	0.0017	0.0009
Makeup Drilling Costs	0.0000	0.0000	0.0000	0.0000	0.0000	0.0000	0.0000	0.0000
Operating Costs ($/kWh)	0.0516	0.0329	0.0321	0.0179	0.0362	0.0150	0.0242	0.0164
O&M - Labor	0.0065	0.0068	0.0054	0.0044	0.0060	0.0036	0.0048	0.0025
Maintenance - Plant	0.0123	0.0002	0.0063	0.0002	0.0074	0.0002	0.0049	0.0047
Maintenance- Wells/Reservoir	0.0120	0.0126	0.0078	0.0064	0.0095	0.0057	0.0056	0.0029
Maintenance- Gathering System	0.0006	0.0006	0.0004	0.0003	0.0006	0.0004	0.0004	0.0002
Water Makeup Costs	0.0000	0.0000	0.0000	0.0000	0.0000	0.0000	0.0000	0.0000
Production Pump Maintenance	0.0015	0.0016	0.0011	0.0009	0.0013	0.0008	0.0015	0.0008
Taxes & Insurance	0.0125	0.0070	0.0073	0.0036	0.0075	0.0027	0.0047	0.0036
Royalties	0.0062	0.0041	0.0037	0.0021	0.0039	0.0016	0.0024	0.0017

Table 13. LCOE of hybrid plant with EGS resources.

Geothermal Reservoir Temperature	150 °C		199 °C		200 °C		250 °C	
Plant Type	Standalone GT	Hybrid GT-PC	Standalone GT	Hybrid GT-PC	Standalone GT	Hybrid GT-PC	Standalone GT	Hybrid GT-PC
LCOE - EERE Methodology								
LCOE, with Royalties ($/kWh)	1.3414	1.7525	0.4630	0.2747	0.9765	0.2524	0.2996	0.1384
Power Sales (MW)	8.51	6.37	19.71	24.31	8.19	23.07	22.54	56.15
Capital Costs ($/kWh)	1.1408	1.5196	0.3845	0.2320	0.8019	0.2130	0.2401	0.1112
Exploration	0.6553	1.1913	0.2249	0.1811	0.4752	0.1349	0.1476	0.0558
Drilling	0.1154	0.2098	0.0396	0.0319	0.0810	0.0230	0.0252	0.0095
Field Gathering System	0.0345	0.0626	0.0117	0.0094	0.0271	0.0077	0.0088	0.0033
Stimulation	0.0176	0.0320	0.0060	0.0049	0.0164	0.0047	0.0051	0.0019
Power Plant	0.3086	0.0066	0.0991	0.0021	0.1456	0.0022	0.0506	0.0395
Permitting	0.0095	0.0173	0.0033	0.0026	0.0090	0.0026	0.0028	0.0011
Makeup Drilling Costs	0.0000	0.0000	0.0000	0.0000	0.0476	0.0380	0.0000	0.0000
Operating Costs ($/kWh)	0.2006	0.2328	0.0785	0.0427	0.1746	0.0394	0.0595	0.0273
O&M - Labor	0.0192	0.0350	0.0095	0.0076	0.0206	0.0058	0.0086	0.0033
Maintenance - Plant	0.0431	0.0009	0.0157	0.0003	0.0251	0.0003	0.0087	0.0060
Maintenance- Wells/Reservoir	0.0310	0.0563	0.0121	0.0097	0.0325	0.0092	0.0101	0.0038
Maintenance- Gathering System	0.0019	0.0034	0.0007	0.0005	0.0022	0.0006	0.0007	0.0003
Water Makeup Costs	0.0029	0.0053	0.0011	0.0009	0.0125	0.0036	0.0044	0.0017
Production Pump Maintenance	0.0291	0.0528	0.0118	0.0095	0.0281	0.0080	0.0099	0.0037
Taxes & Insurance	0.0448	0.0444	0.0169	0.0077	0.0312	0.0058	0.0101	0.0052
Royalties	0.0286	0.0348	0.0107	0.0064	0.0223	0.0060	0.0070	0.0033

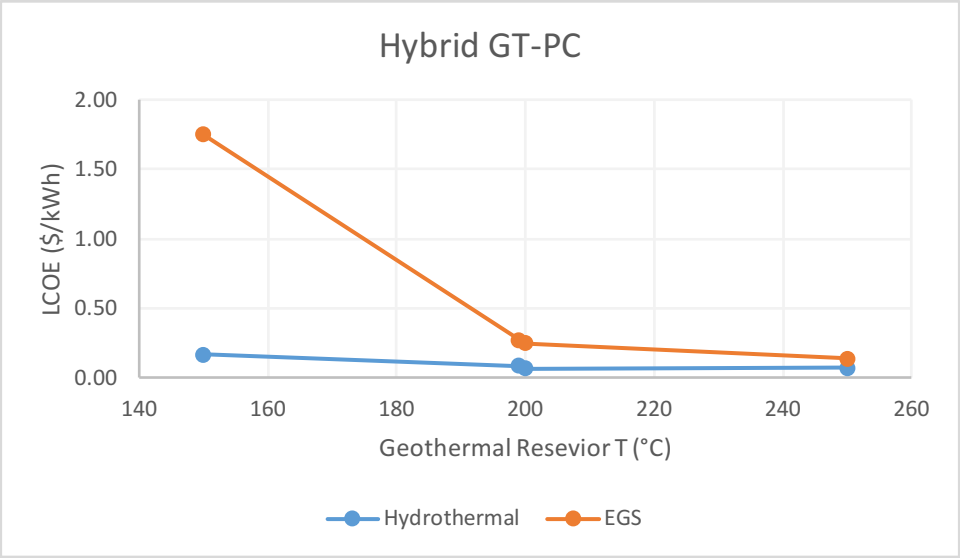

Figure 28. LCOE comparison of hybrid plants with hydrothermal and EGS resources.

4.3.3 Hybrid Plant vs. Standalone Comparison

In addition to understanding the relative power sales and costs of electricity associated with the GT-coal hybrid for each resource class and temperature, it is important to evaluate these against the use of each case study resource for baseload power generation via standalone (non-hybrid) geothermal technologies. Figure 29 and Figure 30 show the net power production for hydrothermal and EGS resources, respectively, with GT-coal hybrid configurations shown in orange and standalone geothermal (binary at 150 and 199 °C, and flash at 200 and 250 °C) in blue. As noted earlier, the net power generated from the 150 °C resource is higher for the standalone plants, and more noticeably so for the EGS resource. For the higher resource temperatures, use of geothermal fluids for boiler feedwater preheating in the coal plant results in higher net power sales than production via standalone technologies.

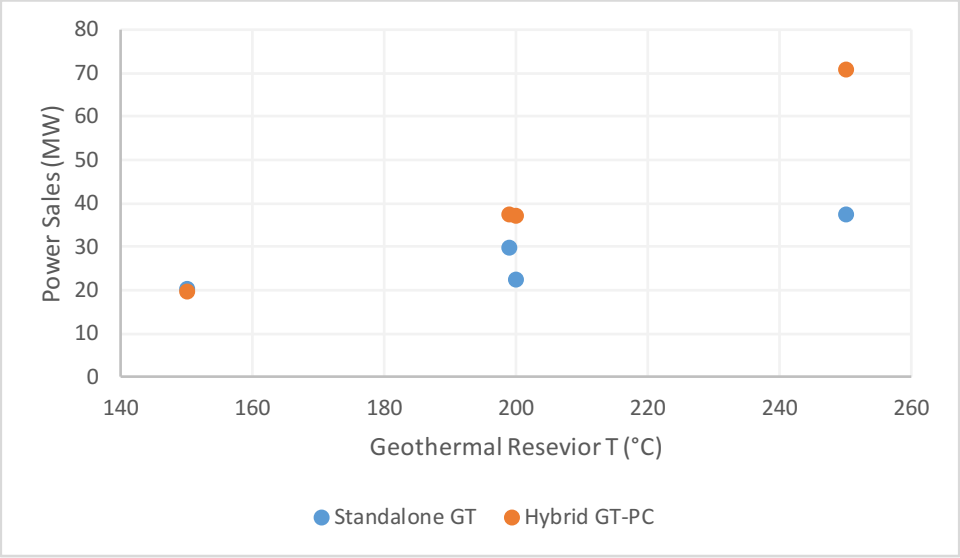

Figure 29. Power sales comparison of standalone and hybrid plant with hydrothermal resources.

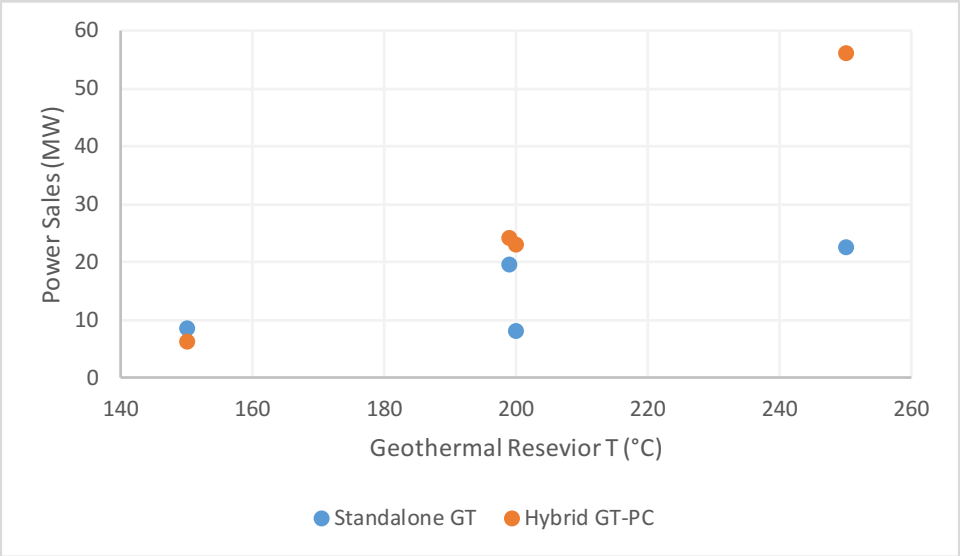

Figure 30. Power sales comparison of standalone and hybrid plant with EGS resources.

One key benefit of using GETEM for the LCOE analysis is that it also enables a common-basis comparison of the standalone and hybrid configurations. Figure 31 and Figure 32 show the LCOEs for hydrothermal and EGS resources, respectively; GT-coal hybrid configurations are shown in orange and standalone geothermal (binary at 150 and 199 °C, and flash at 200 and 250 °C) in blue. Unsurprisingly, LCOEs trend downward for each configuration as resource temperature rises. For both hydrothermal and EGS resources, the gap between hybrid and standalone LCOEs narrows between 200 and 250 °C, but the GT-coal approach remains the lower-cost generation option for each given resource.

Note that, even at 150 °C, where standalone technologies result in more net power generation, the levelized costs for the hybrid configuration are still significantly lower, though only for the hydrothermal resource. Here, the 150 °C EGS case remains the exception, for reasons similar to those noted in the net power discussion: The high cost of obtaining relatively little heat energy for the 150 °C resource results in a higher LCOE for the hybrid configuration ($1.75/kWh) compared to the standalone ($1.34/kWh).

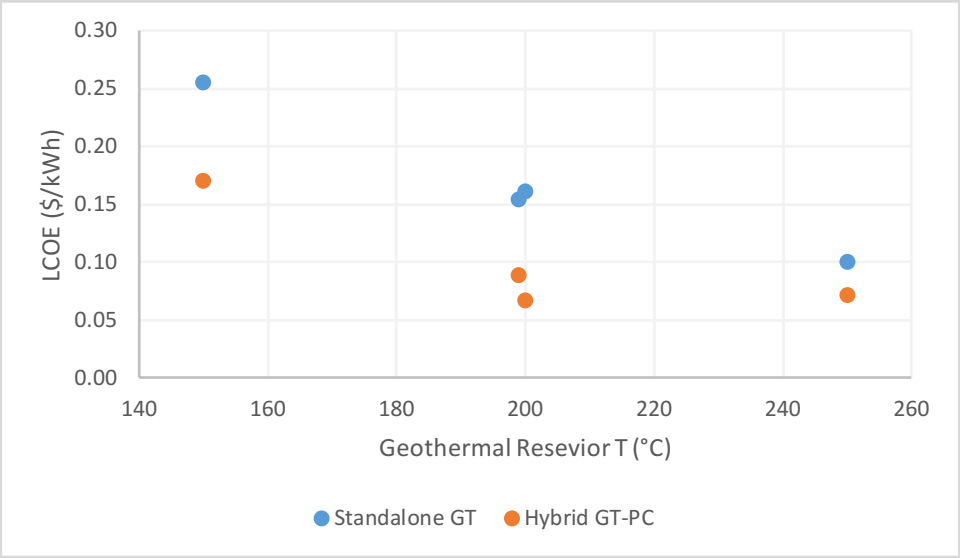

Figure 31. LCOE comparison of standalone and hybrid plant with hydrothermal resources.

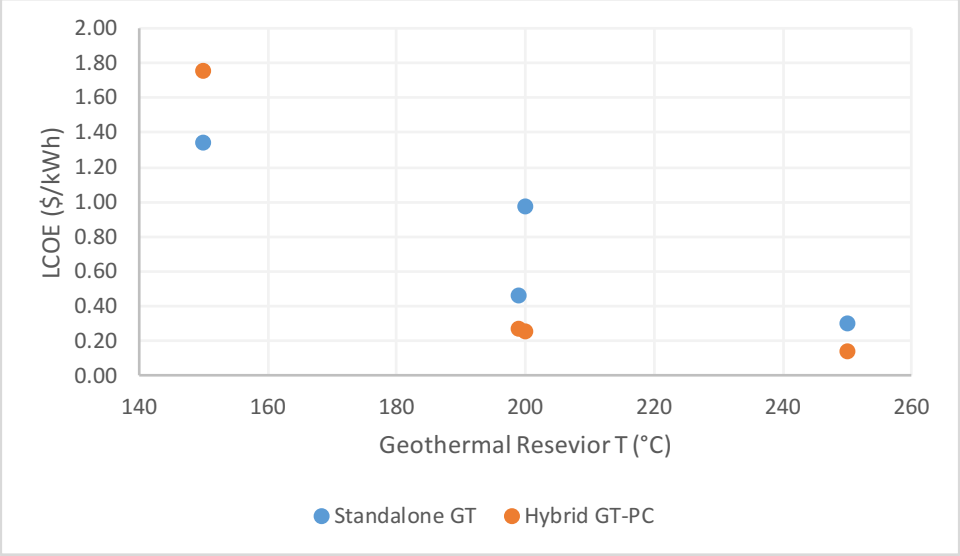

Figure 32. LCOE comparison of standalone and hybrid plant with EGS resources.

4.4 Discussion

Site-specific conditions and individual facility designs vary within industry, and may impact the applicability of this approach for a number of reasons: The power plant must have enough flow capability in the steam turbine, a large enough condenser and cooling system, and a large enough generator to utilize the geothermal heat input. In general though, power plants are designed to operate without one or more of the top (higher temperature) feedwater heaters in operation for maintenance or to produce extra power [123]. For this reason, it's likely that the assumptions that underpin this analysis—specifically regarding the feasibility of using as-built coal-fired power plants without significant retrofit of existing units to handle geothermal temperatures and flow rates—reflect a reasonable application of the hybrid approach evaluated. Table 14 provides the simulated flows, duties, and power production for the benchmark NETL Case 11 operation with and without the top three feedwater heaters, compared to geothermal augmentation. As shown in the table, with the exception of condenser duties for the 200 and 250 °C

geothermal temperatures, the flows, duties, and power production are less than those simulated for the nominal 550 MW power plant operating without the top three feedwater heaters operating.

Table 14. Simulated flows, duties, and power production for NETL benchmark Case 11, without the top three feedwater heaters, as designed, and with geothermal resources at the three temperatures evaluated.

Extraction flows for feedwater heaters, Duties & Net Power (Units: flows lb/hr; Duty MMBtu/hr; Power kW)					
Case	No Geothermal	No Geothermal	150°C Geothermal	200°C Geothermal	250°C Geothermal
Extraction lb/hr	Top 3 Htrs Out	All heaters Used	Bottom 4 Htrs Out	Bottom 4 Htrs Out	All But Htr 8 Out
HTR8		266,033	266,033	327,600	307,700
HTR7		326,725	326,725	317,990	
HTR6		169,216	169,216	76,357	
Deaerator	174,645	133,697	174,645		
HTR4	254,195	198,648			
HTR3	121,882	95,248			
HTR2	122,857	96,010			
HTR1	116,296	90,882			
Total Extraction	789,875	1,376,459	936,619	721,947	307,700
Steam Production	3,669,421	3,669,241	3,669,421	3,640,000	3,620,000
Reheater Flow	3,669,419	3,041,946	3,076,630	2,994,410	3,312,300
Condenser Duty	2,787	2,221	2,663	2,939	3,201
ReheaterDuty	928	744	778	757	837
Boiler Duty	4,242	3,457	3,467	3,481	3,400
Geothermal Duty	0	0	540	877	1,438
Net Power	656,888	550,541	574,568	595,828	645,621

The hybrid use of geothermal fluids in a supercritical coal-fired power plant, under the design specifications and resource assumptions evaluated in this study, appears to yield more net power than standalone geothermal generation at resource temperatures exceeding 175 or 180 °C. And, at all resource temperatures, lower LCOEs are associated with the GT-coal hybrid than standalone geothermal generation. This is largely a function of the higher efficiency of the displaced steam in the coal plant which, when used to generate power in the turbine rather than to preheat water for the boiler, results in more generation relative to using the geothermal fluid for direct power production via standalone geothermal configurations.

While this study examined the integration of geothermal resources at existing coal-fired power plants by holding fuel use constant to simplify estimating LCOE for the additional power produced, it's also possible to use the geothermal resource to maintain the same net output using less fuel. In either case—producing more power with the same fuel or producing the same power with less fuel—the overall emissions and energy intensity of the generation facility are reduced by integrating geothermal as a zero-emissions energy source. This in itself could be monetized separately, as avoided fuel purchase or avoided emissions, offering another possible value stream, depending on the future unit price for that commodity. For now, though, the results of the present study suggest that there may be ways to increase the electricity production possible from a given geothermal resource using today's technologies. Where known geothermal resources are available at or near existing coal plants, or where these can be developed in tandem, this hybrid concept offers an option for expanding geothermal resource utilization in the U.S. and beyond.

5.0 Geothermal Hybrid Gas-Fired Thermoelectric Power Generation

Highlights

- This study examines the use of geothermal energy for feed air precooling in gas-fired power plants.
- Geothermal heat is used in a lithium bromide (LiBr) absorption loop chiller.
- Natural gas plants were represented using NETL Baseline Case B31A (natural gas combined cycle) [124].
- ASPEN design cases were evaluated and modeled for 150 °C geothermal resources.
- Using geothermal resources for feed air precooling in a gas-fired power plant can enable significantly more power generation during summer months, compared to baseline natural gas combined cycle plant.
- Power sales from the GT-NGCC plant are estimated at more than five times the revenues of a standalone binary geothermal plant utilizing the same hydro-thermal resource; equipment costs for the GT-NGCC hybrid are also estimated to be much lower than for the binary GT plant.
- Geothermal resources higher than 150 °C are sufficient for this application, and as a result, this may reflect a significant niche for low-temperature geothermal resource hybrids.

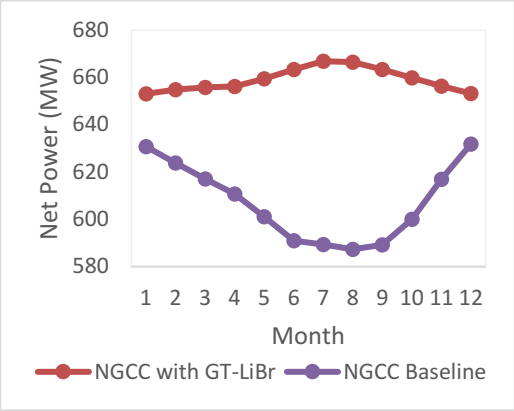

Net power generation, by month, for baseline NGCC (blue) and GT-NGCC hybrid plants.

Incremental power and revenues for GT-NGCC and standalone binary, using average monthly power prices (CA).

2016	CA Average Price $/kWH for All Sectors	Days in Month	Power Sales, kW	Value of Power, $	Power Sales, kW	Value of Power, $
			Incremental power production by the hybrid plant over baseline gas plant:		Alternative production of maximum water from geothermal wells during same period:	
Dec	0.1542	31	22,416	2,571,636	9,466	1,086,028
Nov	0.1503	30	31,056	3,472,997	9,466	1,024,481
Oct	0.1562	31	38,720	4,499,736	9,466	1,100,114
Sep	0.1669	30	45,574	5,659,086	9,466	1,137,555
Aug	0.1715	31	58,386	7,449,790	9,466	1,207,872
Jul	0.1693	31	72,522	9,134,791	9,466	1,192,377
Jun	0.1624	30	80,596	9,738,107	9,466	1,106,884
May	0.1493	31	79,431	8,823,165	9,466	1,051,517
Apr	0.1267	30	74,288	7,002,714	9,466	863,561
Mar	0.1434	31	59,921	6,392,991	9,466	1,009,964
Feb	0.1512	28	39,468	4,439,835	9,466	961,844
Jan	0.1475	31	21,369	2,345,024	9,466	1,038,840
			Total:	**71,529,873**		**12,781,038**

5.1 Overview

A hybridization concept with geothermal-enabled feed air precooling in conventional natural gas power plants are evaluated based on power generation performance. The concept is based on the well-known principle that inlet air cooling increases a gas turbine's power output and efficiency [125]. A combustion turbine's output increases with the air mass flow, but the compressor stage operates with a volume air flow fixed by the design. Cooling the turbine inlet air thus increases air density and raises power output. Lower inlet temperature also allows the compressor stage to operate at higher efficiency, which results in a lower plant heat rate. In warm climate regions, gas power plants with air cooling can avoid a reduction in power output that would otherwise occur when ambient temperature rises. The main economic value of the hybrid air cooling concept is expected to derive from increased power sales in warm months when electricity price is higher due to air conditioning demand.

A LiBr water absorption chiller process was chosen for the turbine air cooling in this study because of its ability to use low-grade heat and the availability of industrial hot-water-driven LiBr units. LiBr water absorption cooling has been commercialized for applications in commercial buildings [126], district, and industrial cooling. Hot-water-driven units in the megawatt size range, suitable for gas turbine air cooling duty, are offered by major industrial cooling manufacturers in the U.S. and world markets.

In LiBr water absorption systems, water evaporation under vacuum provides cooling duty. Water vapor compression is accomplished thermochemically by absorption into a concentrated LiBr solution. The water vapor is boiled off the diluted LiBr solution in the generator with an external heat source. The recovered water vapor is condensed after heat rejection and cycled back to the evaporator. The hybrid plant considered by this study utilizes geothermal hot water as the heat source for the generator. Single-effect LiBr water absorption cycle is the simplest and the least expensive, while double-effect and more complex cycles have higher efficiency at greater capital expense. The current study limits the scope to a single case of 150 °C hydrothermal resources due to budget constraints. With these low-enthalpy geothermal resources, the single-effect LiBr cycle is more favorable because it requires a lower activation temperature than the double-effect cycle. For this reason, hybrid gas plant with a single-effect LiBr absorption cycle was evaluated in this study.

Natural gas plants were represented using NETL Baseline Case B31A (natural gas combined cycle). A hybrid plant with geothermal-fired LiBr absorption for inlet air cooling was modeled using Aspen. Geothermal well field performance and cost were obtained using the GETEM model [127]. The ambient air conditions were simulated using meteorological data for the Geysers field in California. The following sections summarize the model analysis approach and results. Briefly, the model results confirmed that geothermal integration enables additional power output and avoids seasonable reduction in plant output during hot summer months. The additional power output was primarily derived from additional fuel combustion enabled by the air precooling. Direct geothermal contribution to the change in plant heat rate is negligible ($\leq 1\%$).

5.2 Methodology

5.2.1 Approach

The hybrid plant performance was modeled using a combination of Aspen Plus models and the GETEM model. An Aspen Plus baseline NGCC plant was first created to match the specifications of NETL Baseline Case B31A. Next, the model was modified to include an inlet air cooler section between the inlet air filter and the inlet to the turbine compressor stage. The air cooler was a single-effect LiBr water absorption system. The absorption loop was water cooled. The baseline gas plant cooling tower was assumed to be able to provide the additional cooling water utilities. The absorption loop generator was driven with a geothermal hot water stream.

The hybrid plant output was obtained for each month in a full year period using monthly average ambient air temperature and relative humidity (Table 15) based on field meteorological data for Geysers field, California. Ambient pressure was assumed to be at 500 feet above sea level. A greenfield geothermal resource scenario was selected to match the maximum geothermal water demand based on the monthly plant results. The key attributes of these geothermal resource scenarios are summarized in Table 16. This study relies on the GETEM model to provide a full geothermal resource scenario. Besides Table 16, all other parameters needed to describe a geothermal power generation project are taken as the GETEM default values.

The main assumption in the hybrid plant model is that the driving and driven equipment have enough rated capacity to handle the additional power generation enabled by inlet air cooling. The net power output of the hybrid plant was determined from turbine power generation and all parasitic loads. These power values were obtained from the Aspen Plus simulation except for the geofluid pumping power, which was obtained from GETEM model output.

Table 15. Gas Plant ambient air conditions.

Month	Temperature (°F)	Relative Humidity
Jan	47.6	76.0%
Feb	50.4	73.4%
Mar	53.1	69.1%
Apr	56.0	62.8%
May	60.7	59.5%
Jun	65.7	56.4%
Jul	67.8	58.4%
Aug	67.5	58.1%
Sep	66.1	55.6%
Oct	61.2	59.5%
Nov	53.1	70.3%
Dec	47.3	77.4%

Table 16. Geothermal resource scenario key assumptions.

Resource Type	Greenfield Hydrothermal or EGS
Resource Temperature	150 °C
Resource Depth	10,000 ft
Conversion System	Binary (organic Rankine)
Project Life	30 years
Production Well Flow Rate	375,000 lb/hr
Number of Production Wells	3.5
Production Wells Pumping	Yes

5.2.2 Reference Case

5.2.2.1 *Standalone geothermal (GETEM)*

The standalone case was evaluated for a 150 °C hydrothermal resource. The conversion system was selected following GETEM default criteria, i.e., air-cooled binary (organic Rankine cycle) plants for resources below 200 °C. The specific GETEM version used is the 2016 revision provided by the National Renewable Energy Laboratory for the GeoVision Study [121].

Some minor adjustments were made to the GETEM model to accommodate the hybrid approach used in this study. Specifically, the geofluid stream temperature at the inlet to the LiBr absorption loop was

assumed to be 150 °C, the reservoir temperature, and assumed to remain constant through project life. Thermal degradation of the reservoirs was not considered and the well bore temperature loss was ignored in this preliminary evaluation.

5.2.2.2 *Baseline natural gas plant (ASPEN)*

The baseline NGCC plant is chosen as the same specified by the Case B31A in the NETL cost baseline report [124]. The B31A reference plant has 630 MWe net output at a net plant HHV efficiency of 51.5%. The rotor inlet temperature is 1359 °C (2479 °F). Turbine flue enters the heat recovery steam generator (HRSG) at 603 °C (1118 °F) and exits to stack at 117 °C (243 °F). An Aspen Plus model for this baseline case has been created in prior work at PNNL and validated to match the specifications documented in the NETL report.

5.2.3 Hybrid Plant Design Case

The GT-gas hybrid design places the LiBr water absorption cooler after the turbine inlet air filter. A pressure drop of 6-inch-water is specified from the plant air intake to the compressor inlet. The inlet air cooler is configured to reduce the air temperature to 40 °F regardless of the ambient temperature and humidity level. As shown in the block diagram of the hybrid plant in Figure 33, the LiBr absorption section provides the needed cooling duty to the gas turbine inlet air. Details of the gas turbine, HRSG, steam turbine, and cooling tower are shown in Figure 34 to Figure 37. The LiBr absorption cooler is shown in Figure 38. The condenser and absorber in the LiBr absorption process use plant cooling water for heat rejection. In the plant Aspen model, this connection is set up as a utility provided by the cooling tower section. The generator in the LiBr loop is configured with a design spec block to control the geofluid flow rate to achieve a 5 °F approach at the outlets of the geofluid and the strong LiBr solution streams. A separate design spec block adjusts the solution circulation flow rate to match the evaporator duty with cooling demand. When a higher duty is needed for turbine inlet air cooling due to ambient temperature rise, the model increases both the solution circulation flow and the geofluid flow to meet the demand.

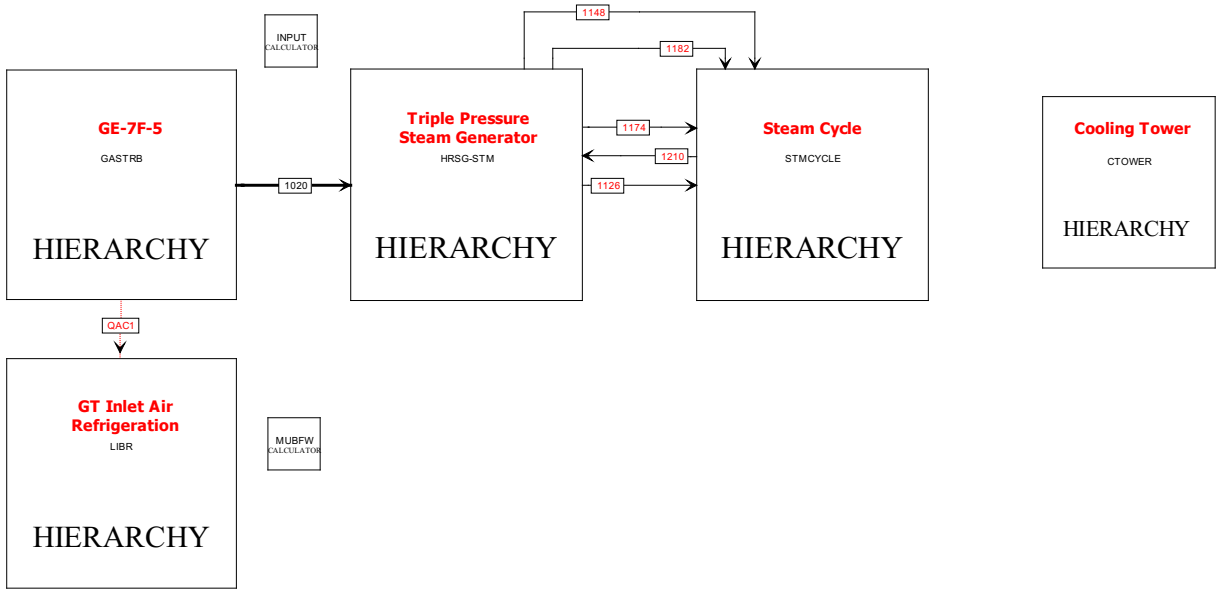

Figure 33. Level-1 block diagram of the hybrid NGCC plant Aspen model.

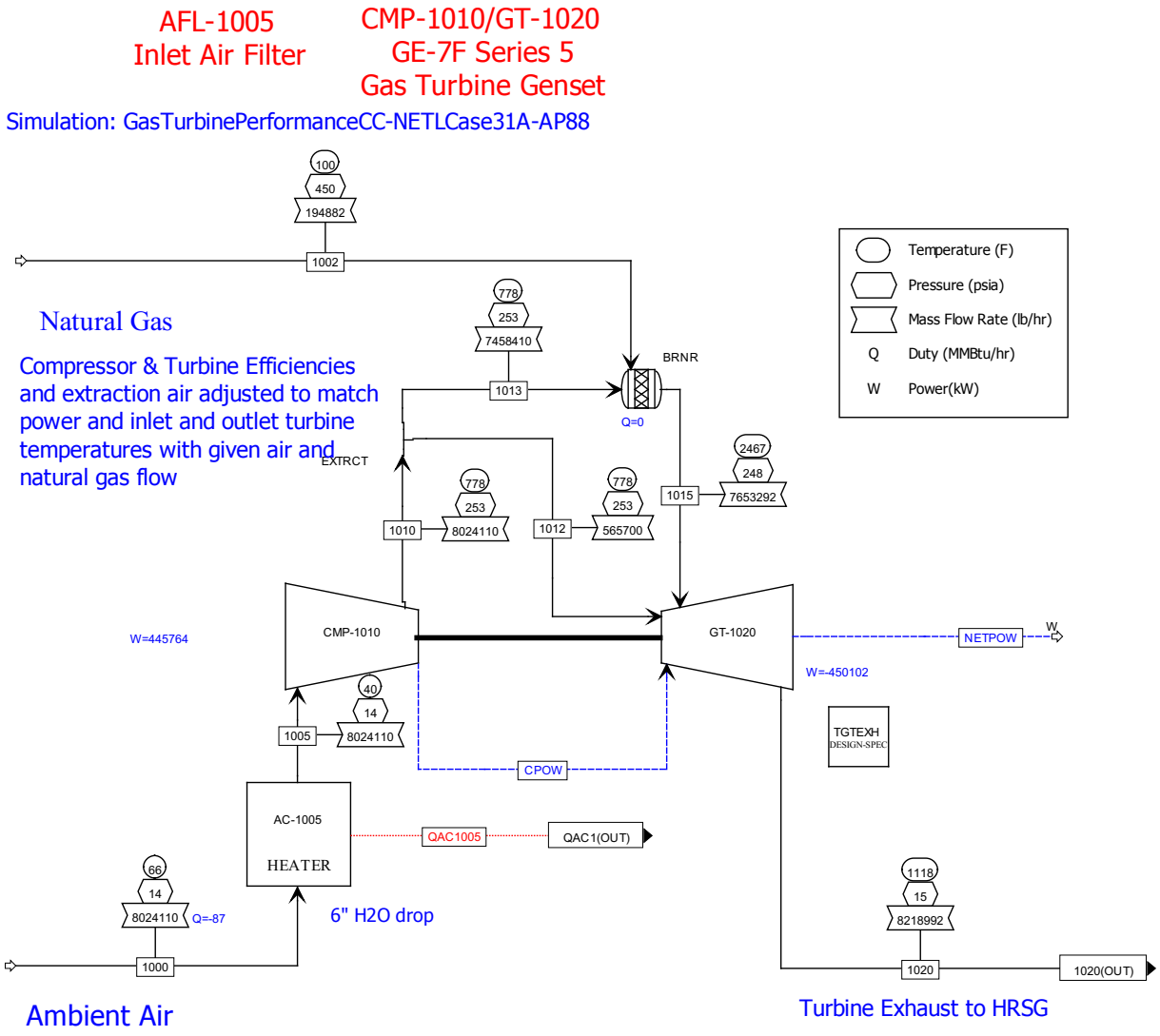

Figure 34. Aspen Plus model of the gas turbine section.

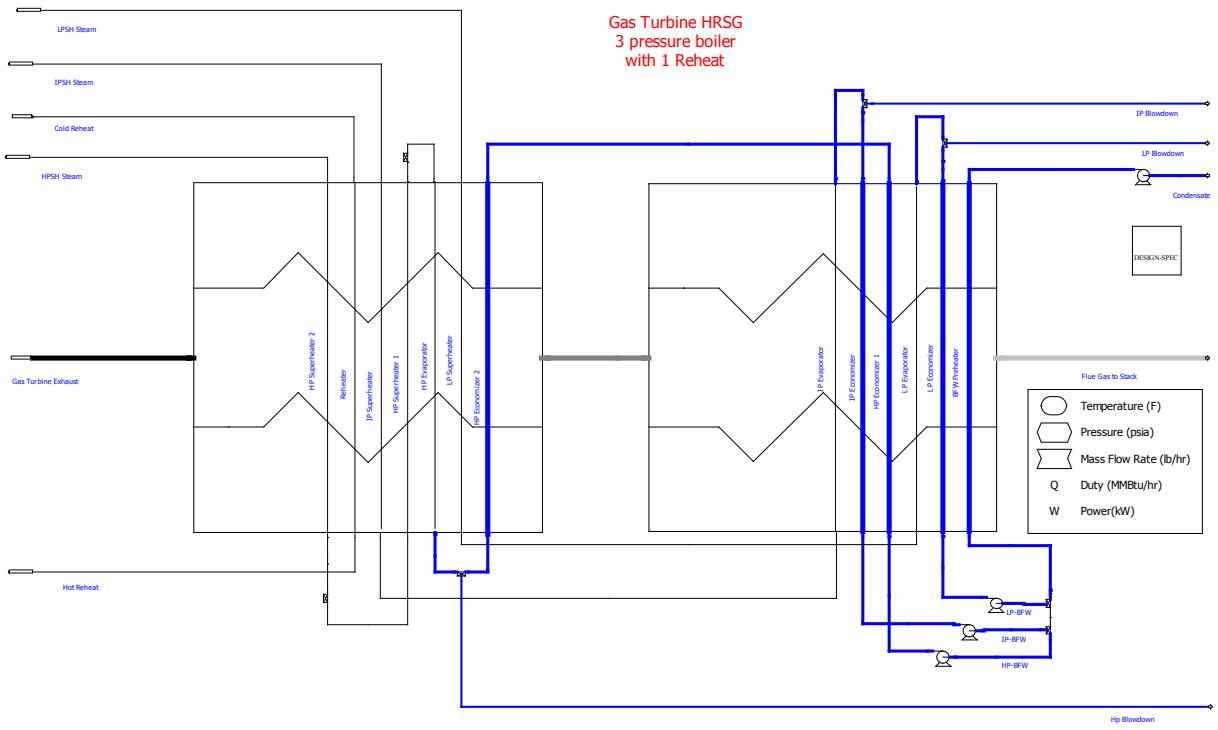

Figure 35. Aspen Plus model of the heat recovery steam generator section.

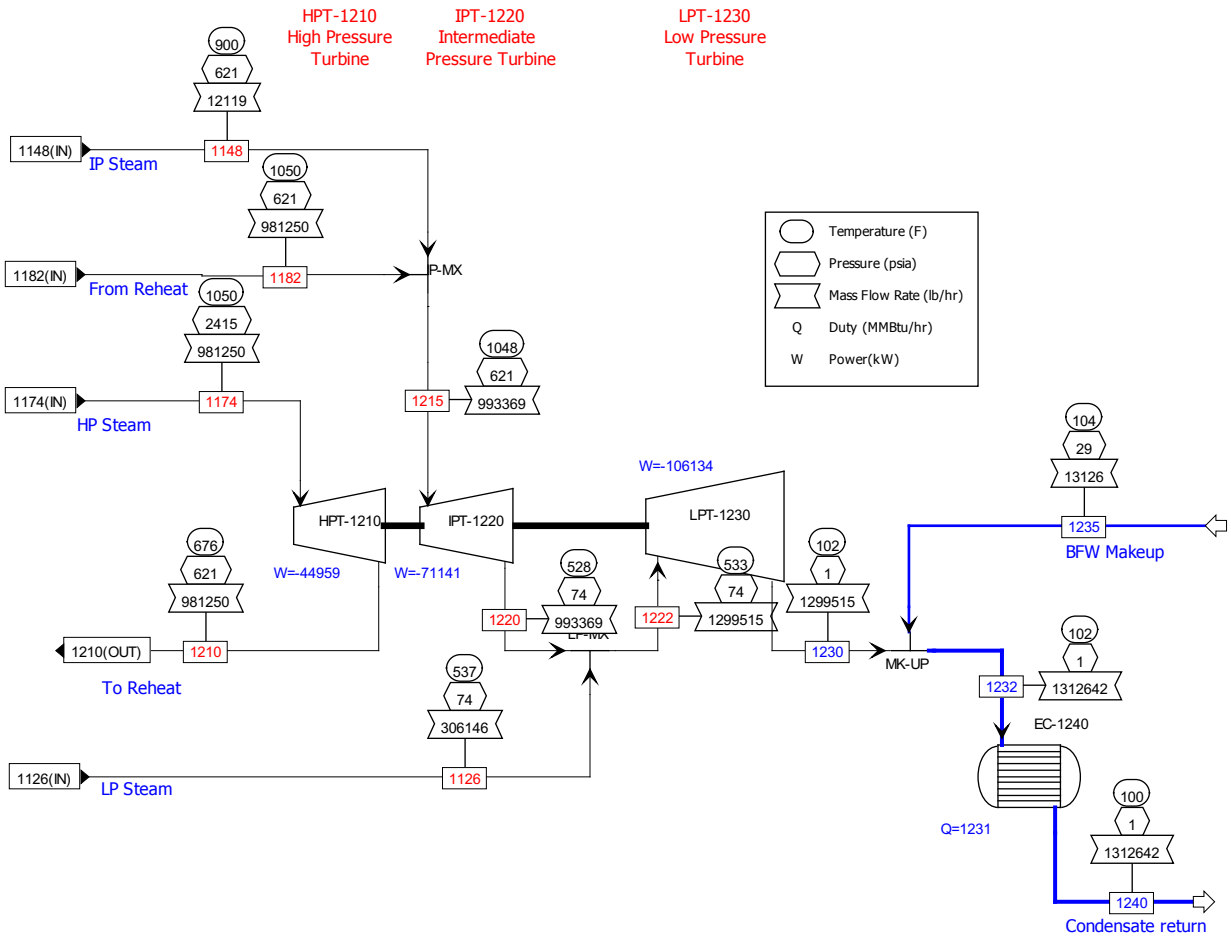

Figure 36. Aspen Plus model of the steam turbine section.

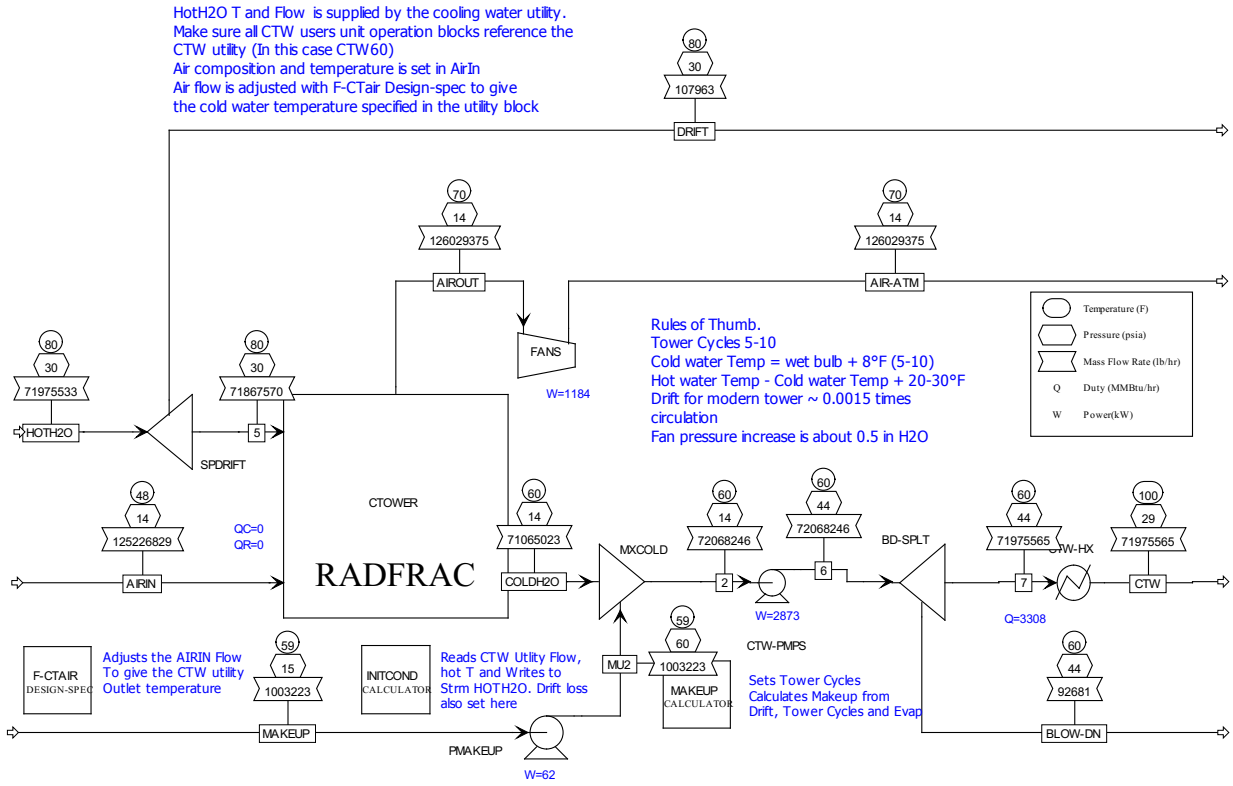

Figure 37. Aspen Plus model of the cooling tower section.

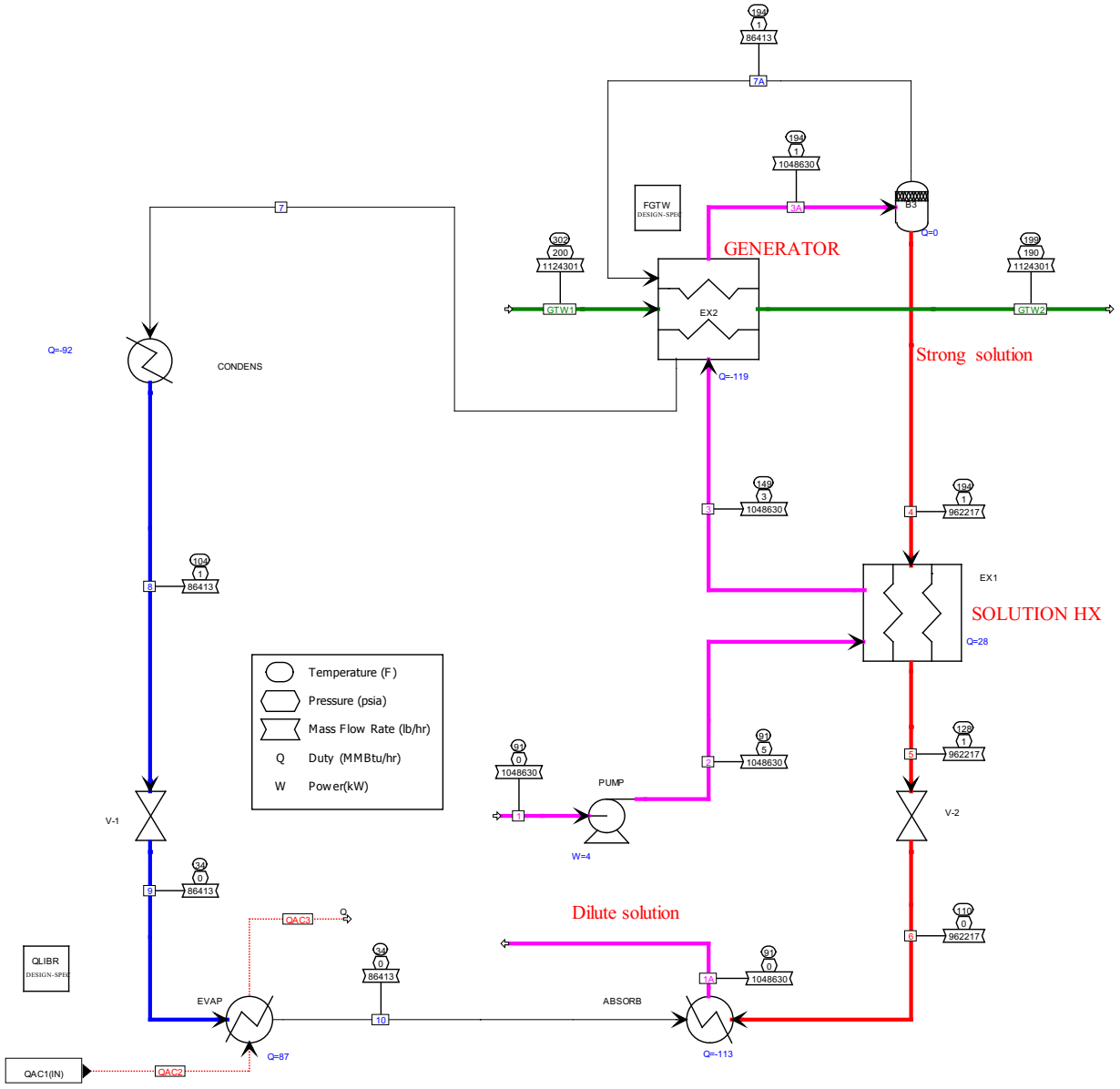

Figure 38. Aspen Plus model of the LiBr water absorption cooler section.

5.2.4 GETEM Integration

The Excel spreadsheet-based GETEM model is used to provide geofluid pumping power requirements. It is assumed that the pumping power for production and injection is the same for geofluid delivery to both the standalone and the hybrid plants. The net power output of the hybrid plant is obtained from the turbine power generation and auxiliary loads given by the Aspen model. The hybrid plant power sales are then calculated by subtracting GETEM's estimated pumping power requirement from the net power output.

The power consumption due to geothermal pumping depends on well depth, bore size, and pump flow. However, for the geothermal scenario considered here, the friction loss contributes much less than the lift work to the overall pumping power. The pumping power is thus approximated by scaling down the power

required at full production flow linearly according to actual geothermal flow demand. This simplification reduces the number of instances of GETEM model runs.

The cooling demand for turbine inlet air varies depending on the time of the year. Because the geothermal well field is sized according to maximum cooling demand during the hottest summer month, turndown of geothermal production is necessary during the rest of the year. It is assumed that this turndown is done by turning down and shutting off wells one by one as opposed to reducing production proportionally across all wells. This approach minimizes the impact of flow reduction on well bore temperature loss, which is typically 2 to 3 °C at the full production rate and is ignored in the current analysis.

5.3 Results

5.3.1 Hybrid Plant Performance

The hybrid plant performance is summarized in Table 10. The hybrid concept plant with turbine inlet air cooling enabled by the geothermally driven absorption cooler allows additional power generation over the baseline NGCC plant. The power increase averages 8.6% on an annual basis and is higher during the hot summer months. Comparing the monthly power generation profiles of the hybrid and the baseline gas plants (Figure 39), not is only the seasonal dip in power output of the baseline plant avoided during high-demand summer season, but the hybrid plant also outputs more power on annual average basis.

The majority of the net power increase achieved with the hybrid plant is attributed to the additional fuel rate enabled by the inlet air cooling. This is easily observable in Figure 40, which compares the net power increases from combustion of additional fuel gas and from geothermal conversion. On an annually averaged basis, out of the 51.63 MW total net power boost, 50.30 MW is due to additional natural gas combustion and only 1.33 MW may be attributed to indirect conversion of geothermal energy. The latter is mainly derived from a higher compressor efficiency at a lower inlet air temperature and is only 3% of the total power increase. The reference standalone geothermal plant outputs a net power of 9.47 MW, more than 7 times greater than the power increase attributable to geothermal input alone to the hybrid plant. The fact that the geothermal wells are not operated at full production for all months for the hybrid plant is also part of the reason why the power production attributable to geothermal is small.

Table 17. Hybrid plant performance.

	Mean	Jan	Feb	Mar	Apr	May	Jun	Jul	Aug	Sep	Oct	Nov	Dec
Net Power – Baseline Gas Plant (MW)	607.43	630.8	623.9	617.0	610.8	601.1	590.9	589.4	587.3	589.2	600.1	616.9	631.8
Net Power – Hybrid Gas Plant (MW)	659.05	653.1	654.8	655.7	656.2	659.4	663.3	666.9	666.5	663.4	659.9	656.4	653.2
Inlet Air Cooling Duty (MW)	18.26	7.76	10.90	13.68	15.62	20.27	25.47	29.03	28.45	25.67	20.81	14.06	7.34
Geothermal Pumping Power (MW)	0.15	0.062	0.087	0.109	0.125	0.162	0.203	0.232	0.227	0.205	0.166	0.112	0.059
Power Increase Total (MW) [(a)]	51.63	22.28	30.94	38.70	45.39	58.36	72.38	77.51	79.17	74.19	59.82	39.45	21.33
Power Increase from Gas (MW) [(b)]	50.30	21.67	30.11	37.67	44.12	56.78	70.55	75.80	77.20	72.37	58.23	38.35	20.75
Power Increase from Geothermal (MW) [(c)]	1.33	0.61	0.83	1.03	1.27	1.58	1.84	1.71	1.97	1.82	1.59	1.10	0.59
Power Increase from Gas – Over Baseline Gas Plant	8.6%	3.5%	5.0%	6.3%	7.4%	9.7%	12.2%	13.2%	13.5%	12.6%	10.0%	6.4%	3.4%
Power Increase from Geothermal – Over Standalone GT Plant	14.0%	6.4%	8.8%	10.9%	13.4%	16.7%	19.4%	18.1%	20.9%	19.2%	16.8%	11.6%	6.2%

(a) Calculated as the difference between the net power of hybrid gas plant and the net power of the baseline gas plant.
(b) Calculated from the baseline gas plant heat rate and the additional fuel rate of the hybrid plant.
(c) Calculated as the power increase total minus the power increase from gas.

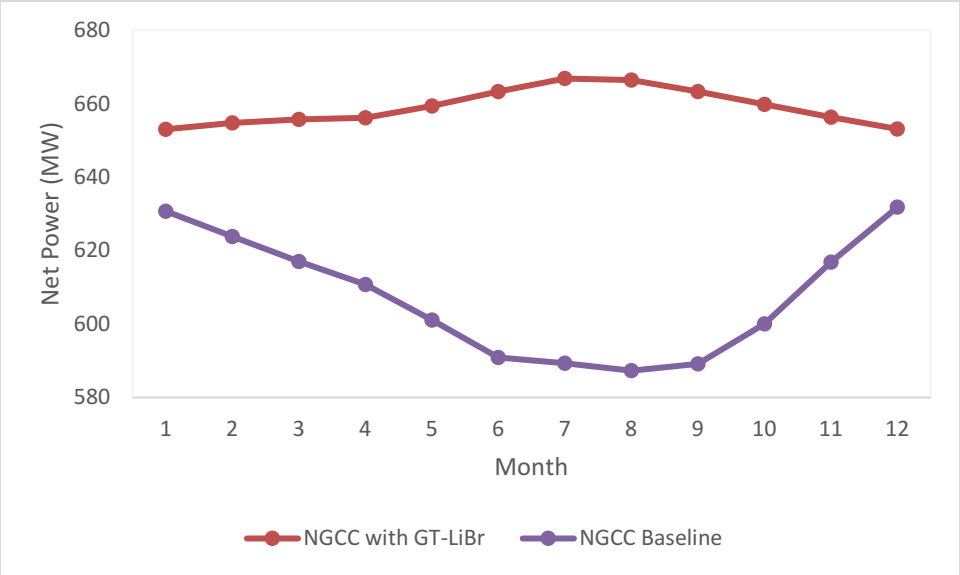

Figure 39. Net power comparison of NGCC plants with and without GT-LiBr inlet air cooling.

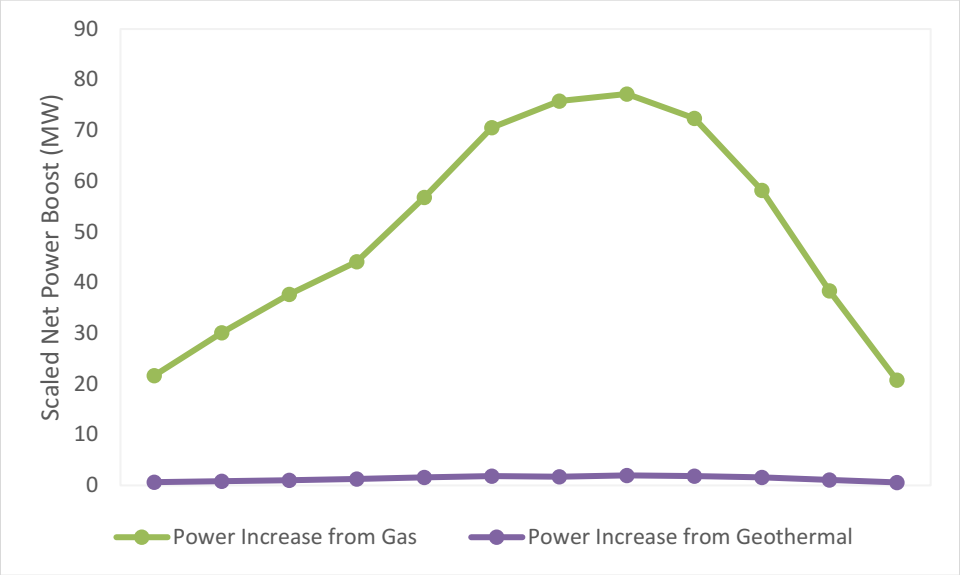

Figure 40. Comparison of contributions to net power increase from additional gas combustion and geothermal conversion.

5.4 Discussion

To evaluate the cost of electricity for the hybrid plant, cost elements from the entire plant including the geothermal well field, the natural gas plant, and the LiBr absorption cooler must be considered. This is different from the hybrid geothermal coal-fired power plant cases, where the LCOE of the geothermal integration can be separately evaluated because the hybrid plant runs at the same fuel rate as the base coal plant. For the hybrid gas plant, the fuel rate is higher than the baseline gas plant. In fact, the real value of the hybrid approach is not solely—or even primarily—a function of the net power generated by the geothermal resource itself, but in the role geothermal-based inlet air cooling plays in enabling power production during the summer months, which would be precluded by ambient air conditions absent the

LiBr system. Because the costing methodologies used in the NETL baseline studies and GETEM model are so disparate, a common-basis cost analysis similar to the one presented for geothermal-hybrid supercritical coal was not feasible.

However, by estimating the additional power generated in the GT-NGCC hybrid system over each month of the year, as well as the power that might be generated from the geothermal resource during the same period, we can examine the relative revenues and costs associated with each use of the resource.

5.4.1 Incremental Power Sales and Revenue

It is useful to consider the value of the additional power sales in reference to the monthly variation in the price of electricity. Future studies can add the cost of electricity to evaluate the full economic value of the geothermal integration. The analysis below can provide at least some bounds on the breakeven costs of the hybrid plant vs. standalone geothermal plant. Electricity price data for California in 2016 are published by the U.S. Energy Information Administration. Table 18 includes these data along with the incremental power sales of the hybrid plant and the power sales of the standalone geothermal plant. The values of the power sales are calculated for each month in 2016. The total value of the hybrid plant incremental power sales is $71.5M, or 5.6 times of the $12.8M revenue generated by a geothermal plant during the same period.

5.4.2 Equipment Costs

To evaluate the economic competiveness of the hybrid plant, we can start by comparing the capital costs of the geothermal integration for turbine inlet air cooling and the binary conversion system in a standalone geothermal plant. GETEM's estimate of equipment procurement cost for the conversion system is $15.1M with the same plant specifications as in Table 16. Detailed costs of the LiBr water absorption system are not available at the time of this study. However, based on the few available online prices, the hot water LiBr absorption chillers cost roughly $200 to $300/refrigeration-ton. From Table 18, the maximum cooling duty occurs in the month of July: 29.03 MW or 8254 RT. Assuming a set of two absorption chillers is needed with one spare, the equipment procurement cost for the hybrid plant LiBr system is roughly $2.4M, which compares favorably with the $15.1M binary conversion system (organic Rankine cycle) needed for a standalone geothermal plant.

From both the above incremental power sales and equipment procurement cost values, the hybrid plant compares favorably to a standalone geothermal plant. While a more detailed cost analysis for a specific plant could shed more light on the applicability of this approach in a given market, the GT-NGCC configuration examined here, using gas turbine air cooling by geothermally driven LiBr water absorption, may well be economically competitive with standalone geothermal plants.

Table 18. Value of additional power sales.

2016	CA Average Price $/kWH for All Sectors	Days in Month	Power Sales (kW)	Value of Power ($)	Power Sales, (kW)	Value of Power, ($)
			Incremental power production by the hybrid plant over baseline gas plant:		Alternative production of maximum water from geothermal wells during the same period:	
Dec	0.1542	31	22,416	2,571,636	9,466	1,086,028
Nov	0.1503	30	31,056	3,472,997	9,466	1,024,481
Oct	0.1562	31	38,720	4,499,736	9,466	1,100,114
Sep	0.1669	30	45,574	5,659,086	9,466	1,137,555
Aug	0.1715	31	58,386	7,449,790	9,466	1,207,872
Jul	0.1693	31	72,522	9,134,791	9,466	1,192,377
Jun	0.1624	30	80,596	9,738,107	9,466	1,106,884
May	0.1493	31	79,431	8,823,165	9,466	1,051,517
Apr	0.1267	30	74,288	7,002,714	9,466	863,561
Mar	0.1434	31	59,921	6,392,991	9,466	1,009,964
Feb	0.1512	28	39,468	4,439,835	9,466	961,844
Jan	0.1475	31	21,369	2,345,024	9,466	1,038,840
			Total:	**71,529,873**		**12,781,038**

5.4.3 New Generation to Meet Peak Load

For gas plant operators in areas with high summertime ambient temperatures and access to low-temperature geothermal resources, the opportunity to use geothermal heat in absorption chilling loops for inlet air precooling could provide an option to more fully utilize existing generation capital during periods of high power demand associated with peak air conditioning season. Where peak demand during these months is driving investment in new generation capacity, this geothermal hybrid approach offers a novel and potentially cost effective alternative to greenfield projects.

Even in off-months, the additional power generated via inlet air precooling—relative to that generated from the same resource via standalone binary cycle geothermal—is significant, valued at nearly 6 times the power generated by the standalone plant (Table 18). As noted above, a quick comparison of the capital costs associated with LiBr implementation at an existing NGCC plant with the costs of installing a new binary geothermal plant might further skew the "incremental" LCOE in favor of the GT-NGCC hybrid. This may offer a "sweet spot" that offers a higher-value use for low-temperature geothermal fluids, and a lower-cost option for increasing nameplate capacity during high-load summer months. Coupled with the ease of permitting and the ability to leverage capital and infrastructure at extant gas plants, this GT-NGCC hybrid approach could be a particularly attractive option for gas plants located near productive hydrothermal resources whose low resource temperatures may diminish their potential for standalone binary development. If so, this approach could increase demand for (and utilization of) lower-temperature geothermal resources while also giving utilities an option for delaying investments in new power plants by helping to make the existing ones more efficient, generating more power while using less fuel and producing fewer emissions per kilowatt-hour by leveraging renewable, domestic energy.

6.0 Evaluation of Geothermal Addition to the Algal Hydrothermal Liquefaction Process

Highlights

- This analysis evaluated the potential for using heat energy from geothermal fluid in a biofuel production process.
- Algal hydrothermal liquefaction (AHTL) was modeled under this approach using system designs presented by Jones et al. [128].
- Geothermal resource integration was modeled for temperatures of 150, 200, and 250 °C.
- Within the hydrotreating process modeled under this study, the resource temperatures evaluated here are insufficient to drive reboilers on any of the distillation columns.
- The hydrocracking process employs a Naphtha reboiler that operates at temperatures between 200 and 250 °C; but with only a small fraction of the heat energy extracted from the geothermal resource for this use, the costs are likely to exceed those of conventional sources here.
- While this analysis focused on the use of geothermal resources as a supplemental heat source in the hydrotreating and hydrocracking processes, there may be potential uses for low-temperature fluids in maintaining pond temperature for algal feedstock production, if the geothermal resource can be obtained at costs well below those of conventional heat sources.
- For specific projects where low-cost geothermal fluid availability and site-specific considerations might make certain applications appealing, the opportunities appear to be limited for using supplemental geothermal heat within the AHTL process evaluated here.

6.1 Overview

Geothermal heat addition at temperature levels of 150, 200, and 250 °C was explored to supplement the AHTL process, as described in report PNNL-23227, prepared for the U.S. Department of Energy Bioenergy Technologies Office [128]. The process converts micro-algae to an oil that is upgradable to a renewable transportation fuel. All AHTL processing discussions and figures are from information in this report [128].

High water content is a principal deterrent to the use of biomass for the production of carbon neutral fuels [128]. Hydrothermal liquefaction employs high-temperature, high-pressure liquid water to produce hydrocarbon liquids from wet biomass feedstocks, including many strains of micro-algae. About two-thirds of the input biomass carbon is transformed into the biomass fuels.

6.2 Evaluating Options for Geothermal Energy Use

6.2.1 Feedstock Cultivation

There are two main alternatives for cultivating photoautotrophic algae for feed to this process: raceway pond systems and photobioreactors (PBRs). A typical raceway pond comprises a closed loop oval channel, less than 0.4 meters deep, open to the air, and mixed with a paddle wheel to circulate the water and prevent sedimentation. (Ponds are kept shallow as optical absorption and self-shading by the algal cells limits light penetration through the algal broth.) In PBRs, the culture medium is enclosed in a transparent array of tubes or plates and the micro-algal broth is circulated from a central reservoir.

PBR systems allow for better control of the algae culture environment, but tend to be more expensive than raceway ponds. Additionally, at least one study found that all PBR systems require more energy than they produce. In contrast, most of the raceway systems were found to produce more energy in biomass than they consumed in pumping power [129].

Algae productivity rates vary significantly as a function of location and season. Main variables affecting the variation are solar insolation and temperature. The variation can be as much as 9/1 and a minimum of at least 2/1 [128].

Maintaining the pond temperature at optimum conditions in periods of low ambient temperature is a logical application for geothermal energy. However, in the case of raceway ponds, the temperature is not normally controlled since it is impractical to do so [129]. The pond interacts strongly with the environment and readily loses heat through evaporation, convection, and radiation. The shallow raceway ponds have maximum algal growth with high surface-to-volume ratios, but also have great potential for heat loss (see, for example, [130]). This heat loss makes it economically unattractive to regulate pond temperature when heat is provided via conventional sources; should geothermal energy offer an option for significantly lower-cost heat (e.g., low-temperature effluent from existing geothermal or oil and gas development projects), there may be opportunities to integrate geothermal heating into this part of the process. However, the incremental costs to a given site would need to be weighed against the temperature support and associated feedstock productivity that might be obtained, relative to the standard option of not supplementing pond temperature during cool ambient conditions.

6.2.2 Feed Preheating and Hydrotreating

After the algae is harvested and concentrated, it is pumped and heated to feed the AHTL reactor. Figure 41 shows the simplified process flow diagram.

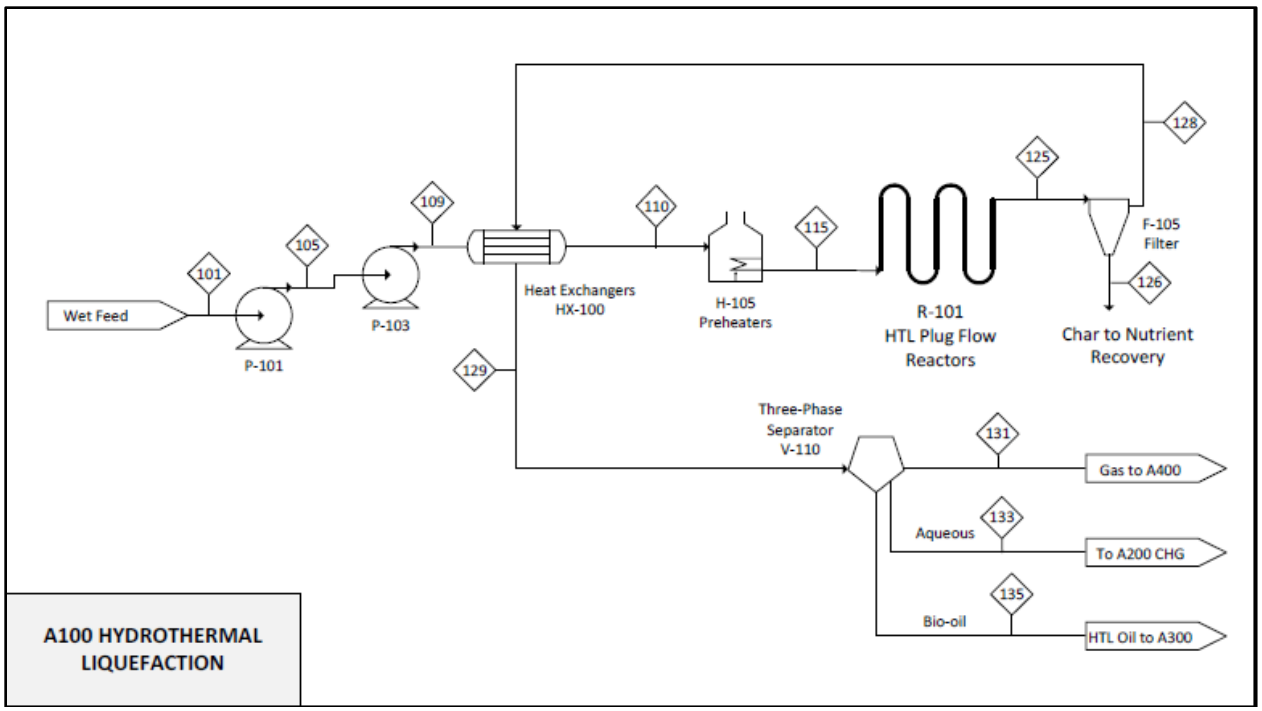

Figure 41. AHTL reactor process flow diagram.

The concentrated algae feedstock is pumped to near the critical water pressure. After pumping, the feed is heated in a cross exchanger with the hot effluent from the AHTL reactor. Here, geothermal heat would not be applied since the heat from the reactor effluent can be applied directly to heat the reactor feed to 315 °C. The gas-fired process heater then heats the feed to the reactor operating temperature of 350 °C, well above the available geothermal temperature of 250 °C. Following reaction, the hot reactor effluent is cooled by the cross exchanger and then phase-separated by gravity. The gas phase is used as fuel in the process heater and for steam generation. The aqueous phase is recycled to the algae pond for nutrient recovery and the oil is forwarded for additional processing, typically hydrogenation for deoxygenation.

Figure 42 is a process flow diagram for the AHTL oil hydrotreating. Here, geothermal heat is not of sufficiently high temperature to drive the reboilers on any of the three distillation columns shown. The Lights Column, T-310, requires more than 250 °C and has the lowest temperature reboiler.

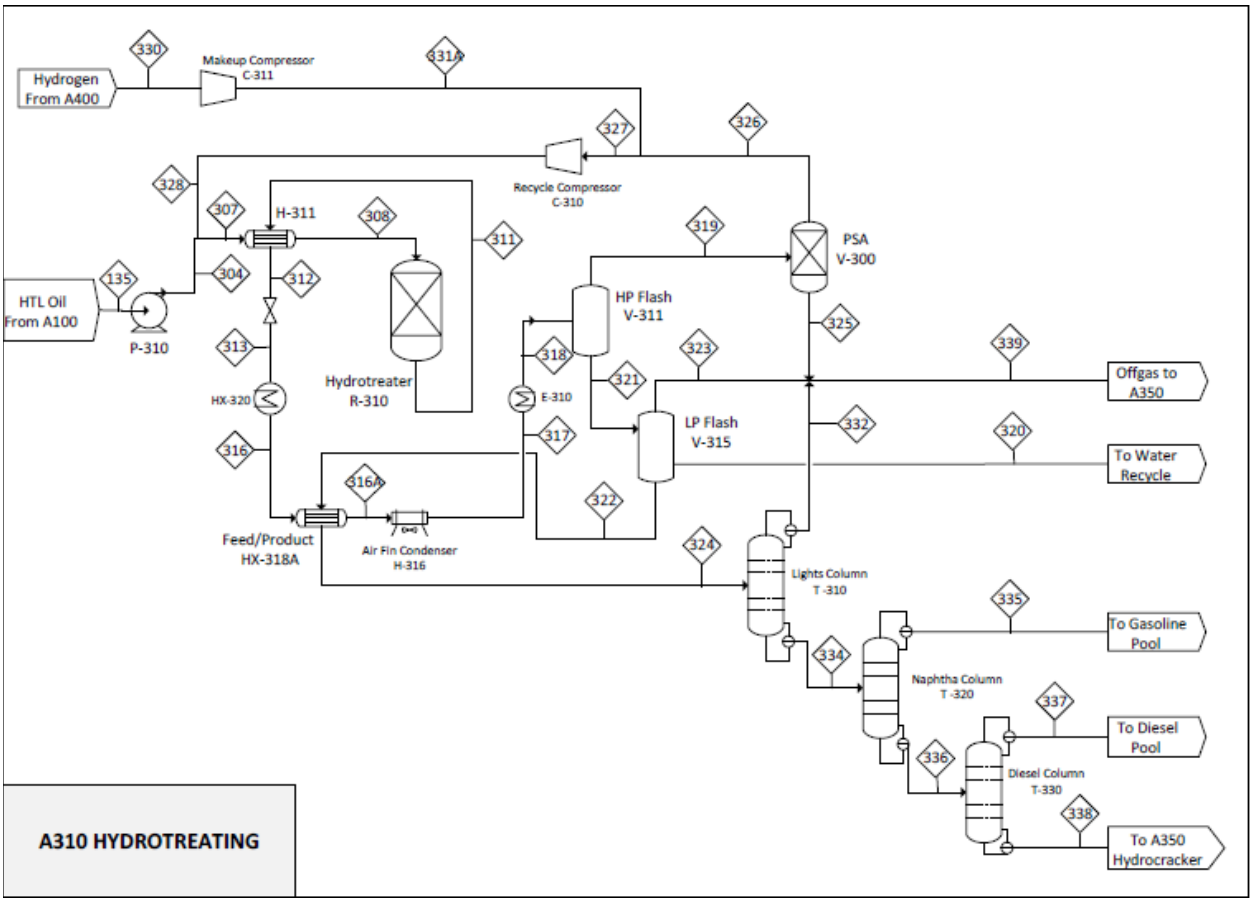

Figure 42. AHTL oil hydrotreating.

6.2.3 Hydrocracking

Compared to the hydrotreating process, hydrocracking converts the higher molecular weight components in heavy oil to lighter components under relatively high temperature and pressure conditions, in the presence of hydrogen and a catalyst. Figure 43 is a process flow diagram for this operation.

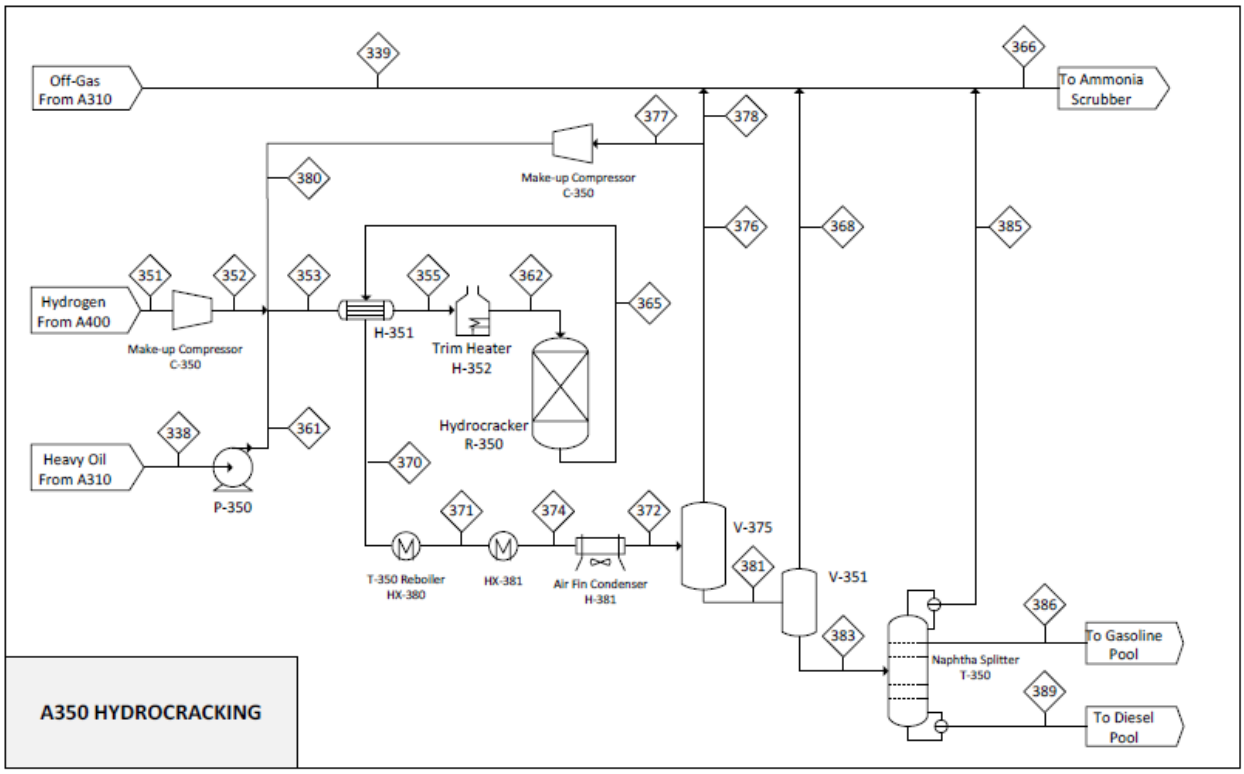

Figure 43. AHTL oil hydrocracking.

The Naphtha splitter reboiler in this process operates within a range of 220 to 250 °C. While geothermal fluid could possibly be used, only a small amount of the available energy could be extracted. There may also be opportunities to use geothermal energy for boiler feedwater heating, though this would require flow rates on the order of 8 MMBtu, translating to a flow on the order of 50,000 lb/hr of geothermal fluid to impact system performance, and would need to be considered as a function of costs to acquire geothermal fluids, given the low utilization of the heat energy within this resource.

6.3 Discussion

While the possibility of low-cost geothermal fluid might make this approach economically appealing within certain site-specific applications, the opportunities appear to be limited for using supplemental geothermal heat within the AHTL process evaluated here. In general, bioenergy processing tends to be relatively self-contained, providing heat where needed within the process, leaving few opportunities for geothermal to offer supplemental heat that would offset significant higher-cost sources. Given the lack of promising opportunities for integrating geothermal heat into a bioenergy production facility as modeled here, additional analytic work and levelized cost analysis was not pursued for this hybrid application.

7.0 Geothermal Hybrid Compressed Air Energy Storage

Highlights

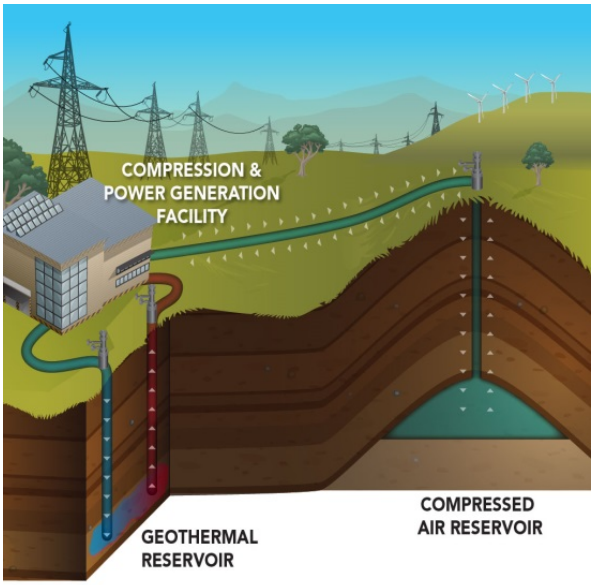

- This study evaluates a compressed air energy storage (CAES) system using geothermal heat for air reheating prior to each stage of turboexpansion.
- Geothermal energy displaces the reheating role of natural gas in conventional CAES plants, with compressed air stored in the subsurface when power prices are low and produced via turboexpansion when power prices are high.
- Systems are optimized to divert geothermal fluid for interstage reheating during the 6-hour diurnal expansion cycle, and to produce geothermal electricity via GETEM-selected technologies during other periods (compression, shut-in).
- Holding compression load constant (43 MW) across resource cases, the power generated during the expansion cycle increases as a function of geothermal resource temperature—from 22 MW at 150 °C to 29 MW at 250 °C.
- Round-trip efficiencies range from 51% for the 150 °C resource to 66% for the 250 °C resource.
- Levelized cost of electricity (LCOE) can vary widely based on how the baseload and CAES portions of the project are dispatched to maximize arbitrage revenues; instead, overnight capital costs are presented for the resource-binned case studies examined in this analysis.
- Previous site-specific analyses of GT-CAES suggest LCOEs could be competitive with peaking gas and intermittent renewables.
- GT-CAES requires both a geothermal resource and a reservoir suitable for compressed air storage. Previous paper studies found that these conditions can be difficult to find in a single location.
- This study assumes the presence of a salt dome for the air storage portion of the project, but salt domes are less ubiquitous than sedimentary reservoirs, which have not been studied as extensively for compressed air storage. Additional field work to validate the use of sedimentary reservoirs or other novel air storage options might increase the number of opportunities to pair CAES with geothermal resources to provide low-emission, grid-scale energy storage.

7.1 Overview

This study examines the application of geothermal resources to CAES. Previous work at PNNL analyzed geothermally coupled CAES (GT-CAES) concepts to provide balancing resources for integration of renewables to grid [53, 131] and to use existing wellbores for compressed air storage [52]. The present study investigates GT-CAES configurations suitable for different grades of geothermal resources and conducts a sensitivity analysis of GT-CAES performance and overall capital costs to geothermal resource temperature.

The analysis presented here, to be consistent with the resource temperature case study approach used across other hybrid technologies, assumes a fixed set of operating parameters. Specifically, the design case used in this analysis is based on previous work on geothermal hybrid CAES, which assumed a diurnal 6-hour compression (load) and 6-hour expansion (generation) cycle. However, the primary market driver for CAES is its ability to provide ancillary services, as these typically represent the highest-value product streams for grid-served power. Thus, despite the simplifying assumptions used to constrain the operational scenarios in this study and previous work upon which it is based, a given GT-CAES plant would be cycled to maximize revenues from a combination of ancillary services and power generation via binary or flash geothermal. Such optimization is heavily dependent on individual market conditions, precluding a generalized estimate of LCOE similar to those presented for other hybrid technologies. However, in a study examining the applicability of GT-CAES in the Pacific Northwest, McGrail et al. [53] found that LCOEs for this hybrid approach could be competitive with intermittent renewables at a low capacity factor (10%), or peaking gas if used at a higher capacity factor (25%).

As discussed later in this section, the impacts of site- and market-specific issues for GT-CAES extend well beyond the specifics of the geothermal resource at a given site. These other issues—including CAES reservoir capacity and quality, market for balancing services provided by the CAES mode of the project, and potential for power arbitrage between peak and off-peak pricing—may have far greater effects on LCOE and dispatch profiles than the geothermal resource temperature. While parameterizing these variables is a highly site-specific task, the spirit of the case study approach selected for evaluating hybrid systems under the GeoVision study is one of high-level, qualitative comparison of highly disparate hybrid applications. The analysis in this section, then, is intended to provide a common-basis comparison of GT-CAES implementation at multiple resource temperatures as part of the overarching goal of the Hybrid Systems Task Force to facilitate a discussion of each hybrid application across a range of geothermal resource temperatures.

7.2 Methodology

The hybrid GT-CAES process is modeled primarily using Aspen Plus. GETEM,[1] a geothermal power analysis model, is also used to provide data on geothermal wells and power plant performance and cost. The Aspen model is similar to those developed in previous PNNL studies [52], but with a modified power recovery block. As shown in the level-1 block diagram in Figure 44, air is compressed using power from grid or associated power plants and injected to an underground storage. During a demand increase, electric power is recovered by expanding the stored air in a series of unfired gas expanders with interstage reheat. Geothermal fluids are used to reheat the expanded air to prevent cooling below the freezing point of water. The top-level material balance is summarized in Table 19.

[1] GETEM: Geothermal Electricity Technology Evaluation Model, U.S. Department of Energy, Geothermal Technologies Office. Revision 2016, GeoVision Study.

Table 19. GT-CAES material balance.

Stream	Compressor Feed Air	Reservoir Air	Air To Expander	Water Condensate	Expander Exhaust *	GT Brine Supply *	GT Brine Return *
Temperature, °F	60	275	205	90	62	392	139
Pressure, psia	15	2406	2324	250	15	300	280
Mass Flow, lb/hr	432,000	429,704	429,704	1876	429,704	396,691	396,691

*Values provided for the 200 °C geothermal resource scenario as examples.

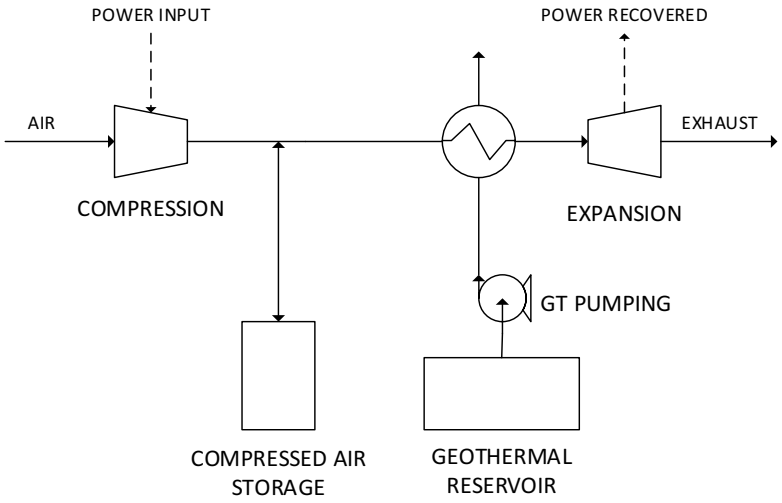

Figure 44. GT-CAES level-1 block diagram.

7.2.1 Compression and power recovery Aspen simulations

Air compression, interstage cooling, air expansion, and reheat are modeled with Aspen Plus. The Aspen flowsheet for the air compression section is shown in Figure 45. Ambient air specified at ISO standard reference conditions is pressurized using an axial flow compressor to an outlet pressure of 265 psia. The compressed air temperature is reduced in series by a pair of air-cooled and water-cooled exchangers to 90 °F. Condensed water is separated out. The air is further compressed to 2406 psia by a three-stage centrifugal compressor with interstage cooling. The above cooling duties for the air compressors are provided by a cooling tower. The Aspen flowsheet of the cooling tower section is shown in Figure 46. After the final compression stage, the air is injected to an underground storage. In this study, the storage vessel is simulated as a 10-inch-diameter, 3750-foot-deep carbon steel pipe, representing a low-grade well casing. Out-of-service wellbores have been identified as a class of low-capital cost reservoirs suitable for CAES applications in a previous report [52].

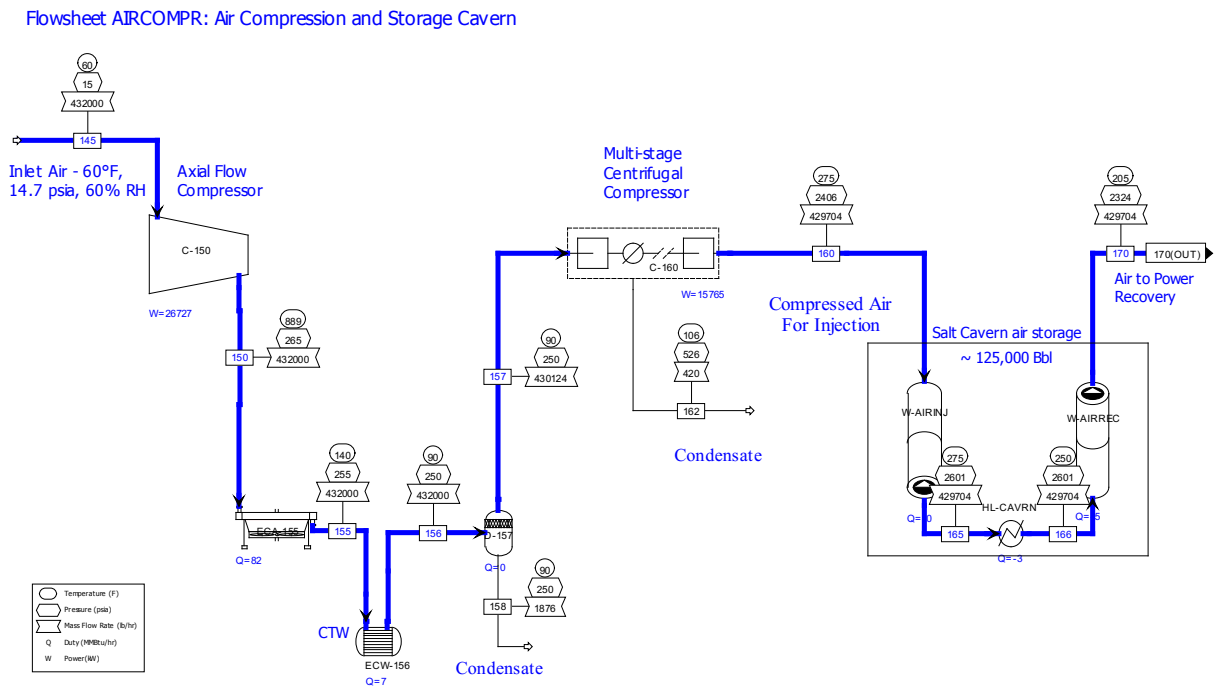

Figure 45. GT-CAES air compression Aspen flowsheet.

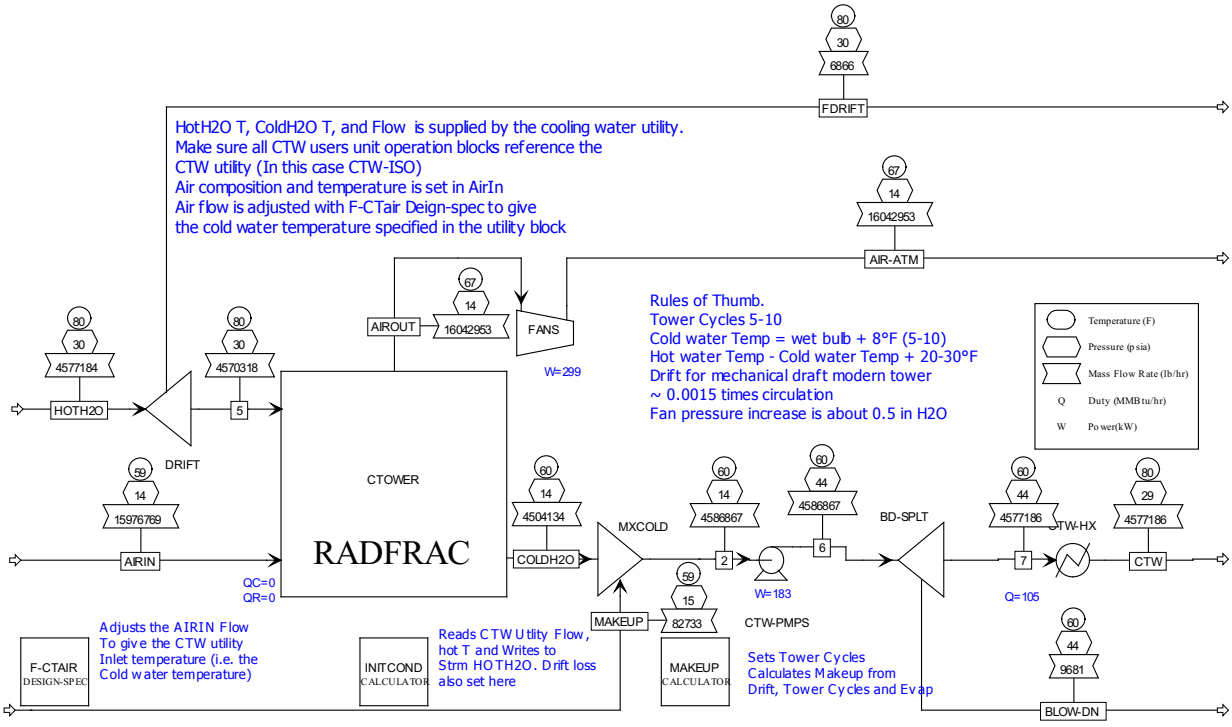

Figure 46. GT-CAES cooling tower Aspen flowsheet.

The Aspen flowsheets for the power recovery section are given in Figure 47 to Figure 49 for three cases of geothermal scenarios: 150, 200, and 250 °C geofluid temperature. The flowsheets are similar; the

difference is in the number of gas expanders. For higher grade geothermal resources, more stages are used to obtain higher efficiency. Identical to each case, the compressed air from the storage reservoir is first heated using the geothermal fluid in a shell and tube exchanger before entering the first gas expander. The expanded air is reheated by the geofluid from the first exchanger. The expansion and reheat steps are repeated with a fixed expansion ratio until the air pressure is slightly above ambient. The reheat exchanger temperature approach is set at 10 °F between the geofluid inlet and the air outlet. For the three geothermal scenarios of 150, 200, and 250 °C reservoir temperatures, four, five, and six expansion turbines are needed, respectively.

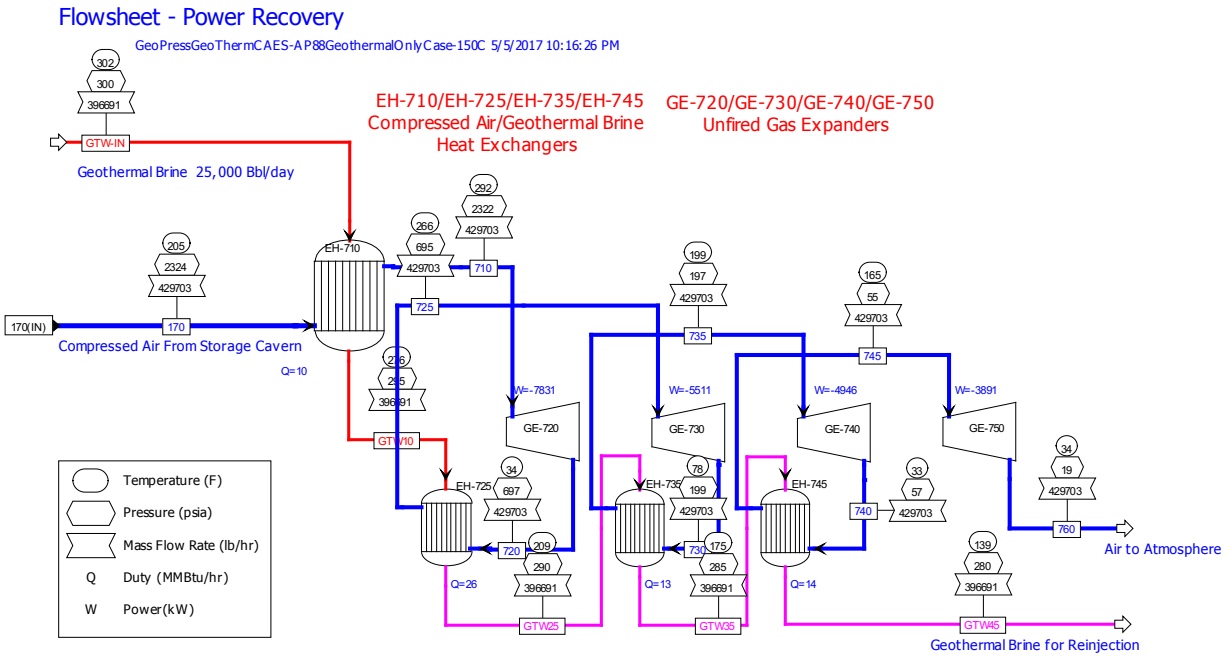

Figure 47. GT-CAES power recovery Aspen flowsheet for the 150°C geothermal scenario.

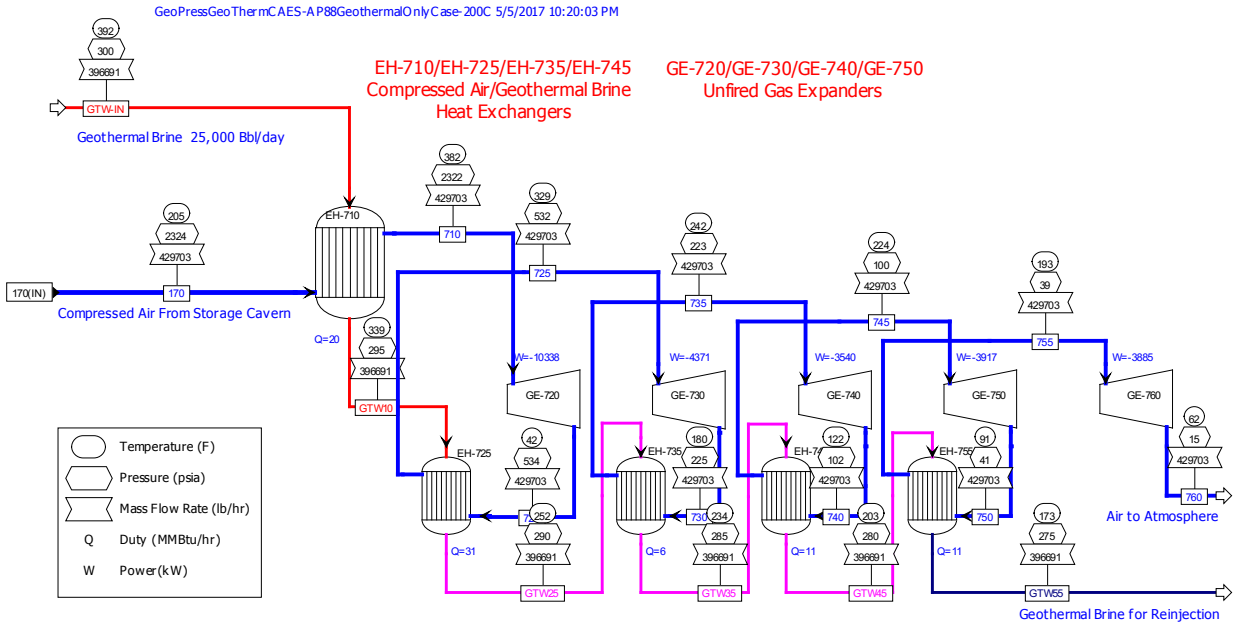

Figure 48. GT-CAES power recovery Aspen flowsheet for the 200 °C geothermal scenario.

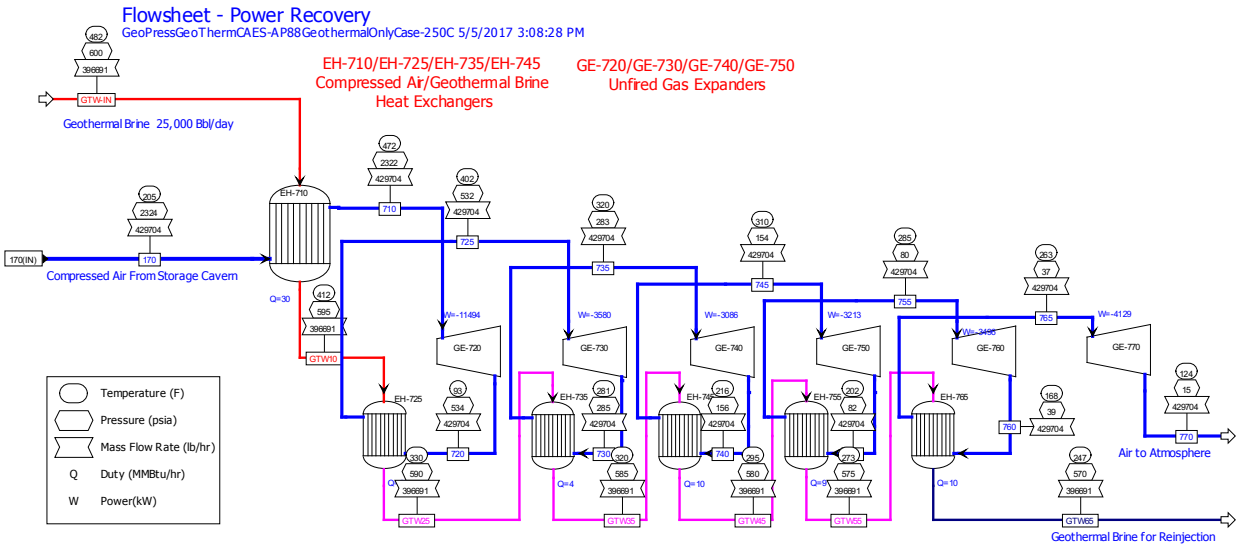

Figure 49. GT-CAES power recovery Aspen flowsheet for the 250 °C geothermal scenario.

7.2.2 Geothermal wells and plant

Referring back to the GT-CAES top-level process shown in Figure 44, the geothermal fluid is extracted from a reservoir and pumped to reheat exchangers. The geothermal wells, fluid-gathering system, and production and injection pumps are not part of the Aspen simulation. They are configured using the GETEM model in greenfield scenarios to obtain the geothermal pumping power requirements. The key attributes of the geothermal resource scenarios under consideration are summarized in Table 16. This study relies on the GETEM model to provide a full geothermal resource scenario. Besides Table 16, all other parameters needed to describe a geothermal power generation project are taken as the GETEM

default values. The conversion system is selected following GETEM default criteria, i.e. air-cooled binary (organic Rankine cycle) plants for below 200 °C and flash steam plant for 200 °C or higher.

Table 20. Geothermal resource scenario key assumptions.

Resource Type	Greenfield Hydrothermal
Resource Temperature	150 °C, 200 °C, 250 °C
Resource Depth	10,000 ft
Conversion System	Binary (Organic Rankine Cycle) or Flash Steam Plant
Project Life	30 years
Production Well Flow Rate	396,691 lb/hr
Number of Production Wells	1
Production Wells Pumping	Yes

7.2.3 GT-CAES performance and costs

The auxiliary loads from air compression are calculated by the Aspen simulation. These include the air compressor power and the cooling tower fan and pump power. Additional auxiliary loads on the geothermal plant side are calculated using the GETEM model. These include the production well pump and injection well pump power. The net power generation by a conventional geothermal plant, when the fluid is not used for air reheating, is also obtained using GETEM. Following GETEM methodology, this geothermal net power does not take into account the geothermal pumping loads. The performance of the GT-CAES hybrid plant is calculated as described below, assuming that the compressed air storage and the power recovery are only run for a portion of the day.

Compression is assumed to occur daily over a 6-hour off-peak period. Expansion and power recovery are assumed to take place over a 6-hour peak period. The geothermal well field is assumed to operate 24 hours per day. During the 18-hour off-peak period, when geothermal brine is not needed for reheating expanded air, the geothermal plant sized to the well field is assumed to be in operation for power generation. The round trip efficiency for energy storage is calculated as

$$[\text{Round Trip Efficiency}] = \frac{\sum[\text{kWh Expander Recovery}]}{\sum[\text{kWh Compression Loads}]+\sum[\text{kWh Geopumping Loads}]} \quad \text{Eq. 7.1}$$

The overnight capital costs are developed using ASPEN Process Economic Analyzer v. 8.8, with the exception of the geothermal plant, which is costed using GETEM.

7.2.4 GETEM integration

Unlike the solar and coal hybrid cases presented in earlier sections, the different revenue streams associated with the various operating conditions of the GT-CAES hybrid facility are difficult to interchangeably or incrementally value in a deterministic way. Like the GT-NGCC hybrid case, the hybrid CAES configuration uses geothermal energy to enable additional generation from another system that is not wholly attributable to use of the geothermal resource, as in the GT-Coal case. Thus, a full GETEM implementation of the GT-CAES hybrid concept was not feasible under the present effort.

7.3 Results

7.3.1 Hybrid plant performance

The GT-CAES hybrid plant performance is summarized in Table 21. Auxiliary loads associated with air compressors, cooling tower fans and pumps, and geothermal pumps are tabulated for the three different geothermal temperatures. Energy storage and recovery over a 24-hour period are calculated based on the

operation schedule described in the previous section. The round trip energy efficiency is calculated according to Eq. 7.1.

Table 21. GT-CAES performance summary.

Geothermal Temperature	Unit	150 °C	200 °C	250 °C
Air Compression Loads	MW	42.97	42.97	42.97
AIRCOMPR.C-150	MW	26.73	26.73	26.73
AIRCOMPR.C-160	MW	15.76	15.76	15.76
CTOWER.CTW-PMPS	MW	0.183	0.183	0.183
CTOWER.FANS	MW	0.299	0.299	0.299
Expanders – Power Recovery	MW	22.18	26.05	29.00
UNIT7000.GE-720	MW	7.83	10.34	11.49
UNIT7000.GE-730	MW	5.51	4.37	3.58
UNIT7000.GE-740	MW	4.95	3.54	3.08
UNIT7000.GE-750	MW	3.89	3.92	3.21
UNIT7000.GE-760	MW	NA	3.88	3.50
UNIT7000.GE-770	MW	NA	NA	4.13
Geothermal Power Generation	MW	3.04	3.14	5.22
Geothermal Pumping	MW	0.08	0.18	0.28
Production Wells	MW	0.05	0.08	0.19
Injection Wells	MW	0.03	0.10	0.09
Daily Production *				
Air Compression & Injection	kWh	257,847	257,847	257,847
Air Expansion & Power Recovery	kWh	133,074	156,298	173,988
Geothermal Power Generation	kWh	54,668	56,540	93,963
Geothermal Pumping	kWh	1991	4254	6778
Round Trip Efficiency		51.2%	59.6%	65.7%

*Daily off-peak 6-hour compression, 6-hour peak power recovery, 24-hour geothermal pumping, 18-hour geothermal power generation.

7.3.2 Hybrid plant cost

Aspen and GETEM use different sets of indirect cost multipliers and assumptions that are difficult to reconcile across models for the GT-CAES concept, precluding a common-basis analysis that defensibly marries the two. Instead, the component costs taken from each model are evaluated on an overnight direct capital costs basis, allowing these to be rolled up and compared across the different resource case study scenarios.

A breakdown of overnight capital costs of the GT-CAES plant is presented in Table 22 and Table 23. CAES costs are obtained using Aspen simulation data and Aspen Process Economic Analyzer in 2014 dollars. Costs associated with geothermal wells and power plant equipment have been estimated using GETEM, and are given in 2014 dollars. The costs are direct costs without contingency. The overnight capital costs of the entire GT-CAES hybrid plant are given in Table 24.

Table 22. CAES direct costs (Aspen Process Economic Analyzer).

Geothermal Temperature	150 °C	200 °C	250 °C
Air Injection	$11,662,109	$11,662,109	$11,662,109
Power Recovery	$8,318,437	$9,297,501	$10,598,701
Cooling Tower	$987,126	$987,126	$987,126

Table 23. Geothermal wells and power plant direct costs (GETEM).

Geothermal Temperature	150 °C	200 °C	250 °C
Permitting (Exploration) & Leasing	$582,276	$568,748	$566,889
Exploration	$1,005,496	$1,340,662	$1,340,662
Exploration Drilling	$18,570,740	$15,441,407	$15,441,407
Drilling Before PPA Obtained	$ -	$ -	$ -
Drilling After PPA Obtained	$3,780,853	$2,446,597	$2,386,227
Permitting (Field and Plant)	$2,369,675	$1,480,172	$1,439,925
Field Gathering System (Surface) Before PPA	$ -	$ -	$ -
Engineering Before PPA	$ -	$ -	$ -
Field Gathering System (Surface) After PPA	$1,117,125	$1,117,125	$1,117,125
Geothermal Pump Installation	$468,336	$495,184	$496,574
Engineering After PPA	$538,293	$383,081	$429,797
Plant Construction	$312,224	$330,123	$331,049
Total	$188,967	$238,448	$299,134

Table 24. Overnight direct capital costs of GT-CAES hybrid plant.

Geothermal Temperature	150 °C	200 °C	250 °C
Geothermal Wells	$29,472,280	$24,224,627	$24,278,587
Geothermal Power Plant	$19,019,694	$13,535,516	$15,186,162
CAES Injection Plant	$12,649,235	$12,649,235	$12,649,235
CAES Recovery Plant	$8,318,437	$9,297,501	$10,598,701
Total	$69,459,646	$59,706,878	$62,712,685
Power Recovery – % of Total Cost	12%	16%	17%

The performance results tabulated in Table 21 show that the round trip efficiency for the lowest grade geothermal resource is 51.2% at 150 °C, consistent with previous studies that evaluated resources over a similar temperature range. The round trip efficiency increases when higher grade geothermal brines are used for air reheating: 59.6% at 200 °C and 65.7% at 250 °C. The efficiency improvement is possible because, for configurations using higher temperature geothermal resources, additional gas expanders and reheating stages can be implemented, and more power can be obtained from each CAES cycle.

The additional capital required to enable these higher thermodynamic efficiencies also results in increased capital costs. The geothermal wells are the largest capital expense for the GT-CAES concept as evaluated here, followed by the geothermal power plant and the compression injection system. The CAES power recovery system is the smallest of the equipment groups in terms of costs. The cost data from Table 24 are plotted in Figure 50 to illustrate the component costs for each resource grade. The improvements to power recovery by the use of additional gas expanders and reheat exchangers can be obtained with a moderate increase in fraction costs of the total plant: in the range of 12% to 17% for the geothermal resources considered (see Figure 51). This suggests that the use of higher grade geothermal resources and the matching multi-stage expansion recovery system to obtain higher energy round trip efficiency may be a viable option in GT-CAES applications.

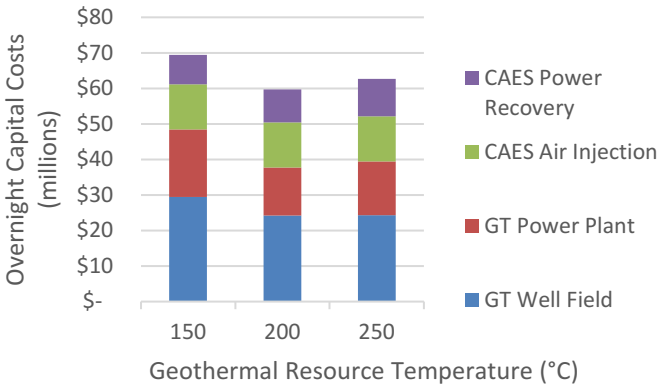

Figure 50. GT-CAES overnight capital costs comparison.

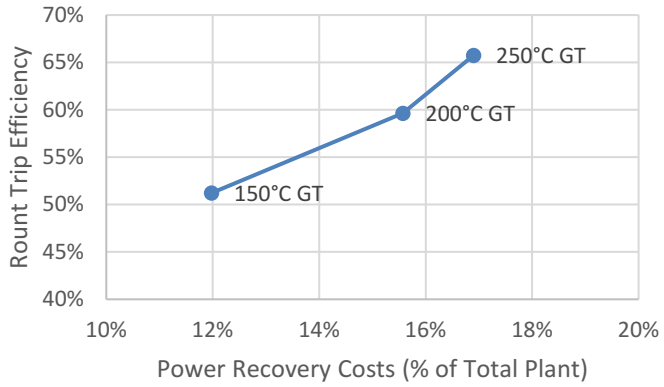

Figure 51. Round trip efficiency and the fraction costs of power recovery system.

7.4 Discussion

This study makes a number of simplifying assumptions that underlie the performance and cost analyses. These assumptions are a function of the common-basis approach taken in the broader geothermal hybrids study, in which a design case was implemented across multiple resource grades to evaluate the relative applicability of hybrid technologies across several resource temperature bins. However, for GT-CAES in particular, the parameters that are necessarily excluded in this approach are many, and include parameters to which GT-CAES costs and applicability are highly sensitive.

For the present study, applications were evaluated against generic geothermal resources, parametrized as a constant flow rate across multiple resource temperature classes. However, the effects of the pressure dynamic on the CAES reservoir associated with diurnal injection and withdrawal of compressed air are not evaluated because they vary so widely from reservoir to reservoir and site to site. As noted in other studies, these pressure excursions can have significant impacts on the local geologic stress regime, which could in turn be a limiting factor for overall air storage potential. This, again, stresses the need for technoeconomic analysis of this complex hybrid application, including its impacts on the subsurface at a site-specific level.

Geofluid temperature will gradually decline over the life of the geothermal field, an effect that could not be readily applied in the present CAES evaluations. Site-specific system design would allow reheaters to

be sized to ensure the expansion air is adequately heated to prevent freezing as the geothermal brine temperature decreases by 20 to 30 °C over the design life of the plant (e.g., by oversizing the initial equipment or building out to meet production decline). The effect of thermal degradation on the round trip efficiency and plant costs would, in turn, depend on the method chosen to address the decline, or impacts to resulting power sales associated with accommodating the decline without system modification in outyears.

Because a GT-CAES facility could be used flexibly—as GT-CAES or as standalone geothermal power generation—a project operator would seek to optimize on revenues associated with ancillary services and baseload generation from the CAES and standalone geothermal modes, respectively. The dispatch price for ancillary services may be significantly higher than that for baseload geothermal, but the market for that higher-value power will also be limited. Similarly, this study assumes that off-peak power is obtained at no cost to the CAES facility operator, with an understanding that the cost of power at times of very low demand may be positive more often than it is negative, but that the proportion and magnitude of these differences will be highly market specific. Operational strategies for optimizing a GT-CAES resource should be based on site-specific parameters, including pricing projections within the local market for the various value streams at the GT-CAES plant. While this sort of site-specific analysis is beyond the scope of the current study, the results presented here are intended to give a sense of how geothermal resource grade impacts overall project economics for GT-CAES projects.

8.0 Geothermal-Enabled Desalination

Highlights

- Geothermal fluid in the temperature range of 100°C to 200°C utilized for heat input to thermal desalination plants
- MED evaluated as the baseline technology for geothermal desalination. MED is a mature technology that can utilize low enthalpy geothermal heat sources and has low electrical power requirements.
- MED desalination plant mass & energy balances were modeled using simplified method described in the open literature

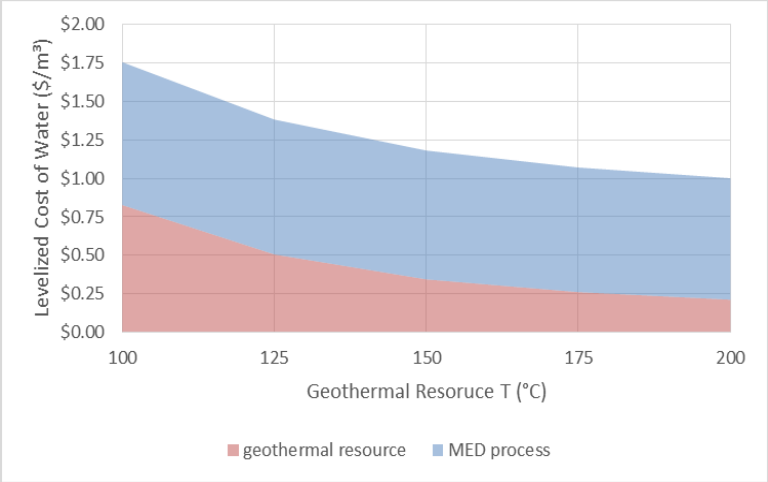

MED Desalination Cost for Hydrothermal Resource in Exploration De-Risk Scenario

- GETEM used to calculate hydrothermal and EGS resource costs in the Business-As-Usual and Exploration De-Risk GeoVision Study Scenarios
- LCOH from geothermal resources in the scenarios evaluated is cost competitive with many of the heat sources examined for MED desalination applications discussed in the literature
- LCOW cost targets are established at $1.50/m³ for the Business-As-Usual (reference) scenario and $1.00/m³ for the Exploration De-Risk (improved) scenario
- In the Business-As-Usual Scenario a hydrothermal resource achieves the LCOW cost target with resource temperatures of approximately 150°C and greater. A hydrothermal resource in the Exploration De-Risk Scenario achieves the LCOW cost target at a resource temperature of 200°C.
- In all cases evaluated, higher temperature geothermal resources demonstrate increased ability to achieve the specified LCOW cost targets
- A literature review indicates that there is significant variability in the reported capital costs for MED desalination plants; more detailed analysis is required to decrease the uncertainty associated with capital costs, feed and cooling water acquisition costs, and concentrated brine disposal costs
- The degree to which the geothermal resource, feed water source, cooling water, water market, and concentrate disposal site are co-located will have a significant impact on the viability of any geothermal desalination application.
- In practice, due to large variations in resource characteristics, site attributes, and application requirements, the economic and logistical feasibility of geothermal desalination is likely to be highly site- and application- dependent

- Although EGS resources in the Exploration De-Risk Scenario do not achieve the LCOW cost target at the resource temperatures evaluated, EGS resources could be deployed at locations where hydrothermal resources do not exist, which would help to address co-location challenges.
- Applications that inherently address co-location issues include treatment of geothermal power plant cooling tower blowdown water and treatment of thermally active co-produced water from oil & gas production operations. GTO is currently supporting research efforts to develop and field demonstrate alternate and/or advanced desalination technologies for these applications.

8.1 Overview

- The most widely used desalination technologies include thermal- and membrane-based technologies. Geothermal energy can be used to drive a desalination process, either through directly providing the heat to drive a thermal desalination process, or by providing electrical power for driving a reverse osmosis (RO) membrane-based desalination process. Numerous different geothermal desalination configurations have been studied, and several have been pilot tested [58, 65-68, 132-136]. As noted by Gude et al [135], there are numerous benefits of using geothermal energy for desalination including:
- Geothermal energy provides a stable and reliable heat supply ensuring the stability of thermal desalination
- Geothermal production technology (extraction of hot water from underground reservoirs) is mature
- Typical geothermal source temperatures are in a temperature range suitable for low-temperature MED desalination
- Geothermal desalination is cost effective, and simultaneous electricity production is possible
- Geothermal desalination is environmental-friendly, as only renewable energy is used with no emissions of air pollutants or greenhouse gases
- Geothermal desalination saves imported fossil fuels which can be used for other purposes.

In this analysis multiple-effect distillation (MED), also known as multiple-effect evaporation (MEE) or multiple effect boiling (MEB), is evaluated as the baseline technology for geothermal desalination. MED is a thermal desalination technology with numerous attributes that make it well suited for use in geothermal desalination applications. MED is a mature technology that has been the process of choice for industrial low-grade-heat-driven desalination since the early 1990s. MED has high reliability with low pretreatment requirements and low electrical power requirements compared to other thermal desalination technologies such as multi-stage flash [137]. Low enthalpy geothermal heat sources (T>60°C) may be utilized for use with MED [132], and MED technology has been demonstrated by Sephton Water Technology to produce up to 20 m^3/day of freshwater from Salton Sea water using 100°C geothermal steam [133] and also utilized on the Greek Island of Kimolos to produce 80 m^3/day of freshwater using a 60-61°C geothermal resource [63]. Additionally, the reliability and robust fouling resistance of MED technology make it suitable for co-produced water treatment [138], which is also a potential geothermal desalination application.

The MED process uses steam to evaporate a portion of the brine fed to the first effect. The distillate vapor is subsequently used to provide heat input to subsequent, lower temperature effects to maximize the energy utilization of the process. Figure 52 illustrates the configuration and operation of a representative MED system [139].

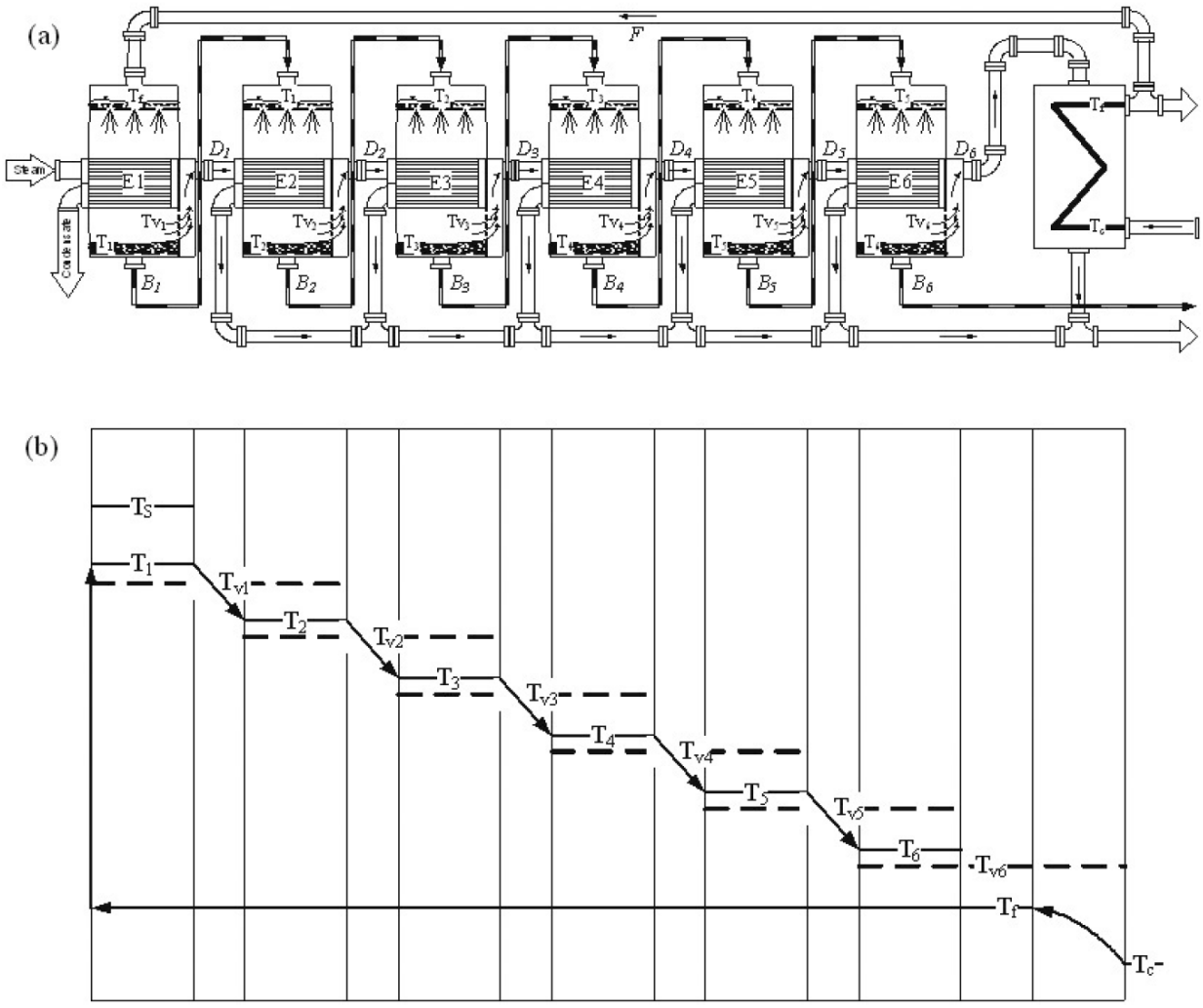

Figure 52. (a) Forward feed six-effect distillation system; (b) temperature distribution through the effects [139].

8.2 Methodology

In order to evaluate the cost of geothermal desalination in each of the scenarios investigated, several case studies were analyzed. Each case study was defined by the selection of a resource type, a GeoVision Study scenario, and the range of resource temperatures evaluated. While in practice geothermal desalination site characteristics and project requirements will vary on a site-by-site basis, the case study analyses were performed using parameters selected to provide generalized results that would be instructive for determining the resource types, resource conditions, and scenarios that would be best suited for geothermal desalination applications.

In this analysis it is assumed that the geothermal resources evaluated are used exclusively for the purpose of providing heat to a geothermal desalination plant. Although the geothermal resource costs are assumed to include the drilling, field gathering system, pumps, and O&M costs, it is assumed that the geothermal resource is developed at an identified site such that there is no cost associated with geothermal exploration. However, the cost of drilling unsuccessful production and injection wells is included in the

drilling costs. The geothermal resource costs are calculated using the GETEM model with input parameters from applicable GeoVision Study scenarios.

The GeoVision scenarios evaluated include the Business-As-Usual Scenario with a brownfield hydrothermal resource and the Exploration De-Risk Scenario with brownfield hydrothermal and EGS resources. Since this analysis assumes a brownfield site it is likely that the desalination process would be located at the same site as new or existing power plants, which would also provide the benefit of readily available electrical power. A listing of the GETEM input variables that differentiate the improved scenarios from the reference scenario is included in Appendix A.

Each case study analysis assumed a project size based on the use of three geothermal production wells, each with a flow rate defined by the applicable GeoVision Scenario evaluated (generally 110 kg/s). Geothermal production fluid temperatures of 100°C to 200°C were evaluated. The steam used for thermal energy input to the MED process is provided by flashing the geothermal production fluid [65, 68, 133, 140]. The flash pressure is selected such that the steam conditions will be consistent with those reported in various MED desalination modeling analyses available in the open literature [140-143]. Geothermal resources with $T \geq 125°C$ are coupled with an 8 effect MED process that uses 0.31 bar steam (70°C), while geothermal resources with $T < 125°C$ are coupled with a 6 effect MED process that utilizes 0.16 bar steam (55°C).

The quantity of water that could be desalinated from each of the geothermal resources evaluated was determined by developing a simplified MED model based on the approach used by Darwish et al [140]. The MED model was used to evaluate gained output ratio (GOR), or the ratio of the distillate output to the steam input for the applicable MED process configuration and operating conditions. The number of effects in the MED model was selected to result in a ΔT between effects of approximately 4°C, which provides a good balance between process cost (lower ΔT results in higher heat exchanger area requirements) and efficiency (higher ΔT results in fewer effects; GOR generally cannot exceed the number of effects).

The feed water is assumed to come from a generic saline water source and to have a total dissolved solids (TDS) concentration of 30,000 ppm. The MED process performance is based on the assumption that the feed water is concentrated to 60,000 ppm. The source of this generic saline feed water could be seawater, water from a saline aquifer, brackish water, wastewater, or geothermal brine. Use of geothermal brine is considered unlikely as use of this fluid could result in reservoir drawdown at hydrothermal sites, and EGS resources require the net addition of water in order to transfer the geothermal heat to the surface.

In this analysis no cost is associated with acquisition of the saline water feed stream, but this assumption is not expected to hold for many potential geothermal desalination applications since at a minimum it would generally be expected that some sort of infrastructure would be required to provide the source water to the desalination process. Additionally, pretreatment is a site specific issue that can contribute to the costs and influence the feasibility of a desalination process. The degree to which the feed stream contains potential fouling agents such as scalants, particulates, and biological components may have a major impact on the overall costs [144]. In this analysis a generic operating cost of $\$0.025/m^3$ was included for cleaning, anti-scalant, and antimicrobial chemicals [145].

Additional site-specific considerations include the MED process cooling source and the concentrated brine disposal. The MED process model assumes use of 28°C cooling water that is provided at no cost. In practice, several process cooling options could be used. Process cooling could be provided by the feed water source, or through use of a cooling tower or air-cooled condenser. Of these options, the use of the feed water source for cooling would likely be the most economical, but includes the limitation that a volume of water in excess of that required for the process feed stream would be required. Similarly, no cost was assigned to disposal of the concentrated brine. In seawater desalination applications the concentrated brine can often be returned to the saline water intake source. Concentrated brine disposal is particularly a problem for inland desalination [144]. The geothermal reservoir may be a suitable

destination for concentrated brine disposal, but further study would be required to determine whether this would adversely impact injection well or reservoir performance.

Another important site-specific consideration is the extent to which the geothermal resource, the saline water source, and an application/market for the purified water product are co-located. If any of these resources is in a location removed from the others, significant costs may be incurred in order to transport all resources to a common site. Since transport costs increase with distance, there will be a maximum allowable radius over which these resources can be obtained; this analysis does not consider costs associated with transporting material or energy for geothermal desalination applications.

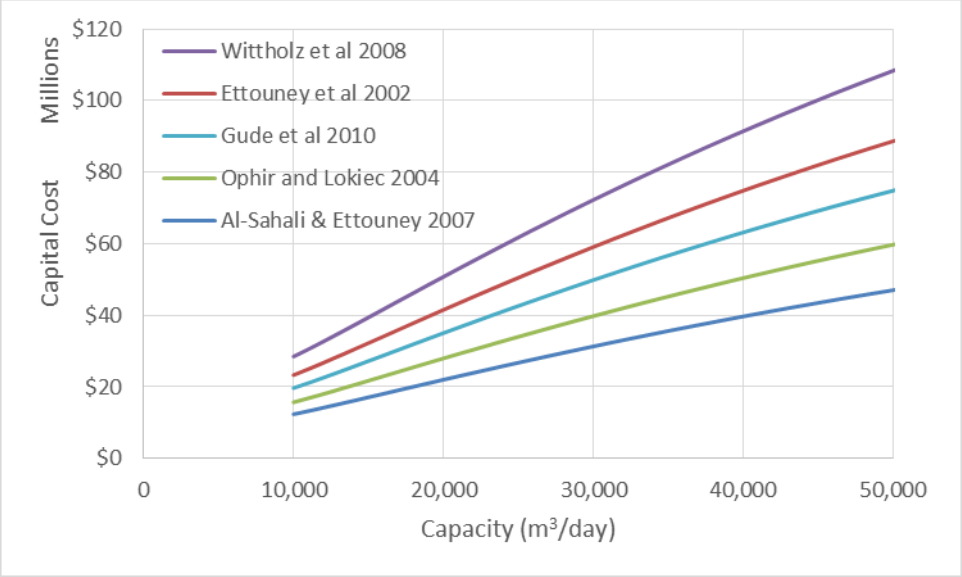

Figure 53. MED desalination plant capital costs vs plant capacity. Curves generated using power law scaling relation based on capital costs reported in referenced literature sources.

MED process capital costs were obtained by scaling values reported in the open literature. The literature includes numerous cost estimates of MED desalination applications, although these costs were reported over a period of several decades for disparate worldwide locations and desalination applications. Figure 53 is a plot of several of the reported capital costs scaled over various MED desalination plant capacities using a scaling exponent of 0.83 as derived from a desalination plant cost database compiled by Wittholz et al [146]. The reference plant capital costs were based on those listed by Gude et al [135] for a 20,000 m^3/day MED desalination plant since this data produced the median capital cost curve from the data evaluated. MED process operating costs include electric power consumption, chemicals, labor, and replacement parts. Estimates for each of these operating cost components were obtained from various literature sources. A summary of all input parameters used to determine the costs of the geothermal resource (calculated using GETEM with applicable GeoVision Scenario inputs) and the MED desalination plant is provided in Table 25.

Table 25. Thermal Desalination Analysis Input Parameters

Input Parameter	Value	Reference or comment
Geothermal Resource		
Resource depth or temperature gradient	1500 m	Hydrothermal resources
	5°C/100 m	EGS resources
Temperature range evaluated	100-200°C	25°C increments evaluated
Reinjection temperature	70°C for production T≥125°C 55°C for production T<125°C	Production fluid flashed to generate steam at pressure corresponding to the reinjection temperature
Production fluid flow rate	330 kg/s	Value corresponds to three production wells at GeoVision Scenario default flow rate (110 kg/s for both Business-As-Usual and Exploration De-Risk Scenarios)
Exploration drilling cost	None	No costs included for exploration drilling; however, geothermal drilling does include costs for failed wells as calculated by GETEM
MED Capital Costs		
Reference plant capacity	20,000 m^3/day	[135]
Reference plant capital cost	$35MM	[135], Additional data for CAPEX estimation provided in [68, 143, 145-151]
Scaling exponent	0.83	[146, 148]
MED Operating Costs		
Plant availability	90%	[143, 145, 146, 148, 150, 151]
electricity cost	$0.05/kWh	[145]
electric power consumption	2.5 kWh/m^3	[143], for fluid pumping power
chemical cost	$0.025/$m^3$	[145]
labor cost	$0.1/$m^3$	[145]
spare parts	1% of CAPEX	[143]
Economic Parameters		
Plant Life	20 years	[68, 136, 137, 143, 146, 152]
Fixed Charge Ratio	0.108	GETEM default input value for legacy FCR based LCOE calculations

8.3 Target Costs and Applications

This analysis did not calculate mass & energy balances or estimate costs for non-geothermal energy based desalination applications. Instead, the literature was reviewed to determine applicable desalination product water costs. The unit cost of large-scale seawater desalination lies in the range of $0.50 and $2.00 per m^3 [146]. Water purchase agreement costs for the Carlsbad RO Desalination Plant are reported as $2131 to $2367 per acre-ft ($1.73 to $1.92 per m^3) [153], although this price is stated to be about twice the price of alternative water sources [154]. While there may be select sites where geothermal energy could be used to desalinate seawater, more opportunities are likely to exist in non-coastal areas of the US where geothermal resources are abundant and fresh water is scarce. Geothermal desalination in the interior US would likely be performed at a smaller scale than the seawater desalination plants, and would likely be used to treat water from saline aquifer, brackish water, or wastewater sources. The current

wholesale cost for small-scale thermal desalination is on the order of $2–$3/m³, which is at the high end of retail water rates in major U.S. cities [154].

Depending on the heat source, a significant fraction of thermal desalination costs can be associated with the thermal energy. Al-Sahali and Ettouney estimate that steam costs account for $0.30/m³ of the product water cost for an MED desalination application in which steam is extracted from a steam Rankine cycle power plant [143]. Following the calculations of Kesieme, it is estimated that steam costs account for approximately $0.70/m³ of the product water cost in an MED application in which the price of the steam is $0.0078/kg ($3.53/MMBtu) and MED process thermal energy requirements per unit of product water equal 60 kWh/m³ [148]. These represent relatively high energy costs for MED desalination, and suggest that there are opportunities for cost reductions through the use of geothermal heat. As noted by Turchi et al, membrane distillation thermal desalination product water cost could be less than $1.00/m³ if thermal energy is inexpensive, as in waste heat or low-cost geothermal energy applications. Such a cost would be competitive with the best desalination applications in the world [154].

For this analysis, desalination applications with water product costs of $1.50/m³ or less are likely cost competitive in various domestic water markets, and deployment of geothermal desalination plants at this price is possible in the Business-As-Usual Scenario provided that low cost sources of feed water and process cooling, as well as suitable water market and/or end use application are readily available. Therefore, $1.50/m³ is specified as the Business-As-Usual (reference) scenario price target in this analysis.

As desalination technology has advanced, the costs of both thermal and RO desalination have decreased. This trend is likely to continue as methods of utilizing low cost heat sources are developed and membrane technologies improve. Therefore, for the Exploration De-Risk (improved) scenario a geothermal desalination a cost of $1.00/m³ is targeted. This cost target is competitive with other desalination technologies that have been deployed in the US. However, in regions with fewer water resources desalination applications with water costs greater than this target value could deploy.

8.4 Results

Geothermal desalination using MED was analyzed in three case studies. The specific case studies evaluated were (1) a hydrothermal resource in the Business-As-Usual Scenario, (2) a hydrothermal resource in the Exploration De-Risk Scenario, and (3) an EGS resource in the Exploration De-Risk Scenario. In all three case studies the geothermal resource temperature was evaluated over the range of 100°C to 200°C in 25°C increments. The scenario selection determined the GETEM inputs used for determining the geothermal resource capital and operating costs.

The capital and operating costs associated with both the geothermal resource and the MED desalination process were evaluated for each case study. Using these costs it was possible to estimate the levelized cost of heat (LCOH) and the levelized cost of water (LCOW) for the range of temperatures evaluated in each case study. The levelized cost of heat calculation uses the geothermal resource capital and operating costs to determine the amortized unit cost of the heat provided by the geothermal resource (Equation 8.1, [154]). This calculation is not specific to the MED application and could be used to estimate the cost of the geothermal energy for any process heat application for which the geothermal heat characteristics were suitable.

$$LCOH = \frac{\left(CAPEX_{geothermal}\right) \cdot FCR + \left(OPEX_{geothermal}\right)}{Annual\ thermal\ generation} \tag{8.1}$$

The levelized cost of water calculation uses the capital and operating costs for both the geothermal resource as well as the MED desalination process to determine the unit cost of the desalinated water

product (Equation 8.2, adapted from [68]). The LCOW reported in this analysis is specific to the use of MED technology for each of the geothermal resources considered.

$$LCOW = \frac{\left(CAPEX_{geothermal} + CAPEX_{desal}\right) \cdot FCR + \left(OPEX_{geothermal} + OPEX_{desal}\right)}{Annual\ water\ production} \quad (8.2)$$

Performance and cost specifications for both the geothermal resource and MED desalination process, in addition to a breakdown of the LCOW cost contributions, are included in Table 26 for the Business-As-Usual Scenario with hydrothermal resources, Table 27 for the Exploration De-Risk Scenario with hydrothermal resources, and Table 28 for the Exploration De-Risk Scenario with EGS resources. Plots of the geothermal resource and MED process cost contributions to the LCOW as a function of geothermal resource temperature are provided for each case study analysis in Figure 54 through Figure 56.

As can be observed from the results presented in Table 26 through Table 28 as well as Figure 54 through Figure 56, the LCOH and LCOW decrease with increasing geothermal resource temperature for all scenarios and resource types evaluated. This is similar to the general trend in which levelized cost of electricity (LCOE) decreases with increasing geothermal resource temperature due to the increase in exergy associated with higher temperature resources (assuming equal development costs and production fluid flow rate for all resources). The higher temperature geothermal resources evaluated in this analysis are therefore most likely to achieve the water purification cost targets listed in Section 3.

In the Business-As-Usual Scenario a hydrothermal resource achieves the reference scenario cost target of \$1.50/m³ with resource temperatures of approximately 150°C and greater. A hydrothermal resource in the Exploration De-Risk Scenario achieves the improved scenario cost target of \$1.00/m³ with a resource temperature of 200°C (although temperatures above 200°C were not evaluated, it is presumed that the LCOW would follow the observed trend of decreasing cost with increasing resource temperature). Although EGS resources in the Exploration De-Risk Scenario do not achieve the improved scenario target cost of \$1.00/m³ at the resource temperatures evaluated, EGS resources have the potential advantage of being deployable at locations where hydrothermal resources do not exist, which would provide much needed flexibility toward meeting the desalination co-location requirements. Ultimately co-location issues, rather than cost targets, are likely to provide the largest barrier to widespread deployment of geothermal energy based desalination processes, and the use of EGS resources in combination with lower cost desalination technologies may be required.

The cost of geothermal heat can also be compared with the cost of heat provided by natural gas combustion, although combustion of natural gas provides heat at a significantly higher exergy which allows for use of a desalination process requiring high-grade heat input and/or cascaded heat use (e.g. power generation and desalination). Nonetheless, a comparison of the cost of geothermal heat versus the cost of steam may be useful in certain circumstances. A review of natural gas prices indicates that \$2/MMBtu (0.68¢/kWh$_t$) is a historically low price. In all of the case studies evaluated, geothermal resources with temperatures ≥150°C are able to provide heat at a lower LCOH (T≥125°C for the hydrothermal Exploration De-Risk Scenario), such that use of geothermal heat would not introduce an economic penalty in thermal desalination applications that would otherwise require a fossil energy heat source. Although not considered in this analysis, analysis by Kesieme et al indicates that the presence of a carbon tax could further improve the economic viability of a renewable energy based desalination process relative to a fossil energy based process [148].

Table 26. Business-As-Usual Scenario with hydrothermal resource

Geothermal Resource					
Resource Temperature (°C)	200	175	150	125	100
reinjection temperature (°C)	70	70	70	70	55
resource depth (m)	1500	1500	1500	1500	1500
No. production wells drilled	3.95	3.95	3.95	3.95	3.95
No. injection wells drilled	2.34	2.34	2.34	2.33	2.33
Avg. distance well to plant (m)	750	750	750	750	750
geothermal pumping power (kW)	2,571	2,613	2,694	2,810	2,946
Geothermal CAPEX					
production well cost	$12,551,000	$12,551,000	$12,551,000	$12,551,000	$12,551,000
injection well cost	$7,437,000	$7,431,000	$7,425,000	$7,421,000	$7,418,000
field gathering system costs	$3,141,000	$3,119,000	$3,102,000	$3,089,000	$3,081,000
GF pump costs	$1,695,000	$1,652,000	$1,639,000	$1,654,000	$1,910,000
indirect costs	$659,000	$651,000	$647,000	$647,000	$681,000
total	$25,484,000	$25,404,000	$25,365,000	$25,362,000	$25,641,000
Geothermal OPEX					
well field maintenance ($/yr)	$353,000	$355,000	$355,000	$356,000	$359,000
pump O&M ($/yr)	$375,000	$332,000	$309,000	$299,000	$298,000
pumping power ($/yr)	$1,014,000	$1,030,000	$1,062,000	$1,108,000	$1,162,000
labor ($/yr)	$137,000	$126,000	$112,000	$95,000	$74,000
MED Desalination Process					
plant capacity (m^3/day)	49,400	39,600	30,000	20,500	12,800
GOR (kg/kg)	7.24	7.24	7.24	7.24	5.63
specific thermal energy (kWh/m^3)	89.3	89.3	89.3	89.3	116.5
MED process equip CAPEX	$74,191,000	$61,715,000	$48,984,000	$35,747,000	$24,176,000
Geothermal Cost Components					
CAPEX ($/$m^3$)	$0.17	$0.21	$0.28	$0.41	$0.66
well field maintenance ($/$m^3$)	$0.02	$0.03	$0.04	$0.05	$0.09
pump maintenance ($/$m^3$)	$0.02	$0.03	$0.03	$0.04	$0.07
pump power ($/$m^3$)	$0.06	$0.08	$0.11	$0.16	$0.28
well field labor ($/$m^3$)	$0.01	$0.01	$0.01	$0.01	$0.02
subtotal ($/$m^3$)	$0.29	$0.35	$0.46	$0.68	$1.11
MED Process Cost Components					
CAPEX ($/$m^3$)	$0.49	$0.51	$0.54	$0.57	$0.62
electric power ($/$m^3$)	$0.13	$0.13	$0.13	$0.13	$0.13
chemicals ($/$m^3$)	$0.03	$0.03	$0.03	$0.03	$0.03
labor ($/$m^3$)	$0.10	$0.10	$0.10	$0.10	$0.10
spare parts ($/$m^3$)	$0.05	$0.05	$0.05	$0.05	$0.06
subtotal ($/$m^3$)	$0.79	$0.81	$0.84	$0.88	$0.93
Cost Summary					
LCOW ($/$m^3$)	$1.07	$1.16	$1.30	$1.56	$2.04
LCOH (¢/kWh)	0.318	0.393	0.519	0.761	0.949

Table 27. Exploration De-Risk Scenario with hydrothermal resource

Geothermal Resource					
Resource Temperature (°C)	200	175	150	125	100
reinjection temperature (°C)	70	70	70	70	55
resource depth (m)	1500	1500	1500	1500	1500
No. production wells drilled	3.95	3.95	3.95	3.95	3.95
No. injection wells drilled	2.34	2.34	2.34	2.33	2.33
Avg. distance well to plant (m)	750	750	750	750	750
geothermal pumping power (kW)	2,571	2,613	2,694	2,810	2,946
Geothermal CAPEX					
production well cost	$6,507,000	$6,507,000	$6,507,000	$6,507,000	$6,507,000
injection well cost	$3,856,000	$3,852,000	$3,849,000	$3,847,000	$3,845,000
field gathering system costs	$3,141,000	$3,119,000	$3,102,000	$3,089,000	$3,081,000
GF pump costs	$1,695,000	$1,652,000	$1,639,000	$1,654,000	$1,910,000
indirect costs	$659,000	$651,000	$647,000	$647,000	$681,000
total	$15,857,000	$15,781,000	$15,744,000	$15,744,000	$16,024,000
Geothermal OPEX					
well field maintenance ($/yr)	$209,000	$210,000	$211,000	$211,000	$215,000
pump O&M ($/yr)	$375,000	$332,000	$309,000	$299,000	$298,000
pumping power ($/yr)	$1,014,000	$1,030,000	$1,062,000	$1,108,000	$1,162,000
labor ($/yr)	$137,000	$126,000	$112,000	$95,000	$74,000
MED Desalination Process					
plant capacity (m^3/day)	49,400	39,600	30,000	20,500	12,800
GOR (kg/kg)	7.24	7.24	7.24	7.24	5.63
specific thermal energy (kWh/m^3)	89.3	89.3	89.3	89.3	116.5
MED process equip CAPEX	$74,191,000	$61,715,000	$48,984,000	$35,747,000	$24,176,000
Geothermal Cost Components					
CAPEX ($/$m^3$)	$0.11	$0.13	$0.17	$0.25	$0.41
well field maintenance ($/$m^3$)	$0.01	$0.02	$0.02	$0.03	$0.05
pump maintenance ($/$m^3$)	$0.02	$0.03	$0.03	$0.04	$0.07
pump power ($/$m^3$)	$0.06	$0.08	$0.11	$0.16	$0.28
well field labor ($/$m^3$)	$0.01	$0.01	$0.01	$0.01	$0.02
subtotal ($/$m^3$)	$0.21	$0.26	$0.34	$0.51	$0.83
MED Process Cost Components					
CAPEX ($/$m^3$)	$0.49	$0.51	$0.54	$0.57	$0.62
electric power ($/$m^3$)	$0.13	$0.13	$0.13	$0.13	$0.13
chemicals ($/$m^3$)	$0.03	$0.03	$0.03	$0.03	$0.03
labor ($/$m^3$)	$0.10	$0.10	$0.10	$0.10	$0.10
spare parts ($/$m^3$)	$0.05	$0.05	$0.05	$0.05	$0.06
subtotal ($/$m^3$)	$0.79	$0.81	$0.84	$0.88	$0.93
Cost Summary					
LCOW ($/$m^3$)	$1.00	$1.07	$1.18	$1.38	$1.76
LCOH (¢/kWh)	0.237	0.292	0.385	0.565	0.708

Table 28. Exploration De-Risk Scenario with EGS resource

Geothermal Resource					
Resource Temperature (°C)	200	175	150	125	100
reinjection temperature (°C)	70	70	70	70	55
resource depth (m)	3800	3300	2800	2300	1800
No. production wells drilled	3.95	3.95	3.95	3.95	3.95
No. injection wells drilled	2.77	2.77	2.77	2.77	2.77
Avg. distance well to plant (m)	500	500	500	500	500
geothermal pumping power (kW)	2,566	3,000	3,465	3,755	3,967
Geothermal CAPEX					
production well cost	$14,672,000	$13,115,000	$11,564,000	$10,022,000	$8,486,000
injection well cost	$10,296,000	$9,203,000	$8,115,000	$7,033,000	$5,955,000
field gathering system costs	$1,392,000	$1,383,000	$1,376,000	$1,371,000	$1,367,000
GF pump costs	$1,715,000	$1,867,000	$2,028,000	$2,129,000	$2,204,000
indirect costs	$424,000	$443,000	$464,000	$477,000	$487,000
total	$28,499,000	$26,011,000	$23,548,000	$21,031,000	$18,500,000
Geothermal OPEX					
well field maintenance ($/yr)	$324,000	$298,000	$273,000	$247,000	$221,000
pump O&M ($/yr)	$247,000	$256,000	$271,000	$283,000	$294,000
pumping power ($/yr)	$1,011,000	$1,183,000	$1,366,000	$1,480,000	$1,564,000
labor ($/yr)	$137,000	$125,000	$111,000	$94,000	$74,000
MED Desalination Process					
plant capacity (m^3/day)	49,400	39,600	30,000	20,500	12,800
GOR (kg/kg)	7.24	7.24	7.24	7.24	5.63
specific thermal energy (kWh/m^3)	89.3	89.3	89.3	89.3	116.5
MED process equip CAPEX	$74,191,000	$61,715,000	$48,984,000	$35,747,000	$24,176,000
Geothermal Cost Components					
CAPEX ($/$m^3$)	$0.19	$0.22	$0.26	$0.34	$0.47
well field maintenance ($/$m^3$)	$0.02	$0.02	$0.03	$0.04	$0.05
pump maintenance ($/$m^3$)	$0.02	$0.02	$0.03	$0.04	$0.07
pump power ($/$m^3$)	$0.06	$0.09	$0.14	$0.22	$0.37
well field labor ($/$m^3$)	$0.01	$0.01	$0.01	$0.01	$0.02
subtotal ($/$m^3$)	$0.30	$0.36	$0.46	$0.65	$0.99
MED Process Cost Components					
CAPEX ($/$m^3$)	$0.49	$0.51	$0.54	$0.57	$0.62
electric power ($/$m^3$)	$0.13	$0.13	$0.13	$0.13	$0.13
chemicals ($/$m^3$)	$0.03	$0.03	$0.03	$0.03	$0.03
labor ($/$m^3$)	$0.10	$0.10	$0.10	$0.10	$0.10
spare parts ($/$m^3$)	$0.05	$0.05	$0.05	$0.05	$0.06
subtotal ($/$m^3$)	$0.79	$0.81	$0.84	$0.88	$0.93
Cost Summary					
LCOW ($/$m^3$)	$1.08	$1.17	$1.30	$1.53	$1.91
LCOH (¢/kWh)	0.330	0.401	0.517	0.725	0.845

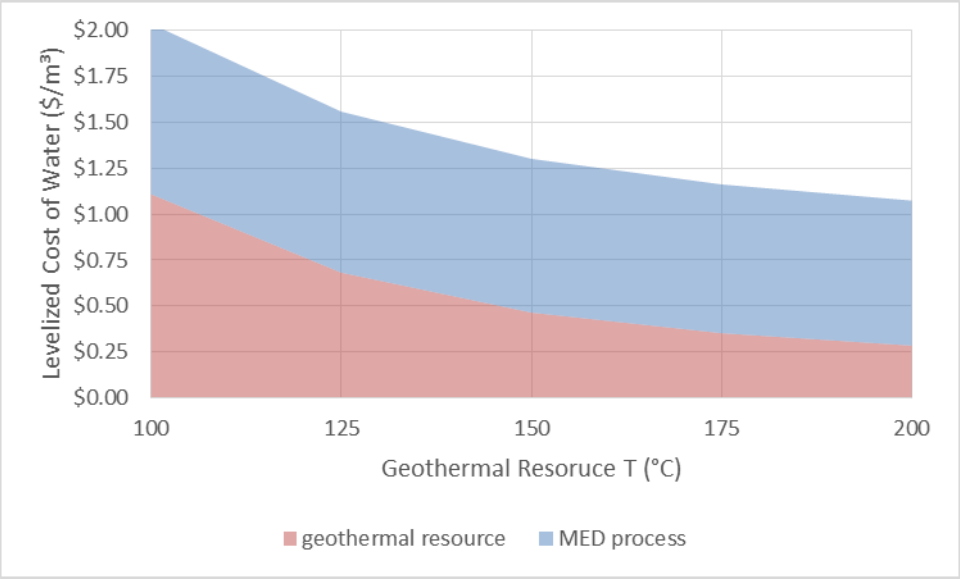

Figure 54. MED Desalination Cost for Hydrothermal Resource in Business-As-Usual Scenario

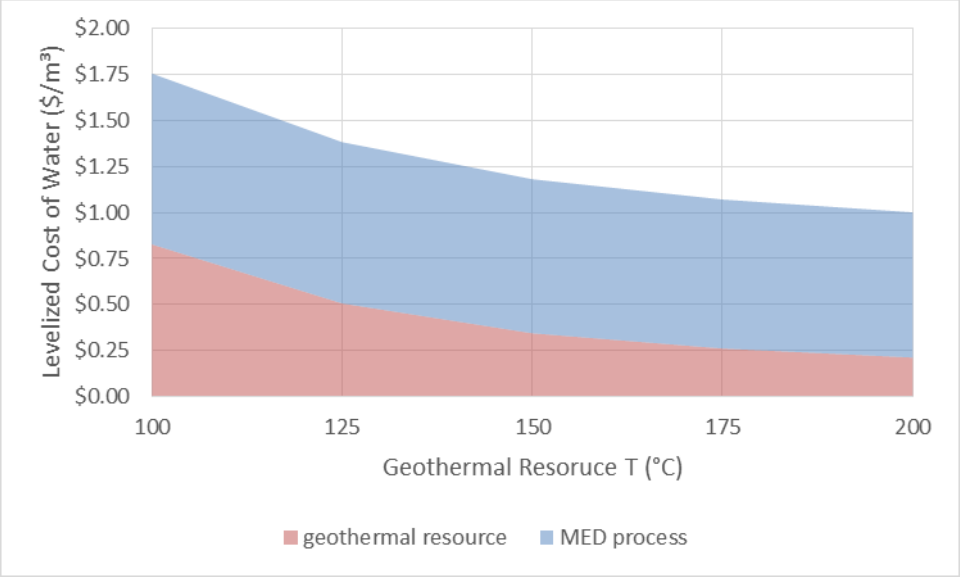

Figure 55. MED Desalination Cost for Hydrothermal Resource in Exploration De-Risk Scenario

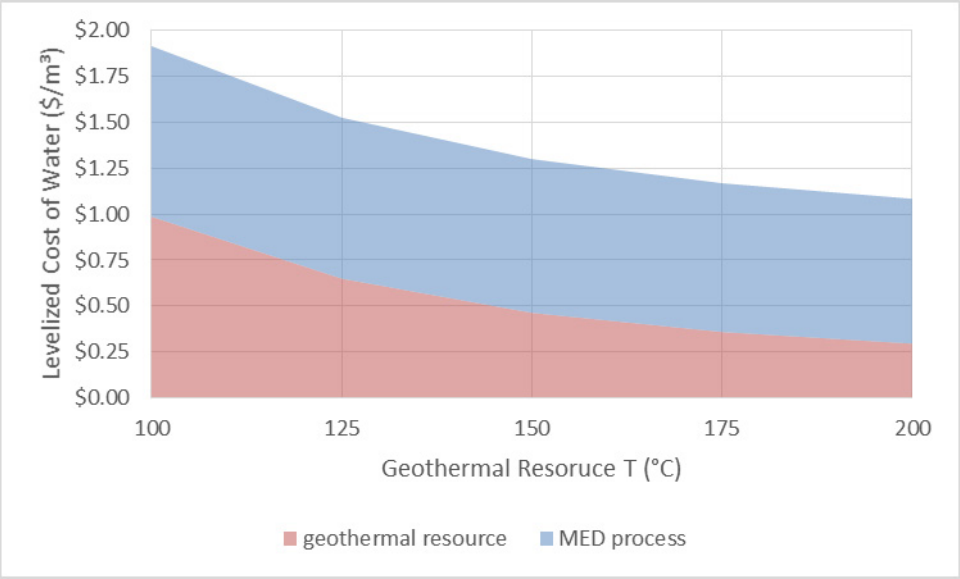

Figure 56. MED Desalination Cost for EGS Resource in Exploration De-Risk Scenario

8.5 Discussion

8.5.1 Limitations and Caveats of the Technology and/or Analysis

The LCOH and LCOW estimates assume that the hydrothermal and EGS resources have the attributes specified in Table 25. Differences in reservoir depth and production fluid flow rate could significantly alter these water purification cost estimates. Further, as previously noted, the LCOW estimates exclude the costs of accessing a saline feed water source, an MED process cooling source, and the disposal of the brine concentrate. The cost associated with each of these requirements is likely to vary widely on a site-by-site basis, and sites where they cannot be provided at low cost are not likely suitable candidates for a geothermal energy based desalination project.

As noted in Section 2, there is significant variability in the capital and operating costs reported for MED desalination processes. A chart of MED process cost components for several cost analyses from the literature is presented in Figure 57. In each of the four literature studies compared in Figure 57 there is also variability in the thermal energy cost component. Kesieme et al assumes use of low pressure steam at a cost of $0.744/m³ with a total product water cost of $1.48/m³ (costs based on 20,000 m³/day capacity without use of waste heat) [148]. Wade presents a case with an MED cost of $0.953/m³ including thermal energy costs of $0.219/m³ from the use of low pressure steam [151]. Al-Sahali & Ettouney assume use of low pressure steam extraction from a power plant at a net cost of $0.30/m³ [143]. NRC [137] reports an estimated seawater desalination cost of $0.72/m³ for a 100,000 m³/day MED plant with a thermal energy cost of $0.27/m³ [137]. The thermal energy costs in these literature studies can be compared with the geothermal energy cost for the various resource types, temperatures, and scenarios reported as the geothermal cost component subtotal in Table 26, Table 27, and Table 28.

For each of the four literature studies cited, the corresponding product water cost is estimated if geothermal heat at temperatures of 200°C and 150°C were substituted for the thermal energy cost used in each of the original analyses (geothermal energy cost estimates correspond to a hydrothermal resource in Exploration De-Risk Scenario). The results of this exercise are displayed using data series with a diagonal fill pattern in Figure 57. Substitution of heat from a 200°C hydrothermal resource in the Exploration De-Risk Scenario results in lower thermal energy costs than used in any of the cases examined from the literature studies referenced. Substitution of a 150°C hydrothermal resource in the Exploration De-Risk

Scenario would result in slightly higher overall product water costs for all of the studies except Kesieme et al, but would nonetheless still result in product water costs of less than the improved scenario cost target of $1.00/m³ if the non-thermal energy cost components from the Al-Sahali & Ettouney or NRC analyses are used.

While this suggests that deployment of cost effective geothermal desalination installations is possible, it also draws attention to the variability of the MED desalination cost estimates available in the literature and highlights that the scaling factor method used in this analysis is not sufficiently accurate for a rigorous determination of the cost effectiveness of a thermal desalination project. Evaluation of the cost effectiveness of a geothermal desalination process will ultimately require use of site- and application-specific operating parameters along with a detailed process design from which all process equipment costs can be determined.

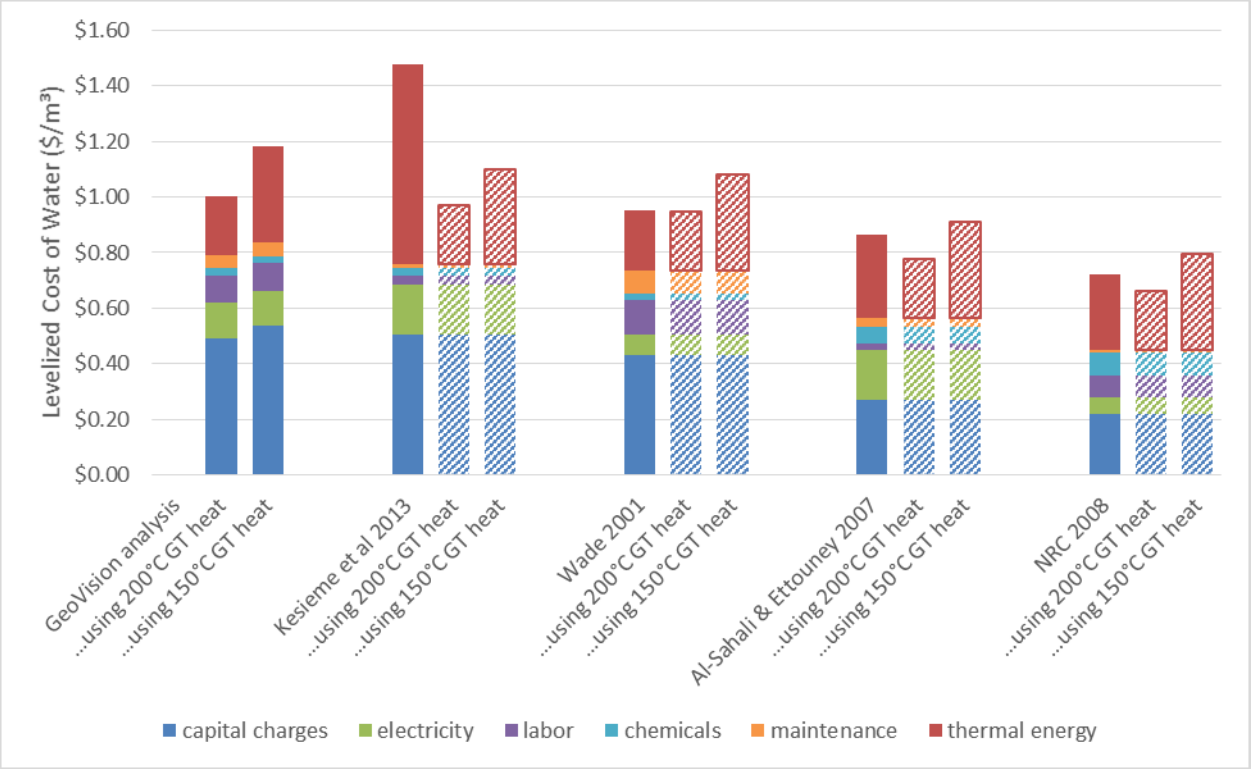

Figure 57. Cost breakdown for several MED thermal desalination cost analyses (Kesieme et al 2013 costs based on 20,000 m³/day capacity without use of waste heat). The second and third columns in each set substitute thermal energy costs corresponding to use of 200°C and 150°C hydrothermal resources in the Exploration De-Risk Scenario.

8.5.2 Benefits and Opportunities for Future Application

Although Figure 57 suggests that MED-based geothermal desalination processes may be able to achieve the specified cost targets, there is additional flexibility with regard to selection of the desalination technology, especially in the case of higher temperature geothermal resources (T>150°C). When higher temperature geothermal resources are available, an alternate thermal desalination technology may increase performance and/or decrease capital costs such that product water costs lower than those reported in this analysis could be achieved. Alternate thermal desalination technologies include membrane distillation (MD), multi-stage flash (MSF), or hybrid technologies such as MED-MSF or MED with thermal vapor compression (MED-TVC) [58, 65, 143, 155-157]. Regardless of the thermal desalination

technology employed, the LCOH values calculated in Table 26, Table 27, and Table 28 can be used to gauge the cost effectiveness of the specified geothermal heat sources relative to other available heat sources.

Thermal desalination based on the use of MED or another technology may be an appealing use of geothermal heat in the cases in which water production costs meet the specified reference or improved scenario cost targets ($1.50/m³ and $1.00/m³, respectively) such that they would be cost competitive with other water sources. However, if the thermal resource, water source, and water market are not co-located for any given application, it is very unlikely that these cost targets will be achievable.

The most likely near term applications for geothermal desalination involve those in which the geothermal heat source is co-located with a wastewater source that can be treated via desalination to offset water purchase or disposal costs. Two candidate applications include treatment of geothermal power plant cooling tower blowdown water and treatment of co-produced water from oil & gas production operations. Both of these applications are currently being investigated by desalination projects supported by the DOE Geothermal Technologies Office.

8.5.3 Cooling Tower Blowdown Water Treatment

Steam geothermal power plants using closed loop cooling towers are reported to have the highest rate of water consumption of all thermoelectric power generation technologies, estimated as 1,400 gal/MWh (5.3 m³/MWh) [158]. This is primarily due to the relatively low efficiency of geothermal power plants, which is inherent to the low temperature characteristics of geothermal heat sources (in comparison with fossil, nuclear, or solar thermal).

Power plants that use evaporative cooling towers consume water through evaporation, blowdown, and drift. Blowdown is the portion of the recirculated cooling water that must be purged to prevent a buildup in the concentration of impurities. The fraction of water consumed via blowdown is a function of cooling tower operating conditions, especially the number of cycles of concentration. When lower quality water is used as the cooling tower makeup water source, the cooling tower must be operated with a lower number of cycles of concentration (5 cycles is considered a low number of cycles [159]) and blowdown can be a significant fraction of the total water consumption (approximately 20% for a cooling tower operating with 5 of cycles of concentration [160]). The cooling tower blowdown requirements for a geothermal power plant could therefore be as much as 280 gal/MWh (1.1 m³/MWh). A thermal desalination technology can be integrated with the power plant to utilize a fraction of the geothermal energy for treatment of the cooling tower blowdown water. The treated blowdown water could then be reused in the cooling tower, which would have the net effect of decreasing total water consumption while simultaneously reducing blowdown water disposal costs.

Membrane distillation (MD) is a thermal desalination technology that can utilize low grade heat to purify a contaminated feed water stream [58, 62, 65, 72]. The National Renewable Energy Laboratory (NREL) and Colorado School of Mines (CSM) are currently working to perform a field demonstration of MD technology for geothermal power plant cooling tower blowdown water treatment [136, 154]. The NREL and CSM project seeks to utilize power plant reinjection fluid to provide the MD process heat requirements.

Due to the large flow rate of injection brine typically available at geothermal power plants, a significant quantity of low-grade heat could be obtained without introducing a large ΔT on the reinjection fluid. Assuming that additional heat can be extracted from the reinjection fluid without violating minimum temperature restrictions (for prevention of geothermal heat exchanger fouling), the only costs associated with this heat source would be any required reinjection piping system modifications and any additional O&M costs associated with pumping the reinjection fluid through the MD heat exchangers. An LCOH estimate for the use of power plant reinjection fluid is provided by Akar & Turchi [136]. The energy harvested from the power plant reinjection water could also be used for purification of water sources other

than cooling tower blowdown, such as saline or brackish water sources located nearby candidate geothermal power plants.

8.5.4 Oil & Gas Wastewater Treatment

Every year tens of billions of barrels of co-produced water are brought to the surface as a byproduct of US oil & gas production. The majority of co-produced water from oil & gas production operations is reinjected into the subsurface. Approximately 45% of produced water is reinjected to for enhanced oil recovery (to maintain reservoir pressure) and ~40% is disposed of via injection [161, 162].

There are numerous potential environmental concerns associated with the handling and disposal of produced water from oil & gas operations, including an increasing number of spills from transport operations and earthquakes from injection into deep disposal wells. Additionally, handling and disposal of produced water is a significant operating costs for oil & gas producers. In general, injection disposal costs have been reported to range from \$0.30/bbl (\$1.88/m³) to as high as \$10.00/bbl (\$62.90/m³) [163]. Cost effective treatment of the produced water stream could simultaneously decrease environmental risks, offset billions of dollars in annual wastewater disposal costs, and provide an additional source of clean water for subsequent beneficial uses.

The MED process reliability and robustness to fouling make it a suitable option for produced water treatment [138]. MED is applicable to all types of water and a wide range of TDS [164], although MED typically achieves a low product water recovery between 20% and 35% [165]. Low product water recovery is problematic for applications in which the goal is to reduce the volume of a wastewater stream.

Forward Osmosis (FO) is a semi-permeable membrane-based thermal desalination technology that can achieve high water recovery from concentrated feed streams. These characteristics make FO well suited for the co-produced water treatment application. The Idaho National Laboratory (INL) and Lawrence Berkeley National Laboratory (LBNL) are currently developing forward osmosis based thermal desalination technologies that could utilize geothermal heat for the treatment of co-produced water. The Switchable Polarity Solvent Forward Osmosis (SPS FO) desalination process requires a heat source of 80°C or greater to regenerate the FO draw solution [77, 166]. An analysis by Augustine and Falkenstern indicates that there are greater than 4 billion barrels per year (~600 million m³/yr) of produced water with an estimated temperature greater than 80°C [167]. The co-produced water could therefore serve as both the feed water source as well as the geothermal energy source for the thermal desalination process. Techno-economic analysis of the SPS FO process estimates water treatment costs of \$3.44/m³ [166]. Assuming 80% water recovery from the SPS FO process and a cost of \$1.00/bbl (\$6.3/m³) for injection disposal of the co-produced water concentrate results in a total water management (treatment plus disposal) cost of \$4.00/m³, which is considerably less than the typical \$1.00/bbl (\$6.3/m³) cost of deep injection disposal of the full co-produced water volume. This suggests that there could be potential for significant deployment of geothermal desalination technology for the treatment of co-produced water.

8.6 Conclusions

In conclusion, the conditions for which geothermal energy based desalination projects will be cost effective are highly site- and application-specific.

- Geothermal resource characteristics are highly variable and the resource characteristics evaluated in this analysis are likely representative for only a small fraction of potential sites
- Desalination requirements are similarly highly variable with differences in the feed water quality and the regional costs of pure water; demand may vary seasonally or annually (due to presence or absence of drought conditions), which further complicates the assessment of the long term viability and applicability of a particular project

- Co-location of resources is a major issue; applications that have the greatest potential for near-term deployment are those where the feed source is a wastewater stream (associated with a geothermal heat source or application) that would otherwise require costly treatment and/or disposal.

In the Business-As-Usual Scenario a hydrothermal resource achieves the reference scenario cost target of $1.50/m³ with resource temperatures of approximately 150°C and greater. A hydrothermal resource in the Exploration De-Risk Scenario achieves the improved scenario cost target of $1.00/m³ with a resource temperature of 200°C. Although EGS resources in the Exploration De-Risk Scenario do not achieve the improved scenario target cost of $1.00/m³ at the resource temperatures evaluated, EGS resources have the potential advantage of being deployable at locations where hydrothermal resources do not exist, which would provide much needed flexibility toward meeting the desalination co-location requirements. Ultimately co-location issues, rather than cost targets, are likely to provide the largest barrier to widespread deployment of geothermal energy based desalination processes, and the use of EGS resources in combination with lower cost desalination technologies may be required.

In addition to applications where resources are naturally co-located, applications where desalination can decrease the volume of water that must be treated or disposed of at a higher cost are most likely to provide sufficient economic benefit to favor deployment. Specific wastewater treatment applications in which geothermal heat is inherently available include the treatment of geothermal power plant cooling tower blowdown water, and treatment of thermally active co-produced water from oil & gas production operations.

In applications where the primary driver for installation of a desalination plant are the demand for purified water, geothermal energy based desalination is expected to be most cost-competitive when using higher temperature geothermal resources, and the cost competitiveness would further increase if the geothermal energy was used in a thermal desalination process with improved performance and/or lower costs relative to the MED baseline desalination process evaluated in this analysis.

9.0 Mineral Recovery: Assessment of Mineral Resources in US Geothermal Brines

Highlights

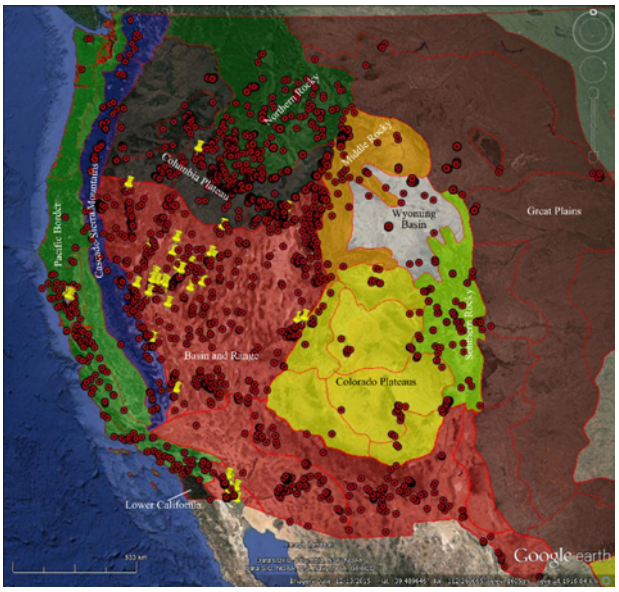

Map of western US brine samples and geographic subdivisions. Geothermal power plant locations designated by yellow push pins.

- Geothermal brines contain dissolved chemical components including critical and strategic mineral commodities at various concentrations. Despite the low concentrations, significant quantities of select minerals could be recovered due to the large volumes of brine utilized by geothermal power plants.
- The potential economic benefits of mineral recovery from geothermal brines has long been identified, however, no commercial recovery of these materials is currently on-going in the US.
- The mineral contents in geothermal brines in the western US geographic provinces were evaluated to identify materials with potential to generate significant revenue. A database of geothermal brine compositions from more than 2250 geothermal features was compiled using various sources. A sub-database for several operational geothermal plants and a separate database for geothermal features with known compositions of rare earth elements (REEs) were also compiled.
- A number of mineral-specific to multi-minerals bench scale extraction technologies are available. Some of these extraction technologies (e.g., SiO_2 and Li) have been successfully tested with pilot-scale facilities in the US.
- The Basin and Range Province has the greatest promise for recovering various minerals. The Great Basin Section of this province offers the best sites for extraction of SiO_2. The geothermal features in the Salton Trough Section of the Basin and Range Province have distinct brine compositions that contain various economic minerals of interest (e.g., Li, Mn, Cs etc.) at higher concentrations.
- Several geothermal brines in the Columbia Plateau Province contain parts-per-billion levels of Ag and Au.
- Geothermal brines that may be good candidates for Li extraction have been identified in various provinces.
- With the exception of a few geothermal features characterized by acidic brines, all geothermal features produce brines with extremely low (ppt to low ppb) levels of REEs. The available data indicate that the extraction of REEs from geothermal brines could be economically prohibitive with the current market forces.
- The extraction of targeted minerals at selected sites could add an additional revenue stream. The potential revenue from recovery of several target minerals for selected operational power plants are

summarized in the table below. However, several outstanding technological, financial, and market challenges currently hinder the recovery of minerals from geothermal brines.

Geothermal Plant	Brine x 1000 (kg/day)[1]	Market values of some recoverable minerals (in $/year @market prices given in Table 29)				
		Ag	Au	Cu	Li	Mn
Beowawe	22,960	78,000		430-4,280	445,000-551,000	1-6
Desert Peak-1	10,230				132,000-529,000	
Dixie	52,610		1,187,000	200-1,600	185,000-1,287,000	0.4-3
Salton Sea	273,130	23,262,000-65,133,000	308,079,000	408,000-6,115,000	226,908,000-1,109,000,000	322,000-1,122,000
Brady	43,190				75,800-1,316,000	60
East Mesa	190,640	325,000-1,948,000	21,504,000-172,029,000	10,700-317,000	1,443,000-70,391,000	10-500
Heber	133,760	911,000		50,000-125,000	3,457,000-8,149,000	320-700
Soda Lake	23,150			430	10,700-363,000	1-4
Desert Peak-2	860				11,100-45,000	
Steamboat Com.	20,830			3,900	12,305,000-19,227,000	11
Stillwater	28,030				388,000-543,000	
Casa Diablo	65,660	22,400-447,000	74,061,000	490-8,600	182,000-2,424,000	0.3-41
Wabuska	14,150	20	8,000	16-260	33,000-69,000	1
Raft River	34,400		32,000	5,100	381,000-953,000	5-7
Tuscarora	31,300				173,000-202,000	
San Emidio	23,130	40	20,900	36-430	470,000-534,000	8-9
Neal[2]	51,060	174,000	57,596,790	1,900	141,000	8
Roosevelt	24,490	375,000		1,400	3,618,000-5,992,000	10

9.1 Introduction

Geothermal fluids are the product of water-rock interactions over a long time at a high temperature and depth. In the process of this prolonged high-temperature water-rock interaction, geothermal fluids pick up several chemical species including some valuable metals from the rock. Specifically, the chemically corrosive and complexing species such as hydrogen, chloride, sulfate, etc., ions in the geothermal fluids help leach out metals from the rocks and sustain their mobility in the geothermal brines. Therefore, the large-volume geothermal brines produced in power plants are likely to contain significant amount of valuable mineral resources. However, traditionally geothermal power plants are built to recoup heat from the brines. The post-production brines are injected back into the geologic formations without intercepting any valuable minerals therein. Therefore, development of cost-effective and deployable mineral recovery technologies can add an additional revenue stream and improve the economics of the geothermal energy.

The western states of the US have been known to have higher geothermal activities with numerous sampling features (Figure 58). Several geothermal power plants have been established at various locations in these areas over the last four decades, and there are numerous additional sites with potential power production using natural hydrothermal or engineered geothermal resources. Over the years, the chemical compositions of geothermal brines/waters of numerous hot springs and wells have been measured. In this paper, we assembled composition data for more than 2250 features scattered all over the US. The chemical dataset was used to assess the potential minerals resources in the US geothermal resources. This paper focuses the general assessment of mineral resources in the US geothermal brines and the existing/available mineral extraction technologies. We identify some target metals/minerals in geothermal brines from several western US geographic provinces. Similarly, we also present preliminary results on the economic values of several minerals in the brines of some operating power plants. Finally, we briefly

present the barriers and challenges that may be hindering for the incorporation of mineral recovery facilities in power plants.

9.2 Approach

We compiled a database for US geothermal brine compositions using various sources such as past reports of the USGS, states water resources management agencies, conference papers, and journal articles. We started data compilation with the USGS open file database for geothermal brines (http://gdr.openei.org/files/194/GEOTHERM_ALL.xls). This database contains over 8000 entries for US geothermal brines. We removed incomplete and redundant data entries of this file. We also assembled as many original sources as possible to make sure the reported concentrations and units in the database were valid. We incorporated additional data to our database for geothermal features that are not included in the USGS data file, and for some features, we replaced the existing incomplete data with the complete data from other sources. For this study, we have compiled a database containing brine compositions for more than 2250 geothermal features (hot springs and wells) (Figure 58a). In addition to this, we prepared a sub-database for several operational geothermal plants (Figure 58b).

A separate database was also prepared for geothermal features with known compositions of rare earth elements (REEs). The REEs data for geothermal brines were primarily assembled from reports and journal articles published by Scott Wood and his groups [103, 168, 169]. Ongoing Idaho National Laboratory (INL) projects have collected and analyzed REEs in several geothermal/oil and gas wells brines of the eastern Snake River Plain (ESRP), southeastern Idaho, and Wyoming Basin. Including the INL's unpublished data, our REEs database includes measured concentrations for about 230 geothermal features in the US.

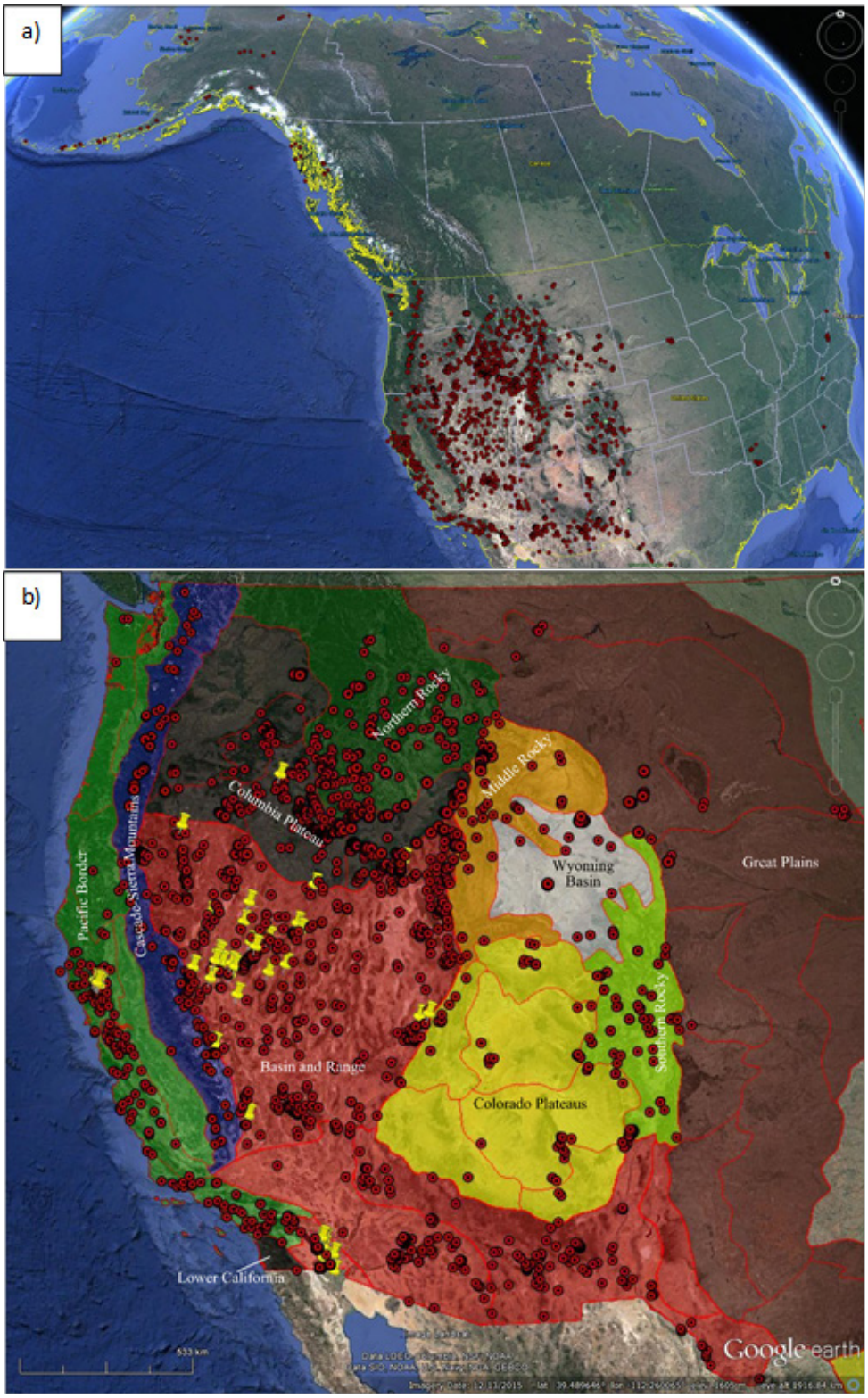

Figure 58. Distribution of the US geothermal brine samples (~2275 samples) with known chemistry. (b) The western US brine samples are plotted on a map with boundaries of geographic subdivisions [170]. Locations of operational (as well as a few planned) geothermal plants are indicated with yellow push pins.

Table 29. Demand and sources of mineral commodities in the US.

Mineral	Demand/ consumption	Price ($)	Purity	Domestic source	Imports (% re-calculated for non-domestic sources)	Ref.
Ag	6900[a]	20.16[b]	99.99%	63%	Mexico (53%), Canada (28%), Poland (6%), Peru (3%), and other (10%).	[171, 172]
Au	165[a]	1335[b]	99.99%	Net exporter[c]	Mexico (52%), Canada (17%), Colombia (11%), Peru (7%), and other (13%).	[172, 173]
B	NA[d]	630[e]	B minerals	~100%	Turkey (81%), China (3%), Argentina (3%), Austria (2%), and other (11%).	[172]
$BaSO_4$	3,420,000[a]	125[e]	$BaSO_4$	21%	China (80%), India (11%), Morocco (4%), Mexico (3%), and other (2%).	[172]
Cs	Few thousands[f]	2020[g]	99.98%	None	Canada (~100%).	[172]
Cu	1,830,000[a]	3.22[h]	Cathode grade	69%	Chile (51%), Canada (26%), Mexico (13%), Peru (6%), and other (4%).	[172]
Li_2CO_3	21300[a,i]	6,600[e]	Li_2CO_3	<50%	Chile (50%), Argentina (46%), other (4%)	[172]
K_2O	5,500,000[a]	730[e]	K_2O	16%	Canada (85%), Russia (10%), Israel (2%), Chile (2%), and other (1%).	[172]
Mn ore	500,000[a]	5.01[e]	46-48% Mn content	None	Gabon (61%), Australia (16%), south Africa (14%), Ghana (4%), other (5%).	[172]
Fe-Mn	370,000[a]	5.01[e]			South Africa (57%), Norway (9%), Ukraine (8%), South Korea (7%), other (19%).	[172]
Si-Mn	150,000[a]	5.01[e]			South Africa (32%), Gabon (22%), Georgia (8%), Australia (12%), and other (26%).	[172]
Pb	1,660,000[a]	1.07[h]	Pb metal	70%	Canada (68%) Mexico (18%), Australia (5%), and other (9%).	[172]
Rb	2000[f]	1472[g]	99.75%	None	Canada (~100%).	[172]
SiO_2 (col.)		1750[e]	30%			[83]
Sn	42,300[a]	8.1[h]	Sn metal	26%	Peru (40%), Bolivia (17%), Indonesia (15%), Malaysia (12%), and other (16%).	[172]
Sr	33,000[a]	50[e]	Sr minerals	None	Mexico (89%), Germany (7%), China (3%), and other (1%).	[172]
Zn	990,000[a]	1.075[h]	Zn metal	19%	Canada (68%), Mexico (13%), Peru (9%), and other (10%).	[172]
Ce_2O_3	17,000[a] (total REEs)	2.5[j]	99% Bulk	None	China (75%), France (6%), Japan (6%), Estonia (4%), and other (9%).	[172, 174, 175]
Dy_2O_3		250[j]				
Eu_2O_3		225[j]				
La_2O_3		2.5[j]				
Nd_2O_3		46[j]				
Pr_2O_3		62[j]				
Sm_2O_3		3.1[j]				

a. metric tons/year. b. per troy ounce (31.104 g). c. In 2015, US mined 211 metric tons of gold, US also imported 315 metric tons and exported 430 metric tons of gold. d. Consumption data not available, but the US also imported and exported B compounds, global production in 2014 was 3,720,000 metric tons. e. per metric ton. f. kilograms. g. per 100 grams. h. per pound. i. converted from Li content to Li_2CO_3. j. per kilograms.

9.2.1 Data Reduction/Illustration

Two approaches were used for data reduction and illustrations. First, we treated all of the US brine samples as a single group and plotted them on a series of maps to illustrate how the concentrations of various minerals of economic interest are distributed in the US. Second, the assembled data were separated into groups depending on their geographic locations. For the contiguous US, we adopted physiographic subdivisions (provinces) given by Fenneman [170] to separate samples into different groups. The brines samples from Alaska and Hawaii (which are given a low priority, and are not discussed in detail here) were grouped state-wise. This grouping of data helped identify potential economic minerals in each of the geographic subdivisions. Finally, annual brine flow rates produced by several geothermal power plants in the US were also assembled. The mass flow rates and concentration of minerals in the brines were used for general estimation of potential new revenue to geothermal power plants from the brine mining.

9.3 The US Demands and Sources of Mineral Commodities

We assembled the US demands, sources, and prevailing market prices of various mineral commodities (Table 29). Specifically, the latest USGS mineral commodity summary [172], reports of the US Congressional Research Service [176], and other sources [174, 175] were used to assemble market parameters for various mineral commodities that could potentially be recovered from the US geothermal brines. Table 29 shows that the US is completely or mostly dependent upon foreign sources for several mineral commodities. Specifically, the US is fully dependent on foreign sources for the Cs, Mn, Rb, Sr, and REEs minerals. Similarly, it imports most of the Ba, Li, K, Sn, and Zn from various countries.

9.4 Distributions of Economic Minerals in the US Geothermal Brines

9.4.1 Precious Metals

More than 150 (7% of the samples in the database) of the US geothermal brine samples (mostly distributed in the Basin and Range and Columbia Plateau Provinces) have known Ag concentrations (Figure 59), and the majority (117) of them have values between 0.01 to 0.1 mg/kg. A good number of samples (ca. 15) have Ag concentration > 0.1 mg/kg, and a few samples from Salton Sea area are reported to have concentration up to 1.4 mg/kg [86]. Figure 60 shows the distribution of geothermal brine samples [about 90 (4% of the) samples in the database] with known Au concentrations. The reported values of Au in geothermal brines range from sub-detection limit to 0.11 mg/kg. Of the samples with known concentrations, 65 samples have Au level ca. 0.1 mg/kg, and majority of these high Au samples are located in Oregon covering both the Basin and Range Province (Great Basin Section) and the Columbia Plateau Province (Blue Mountain and Harney Sections).

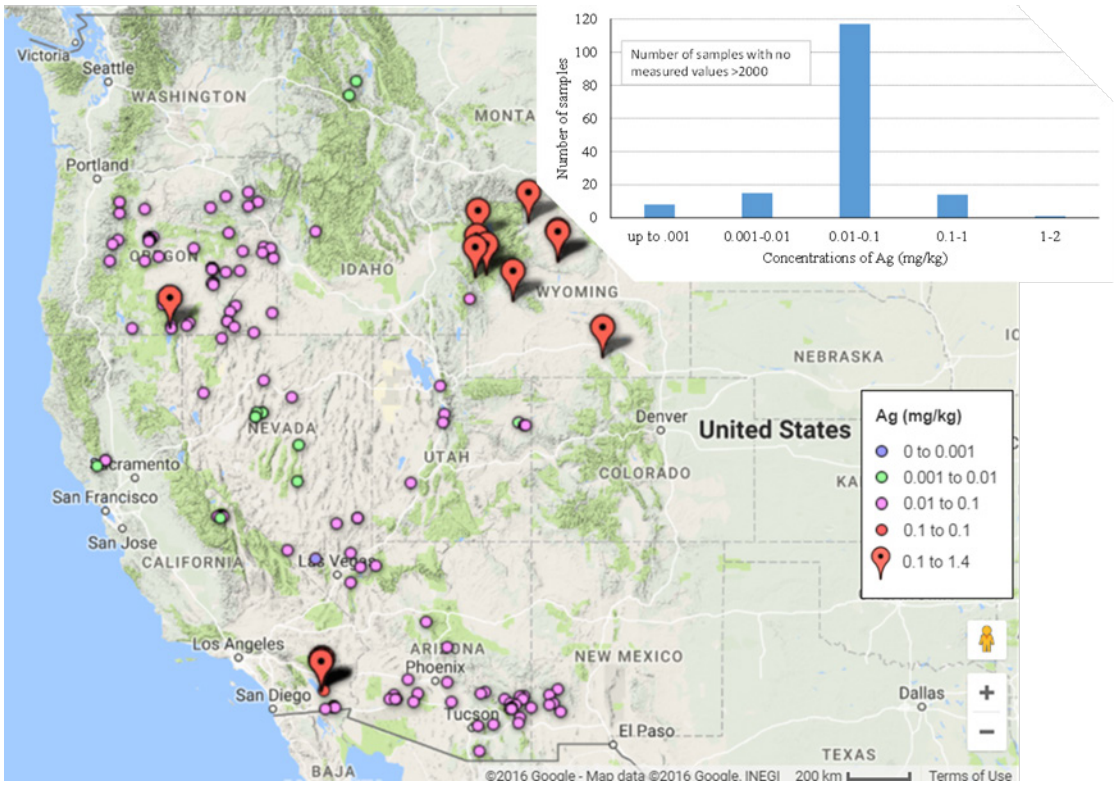

Figure 59. Distribution of geothermal brine samples with measured Ag concentrations.

9.4.2 Copper

In our database, about 500 (22% of the) geothermal brine samples in the database have measured Cu concentrations (Figure 61). The majority of samples with known Cu values have concentrations in the range of 0.001 to 0.01 mg/kg (230 samples) and 0.01 to 0.1 mg/kg (187 samples). About 38 samples have Cu concentrations in the range from 0.1 to 1 mg/kg. However, some samples (9) from Salton Sea area have Cu concentrations >12 mg/kg.

9.4.3 Lithium

Figure 62 shows the distribution of geothermal brine samples (about 1200 or 53% of the samples in the database) in the US with known Li concentrations. The majority of geothermal brines (>900 samples) have the Li concentrations <1 mg/kg. About 263 samples have concentrations in the range from 1 to 10 mg/kg, and about 14 samples are reported to have concentrations in the range from 10 to 20 mg/kg.

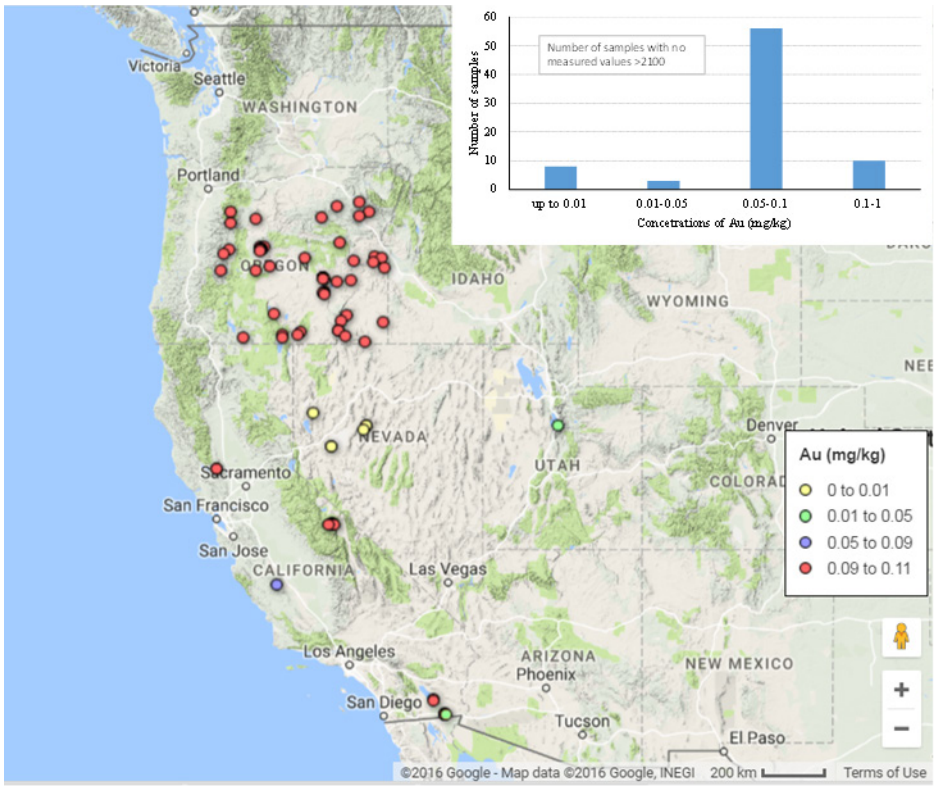

Figure 60. Distribution of geothermal brine samples with measured Au concentrations.

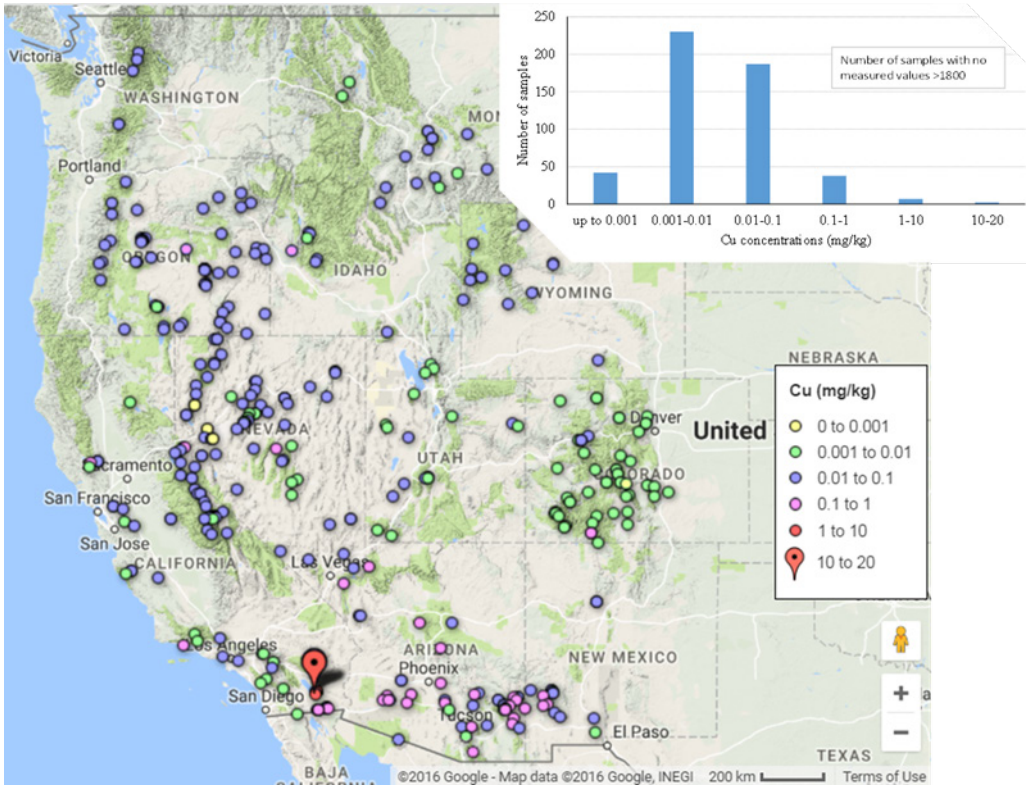

Figure 61. Distribution of geothermal brine samples with measured Cu concentrations

Some brine samples (about 21) have Li concentrations >20 mg/kg. Specifically, brine samples with higher Li concentrations are confined to the Salton Sea area, and several of these brines have up to 400 mg/kg of Li. In the past, several Li extraction technologies were developed for processing brines with Li concentrations typical of the Salton Sea area, and a few of them were successfully demonstrated with a pilot scale plant [177].

9.4.4 Manganese

Our database include about 800 (36% of the) geothermal brine samples with known Mn concentrations (Figure 63). Most of the geothermal brine samples (>700) with reported concentrations have Mn values <1 mg/kg. There are over 50 geothermal brines with Mn concentrations in the range from 1 to 10 mg/kg. Similarly, about 10 geothermal samples have Mn concentrations in the range from 10 to 50 mg/kg, and more than 15 additional samples are reported to have concentrations up to 4000 mg/kg. As with the other minerals of interest, the high Mn brine samples are confined to the Salton Sea area.

9.4.5 REEs

Measured REEs concentrations are available (including published and unpublished data) for about 230 geothermal features and groundwater samples (Figure 64). The majority of the data represent brines collected in Oregon, Idaho, and Wyoming. A few features in California, Nevada, New Mexico, and Washington also have measured values of REEs. In general, the geothermal brines have very minute levels of REEs. With the exceptions of a few features in Yellowstone National Park in Wyoming and Valles Caldera National Preserve in New Mexico, the total REEs in filtered brine samples do not exceed 1 μg/kg (parts-per-billion, ppb). Those samples with >1 μg/kg levels of REEs are from the acidic hot springs with pH <3.5 (Figure 65). All other filtered brines with near-neutral to alkaline pH have ng/kg (parts-per-trillion, ppt) levels of REEs concentrations.

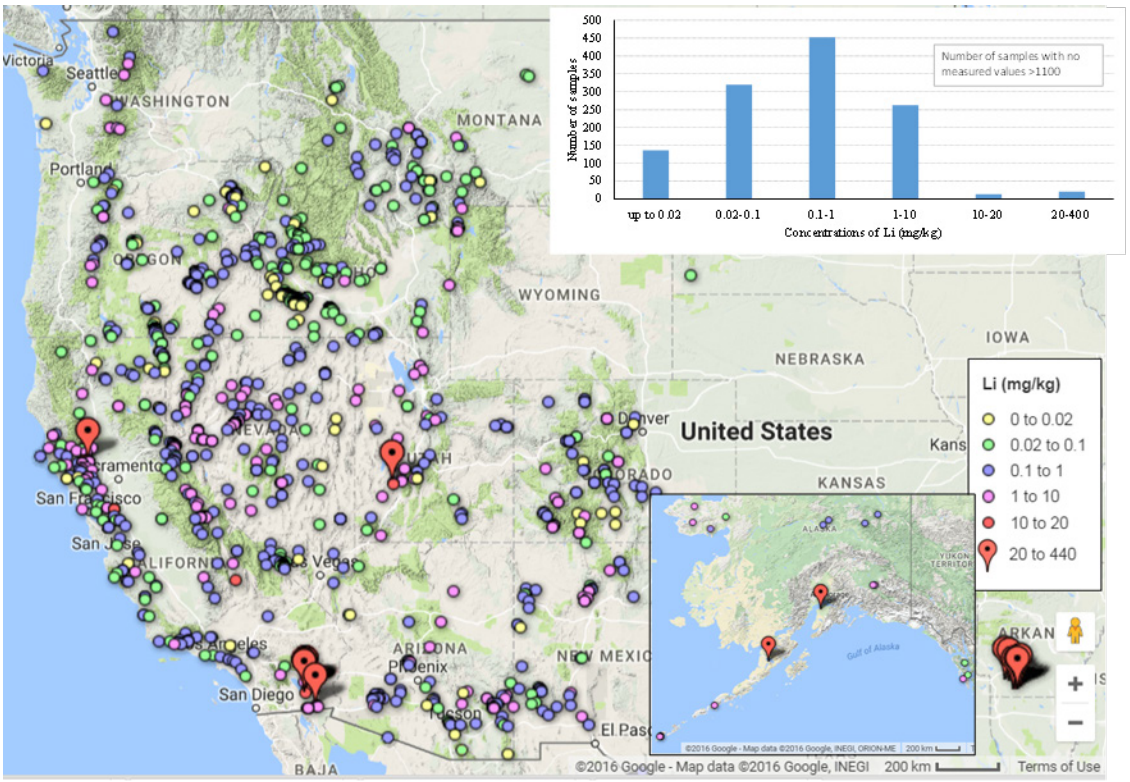

Figure 62. Distribution of geothermal brine samples with measured Li concentrations.

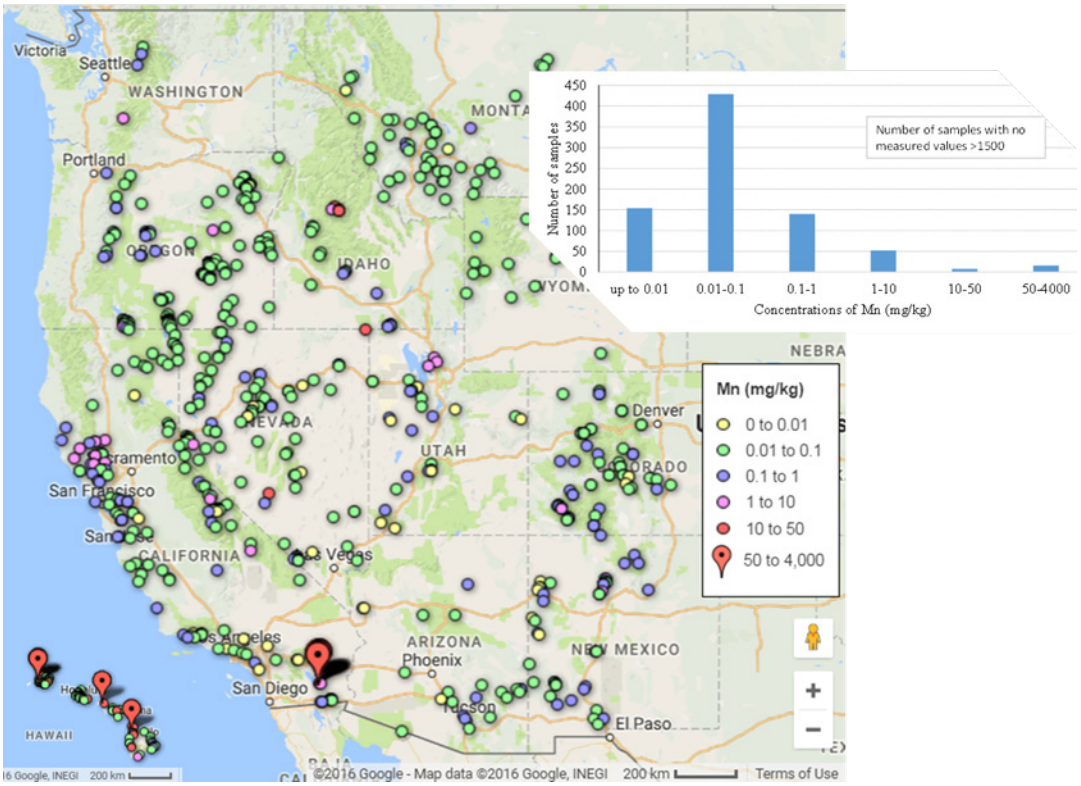

Figure 63. Distribution of geothermal brine samples with measured Mn concentrations.

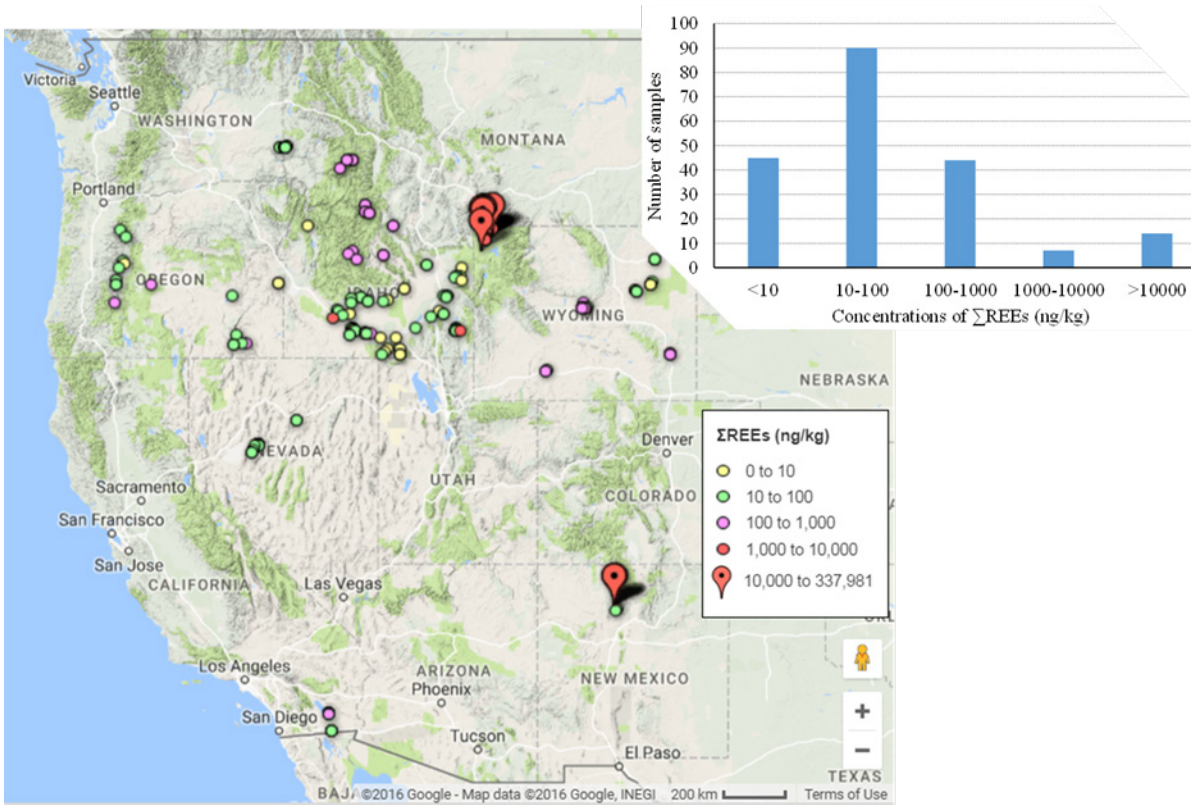

Figure 64. Distribution of geothermal brine samples with measured REEs (total REEs) concentrations.

9.4.6 Silica

Silica is fairly ubiquitous in geothermal brines, and its concentration is reported for most of the brines (over 2200 samples, i.e., 98% of the samples in the database have reported SiO_2 concentrations). In general, the concentration of SiO_2 increases with increasing temperature of the reservoir. Therefore, all operational geothermal power plants or the geothermal sites with potential for power production are likely to have economic level of SiO_2 in their brines. However, not all brines with very high SiO_2 concentrations are economically attractive. Harrison [177] mentions the possibility of extracting SiO_2 and other products from hyper-saline brines, however, it could be a challenge to do so economically. In general, the brines containing relatively low total dissolved solid (TDS) and higher level of SiO_2 could produce high-value SiO_2 products with favorable economics because pre-processing of these brines to remove potential impurities can be avoided. Bourcier et al. [83] demonstrated a SiO_2 extraction scheme with a pilot plant at the Mammoth Lake geothermal site in California. The Mammoth Lake wells produce low TDS (up to 1500 mg/L) brines containing ca. 250 mg/L of aqueous SiO_2. For direct SiO_2 extraction, this is a low level of aqueous SiO_2 and economic recovery of SiO_2 from such brines would require pre-concentration. Bourcier et al. [83] deployed reverse osmosis to pre-concentrate aqueous SiO_2 by a factor of 2.5 to 3.5. The total TDS and SiO_2 in the pre-concentrated brine would then be present at concentrations of 5400 mg/L and 600-900 mg/L, respectively.

The TDS and SiO_2 levels in the original and pre-concentrated Mammoth Lake brines can be used to define a tentative criterion for the selection of potential SiO_2 extraction target brines (Figure 66a). The samples plotted on the lower TDS sides of T1 in Figure 66a are considered good brines for SiO_2 recovery whereas samples plotted between T1 and T2 could be useful for SiO_2 recovery. However, further geochemical analysis with specific composition will be required to assess whether the brines between T1 and T2 could produce high quality SiO_2. All samples that are plotted on the higher TDS side of T2 could

potentially yield poor quality SiO_2 products without pre-removal of impurities. This selection tool indicates that there are about 164 (7% of the) geothermal brines in the database that could be used for recovery of good quality SiO_2 (Figure 66b).

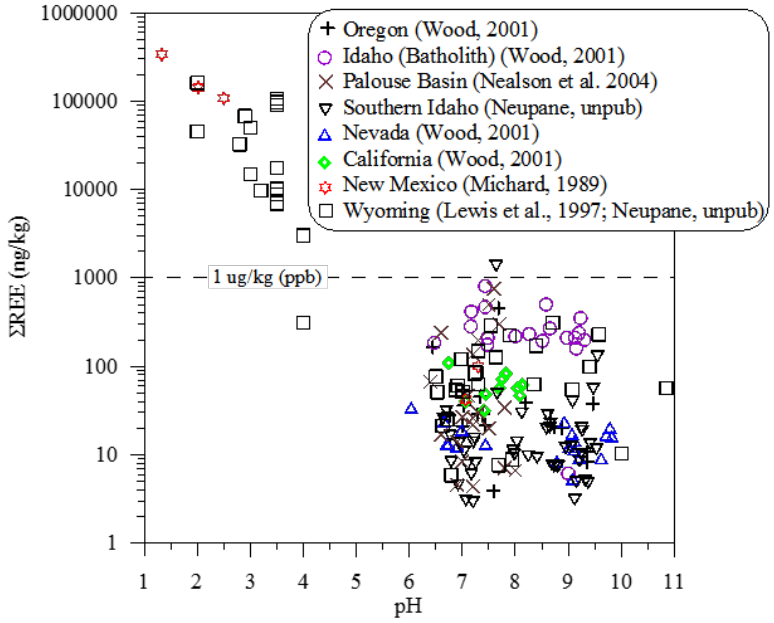

Figure 65. Brine (filtered) concentrations of total REEs plotted against pH. Only acidic brines tend to have > 1 µg/kg (ppb) levels of total REEs.

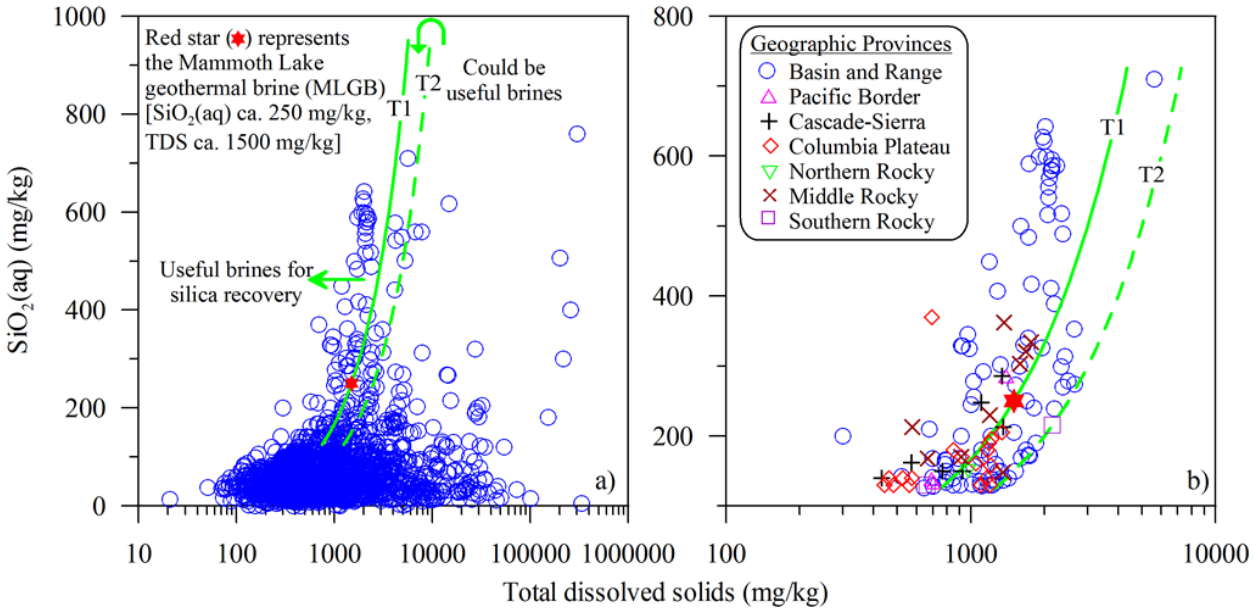

Figure 66. (a) Concentrations of aqueous SiO_2 plotted against total dissolved solids (TDS) in the US geothermal brines. The solid green line (T1) represents the reverse osmosis pre-concentration trend for the Mammoth Lake geothermal brine (MLGB) [SiO_2(aq) ca. 250 mg/kg and TDS ca. 1500 mg/kg [83]]. The dashed green line (T2) is arbitrarily constructed to represent a trend for a brine containing the MLGB level of SiO_2(aq) and the TDS level of about (MLGB+1000) mg/kg. (b) The western US brine samples with positive attributes (TDS level on the lower side of T2 and SiO_2(aq) >125 mg/kg) are grouped according to their geographic provinces.

9.4.7 Potassium

Potassium is one of the major cations in the geothermal brines, and its concentration is commonly measured and reported in general water chemistry data. The majority of the samples in our database have measured concentration of K (Figure 67a). Nearly 2000 geothermal samples in the database have concentrations of K <100 mg/kg. However, there are over 150 samples that have K in excess of 100 mg/kg, and over 20 samples have K concentration >1000 mg/kg. Several hypersaline samples (mostly from the Salton Sea area) have K concentration as high as 24000 mg/kg.

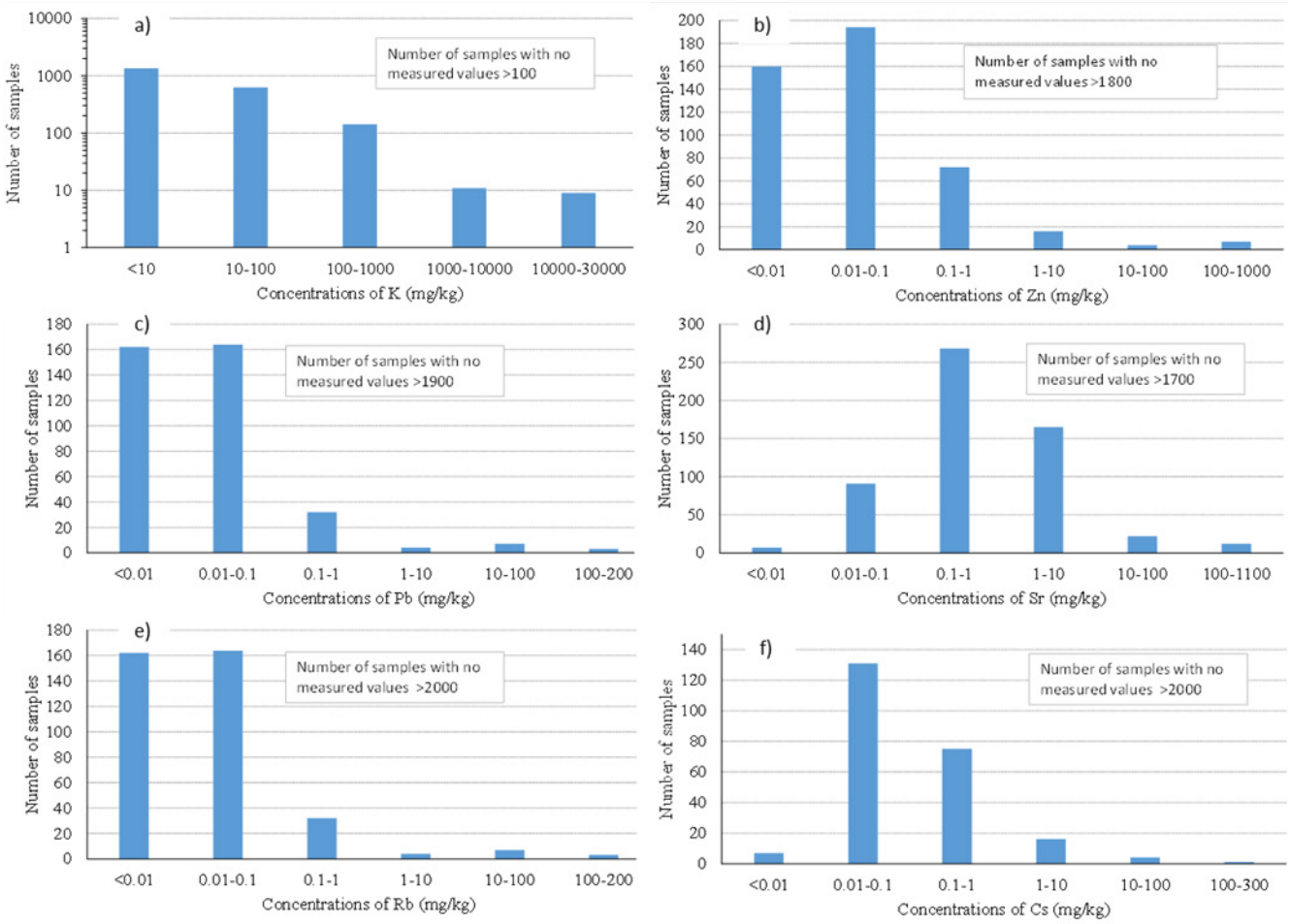

Figure 67. Number of brine samples with various concentrations of K (a), Zn (b), Pb (c), Sr (d), Rb (e), and Cs (f).

9.4.8 Other Minerals in the US Geothermal Brines

In our database, over 450 (20%), 350 (16%), 550 (24%), 250 (11%), and 230 (10) samples in the database have the measured concentrations of Zn, Pb, Rb, Sr, and Cs, respectively. Figure 67b through Figure 67f illustrate the concentration ranges of these minerals in the geothermal brines represented in the database. Most of the brines with measured concentrations have very low values of these elements. For example, only ca. 10 brines samples have the Zn and Pb concentrations >10 mg/kg. Similarly, ca. 35 samples have Sr concentrations in excess of 10 mg/kg. Only five samples have Rb and Cs concentrations >10 mg/kg. Moreover, all the samples with higher levels of these minerals are reported from the Salton Sea area geothermal fields (Salton Sea, East Mesa, Heber, etc.).

9.5 Target Minerals in the US Geothermal Brines

An effort was made to identify a list of target minerals that could have the greatest potential for recovery. For this, the brine samples were grouped according to their locations on a map of the US geographic subdivisions [170]. Specifically, we focused our mineral assessments on several geographic provinces in the western US because the majority of the geothermal features (and available data) are located in this part of the country (Figure 58b). These provinces are: 1) Basin and Range, 2) Columbia Plateau, 3) Colorado Plateau, 4) Northern Rocky, 5) Middle Rocky, 6) Wyoming Bain, 7) Southern Rocky, 8) Cascade-Sierra, and 9) Pacific Border.

Table 30 presents a list of minerals with potential for recovery in each of the province in the western US (Figure 58b). The Basin and Range Province has the greatest promise for recovering various minerals. The Great Basin Section of this province offers the best sites for extraction of SiO_2. Very few sites in other provinces have suitable water chemistry for SiO_2 extraction. The geothermal features in the Salton Trough Section of the Basin and Range Province have distinct brine compositions such as having very high TDS. These high TDS brines also contain various economic minerals of interest (e.g., Li, Mn, Cs etc.) at higher concentrations. Several geothermal brines in the Columbia Plateau Province (Walla Walla, Harney, and Blue Mountains Sections) contain parts-per-billion levels of Ag and Au. Several geothermal brines likely to be good candidates for Li extraction have been identified in various provinces. With the exception of a few geothermal features characterized by acidic brines [e.g., in the Middle Rocky Province (Yellowstone National Park) and Southern Rocky Province (Valles Caldera National Preserve)], all other geothermal features produce brines with extremely low (ppt to low ppb) levels of REEs. The available data indicate that the extraction of REEs from the US geothermal brines could be economically prohibitive with the current market forces.

Table 30. List of minerals with potential of recovery from brines of various geographic provinces.

Geographic Province	Potential Minerals	Remarks
Basin and Range	SiO_2, Ag, Au, B, Cs, Cu, Li, K, Mn, Pb, Rb, and Zn	SiO_2 and K can be recovered from numerous brines; Ag, Au, Cu, Li, Mn, Pb, Zn have recovery potential from Salton Trough Section of this province; Li could be recovered from some brines in the Great Bain Section in Utah and Nevada; B, Cs, and Rb could be recovered from some brines in the Great Basin and Salton Trough Sections.
Columbia Plateau	SiO_2, Ag, Au	Some brines from Walla Walla, Harney, and Blue Mountains Sections have Ag and Au in µg/kg (ppb) levels of concentration. Several brines in this province are identified with positive attributes for SiO_2 recovery.
Northern Rocky	SiO_2	SiO_2 concentrations are relatively low (<125 mg/kg) in most of the brines. One sample is identified with SiO_2 and TDS level suitable for recovery (Figure 66b).
Middle Rocky	SiO_2, Ag, Li	The geothermal features with some recovery potential of these minerals are located in Yellowstone National Park, Wyoming.
Wyoming Basin	Ag	A small number of samples are reported to have about 50 µg/kg (ppb) silver content.
Southern Rocky	SiO_2, Li	Li could be recovered from brines around Vales Caldera National Preserve. Only two brine samples are identified with good attributes for SiO_2 recovery.
Colorado Plateau	Li, K	Li can be recovered from brines located in the Datil and Navajo Sections; K has higher recovery potential from brines in the Canyon Lands Section
Cascade-Sierra	SiO_2, B, Li	A small number of sites have SiO_2 recovery potential; a small number of geothermal waters in the Northern Cascade have B and Li concentrations up to 40 mg/kg and 10 mg/kg, respectively.
Pacific Border	SiO_2, Li,	A small number of sites have SiO_2 recovery potential; a small number of sites have Li concentrations between 10-33 mg/kg.

9.6 Technologies for Mineral Recovery from Brines

Since the 1940s, the possibility of extracting minerals from large-volume of produced geothermal fluids and creating a new revenue stream has been enticing to geothermal communities including private industries and geothermal program at DOE [82, 91, 92, 94, 100, 101, 178]. Early research on mineral recovery from geothermal fluids was conducted in Japan and New Zealand [91, 92]. Since then numerous studies and works, ranging from chemical characterization of geothermal fluids [86, 103] to operation of pilot-scale onsite extraction facilities [83, 177] have been conducted over the years. Table 31 summarizes several technologies suggested for extraction of various minerals from geothermal brines.

In the US, the Salton Sea geothermal brines are known for having high concentrations of metals and other minerals. Initially, these hyper saline brines got attention because of the problems they created such as fouling (scaling) of the wells and waste disposal [78]. Eventually, several studies were carried out aiming to extract minerals from these brines. Werner [101] suggested a serial approach involving sorption of aminated metal complexes on activated charcoal/coke followed by leaching and sequential evaporations in multiple ponds to precipitate chloride salts of Na, K, Ca, Mg, Li, and others from the Salton Sea geothermal brines. Later researchers associated with Hazen Research, Inc. in Golden, Colorado published a series of works on Li recovery from Salton Sea brines for the US Bureau of Mines. Specifically, Berthold and Baker [81] put forward a method for recovering Li from the brines by chemical precipitation and ion-exchange. Their extraction method involved cleaning up post-flash brines (from the Salton Sea Sinclair No. 4) for removal of SiO_2, Fe, Mn, Zn, and Pb prior to Li recovery. In their work, the "clean up" was achieved by adjusting pH to 7.5-8.0. Then the "cleaned up" brine was treated with aluminum chloride (Al:Li ratio 3) to precipitate Li aluminate complex at pH 7.5. Besides suggesting the Li recovery method, Berthold and Baker [81] also identified two important constraints to be considered while developing mineral recovery infrastructure at power producing geothermal sites. These two constraints are: 1) the post-flash brine need to be re-injected regardless of whether or not mineral recovery is performed to sustain the reservoir for a long time, and 2) the post-flash brine should not be chemically altered to the point that it becomes unsuitable for re-injection (left over resin or other chemicals used during recovery).

Maimoni [94] conducted an extensive study on mineral recovery from Salton Sea geothermal brines. Chemical compositions of brines and scales were found to have promising levels of concentrations for several precious and economic metals that could be extracted as value-added commodities. Maimoni [94] notes that for a 1000 MWe geothermal power plant at Salton Sea, the potential revenue from the extraction of metals could exceed the revenue from power production. As an extraction technique, Maimoni [94] suggested a fluidized-bed cementation reaction with metallic iron to recover precious metals, lead, and tin. The post-extraction brines could be injected back to the reservoir through injection wells.

Table 31. Technologies of mineral recovery from geothermal brines.

Mineral	Technology	Remarks	Ref.
Ag	a. Sulphidization using H_2S, NaHS, or Na_2S	Technologies tailored for Salton Sea area brines. Extraction efficiency ca. 100%.	[179]
	b. Metallic iron induced precipitation as sulfide from acidified post-flash brine, magnetic separator/thickener/centrifugation		[94]
	c. Ag recovery/deposition by passing brines through mild steel collection vessel	Extraction in the range of 0.096-0.84 mg/tonne (brine)	[180]
	d. Ag recovery from geothermal scales		[89]

Mineral	Technology	Remarks	Ref.
Au	a. Au deposits in scale		[88, 181]
	b. Au recovery/deposition by passing brines through mild steel collection vessel (plates)	Extraction in the range of 0.007-0.24 mg/tonne (brine)	[180]
	c. Biochemical leaching of geothermal sludge/scales		[182]
B	a. Evaporation of brines, steam heated system (extracted borax salt)	First mineral recovered (Larderello, Italy); facility was run for decades.	[183, 184]
	b. B removal by resin	Developed environmental purposes (not intended for B recovery).	[185-187]
	c. B recovery by sorption on resin	Vionit AS-116 resin tested with brine containing 59-100 mg/kg B for recovery	[188]
	d. B removal by electrocoagulation	Developed for environmental purposes. Removal efficiency ca. 95%.	[189]
Ba (as $BaSO_4$)	a. Gypsum-induced precipitation of Ba-salt, non-evaporative	Achieved partial success.	[190]
Cs and Rb	a. Fractional precipitation	Extraction efficiency ca. 70-80%.	[191]
	b. Ion-exchange (e.g., sorption on zeolites)	Extraction efficiency ca. 92%.	[191]
	c. Solvent extraction	Extraction efficiency ca. 96-99%.	[191]
	d. Removal of Cs and Rb (along with K) with tetrafluroborate from desilicated and deferricated brines		[192]
Cu	a. Metallic iron induced precipitation as sulfide from acidified post-flash brine, magnetic separator/thickener/centrifugation		[94]
Li	a. Precipitation of Li as aluminate, non-evaporative	Good recovery (99%), no further refinement process suggested.	[190]
	b. Precipitation as Li-Al by addition of $AlCl_3$ and raising pH to 7.5 with lime slurry, precipitate dissolved in HCl and evaporated at 100ºC to obtain a mixture of chlorides	Further processing include leaching with tetrahydrofuran, evaporation, and re-dissolution in water and treatment with oxalic acid. Extraction efficiency ca. 97%.	[193]
	c. Li co-precipitation with aluminum hydroxide at pH 10±0.5	For Al recycling, desilicate prior to Li extraction. Extraction of ca. 50% (at 64 ºC) and 95% (at 30 ºC).	[99]
	d. LiCl-alumina pellets used to recover (sorb) Li, process can be repeated by unloading (water washing) and loading (reacting with brine)		[79, 80]
	e. Li sorption on improved sorbents from post-flash and SiO_2 removed brine	Demonstrated in a pilot plant. Extraction efficiency ca. 95%.	[194]
	f. Li sorption on Li-Mn or Li-Fe-Mn oxides (spinel)	Extraction efficiency ca. 20 to 96%.	[96, 195-197]
	g. Electrodialysis of desilicated brine (13 ppm Li)	Experimentally verified, pilot-test ready. Extraction efficiency ca. 87%.	[198]
	h. Evaporation and extraction of LiCl along with others		[95]
K (as K_2O)	a. Evaporation and extraction of KCl along with others	Extraction efficiency ca. 80%	[95, 199]
	b. Cation exchange uptake of K by zeolites	Targeted for 50% recovery, process cost found to be unfavorable.	[177]

Mineral	Technology	Remarks	Ref.
Mn	a. Lime-induced selective precipitation of Mn-oxides	Desilication advantageous, mixed precipitates (Fe, Pb, Zn oxides) create difficulty in separation.	[192]
	b. Precipitation from post-flash and desilicated brine		[194]
	c. Precipitation as hydroxides at pH about 8-9	95% extraction, could be economic and competitive with the other commercial operations.	[177]
Pb	a. Lime-induced selective precipitation of Pb-oxides		[190]
	b Sulphidization using H_2S, NaHS, or Na_2S	Targeted for 100% extraction.	[179]
	c. Metallic iron induced precipitation as sulfide from acidified post-flash brine, magnetic separator/thickener/centrifugation		[94]
	d. Precipitation by treating pH-stabilized (with lime) brine with H_2S	Extraction efficiency ca. 99%.	[200]
Pt	a. Recovery of Pt by contacting geothermal brine with carbon	Technology refers to Salton Sea brines	[201]
SiO_2 (col.)	a. SiO_2 pre-concentrated to 1250 ppm (by reverse osmosis) and aged to grow SiO_2 colloids and filtered	Demonstrated with a 20 gpm pilot plant at the Mammoth Lake site.	[83]
	b. Precipitation of SiO_2 as calcium silicates by lime treatment		[202-204]
Sn	a. Metallic iron induced precipitation as sulfide from acidified post-flash brine, magnetic separator/thickner/centrifugation		[94]
Sr	a. Evaporative extraction		[190]
Zn	a. Lime-induced selective precipitation Zn-oxides	Used aqueous ammonia and ammonium chloride solutions to separate Zn. Extraction efficiency ca. 50%.	[190]
	b Sulphidization using H_2S, NaHS, or Na_2S	H_2S at about 1 atm led to precipitate 50% of Zn. With Na_2S treatment, 85% Zn recovered, precipitates contain 31% ZnS, 5% PbS, 14% MnS, and 41% SiO_2.	[179]
	c. Zn precipitation from post-Ag, Cu, Pb, Sn, and Fe (added) recovery brines.		[94, 190]
	d. Precipitation from post-flash, desilicated brine		[194]
	e. Precipitation as hydroxides at pH about 8-9	95% extraction, could be economic and competitive with the other commercial operations.	[177]
	f. Precipitation by treating pH-stabilized (with lime) brine with H_2S	Extraction efficiency ca. 99%.	[200]
REEs	a. Pre-concentration of REEs on the specialized resin and recovery by acid elution		[100, 178, 205]
	b. Capturing REEs in geothermal fluids by highly-selective engineered microbes		[100, 178, 206]
	c. Recovery of REEs from brines using functionalized magnetic-core nanoparticles	Extraction efficiency up to ca. 95%.	[100, 178, 207]
	d. Sequestration of REEs from geothermal brines on proprietary media		[100, 178, 208]
	e. Recovery of REEs from geothermal waters with advanced sorbet structures		[100, 178, 209]
	f. Magnetic segregation of REEs from hydrothermal products		[210]

Gallup et al. [89, 90] described an electrochemical method to recover Ag and other precious metals from the Salton Sea geothermal brines. Their method involves passing the pH adjusted (to 5) brine through a conduit packed with metal higher in the electromotive series than Ag to precipitate Ag and other precious metals. The suggested packed material is Zn-galvanized steel chicken wire mesh which facilitates precipitation of iron silicate and heavy metal scales. The mesh also acts as a filter where the suspended particles are trapped. The precipitate is then dissolved with acid that leaves precious metal residue. The post-extraction water, which has much less dissolved/suspended load, would extend (x3) the useful life of injection wells. A US patent was granted for this technology. However, no production plant is built employing this technology.

A few years ago, Simbol Materials Inc. operated a pilot-scale Li extraction plant at the Salton Sea [177]. The extraction technology used in the pilot-plant likely involved the co-precipitation of Li with aluminate complex as described in a series of US patents by company employees [79, 80, 192]. Although it was claimed that the pilot-plant successfully extracted the battery-grade Li, a plan to build a full-fledged extraction facility was suddenly stopped because of lack of investors [98]. Recently, it has been reported that a new company (Alger Alternative Energy, LLC.) has acquired Simbol's assets at the Salton Sea site, and is trying to attract new investors to build a full-fledged Li extraction plant [98]. However, it is too early to see how this new effort pans out in enticing new investors for this endeavor.

Bourcier et al. [83] reported a pilot-scale SiO_2 extraction demonstration facility at the Mammoth Lakes geothermal power plant in California. For this technology demonstration pilot plant, about 20 gpm post-production brines (at 50-80 ºC) was routed to the recovery system, which consisted of a two-step process: 1) reverse osmosis, and 2) ultrafiltration. Reverse osmosis concentrated SiO_2 (initial concentration of 250 ppm) to 1250 ppm without SiO_2 fouling, the concentrate was aged to grow SiO_2 colloids and then passed through a cross-flow ultra-filter to extract the SiO_2 colloids. This pilot-scale work demonstrated that the extraction of colloidal SiO_2 with specifications comparable to known commercial colloidal SiO_2 products is possible from geothermal brines.

Currently, DOE is funding several projects to develop technology to extract REEs, Li, and Mn from geothermal brines [100, 178]. In the case of REEs, it is not yet fully understood whether there exist economic levels of concentrations of these elements in geothermal brines. Available data (Figure 65) show very low levels of REEs in geothermal brines. An ongoing research project led by the University of Wyoming [211] is measuring REEs in produced waters from oil and gas wells.

Besides the ongoing and previous mineral recovery work in the US, there have been several mineral extraction studies performed in other countries. Particularly, researchers in New Zealand and Japan have conducted several mineral recovery studies and developed extraction technologies [91, 92, 212]. For example, researchers worked on developing technologies such as co-precipitation of Li-aluminate complex [99] as well as adsorbing Li on manganese oxide and resins [96]. Similarly, some other technologies (e.g., electrochemical, evaporation, etc.) were also included for Li extraction in some studies conducted in New Zealand [91]. In Mexico, Mercado et al. [95] came up with a recommendation for recovering K and Li minerals from Cerro Prieto geothermal brines. They suggested that by recovering salt by evaporating geothermal brines in disposal ponds, the Cerro Prieto geothermal plant could have solved two problems: 1) disposal of a large volume of brine, and 2) developing a domestic source of K and Li for Mexico. However, evaporating a large volume of brines could jeopardize the longevity of a geothermal reservoir by depriving the water to inject back into the formations. Furthermore, the creation of massive evaporating ponds could also be environmentally problematic.

There has also been research performed for extracting B, Mn, Rb, and Cs from geothermal brines (Table 31). These technologies range from absorption of target metals on metal oxides, clays, and resins to electrochemical extractions. Several of these technologies are reported to be effective in test cases; however, further tests mimicking natural scenarios (such as natural brines and T) need to be completed before deploying them for mineral recovery.

9.7 Economic Values of Minerals in Brines of Some Geothermal Plants

For some operational geothermal plants in the US, we assembled both the chemistry and total mass flow rates of brines produced for power generation to assess the revenue that could potentially be generated from the recovery of various minerals. Table 32 includes brines mass flow rates, concentrations, recoverable masses, and market values of Ag, Au, Cu, Li, and Mn. Several assumptions were made to generate the recoverable masses and market values of these minerals. The most important assumptions are that the concentrations of minerals in the brine will not change significantly over time, all of production volume will be available for extraction of minerals, plant outages will be limited (operating 90% of the time), the extraction technology operates at a certain efficiency (80% extraction from brines), there will be minimum market pricing volatility for the minerals of interest, and so on. Similarly, no specific capital and operating costs for any of the potential extraction plants are considered. Data included in Table 32 show that geothermal brines produced in southern California areas have the highest levels of recoverable masses of Ag, Au, Cu, Li, and Mn. Specifically, geothermal plants in the Salton Sea area produce brines rich in these minerals. As with the previous estimates [94], our general estimates show that the Salton Sea area brines could generate substantial revenue from recovery of minerals. However, all past attempts to recover Li and Mn from these brines has been limited to pilot-scale activities, and fully commercial mineral recovery plants have yet to be realized.

9.8 Capital Costs, Operating Costs, and Market Values of Recovered Minerals

Information related to the costs for deployment of mineral extraction technologies is scarce in the literature. Only a few studies with pilot-scale demonstration facilities [83] provide some detailed economics for the deployment of mineral recovery technologies. Simbol's economic analysis for Li and Mn recovery was not accessible to us. Some recent reports [213-215] submitted to DOE by various research groups working on developing new mineral extraction technologies include some preliminary economic analysis. Here we first summarize the results presented by Bourcier et al. [83] as a guide for the potential upfront costs related to a SiO_2 extraction facility. Bourcier et al. [83] did their cost calculations for a facility that would involve both a reverse osmosis process for increasing the brine SiO_2 concentrations and a SiO_2 seeding process for actual SiO_2 extraction. One of the tools they used for estimating the capital and operating costs is used for estimating costs for water treatment facilities (WTCOST [216]). With this tool, they reported a total capital costs of about 25 million dollars and a total operating cost of about 16 million dollars for the SiO_2 extraction plant at a geothermal site producing a brine volumes of 18 million gallon-per-day. Bourcier et al. [83] noted that the calculations they presented have several assumptions and uncertainties, and the cost associated with staffing was considered one of the major uncertainties. Overall, Bourcier et al. [83] show positive economic impacts to the geothermal operator from SiO_2 recovery. Their analysis indicated that SiO_2 extraction could offset the cost of geothermal power by more than \$0.01/kWh and extraction of other metals could generate about \$0.005/kWh per metal.

Table 32. Concentrations, recoverable mass, and market values of some minerals in brines of some US geothermal plants

Geothermal Plant	Brine x 1000 (kg/day)[1]	Concentration (mg/kg)				
		Ag	Au	Cu	Li	Mn
Beowawe	22,960	0.02		0.01-0.1	2.1-2.6	0.014-0.1
Desert Peak-1	10,230				1.4-5.6	
Dixie	52,610		0.002	0.002-0.016	0.38-2.65	0.003-0.02
Salton Sea	273,130	0.5-1.4	0.1	0.8-12	90-440	448-1560
Brady	43,190				0.19-3.3	0.5-0.5
East Mesa	190,640	0.01-0.06	.01-0.08	0.03-0.89	0.8-40	0.02-0.95
Heber	133,760	0.04		0.2-0.8	2.8-6.6	0.9-1.9
Soda Lake	23,150			0.01	0.05-1.7	0.02-0.07
Desert Peak-2	860				1.4-5.6	
Steamboat Com.	20,830			0.01	6.4-10	0.02
Stillwater	28,030				1.5-2.1	
Casa Diablo	65,660	0.002-0.04	0.1	0.004-0.07	0.3-4	0.002-0.24
Wabuska	14,150	0.00001	0.00005	0.00062-0.01	0.26-0.53	0.02
Raft River	34,400		0.000082	0.08	1.2-3	0.06-0.08
Tuscarora	31,300				0.6-0.7	
San Emidio	23,130	0.00001	0.00008	0.00084-0.01	2.2-2.5	0.13-0.15
Neal[2]	51,060	0.02	0.1	0.02-0.02	0.3	0.06
Roosevelt	24,490	0.09		0.03	16-27	0.15
Recoverable masses of some minerals [in troy ounce (31.1 g) per year for Ag and Au, and in metric ton per year for Cu, Li and Mn][3]						
Beowawe		3880		0.06-0.6	13-16	0.08-1
Desert Peak-1					4-15	
Dixie			890	0.028-0.22	5-37	0.04-0.3
Salton Sea		1,154,000-3,231,000	230,800	57-860	6,460-31,580	32,000-112,000
Brady					2-37	6
East Mesa		16,100-96,600	16,100-128,900	1.5-45	41-2000	1-48
Heber		45,200		7-18	98-230	32-67
Soda Lake				0.06	0-10	0.12-0.43
Desert Peak-2					0-1	
Steamboat Com.				0.5	350-550	1.1
Stillwater					11-15	
Casa Diablo		1,110-2,2200	55,500	0.07-1.2	5-69	0.3-4.1
Wabuska		1	6	0.002-0.037	1-2	0.1
Raft River			24	0.723	11-27	0.5-0.7
Tuscarora					5-6	
San Emidio		2	16	0.005-0.06	13-15	0.8-0.9
Neal		8630	43,100	0.27	4-4	0.8
Roosevelt		18,630		0.19	100-170	1
Market values of some recoverable minerals (in $/year @market prices given in Table 29)						
Beowawe		78,000		430-4,280	445,000-551,000	1-6
Desert Peak-1					132,000-529,000	
Dixie			1,187,000	200-1,600	185,000-1,287,000	0.4-3
Salton Sea		23,262,000-65,133,000	308,079,000	408,000-6,115,000	226,908,000-1,109,000,000	322,000-1,122,000
Brady					75,800-1,316,000	60
East Mesa		325,000-1,948,000	21,504,000-172,029,000	10,700-317,000	1,443,000-70,391,000	10-500
Heber		911,000		50,000-125,000	3,457,000-8,149,000	320-700
Soda Lake				430	10,700-363,000	1-4
Desert Peak-2					11,100-45,000	
Steamboat Com.				3,900	12,305,000-19,227,000	11
Stillwater					388,000-543,000	
Casa Diablo		22,400-447,000	74,061,000	490-8,600	182,000-2,424,000	0.3-41
Wabuska		20	8,000	16-260	33,000-69,000	1
Raft River			32,000	5,100	381,000-953,000	5-7
Tuscarora					173,000-202,000	
San Emidio		40	20,900	36-430	470,000-534,000	8-9
Neal		174,000	57,596,790	1,900	141,000	8
Roosevelt		375,000		1,400	3,618,000-5,992,000	10

[1] Brine masses [tentatively (without considering TDS effect) converted from volumes to mass] are obtained from Clark et al. [217] and other open source documents.
[2] Concentrations are reported for the Neal Hot Spring [218]. Available production wells' water chemistry data do not include concentrations for these elements.
[3]Recovery mass calculated assuming 80% efficiency of recovery method(s) and 90% operation time

Ventura et al. [215] presented a preliminary process cost assessment for the recovery of Li and production of Li_2CO_3 from geothermal brines. Their general estimates for a Li plant capable of processing 6000 gallons of brine per minute (containing 400 mg/kg of Li) would have total capital and annual (running for 300 days/year) operating costs of about $20.5 million and $11.1 million, respectively. With a production rate of 49 kg/min of Li_2CO_3 and a very conservative market price ($2000/ton; USGS market price in Table 29 is $6,600/metric ton), Ventura et al. [215] conclude that the Li extraction plant would generate a revenue over $40 million per year. Stull [214] also provides a preliminary cost estimate for recovering REEs from geothermal brines. His study showed the total cost of recovering REEs could be about $89.90/kg whereas the current market price for a blended REEs was reported to be $15.90/kg. Stull [214] concludes that without the improvement in market economics, the extraction of REEs from geothermal brines could be economically prohibitive. Addleman et al. [213] also provide a similarly unfavorable conclusion for the recovery of REEs from geothermal brines. However, they show very optimistic economics for the recovery of precious and base metals. Their preliminary techno-economic analysis estimates a total capital cost of about $43.8 million and an annual operating costs of about $17.2 million for a mineral extraction plant with a processing capacity of 6000 gallons of brine per minute (having "average" mineral contents) generating a gross revenue of about $27.4 million and a net revenue of about $10.2 million with a rate of 23% return on investment (ROI).

9.9 Barriers and Challenges in Mineral Recovery

Review of available literature indicates that the geothermal community has long ago identified that recovery of minerals could be a new and net positive stream of revenue. Some previous studies, for example, Maimoni [94], suggested that the Salton Sea geothermal site could generate more revenue from minerals recovered from the brines than from electricity. Such optimism led industry as well as the US DOE to fund numerous research projects aiming to develop and field test recovery technologies. Outcomes from previous efforts indicate that mineral extraction from the geothermal brines is possible. Specifically, technologies for the extraction of commercial grade SiO_2 and Li have been successfully demonstrated in pilot-scale plants in the US. Nevertheless, the deployment of these extraction technologies at a large scale at any geothermal site has not yet been realized. Therefore, it is equally important to recognize the outstanding issues that may have hindered the construction and operation of extraction facilities alongside geothermal power production.

Major barriers for the large-scale mineral extraction from geothermal brines can range from the lack of deployable technologies to the presence of very low mineral contents in brines. As noted earlier by Berthold and Baker [81], the extraction process should keep the post-mining brines chemically acceptable for reinjection back into the formations for a sustainable operation of power plants. The industrial scale mineral recovery technologies need to be successfully verified for the target brines with onsite pilot plants. Aside from Li and SiO_2 extraction technologies, the other extraction technologies have not been tested in pilot-scale plants in the US. Several mineral recovery technologies presented in Table 31 seem very promising (showing high recovery efficiency); however, most of the performance results were based on laboratory bench-scale experiments that used simple brines with far less chemical complexity than real brines. Even for the field-tested technologies, full-fledged recovery plant have not yet materialized. Specifically, the early optimism generated by Simbol's plan for Li extraction from the Salton Sea geothermal brines decreased over time due to a lack of investors to build an extraction plant [98]. The general hesitancy of investors to invest in such plants could have stemmed from the fear that the expected economic benefits may soon vanish because of market forces such as competition from traditional miners/producers. Roth [98] noted that the Simbol's plan was likely failed to entice new investors because the currently dominant Li mining companies might have discouraged them for investing in a new approach of Li recovery from geothermal brine. Therefore, it is likely that the risk-averse geothermal power operators and hesitant investors will remain one of the greatest challenges for future industrial scale brine mining from geothermal brines.

Other issues such as the presence of low mineral content in the brine could be prohibitive for extraction. For example, the concentrations of REEs in near-neutral to alkaline geothermal brines tend to be very low, and economical extraction of these elements may not be possible. Both Stull [214] and Addleman et al. [213] show that the recovery of REEs from geothermal brines is not economic with current market prices.

9.10 Conclusions

In this study, we assembled over 2250 compositions of geothermal brines representing numerous hot springs and thermal wells in the US and assessed them for their contents of economic minerals. The mineral loadings in geothermal brines vary, ranging from extremely low levels for some minerals to high levels for others. In general, our resource assessment shows that numerous geothermal brines in the US contain concentrations for some minerals that could, if successfully recovered, potentially provide a new value-adding revenue stream to the geothermal industry.

Brine contents of precious metals (Ag and Au) stand out in their potential for positive economic impact to the geothermal operators in the Salton Sea geothermal areas. Furthermore, the Salton Sea geothermal brines also contain economic levels of Li, Mn, and K among others. Some brine samples from the Columbia Plateau Province (Walla Walla, Harney, and Blue Mountains Sections) also contain parts-per-billion levels of Ag and Au. The Middle Rocky Province and Wyoming Basin Province are other areas with geothermal brines having detectable levels of Ag.

Most of the geographic provinces in the western US have geothermal brines with positive attributes for SiO_2 recovery. Particularly, several geothermal systems in the Basin and Range Province produce brines suitable for SiO_2 recovery.

Recovery of Li could be done from brines from the Basin and Range (besides the brines of the Salton Trough Section), Middle Rocky, Southern Rocky, Colorado Plateau, Cascade-Sierra, and Pacific Boarder Provinces. Similarly, the recovery of K could be done from geothermal brines in the Basin and Range and Colorado Plateau Provinces.

The concentrations of REEs in (filtered) geothermal brines are very low. Available REEs data for the US geothermal brines with potential for high volume production do not appear promising for economic recovery of these elements.

Despite extraction technologies having been verified for economic recovery of some minerals (e.g., Li, and SiO_2) the commercial extraction of minerals have yet to be started in the US. Even though the Salton Sea geothermal brines show very profitable mineral recovery scenarios, the latest effort to recover industrial scale Li from these brines by Simbol Materials Inc. did not come to fruition. For other minerals, the recovery technologies are limited to laboratory bench-scale experiments/performance tests. For these low technical readiness level (TRL) technologies, it is important to perform pilot-scale testing prior to commercial-scale deployment. For sustainable recovery, the extraction technology needs to be designed for the mineral types, contents, overall chemistry of the target brines, and likely future market conditions for the mineral commodities.

10.0 Mineral Recovery: Potential Economic Values of Minerals in Brines of Identified Hydrothermal Systems in the U.S.

Highlights

- Brine compositions for several identified hydrothermal resource areas are assembled from various publicly available sources. The mineral loadings in the geothermal brines from these areas vary, ranging from extremely low levels for some minerals to high levels for others.
- In general, our resource assessment shows that numerous geothermal brines in the US contain concentrations for some minerals that could, if successfully recovered, potentially provide a new value-added revenue stream to the geothermal industry.
- This case study analysis identifies some target metals/minerals in geothermal brines and presents potential economic revenues from recovery of these minerals. The analysis considers the 92 identified hydrothermal resource areas in the U.S. included in the Potential to Penetration (P2P) task force geothermal resource database.
- Our assessment shows that for several hydrothermal resource areas, economic potential from recovery of precious metals (Ag and Au), Cs, Rb, Li, and SiO_2 are very promising. However, none of these minerals are currently recovered from US geothermal brines. Recovery technologies for the majority of these minerals are at low technology readiness levels (TRL), and mostly limited to laboratory bench-scale level analyses. Only Li and SiO_2 extraction technologies have been tested at the pilot-plant scale.
- The unit value of all recoverable minerals at each site, both with and without silica recovery, was estimated in units of $/kWh (potential value of mineral recovery revenue per unit of electrical power generation). Sites that appear to be candidates for mineral recovery based on an initial screening of potential revenue should be further evaluated to determine the potential net profits from mineral recovery activities (net profit calculation must include capital, operating, maintenance, and other financial costs).
- The potential unit value of minerals (with or without SiO_2) for these sites ranges from negligible to up to $13.9/kWh. When all recoverable minerals are considered, 15% of the sites (14 of 92) have negligible (<$0.01/kWh) value of minerals, although the number of sites with negligible mineral content increases to 54% (50 of 92) when the potential value from extraction of SiO_2 is excluded. However, the sites with the highest economic impacts from mineral recovery include potential revenue from non-SiO_2 minerals such as Cs, Li, Rb, and precious minerals.
- For several sites, the potential revenue from mineral recovery outweigh the cost of power generation. When all recoverable minerals are considered, brines of 25% of the sites (23 of 92) contain greater value of minerals than the cost to generate power from those brines. Although extraction of all recoverable minerals may not be feasible, if targeted mineral extraction at candidate sites is performed it is very likely that the revenue from minerals could offset some of the cost associated with power generation.

10.1 Introduction

Several states in the western US have high potential to use geothermal energy. The United States Geological Survey (USGS) has defined multiple geothermal areas in the western US as identified

hydrothermal resource areas [219]. Geothermal power plants have been established at various hydrothermal resource areas over the last several decades, and there are numerous additional sites with power production potential.

Geothermal power plants utilize subsurface natural heat for power production. The heat brought up to the surface via a large volume of hot brine (or steam) is captured for power production, and the post-power production brine is pumped back into the geologic formation to sustain the reservoir productivity. Chemical compounds contained in geothermal fluids are the product of long-duration subsurface water-rock interactions at high temperature. Specifically, chemically corrosive and complexing species such as hydrogen, chloride, sulfate, etc., ions in the geothermal fluids help leach metals from the rocks and sustain their mobility in the geothermal brines. Since geothermal plants utilize large volumes of brine, the overall extractable mass of certain minerals could be a source of significant additional revenue. However, geothermal power plants are conventionally built to recoup heat but not minerals. Therefore, development of cost-effective mineral recovery technologies could add an additional revenue stream and improve the economics of geothermal resource utilization.

This analysis assesses the content of economic minerals and their potential values in brines of several identified hydrothermal resources. In our previous work [220], we assessed the mineral contents in numerous US geothermal features and presented economic values of various minerals at several operational geothermal power plants. In this chapter, the analysis is extended to additional hydrothermal resource areas in the US. The majority of these areas do not have operational geothermal power plants, but they could be developed for power production and additional resources such as extractable minerals. In this study, we identify some target metals/minerals in geothermal brines and present potential economic revenues from recovery of these minerals. Our results are preliminary estimates, and we recommend further case-by-case detailed evaluations of the brine chemistry; sustainability; availability, efficiency, and processing costs for applicable extraction technologies; as well as analysis of potential market forces that could affect mineral commodity pricing.

10.2 Approach

Over the years, the chemical compositions of US geothermal brines have been measured and reported by various institutions and groups (e.g., USGS, DOE, states' water resources management agencies). Neupane and Wendt [220] compiled a chemical database for over 2250 geothermal brines in the US. From that database, we selected a subset of data for several identified hydrothermal resource areas. The composition of brines representing these hydrothermal resource areas were assembled from various publicly available sources, e.g. [86, 218, 221-248].

Brine mineral content and mass-flow rates are required to calculate the potential mass of minerals that could be recovered. The mass-flow rates of the potential geothermal plants at several hydrothermal resource sites are estimated using Geothermal Electricity Technology Evaluation Model (GETEM). GETEM is an Excel-based tool that estimates the cost associated with exploration, well field development, power plant construction along with operational costs and levelized cost of electricity (LCOE) from geothermal resource input specifications [249]. In this analysis the resource input parameters for each site were obtained from the geothermal resource database used in the GeoVision Study market penetration analysis. When both the mass-flow rate and concentration of minerals are known, the total mass of minerals that could be recovered from the brines can be estimated.

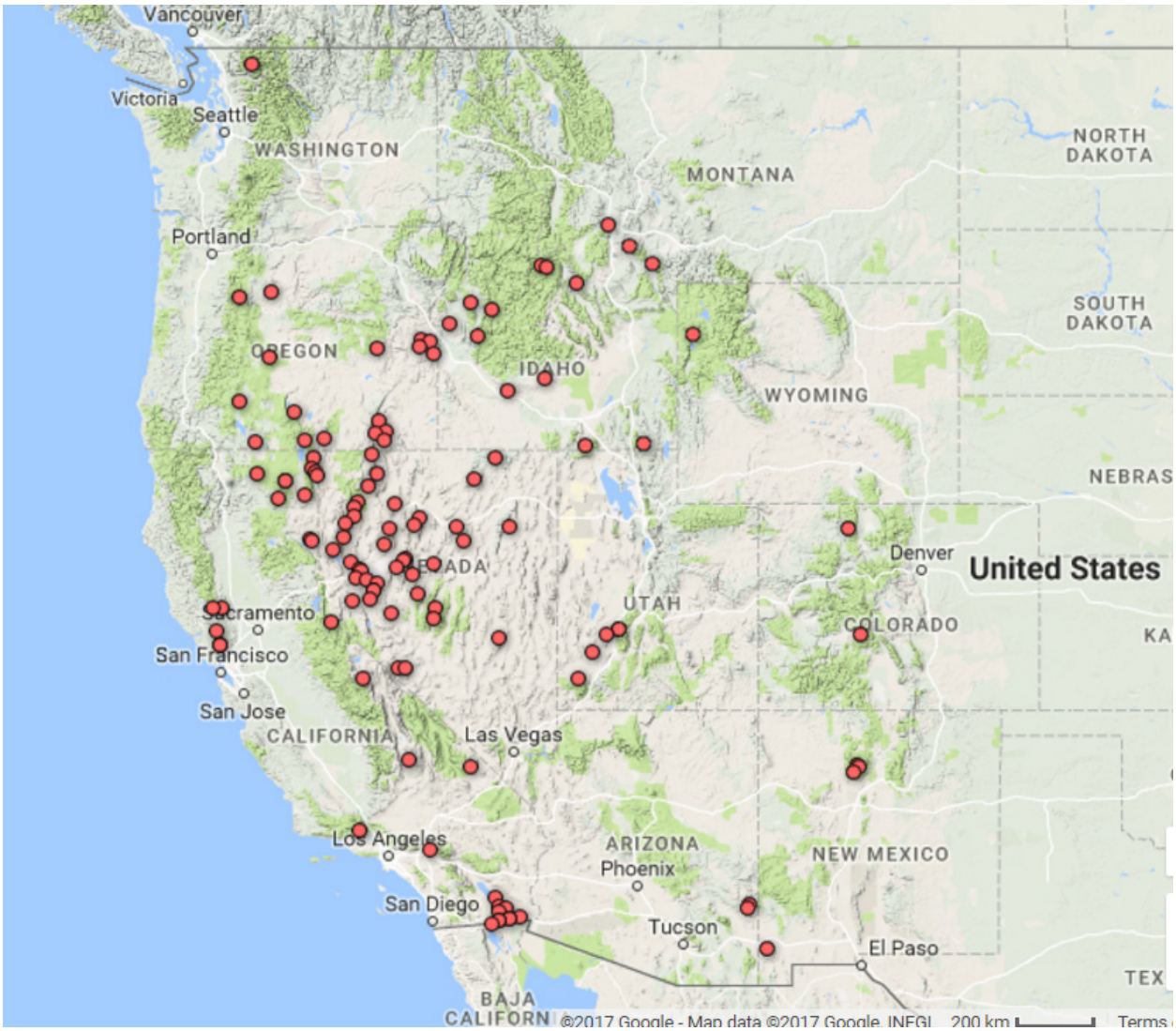

Figure 68: Map showing locations of identified hydrothermal resource areas in the western United States.

For this study, we have selected 92 identified hydrothermal resource sites in the US (Table 33). The main selection criteria for these sites was the availability of both brine chemical composition data and an estimate of brine mass-flow rate (estimated using GETEM with geothermal resource temperature and power generation potential input from the GeoVision Study geothermal resource database). Sites in Hawaii and Alaska are excluded in this study. The geographic distribution of these sites is shown in Figure 68. Table 33 lists GETEM-predicted mass-flow rates along with power generation capacity included in the GeoVision Study geothermal resource database. Using the mass flow rate and concentration of various minerals in brine for each hydrothermal site, we calculated the potential mass of minerals that could be available for recovery. Economic values of various minerals are calculated using market prices for various minerals listed in our previous paper [220].

Table 33. Potential power capacity and GETEM estimated flow rates for several hydrothermal areas.

Site	Capacity (MW)	Flow rate (kg/s)	Site	Capacity (MW)	Flow rate (kg/s)
Alvord HS	24.4	1011	Lake City HS	125.9	3543
Amedee	7.0	525	Lakeview area	25.2	1096
Arrowhead HS	8.8	621	Latty HS	7.9	626
Baker HS	28.4	1901	Leach HS	9.4	565
Baltazor HS	25.7	1015	Lee HS	33.0	1068
Beowawe HS	51.6	706	Leonards/Seyferth HS	12.4	651
Big Creek HS	26.3	1109	Lightning Dock	5.7	293
Black Rock Point area	10.7	641	Little Valley area	18.3	976
Boyes HS	10.5	850	Long Valley - deep	59.4	920
Brady HS	22.6	485	Magic Reservoir area	11.3	939
Breitenbush HS	9.9	330	McLeod	12.3	741
Butte Springs (Trego)	9.1	632	Mickey HS	51.3	1297
Calistoga HS	21.1	810	Mitchell Butte	12.6	784
Canby (I'SOT)	11.8	709	Neal HS	37.0	1235
Clear Lake	36.5	241	Olene HS	10.3	840
Clifton HS	18.1	1466	Pinto HS	32.5	1139
Colado area	13.5	1129	Raft River	33.7	1159
Coso area	347.1	2501	Roosevelt HS	64.4	615
Cove Fort - Liquid	12.2	418	Routt	10.4	842
Crane/Cove Creek area	68.5	2040	Rowland HS	7.3	595
Crump's HS	55.0	1776	Salton Sea area	2103.1	12603
Darrough HS	14.2	913	San Emidio Desert area	77.2	1475
Deer Creek HS	19.6	980	Sespe HS	13.4	807
Desert Peak	19.3	262	Sharkey HS	12.5	851
Dixie HS	12.1	525	Silver Star HS	11.4	791
Dixie Valley Geothermal Field	116.6	1415	Smith Creek Valley	15.6	810
Dixie Valley Power Partners	97.4	729	Soda Lake area	46.5	705
Double HS area	11.7	705	Sonoma Mission Inn	7.9	625
Dyke HS area	6.8	553	Squaw HS	17.4	817
East Mesa (Deep)	66.3	1243	Stillwater area	60.8	1766
East Mesa (Shallow)	45.6	1231	Summer Lake HS	10.3	870
Emigrant	50.1	1255	Surprise Valley HS	9.7	676
Ennis HS	16.2	1121	Tecopa HS	11.3	643
Fernley area	27.8	829	The Needles	21.7	1346
Fort Bidwell	11.4	947	Thermo HS	6.9	386
Gillard HS	14.7	1197	Trout Creek	11.4	827
Gerlach HS	61.6	1504	Vale HS	56.5	2037
Gregson HS	8.9	722	Sulphur Spring/Valles	34.4	426
Hot Borax Lake	53.6	1732	Vulcan HS	12.6	876
Tuscarora HS	44.9	1419	Wabuska HS	9.5	634
Huckleberry HS	48.4	2884	Waunita HS	15.3	920
Humboldt House	113.0	1703	Battle Creek HS	17.5	804
Jemez Springs	10.8	876	Wendel	14.2	751
Kahneetah HS	7.6	545	West Valley Reservoir	15.7	725
Kellog HS	6.7	547	White Licks HS	11.3	937
Kelly HS	11.8	699	Wilbur Springs	36.7	1060

10.3 Concentrations and economic values of recoverable mass of minerals

Since the measured values of all potentially economic minerals are not available for all brines, we have presented their concentrations and potential economic values of recoverable mass in separate tables (Table 34 through Table 36). Specifically, Table 34 includes concentrations and economic values of precious metals (Au and Ag), Cs, Cu, Mn, Pb, Rb, Sr, and Zn. Similarly, Table 35 includes concentrations and economic values of Li, K, and B in geothermal brines. Table 36 shows concentrations and economic values of silica for some hydrothermal systems that have positive attributes for silica recovery.

Several assumptions were made to calculate the annual recoverable mass and potential revenue. As noted in our previous study, the most important assumptions are: the contents of minerals in the brine will not change significantly over time, all of production volume will be available for extraction of minerals, plant outages will be limited (operating 90% of the time), the extraction technology operates at a certain efficiency (80% extraction of each mineral from the brines), and there will be minimum market pricing volatility for the minerals of interest.

Table 34. Concentrations and potential economic values of various minerals in geothermal brines.

Site	Ag	Au	Cs	Cu	Mn	Pb	Rb	Sr	Zn
Concentration (mg/kg)									
Alvord HS	0.02	0.1	0.2	0.05	0.02	0.06	0.33	0.92	
Beowawe HS	0.02		1.04	0.01	0.014	0.06	0.266	0.015	2.3
Breitenbush HS	0.02	0.1	0.1	0.01	0.22	0.06	0.18	0.73	
Crump's HS	0.02	0.1	0.1	0.01	0.03	0.06	0.07	0.12	
Dixie Valley Geothermal Field	<0.001	0.002	0.6	0.002	<0.002	0.002	0.62	0.45	0.02
East Mesa (Deep)	0.06	0.01		0.1	0.95	0.5		320	0.07
East Mesa (Shallow)	0.01	0.01	1.8	0.89	0.05	0.5	0.6	6.4	0.01
Gillard HS	0.07		0.1	0.12	0.02		0.02	0.09	0.13
Gerlach HS	0.02			0.01	0.02				
Hot Borax Lake	0.02	0.1	0.1	0.03	0.03	0.06	0.23	0.42	
Huckleberry HS	0.5			0.01	0.06	0.1			0.02
Kahneetah HS	0.02	0.1	0.1	0.01	0.02	0.06	0.02	0.05	
Lakeview area	0.02	0.1	0.1	0.01	0.02	0.06	0.04	0.32	
Little Valley area	0.02	0.1	0.1	0.01	0.02	0.06	0.02	0.05	
Long Valley - deep	0.04	0.1	0.6	0.03	0.02	0.1	0.48	0.14	0.19
Mickey HS	0.02	0.1	0.1	0.05	0.02	0.06	0.2	0.15	
Mitchell Butte	0.02	0.1	0.1	0.01	0.02	0.06	0.02	0.05	
Neal HS	0.02	0.1	0.1	0.02	0.06	0.06	0.09	0.16	
Olene HS	0.02	0.1	0.1	0.01	0.02	0.06	0.02	0.58	
Salton Sea area	0.5	0.1	20	3	1260	90	25	600	500
Soda Lake area			1.1				0.47	3.77	
Summer Lake	0.02	0.1	0.1	0.02	0.02	0.06	0.02	0.07	
Trout Creek	0.02	0.1	0.1	0.03	0.02	0.06	0.1	0.3	
Vale HS	0.02	0.1	0.1	0.01	0.04	0.06	0.09		
Potential annual economic revenue ($/yr)									
Alvord HS	3.0×10^{5}	9.9×10^{7}	9.3×10^{7}	8.1×10^{3}	5	3.2×10^{3}	1.1×10^{8}	1.1×10^{3}	
Beowawe HS	2.1×10^{5}		3.4×10^{8}	1.1×10^{3}	2	2.3×10^{3}	6.3×10^{7}	12	8.7×10^{4}
Breitenbush HS	9.7×10^{4}	3.2×10^{7}	1.5×10^{7}	530	20	1.1×10^{3}	2.0×10^{7}	270	
Crump's HS	5.2×10^{5}	1.7×10^{8}	8.1×10^{7}	2.9×10^{3}	10	5.7×10^{3}	4.2×10^{7}	240	
Dixie Valley Geothermal Field	2.1×10^{4}	2.8×10^{6}	3.9×10^{8}	460	1	150	2.9×10^{8}	720	1.5×10^{3}
East Mesa (Deep)	1.1×10^{6}	1.2×10^{7}		2.0×10^{4}	280	3.3×10^{4}		4.5×10^{5}	4.7×10^{3}
East Mesa (Shallow)	1.8×10^{5}	1.2×10^{7}	1.0×10^{9}	1.8×10^{5}	20	3.3×10^{4}	2.5×10^{8}	8.9×10^{3}	660
Gillard HS	1.2×10^{6}		5.5×10^{7}	2.3×10^{4}	6		8.0×10^{6}	120	8.4×10^{3}
Gerlach HS	4.4×10^{5}			2.4×10^{3}	6				
Hot Borax Lake	5.1×10^{5}	1.7×10^{8}	7.9×10^{7}	8.4×10^{3}	10	5.6×10^{3}	1.3×10^{8}	830	
Huckleberry HS	2.1×10^{7}			4.6×10^{3}	40	1.5×10^{4}			3.1×10^{3}
Kahneetah HS	1.6×10^{5}	5.3×10^{7}	2.5×10^{7}	880	3	1.8×10^{3}	3.6×10^{6}	30	
Lakeview area	3.2×10^{5}	1.1×10^{8}	5.0×10^{7}	1.8×10^{3}	5	3.5×10^{3}	1.5×10^{7}	400	
Little Valley area	2.9×10^{5}	9.5×10^{7}	4.5×10^{7}	1.6×10^{3}	5	3.1×10^{3}	6.5×10^{6}	60	
Long Valley - deep	5.4×10^{5}	9.0×10^{7}	2.5×10^{8}	4.4×10^{3}	4	4.9×10^{3}	1.5×10^{8}	150	9.4×10^{3}
Mickey HS	3.8×10^{5}	1.3×10^{8}	5.9×10^{7}	1.0×10^{4}	6	4.2×103	8.7×10^{7}	220	
Mitchell Butte	2.3×10^{5}	7.6×10^{7}	3.6×10^{7}	1.3×10^{3}	4	2.5×10^{3}	5.2×10^{6}	40	
Neal HS	3.6×10^{5}	1.2×10^{8}	5.7×10^{7}	4.0×10^{3}	20	4.0×10^{3}	3.7×10^{7}	220	
Olene HS	2.5×10^{5}	8.2×10^{7}	3.9×10^{7}	1.4×10^{3}	4	2.7×10^{3}	5.6×10^{6}	550	
Salton Sea area	9.3×10^{7}	1.2×10^{9}	1.2×10^{11}	6.1×10^{6}	3.8×10^{6}	6.1×10^{7}	1.1×10^{11}	8.6×10^{6}	3.4×10^{8}
Soda Lake area	100	3.7×10^{4}	3.6×10^{8}	70		2	1.1×10^{8}	3.0×10^{3}	20
Summer Lake	2.6×10^{5}	8.5×10^{7}	4.0×10^{7}	2.8×10^{3}	4	2.8×10^{3}	5.8×10^{6}	70	
Trout Creek	2.4×10^{5}	8.1×10^{7}	3.8×10^{7}	4.0×10^{3}	4	2.7×10^{3}	2.8×10^{7}	280	
Vale HS	6.0×10^{5}	2.0×10^{8}	9.3×10^{7}	3.3×10^{3}	20	6.5×10^{3}	6.1×10^{7}		

Potential economic revenues from recovery of Au, Cs, and Rb appear to be promising for numerous sites (Table 34). For example, from the brine that could be used to generate 53.6 MW at the Hot Borax Lake

hydrothermal system power could also yield over 350 million dollars of Au, Cs, and Rb each year. Economic values of Li for several hydrothermal systems are promising (Table 35). For some sites, the revenue from recoverable K could be attractive. For example, brines of the Salton Sea area, East Mesa, Battle Creek Hot Springs, and Wilber Hot Springs could provide millions of dollars' worth of K annually. However, the economic value of B does not appear promising for the majority of the hydrothermal system examined in this study.

Table 35. Concentrations and economic values of recoverable Li, K and B in geothermal brines.

	Concentrations (mg/kg)			Economic value ($/yr)		
Site	Li	K	B	Li	K	B
Alvord HS	2.1	69	30	1.7×10^{6}	1.4×10^{6}	4.3×10^{5}
Amedee	0.1	5.4	4.7	4.2×10^{4}	5.7×10^{4}	3.5×10^{4}
Arrowhead HS	0.4	12	3.2	2.0×10^{5}	1.5×10^{5}	2.8×10^{4}
Baker HS	0.4	10		6.0×10^{5}	3.8×10^{5}	
Baltazor HS	0.22	8.2	2.1	1.8×10^{5}	1.7×10^{5}	3.0×10^{4}
Beowawe HS	2.6	14		1.5×10^{6}	2.0×10^{5}	
Big Creek HS		14			3.1×10^{5}	
Black Rock Point area		12	2.8		1.5×10^{5}	2.6×10^{4}
Boyes HS	1.65	20.2	15.7	1.1×10^{6}	3.4×10^{5}	1.9×10^{5}
Brady HS	1.3	62	4.7	5.0×10^{5}	6.0×10^{5}	3.3×10^{4}
Breitenbush HS	1.8	31	4.1	4.7×10^{5}	2.0×10^{5}	1.9×10^{4}
Butte Springs (Trego)		9.3			1.2×10^{5}	
Calistoga HS	1.8	8.9	11	1.2×10^{6}	1.4×10^{5}	1.3×10^{5}
Canby (I'SOT)		6.2	2.9		8.8×10^{4}	2.9×10^{4}
Clear Lake (	3.1	23	680	5.9×10^{5}	1.1×10^{5}	2.3×10^{6}
Clifton HS	2.6	82	0.64	3.0×10^{6}	2.4×10^{6}	1.3×10^{4}
Colado area	2.5	120	8.7	2.2×10^{6}	2.7×10^{6}	1.4×10^{5}
Coso area		12			6.0×10^{5}	
Cove Fort - Liquid	5	254	10	1.7×10^{6}	2.1×10^{6}	6.0×10^{4}
Crane/Cove Creek area	0.62	18	10	1.0×10^{6}	7.3×10^{5}	2.9×10^{5}
Crump's HS	0.4	11	14	5.6×10^{5}	3.9×10^{5}	3.6×10^{5}
Darrough HS	0.4	2.6	0.1	2.9×10^{5}	4.7×10^{4}	1.3×10^{3}
Deer Creek HS	0.15	5.3	0.24	1.2×10^{5}	1.0×10^{5}	3.4×10^{3}
Desert Peak	1.4	250	16	2.9×10^{5}	1.3×10^{6}	6.0×10^{4}
Dixie HS	0.38	6.5	0.89	1.6×10^{5}	6.8×10^{4}	6.7×10^{3}
Dixie Valley Geothermal Field	2.34	76.4	11.7	2.6×10^{6}	2.2×10^{6}	2.4×10^{5}
Dixie Valley Power Partners	2.29	69.5	11.6	1.3×10^{6}	1.0×10^{6}	1.2×10^{5}
Double HS area	0.06	4.5	1.8	3.3×10^{4}	6.3×10^{4}	1.8×10^{4}
Dyke HS area	0.09	4.3	1	3.9×10^{4}	4.7×10^{4}	7.9×10^{3}
East Mesa (Deep)	40	1050	9.8	3.9×10^{7}	2.6×10^{7}	1.7×10^{5}
East Mesa (Shallow)	4	150	7.5	3.9×10^{6}	3.7×10^{6}	1.3×10^{5}
Emigrant		2.5			6.3×10^{4}	
Ennis HS	0.26	17	0.61	2.3×10^{5}	3.8×10^{5}	9.8×10^{3}
Fernley area	1.6	38	5.6	1.0×10^{6}	6.3×10^{5}	6.6×10^{4}
Fort Bidwell	0.03	9.5	0.61	2.2×10^{4}	1.8×10^{5}	8.3×10^{3}
Gillard HS	1.01	13.2	0.4	9.6×10^{5}	3.2×10^{5}	6.8×10^{3}
Gerlach HS	1.9	124	0.1	2.3×10^{6}	3.7×10^{6}	2.2×10^{3}
Gregson HS	0.64	3.9	0.3	3.7×10^{5}	5.6×10^{4}	3.1×10^{3}
Hot Borax Lake	0.65	31	17	8.9×10^{5}	1.1×10^{6}	4.2×10^{5}
Tuscarora HS	0.7	41	0.77	7.9×10^{5}	1.2×10^{6}	1.6×10^{4}
Huckleberry HS		8.6	0.74		5.0×10^{5}	3.1×10^{4}
Humboldt House - Rye Patch	5.76	256	8.12	7.8×10^{6}	8.7×10^{6}	2.0×10^{5}
Jemez Springs	10.1	74.2	7.86	7.0×10^{6}	1.3×10^{6}	9.8×10^{4}
Kahneetah HS	0.52	3.4	2.6	2.2×10^{5}	3.7×10^{4}	2.0×10^{4}
Kellog HS	0.12	5.9	3.2	5.2×10^{4}	6.4×10^{4}	2.5×10^{4}
Kelly HS	0.15	6.5	3.8	8.3×10^{4}	9.1×10^{4}	3.8×10^{4}
Lake City HS		18	6.8		1.3×10^{6}	3.4×10^{5}
Lakeview area	0.15	8.5	6.9	1.3×10^{5}	1.9×10^{5}	1.1×10^{5}
Latty HS		1.7			2.1×10^{4}	
Leach HS	5.3	80		2.4×10^{6}	9.0×10^{5}	
Lee HS	0.7	26	2.4	5.9×10^{5}	5.5×10^{5}	3.7×10^{4}
Leonards/Seyferth HS	0.13	8.5	7.6	6.7×10^{4}	1.1×10^{5}	7.1×10^{4}

	Concentrations (mg/kg)			Economic value ($/yr)		
Site	Li	K	B	Li	K	B
Lightning Dock		21			1.2×10^{5}	
Little Valley area	0.11	3.2	4.7	8.5×10^{4}	6.2×10^{4}	6.6×10^{4}
Long Valley - deep	2.8	45	15	2.0×10^{6}	8.3×10^{5}	2.0×10^{5}
Magic Reservoir area	1.18	23	0.08	8.8×10^{5}	4.3×10^{5}	1.1×10^{3}
McLeod	1.7	38	3.5	1.0×10^{6}	5.6×10^{5}	3.7×10^{4}
Mickey HS	1.1	35	11	1.1×10^{6}	9.1×10^{5}	2.0×10^{5}
Mitchell Butte	0.03	1.6	0.49	1.9×10^{4}	2.5×10^{4}	5.5×10^{3}
Neal HS	0.3	16	4.1	2.9×10^{5}	3.9×10^{5}	7.2×10^{4}
Olene HS	0.15	7.2	1	1.0×10^{5}	1.2×10^{5}	1.2×10^{4}
Pinto HS	0.45	23	7.5	4.1×10^{5}	5.2×10^{5}	1.2×10^{5}
Raft River	1.31	100		1.2×10^{6}	2.3×10^{6}	
Roosevelt HS	0.27	488	38	1.3×10^{5}	6.0×10^{6}	3.3×10^{5}
Routt	0.29	9	0.28	1.9×10^{5}	1.5×10^{5}	3.4×10^{3}
Rowland HS		4	0.41		4.8×10^{4}	3.5×10^{3}
Salton Sea area	440	14300	332	4.4×10^{9}	3.6×10^{9}	6.0×10^{7}
San Emidio Desert area	2.2	110	6.5	2.6×10^{6}	3.2×10^{6}	1.4×10^{5}
Sespe HS	0.76	16	13	4.9×10^{5}	2.6×10^{5}	1.5×10^{5}
Sharkey HS	0.47	16	1.6	3.2×10^{5}	2.7×10^{5}	1.9×10^{4}
Silver Star HS	0.38	6.7	0.26	2.4×10^{5}	1.1×10^{5}	2.9×10^{3}
Smith Creek Valley		8.1			1.3×10^{5}	
Soda Lake area	2.7	143	11.2	1.5×10^{6}	2.0×10^{6}	1.1×10^{5}
Sonoma Mission Inn	0.09	12	0.8	4.5×10^{4}	1.5×10^{5}	7.2×10^{3}
Squaw HS		533	9.7		8.7×10^{6}	1.1×10^{5}
Stillwater area	1.9	42	15	2.7×10^{6}	1.5×10^{6}	3.8×10^{5}
Summer Lake HS	0.15	4.6	6.9	1.0×10^{5}	8.0×10^{4}	8.6×10^{4}
Surprise Valley HS	0.1	5.5	5.7	5.3×10^{4}	7.4×10^{4}	5.5×10^{4}
Tecopa HS		16	5.1		2.1×10^{5}	4.7×10^{4}
The Needles	0.61	160	6.1	6.5×10^{5}	4.3×10^{6}	1.2×10^{5}
Thermo HS	1.3	52	0.93	4.0×10^{5}	4.0×10^{5}	5.1×10^{3}
Trout Creek	0.68	11	0.89	4.5×10^{5}	1.8×10^{5}	1.1×10^{4}
Vale HS	0.28	16	9.4	4.5×10^{5}	6.5×10^{5}	2.7×10^{5}
Sulphur Spring/Valles		24			2.0×10^{5}	
Vulcan HS		3			5.2×10^{4}	
Wabuska HS	0.53	15	1.8	2.7×10^{5}	1.9×10^{5}	1.6×10^{4}
Waunita HS	0.2	10	0.07	1.5×10^{5}	1.8×10^{5}	9.2×10^{2}
Battle Creek HS		552	7.6		8.9×10^{6}	8.7×10^{4}
Wendel	0.12	7.5	5.5	7.1×10^{4}	1.1×10^{5}	5.9×10^{4}
West Valley Reservoir	0.4	11	4.5	2.3×10^{5}	1.6×10^{5}	4.7×10^{4}
White Licks HS	0.24	17		1.8×10^{5}	3.2×10^{5}	
Wilbur Springs	33	493	0.21	2.8×10^{7}	1.0×10^{7}	3.2×10^{3}

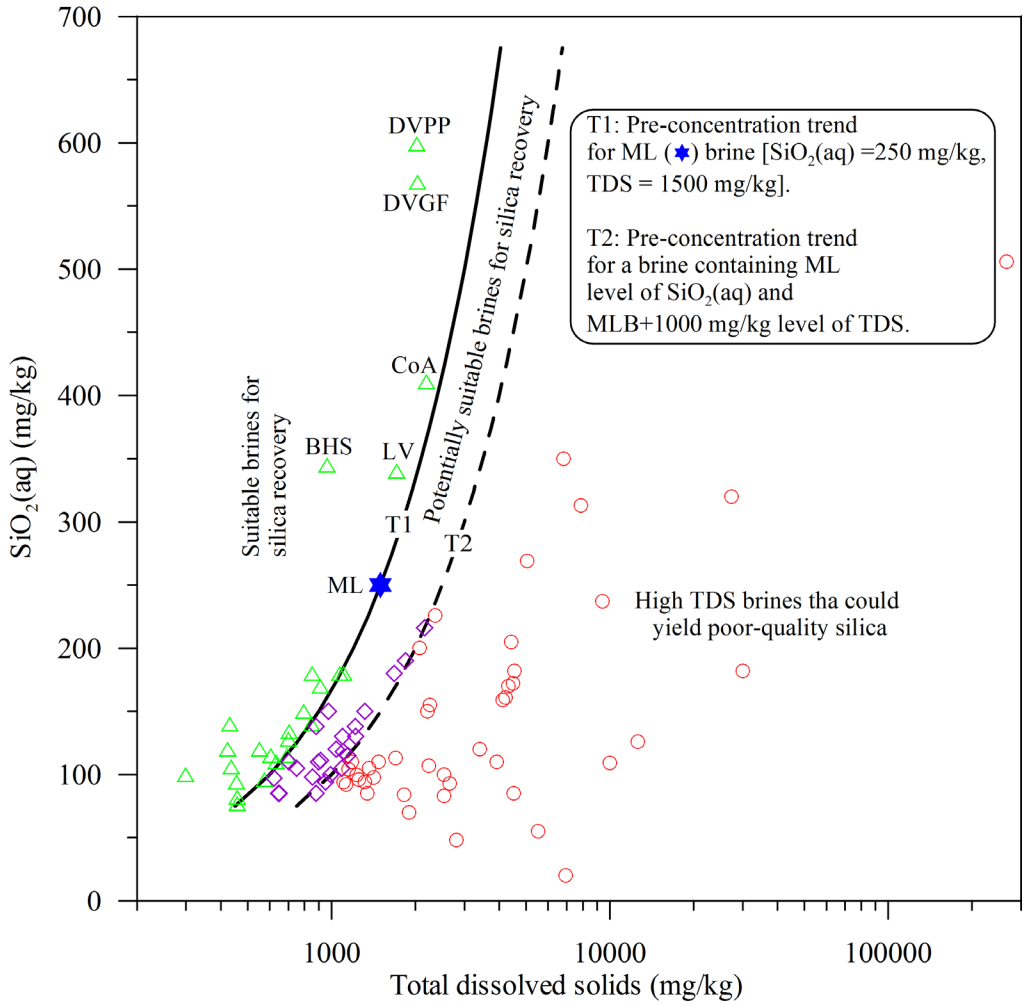

Figure 69. Concentrations of aqueous SiO_2 plotted against total dissolved solids (TDS) in geothermal brines. The brines with good, potentially suitable, and poor attributes for SiO_2 recovery are represented by green triangles (Δ), purple diamonds (◊), and red circles (○), respectively. (ML: Mammoth Lake, LV: Long Valley-deep, BHS: Beowawe Hot Springs, CoA: Coso area, DVGF: Dixie Valley Geothermal Field, DVPP: Dixie Valley Power Partners).

All geothermal brines are enriched in silica. For this study, we used our previous approach [220] to identify brines with positive attributes for silica recovery. This approach (Figure 69) uses the composition of the Mammoth Lake (ML) geothermal brine (TDS up to 1500 mg/kg, SiO_2 = 250 mg/kg) as a reference composition to develop a screening tool for identifying brines that could be used for SiO_2 recovery. The ML was selected as a reference brine because it was used in a pilot-plant for SiO_2 recovery by Bourcier et al. [83]. Since the natural concentration of SiO_2 in the ML brine is deemed low for direct extraction, Bourcier et al. [83] employed a reverse osmosis technology to pre-concentrate aqueous SiO_2 by a factor of 2.5 to 3.5. Therefore, the dilution/concentration trends of ML are used as baselines to separate brines with good attributes for silica recovery. Any brine having ML+1000 mg/kg total dissolved solids could be considered as brine that could produce poor-quality silica. With this screening tool (Figure 69), we identified several identified hydrothermal systems that have brines potentially suitable for silica recovery. For these hydrothermal systems, the recovery of SiO_2 alone could potentially add millions of dollars of additional revenue (Table 36).

Table 36. Concentrations of SiO_2 and potential annual revenues ($/yr) from silica recovery.

Good brines			Potentially suitable brines		
Site	SiO_2 (mg/kg)	Revenue ($/yr)	Site	SiO_2 (mg/kg)	Revenue ($/yr)
Baker HS	140	1.1×10^7	Amedee	138	2.9×10^6
Baltazor HS	150	6.0×10^6	Arrowhead HS	94	2.3×10^6
Beowawe HS	345	9.7×10^6	Big Creek HS	150	6.6×10^6
Calistoga HS	134	4.3×10^6	Canby (I'SOT)	111	3.1×10^6
Coso area	411	4.1×10^7	Double HS area	105	2.9×10^6
Crane/Cove Creek area	180	1.5×10^7	Dyke HS area	85	1.9×10^6
Crump's HS	180	1.3×10^7	Gregson HS	85	2.4×10^6
Darrough HS	106	3.8×10^6	Hot Borax Lake	190	1.3×10^7
Deer Creek HS	120	4.7×10^6	Kellog HS	85	1.8×10^6
Dixie HS	115	2.4×10^6	Kelly HS	110	3.1×10^6
Dixie Valley Geothermal Field	569	3.2×10^7	Lake City HS	118	1.7×10^7
Dixie Valley Power Partners	599	1.7×10^7	Lee HS	180	7.6×10^6
Fort Bidwell	82	3.1×10^6	Lightning Dock	138	1.6×10^6
Huckleberry HS	170	1.9×10^7	Olene HS	98	3.3×10^6
Lakeview area	140	6.1×10^6	Pinto HS	150	6.8×10^6
Latty HS	100	2.5×10^6	Routt	97	3.2×10^6
Little Valley area	115	4.5×10^6	Silver Star HS	110	3.5×10^6
Long Valley - deep	340	1.2×10^7	Surprise Valley HS	100	2.7×10^6
Mitchell Butte	94	2.9×10^6	Trout Creek	105	3.5×10^6
Neal HS	180	8.8×10^6	Vale HS	130	1.1×10^7
Rowland HS	96	2.3×10^6	Sulphur Spring/Valles	216	3.7×10^6
Smith Creek Valley	128	4.1×10^6	Wabuska HS	115	2.9×10^6
Sonoma Mission Inn	77	1.9×10^6	Wendel	120	3.6×10^6
Vulcan HS	120	4.2×10^6	West Valley Reservoir	130	3.7×10^6
Waunita HS	110	4.0×10^6			

10.4 Cost of power and comparative values of recoverable minerals

10.4.1 Cost of power generation

The Business-As-Usual Scenario GETEM-estimated costs of power generation (as LCOE) for the sites considered in this study range from $0.045 to $0.368 per kWh (Figure 70). The DOE-GTO seeks to lower the LCOE of the near-term hydrothermal growth to $0.06/kWh by 2020 through developing, demonstrating, and deploying innovative technologies [250]. The GETEM simulations indicate that only 5 sites out of the 92 sites can produce electricity at that desired level of LCOE in the Business-As-Usual scenario, and the remaining sites will have LCOE > $0.06 /kWh (Figure 71). It is expected that the potential additional revenue from the recovery of minerals (or development of some other cost saving technologies) could help decrease the LCOE for these sites and make them competitive resources in the future.

Figure 70. Cost of power generation and economic value of recoverable minerals in the brines.

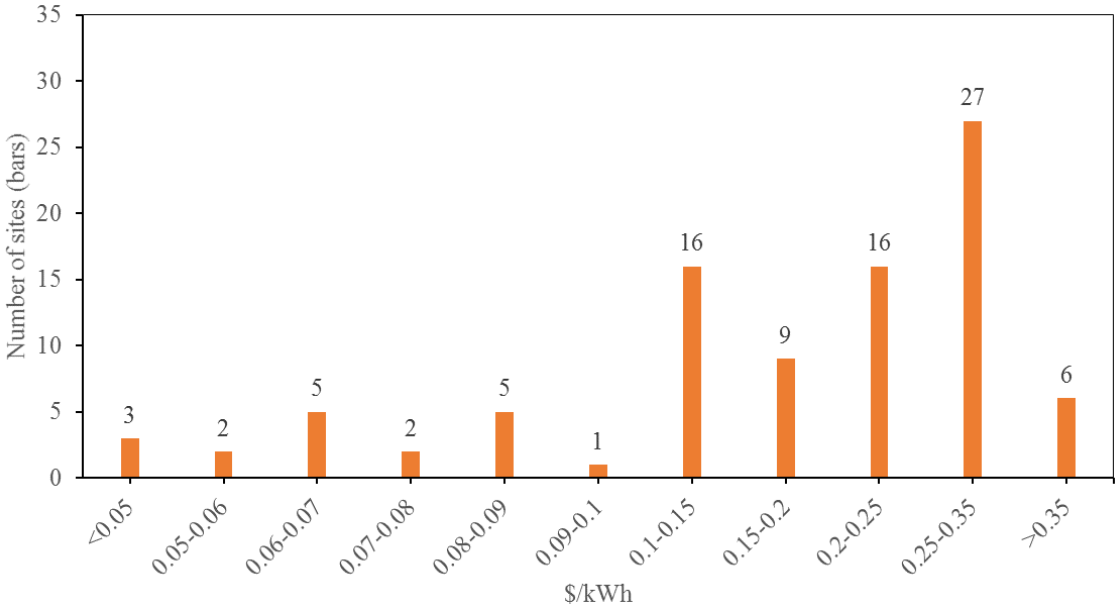

Figure 71. Cost of geothermal power generation without extraction of minerals from brines.

10.4.2 Unit value of recoverable minerals

To assess the economic effect of minerals' extraction on LCOE, we calculated the per unit value of recoverable minerals from brines for all hydrothermal sites. For this calculation, we again assumed that all plants will be operated for 90% of the year at the capacity given in Table 33. Then the total annual economic value (in $/yr) of minerals for each site was obtained by adding economic values of all recoverable minerals (Table 34 through Table 36). Similarly, the total annual power (in kWh) was calculated assuming a 0.9 capacity factor for each site with the power capacity given in Table 33. Finally, the unit value (in $/kWh) of recoverable minerals for each site was calculated by dividing the total annual economic values of minerals by the total annual power. This calculation provides the unit value of minerals from the total mass of brine used to generate 1 kWh of electricity [hereafter, we express this directly as 1 unit (or 1 kWh) value of minerals] and also helps compare mineral value directly with the cost of power generation. Besides calculating the total value of minerals, a set of similar calculations were carried out without accounting for the economic values of recoverable SiO_2. It is assumed that the market for high-quality SiO_2 may not be adequate for a sustainable recovery of SiO_2 from all potential geothermal sites. Non-silica per unit value of minerals would help evaluate the impact of other minerals' to lower LCOE.

An important limitation in our approach for direct comparison between the cost of power generation and the value of minerals is that unlike the cost of power generation, our economic value of minerals does not include the upfront capital and operational costs for the recovery system. We used GETEM estimated LCOE as a cost of power generation to these sites. GETEM includes the capital, operation, maintenance, financial, etc., costs while estimating LCOE [249]. However, our economic value of minerals does not account for any of the costs that would be incurred when establishing and operating mineral extraction facilities. For more meaningful comparison, unit economic value of minerals derived by accounting for capital, operation, maintenance, and other financial costs would be required. As we stated in our previous work [220], we do not have adequate information regarding the technology deployment as well as capital and other associated costs for mineral extraction facilities and activities.

Figure 70 shows the value of recoverable minerals for all sites both including and excluding the potential revenue from extraction of SiO_2. The potential unit value of minerals (with or without SiO_2) for these

sites ranges from negligible to up to $13.9/kWh. Figure 72a illustrates the distributions of hydrothermal sites according to the per unit value of minerals. When all recoverable minerals are considered, 15% of the sites (14) have negligible (<$0.01/kWh) value of minerals. Furthermore, the number of sites (50) with mineral value <$0.01/kWh increased to more than half of the total sites examined in this study when the potential value from extraction of SiO_2 was excluded from the calculations (Figure 72b). For most of the sites with $0.01 to 0.05/kWh value of minerals, the potential mineral revenue is likely to be eliminated if the extraction of SiO_2 is excluded. However, the sites with the highest economic impacts from mineral recovery maintain the similar level of potential revenue from minerals since the main minerals to be extracted from these sites are non-SiO_2, such as Cs, Li, Rb, and precious minerals (Table 34 through Table 36; Figure 72).

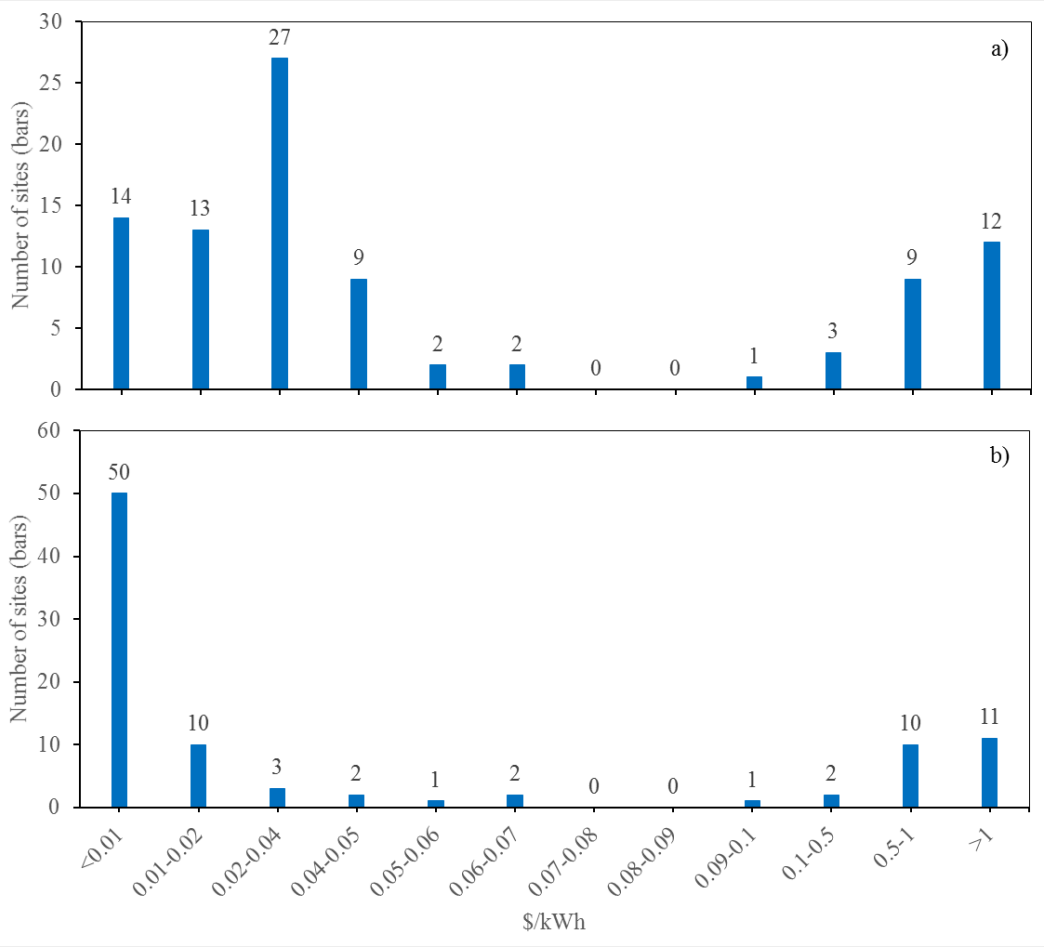

Figure 72. Economic values of recoverable minerals including silica (a) and excluding silica (b) in geothermal brines.

10.4.3 Impact of minerals on cost of power generation

Figure 73 shows the distribution of the cost of power generation if the revenue from potential mineral extractions is included. Inclusion of revenue from all recoverable minerals could increase the number of sites with LCOE ≤ 0.06 $/kWh from 5 sites (Figure 71) to 29 (Figure 73a). Similarly, if potential revenue from SiO_2 is excluded, about 28 sites are likely to generate power with LCOE ≤ 0.06 $/kWh (Figure 73b).

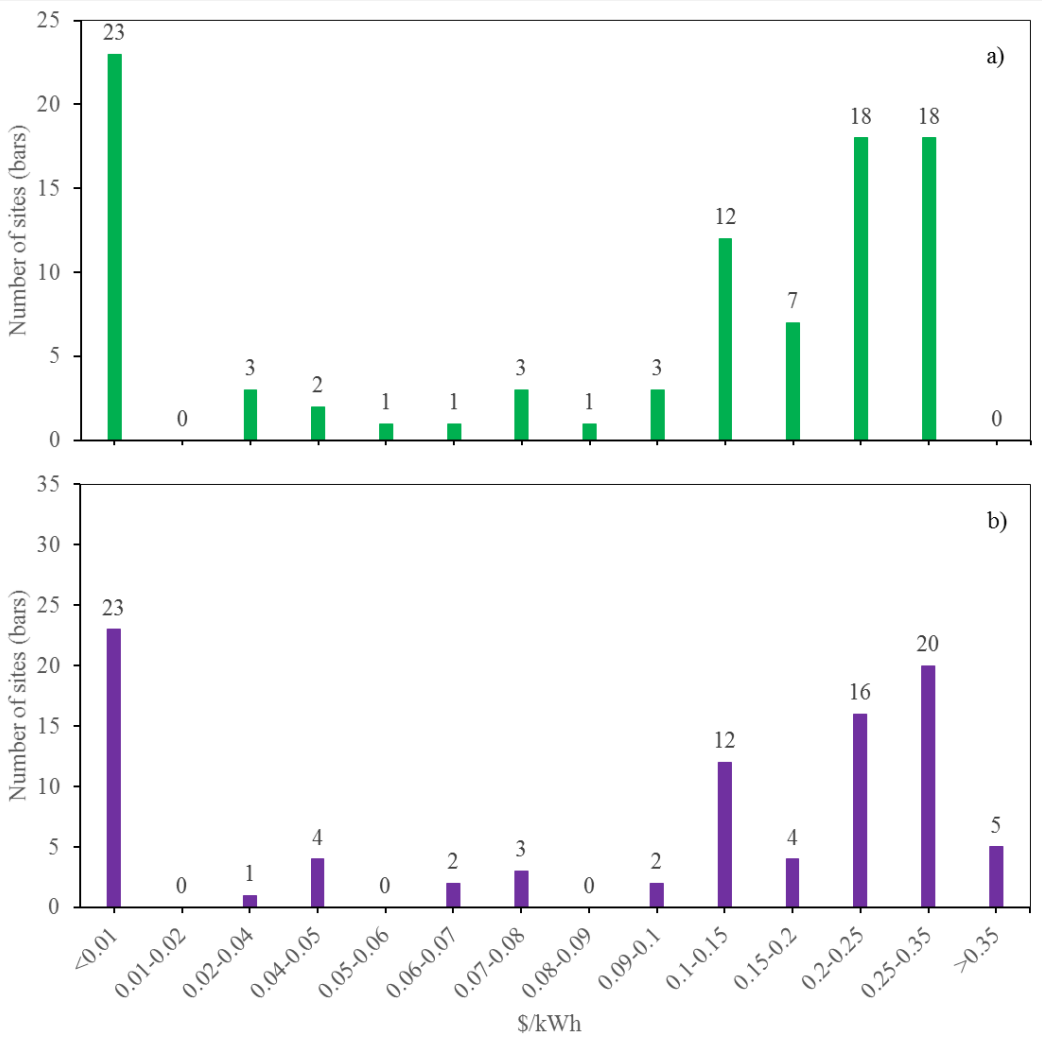

Figure 73. Cost of geothermal power generation with extraction of all recoverable minerals (a) and all but silica minerals (b) from brines.

10.4.4 Relative value of minerals in brines

The value of minerals in terms of the percentage of the power generation cost is also calculated and presented in Figure 74. The US hydrothermal resource areas mostly show a bimodal distribution in terms of their potential mineral values relative to the cost of power production. Many sites generate small revenue from potential mineral recovery. The number of sites that would yield <10% of revenue (relative to power) from all recoverable minerals is 20, and this number increases to 54 if the potential revenue from recoverable SiO_2 is excluded. A large number of sites (40) could yield 10-25% of relative revenue if all minerals are considered. Only a few sites (8 and 1 sites, respectively) have potential revenue from mineral recovery that could account about 25-50% and 50-100% relative revenue. However, there are some other sites that can add significant revenue from minerals, potentially exceeding the cost to generate power. For example, the value of minerals in brines from 23 sites are high enough to completely offset the cost of power generation. Therefore, it appears that the sites that show the greatest promise for mineral recovery are very good, and could provide better revenue from minerals than from power. Even though we did not include the capital and operational costs for the mineral extraction facilities and activities, these findings indicate that for these high-mineral-potential sites, the augmentation of mineral extraction

plants along with power plants could be very economic, or at minimum, such efforts could help make geothermal power more cost competitive by decreasing LCOE. In the meantime, they could also be reliable domestic sources for some minerals. In contrast, for many sites, the relative revenue contribution from recoverable minerals is likely marginal and may not be adequate to decrease the LCOE to the GTO's desired level.

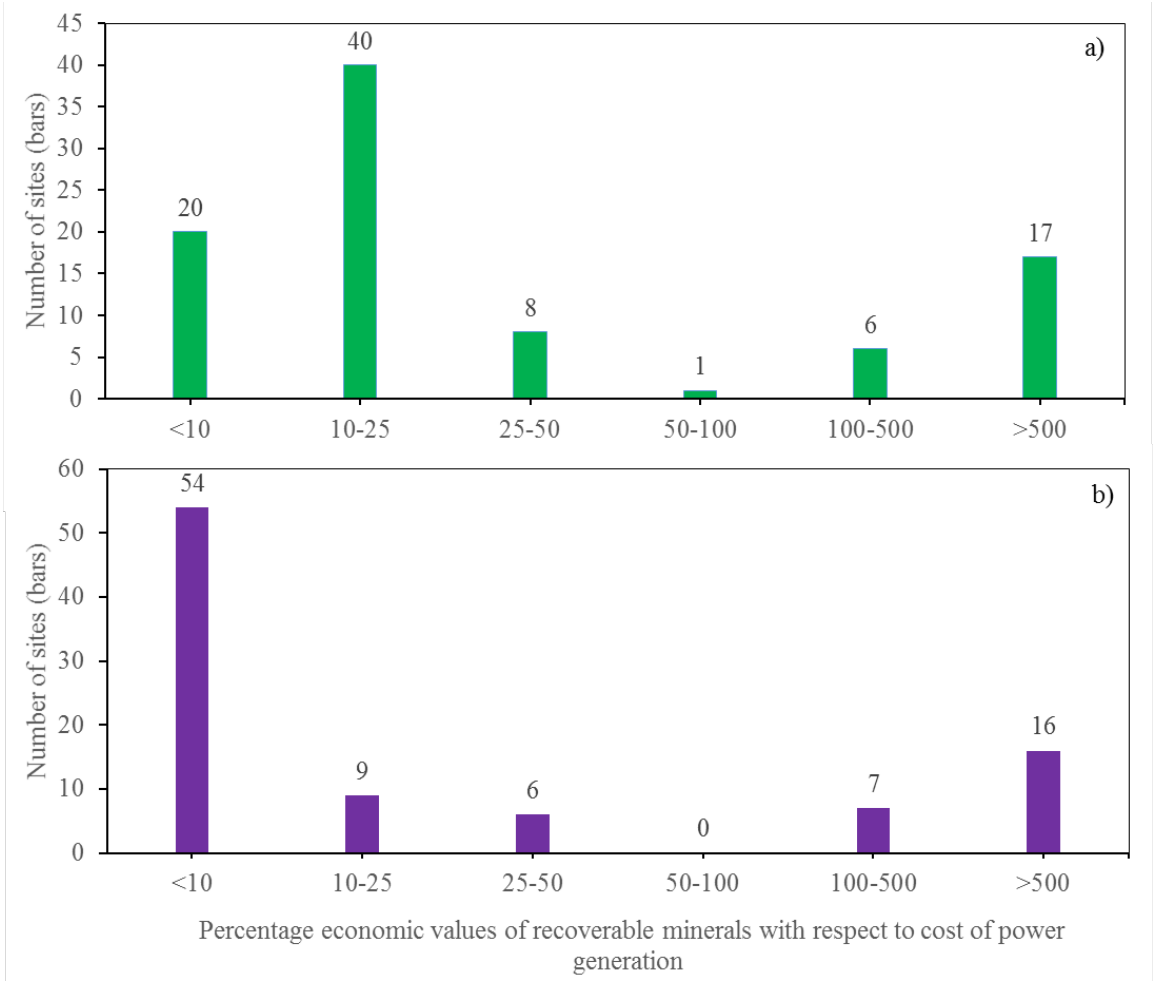

Figure 74. Relative economic values of recoverable all minerals (a) and all but silica minerals (b) with respect to the cost of power generation.

10.5 Conclusions

In this study, we assembled brine compositions for several identified hydrothermal resource areas. The mineral loadings in the geothermal brines from these areas vary, ranging from extremely low levels for some minerals to high levels for others. In general, our resource assessment shows that numerous geothermal brines in the US contain concentrations for some minerals that could, if successfully recovered, potentially provide a new value-added revenue stream to the geothermal industry.

Our assessment shows that for several hydrothermal resource areas, economic potential from recovery of precious metals (Ag and Au), Cs, Rb, Li, and SiO_2 are very promising. However, none of these minerals are currently recovered from the geothermal brines in the US. As we reported previously, recovery technologies for the majority of these minerals have been at low technology readiness level (TRL), and mostly limited to laboratory bench-scale level analyses. Only technologies for extraction of Li and SiO_2

have been tested with pilot-scale plants. Pilot-scale testing of other mineral recovery technologies needs to be performed prior to commercial-scale deployment. For sustainable recovery, the extraction technology needs to be designed for the mineral types, contents, overall chemistry of the target brines, and likely future market conditions for the mineral commodities.

Our comparative assessments indicate that for several sites the value of minerals in brines outweigh the cost of power generation. When all recoverable minerals are considered, brines of 23 sites (out of 92 sites) contain greater value of minerals than the cost to generate power from those brines. Although extraction of all recoverable minerals may not be feasible because of the minimum total value of individual minerals, lower technology readiness levels of extraction technologies, and adverse market forces, some site-specific minerals can be chosen from a list of recoverable minerals for extraction. If such targeted mineral(s) extraction facilities are added or established along with power generation infrastructure, it is very likely that the revenue from minerals could offset some of the cost associated with generation of power. Our study indicate the number sites that could generate power at GTO's desired 2020 LCOE value of $0.06 /kWh could increase from 5 to 29 if revenues from all recoverable minerals are considered. However, evaluation and identification of the most valuable minerals along with the evaluation of extraction technology readiness levels, capital/operating costs, and market forces needs to be performed before establishing mineral extraction facilities at each geothermal site.

11.0 Discussion

11.1 Flexible Power Generation and Grid Stability

Unlike other technologies within the renewable generation portfolio, geothermal energy can be dispatched as baseload power. Where market incentives exist to use it as such, geothermal can also be used as a balancing resource [251] to support variable (non-dispatchable) generation from wind and solar. By combining geothermal energy with other technologies, hybrid approaches can offer additional options for providing flexible generation and grid stability.

- **Solar.** This analysis concludes that hybrid geo-solar plants can provide improved correlation with demand (demonstrated through calculation of lower LCOE for hybrid plants than for stand-alone plants in time-of-delivery pricing scenarios), while remaining candidates for the modifications that can be made to stand-alone geothermal power plants to provide flexible power generation. The hybrid-geo solar plant can provide base load power generation that is well-matched with demand, while retaining the ability to be configured for flexible power generation. This flexibility can be increased by adding solar thermal storage capabilities to allow sustained high power output during intermittent cloud cover and/or during the hours surrounding dusk (a challenging period of the day when solar PV generation rapidly decreases and load increases; this period is very apparent in the famous 'duck curve'). Despite the potential advantages associated with geo-solar hybrid plants (efficiency increases, overall reduction in power block equipment requirements, improved power generation during high ambient temperatures, etc.) a highly efficient and cost effective geo-solar power plant configuration has not yet been realized. *Hybrid geo-solar power plant technology could be advanced by researching and developing power plant configurations that can operate with high efficiency at partial load conditions (in response to intermittent solar heat input) and that do not include large investments in equipment that is only intermittently used (i.e. turbines that are not used at night when the solar field is not providing heat output). Additionally, the use of thermal storage should be considered in markets with variable electrical pricing.*
- **Fossil Generation Hybrids.** Integration of geothermal heat into fossil-fired power stations can increase the total effective capacity of the generation unit by improving efficiency. For coal plants, geothermal energy increases the amount of power generated by reducing the amount of process steam diverted to heat feedwater, and allowing that steam to do higher-value work in the turbine. Adding the geothermal feedwater preheating enables additional power to be generated without increasing the amount of coal used. For baseload natural gas plants, where generation capacity is sensitive to ambient temperature, the geothermal integration could enable inlet air to be cooled to optimal temperatures, which in turn prevents the summer capacity reduction associated with high ambient conditions. In this case, the gas plant can maintain a more stable capacity—and gas consumption rate—over the course of the year. In both fossil cases, the geothermal component increases the overall capacity of the existing generation unit, offering an opportunity for increasing efficiency at existing plants to defer capital investments in new conventional generation. This is particularly true for the gas case, where generation capacity falls as a result of high air temperature, which also drives demand for space cooling. However, significant questions remain. *In particular, understanding the potential for these hybrid systems could include: Evaluation of the geospatial match between known hydrothermal resources and existing fossil-fired power facilities that might be amenable to hybridization; extending this analysis to include prospective sites for greenfield development of purpose-built GT-fossil hybrid generation; analysis of the differential costs and market potential of extending this approach to EGS resources (fully internalized development costs); and evaluation of how the geothermal component*

might be credited under state RPS mechanisms and/or efforts to monetize deferred investment in new capital (e.g., existing gas plants).

- **Compressed Air Energy Storage.** Perhaps the most direct application of geothermal heat for grid stability is its use for compressed air energy storage (CAES). This approach, which could offer grid-scale balancing services for both increasing and decreasing reserves, could run compressors during periods when load is exceeded by generation—particularly from intermittent renewable resources like wind and stand-alone solar—and expand the air during times of peak load and/or intermittent generation drop-off.
- **Desalination.** Desalination could be effectively used with geothermal resources having temperatures similar to those utilized by many geothermal power plants. It would therefore be possible for the power plant and desalination plant to both utilize the same geothermal resource (thereby reducing overall resource development costs). Desalination could be performed during periods of off-peak electrical power demand to continue to utilize the geothermal resource for the purification of water (the purified water product could also be more readily stored than excess electrical output from the plant). Power generation and desalination could also be performed simultaneously in a cascaded configuration in which the power plant brine outlet temperature was increased. Since the heat content in the intermediate temperature brine is converted to electricity with relatively low efficiency, this energy could potentially be used more cost-effectively for low grade heat thermal applications, especially thermal desalination. However, simultaneous operation of power and desalination plants [in either a parallel or series configuration] with one or both plants at less than full capacity would introduce challenges for cost-effective operation. *Deployment of flexible hybrid geothermal power generation and desalination plants would require identification of suitable geothermal resources and co-located power/water markets, research and development of applicable plant configurations, as well as an evaluation of whether the cost of the electricity and water products produced by the hybrid plant would be cost competitive (if not what market drivers would result in favorable economics for the water-power hybrid, e.g. time-of-delivery pricing or capacity payments, favorable water sales pricing, etc.).*

11.2 Energy Security

In addition to the "always available" attribute of geothermal energy, it is a renewable energy source with no operating cost associated with the usage of a consumable fuel source. Instead, the primary costs of geothermal energy are those associated with exploration and development of the well field and power plant, in addition to maintenance and personnel related operating costs. As a result, geothermal energy costs are not subject to fuel price fluctuations or supply chain disruptions.

- **Solar** energy, like geothermal, is a renewable energy source with costs that are largely independent of fluctuations in global energy commodities prices. Additionally, the hybrid geo-solar plant configurations evaluated in the GeoVision Hybrid Systems analysis are assumed to be configured with air-cooled condensers that do not require use of cooling water, allowing these facilities to continue to operate independently of drought or water shortage conditions, insulating them from local water use conflicts. This would be especially beneficial for addressing recent trends toward increased water shortages, which have been responsible for numerous water-cooled power plant curtailment events [252]. *The energy security attributes of hybrid geo-solar power plants could be enhanced through the development of power plant configurations that are specifically designed to incorporate*

an increasing amount of solar heat in the event of geothermal resource productivity decline (e.g. use of mixed working fluids, combined cycles, etc.).

- For **coal-fired power generation**, fuel availability and cost risks can be reduced on a per-kWh basis by increasing the amount of power than can be generated from the same quantity of fuel, while also (in some cases, see Chapter 4.0: Coal) offering a more efficient use of the geothermal resource itself. *As previously discussed, future research necessary to understand the potential of hybrid geothermal fossil systems includes evaluation of the geospatial match between hydrothermal resources (identified sites and potential EGS sites) and fossil-fired power facilities (existing and possible greenfield), and evaluation of how the geothermal component might be credited under state RPS mechanisms and/or efforts to monetize deferred investment in new capital (e.g., existing gas plants).*

11.3 Risk Reduction

Resource development and productivity. Geothermal power projects include significant risks in the areas of geothermal resource development and long-term resource productivity. Power generation projects that hybridize geothermal resources with another heat source—such as in solar, coal and gas configurations—may reduce overall risk to the project by offering flexibility in project development and management. Differences between planned and actual geothermal reservoir performance can be mitigated using the secondary heat source. This flexibility could also be leveraged to decrease the project development schedule (by increasing the amount of overlap of drilling, confirmation, and power plant construction) and/or to decrease project financing costs (by reducing risk to investors).

Emissions liability. Power plants that derive some portion of their energy from geothermal can reduce their long-range cost risk associated with greenhouse gas or pollutant emissions. Because of the non-emitting nature of power generated from both energy sources, hybrid geo-solar power plants would not be impacted by future carbon tax or air-quality regulations. For coal-fired plants, the emissions intensity (emissions per unit of power generated) would decrease via geothermal integration. This is also true for processes where geothermal is used to partially or fully offset fossil-generated electricity or fossil fuel combustion, and associated emissions. For example, the geothermal hybrid CAES and desalination approaches evaluated in this study both use geothermal heat to displace emitting heat sources used in non-hybrid version of those technologies, thus reducing the overall emissions liability associated with the process.

11.4 Critical and strategic materials

An assessment of available composition data of geothermal brines in the US shows the presence of some minerals at potentially economic levels. For example, brines of multiple geothermal sites in the Basin and Range Province contain Cs, Li, and Mn at higher concentrations that may be feasible for economic recovery. Similarly, numerous brines in the same province also show positive attributes for extraction of good quality SiO_2. Some geothermal brines in the Columbia Plateau Province contain parts-per-billion levels of Ag and Au. While recovery of rare earth elements (REE) from geothermal brines may not be economically viable at present market prices because of their very low (parts-per-trillions) concentrations, the possibility for developing domestic sources of particularly strategic REEs (e.g., Li) may become attractive even at costs higher than resources available for import.

11.5 Value added revenue streams

Geothermal resources have long been used as a source of clean and sustainable baseload power. However, the upfront deployment costs of geothermal technologies are high. Various approaches are considered to make geothermal energy more economically attractive over other sources of energy.

Mineral recovery from the large volume of brines used to generate power at geothermal sites. Several bench-scale single- and multi-minerals recovery technologies have been developed and tested over the years. For several minerals of interest, the bench-scale experiments yielded excellent (as high as 95-99%) extraction efficiency. However, most of these technologies are yet to be tested on a scale comparable to any future commercial deployments. Only a few of them (for SiO_2 and Li) have been tested in pilot-scale plants in the US and New Zealand, and capital and operation costs of these processes at commercial scale remain uncertain.

Currently the lack of information regarding processing costs prevents a full detailed economic analysis of mineral recovery from being performed. *In order to obtain a complete picture of the economic viability of mineral recovery activities, future research activities should include a detailed market analysis of recovery of target minerals, and a detailed techno-economic analysis of the mineral recovery technologies/processes such that a complete picture of potential mineral recovery profits can be determined. In addition to processing costs, any impacts on existing geothermal power plant (or other geothermal project) operation and associated expenses must also be included in the analysis.*

Thermal desalination using low-grade heat recovered from the power plant reinjection brine. Geothermal desalination technologies could utilize the low-grade heat in power plant reinjection brine to treat cooling tower blowdown water, simultaneously reducing water consumption and blowdown water management costs (treatment and/or disposal). In applications where once-through or air-cooling is utilized, the low grade heat in the reinjection brine could be used for treating another saline or waste water source to provide an additional revenue stream for the geothermal project. *Additional desalination technology research areas should include the continued identification and development of efficient and cost effective thermal desalination technologies with attributes suitable for use with geothermal energy (especially low temperature), as well as continued identification and development of geothermal desalination applications.*

Grid services from stand-alone CAES plants or those coupled with a baseload geothermal site may offer an opportunity to capture higher-price power sales during times of peak demand. The degree to which geothermal-coupled CAES may be profitable, and at what optimal project size, depends heavily on the market dynamics and regulatory structure in which the project might deploy. While creating a market structure that incentivizes new capital development for grid-scale balancing has lagged the demand for these services, the increasing curtailments of wind power has driven a move to catch up on the market and regulatory side.

Carbon credits generated via geothermal energy use in a given process will be driven, in part, by the degree to which its use displaces emissions that would have resulted from a conventional (non-hybrid) approach. Thus, credits could be generated by coal-fired power plants using geothermal heat to offset the efficiency losses associated with CO_2 capture, or to provide reboiler duty for capture solvent regeneration; they might also be able to generate credits associated with the additional power enabled by boiler feedwater preheating, since this would result in no additional coal combustion (e.g., production would be credited to the geothermal resource). However, for the natural gas plant configuration where geothermal heat facilitates increased power generation via increased gas combustion, the geothermal portion of actual generation—and thus any associated zero-carbon energy credits—would be small. Credits could also be available to industrial projects that replace fossil combustion with geothermal energy.

The market potential for GT-hybrid CAES and CO_2 capture cannot be evaluated without an understanding of both potential costs and revenue streams. The increased proportion of intermittent renewables deployment in the U.S. will create a proportional increase in the market for ancillary grid services from facilities such as GT-CAES plants. Similarly, the potential to use geothermal energy to offset efficiency losses in a power plant due to the need to capture CO_2 from flue gas—rather than simply using the geothermal heat to improve efficiency of a non-capturing system, and selling the additional power—will result in a revenue stream (or avoided cost stream) that is distinct from the revenue

associated with scheduled power sales. While project development costs may be relatively deterministic, the value of revenue streams rests heavily on societal decisions that will drive demand for low-carbon power. ReEDS is designed with this scenario-based approach in mind, but again, is not currently configured to take hybrid systems into account. This could be addressed by:

- *Fleshing out case studies with ASPEN-level sensitivity analyses that evaluate a range of operating conditions, including changes in fuel price, market value of differential product streams (e.g., renewable credits vs CO_2 credits vs ancillary services vs baseload) for development of reduced-order models (ROMs) that can be integrated with GETEM and applied more natively to ReEDS.*
- *Modification to ReEDS to accommodate the ROMs for hybrid techs that allow them to be integrated at a level of rigor that allows for defensible comparison between the hybrid technologies and other non-hybrid generation.*
- *While not specific to the geothermal hybrid concept, integration of grid services pricing into ReEDS would be a meaningful investment, allowing for a deeper understanding of the demand for grid services associated with increased build-out in variable renewable generation. As renewable LCOEs continue to drop, local and regional grid infrastructure will continue to hit its carrying capacity for intermittency, resulting in curtailment and/or instabilities in the grid over time. These forces will drive markets for ancillary services, and it's essential to capture those price signals as externalities to the wind and solar power markets which reflect the potential for new development of support technologies like GT-CAES and thermal storage.*

11.6 Energy and materials for multi-purpose applications through cascaded-use and hybrid applications

Different geothermal resources are able to provide heat at different temperatures. As a result, most geothermal projects differ in the exact way that they utilize this heat. Fortunately, geothermal heat can be used for numerous applications that are practical over a range of temperatures. High temperature geothermal heat is most frequently used for power generation. However, in cases where flexible power generation is required or there are significant markets for products other than electrical power, geothermal energy could be used in cascaded-use or other value-added applications.

Electricity production and water resources are interrelated. Energy production is highly dependent on water usage; purification and distribution of water requires energy. As a means of addressing the water energy nexus, desalination and power generation could be combined in a geothermal energy driven hybrid plant or cascaded-use installation.

- A hybrid power/desalination plant could vary the geothermal resource utilization between power generation and water production to perform load following in response to changes in electrical power demand. A hybrid power/desalination plant would incorporate a desalination technology capable of utilizing a significant amount of the energy provided by the geothermal resource to shift the hybrid plant output from electrical power to water production. Since water is more easily stored than electrical power, such a hybrid is envisioned to be capable of simultaneously providing valuable products and services to multiple markets. While high-temperature resources are best suited to large-scale water desalination operations, low grade or waste heat may be used for applications where an ancillary water product would be beneficial for site or project use. *Deployment of flexible hybrid geothermal power generation and desalination plants would require a resource assessment to identify suitable geothermal resources (in areas where no geothermal heat source exists, EGS potential should be evaluated for their ability to provide a cost competitive desalination heat source) and co-*

located power/water markets (water market could also include waste treatment), research and development of applicable plant configurations, as well as a market analysis of the economic feasibility of geothermal desalination.

- An air-cooled geothermal power plant with access to a purified water source, such as that from desalination operations, could also be configured with hybrid cooling (air-cooling that can be augmented by adding water to provide additional evaporative cooling duty) to enhance power plant output during periods of peak demand. Since hybrid cooling enhances power generation through increased heat rejection rather than through increased heat input, this technology could be used with hybrid or stand-alone geothermal power plants to improve performance in a flexible manner (i.e. to provide a better temporal match between power output and load).
- Geothermal facilities based on enhanced geothermal systems could also benefit from access to purified water. EGS resources are generally expected to require the addition of water as a working fluid for extracting the geothermal heat from the reservoir. Some of this water is expected to be lost during the normal operations of the EGS reservoir such that a source of makeup water will be required to maintain the resource productivity. EGS power plants could therefore be coupled with desalination in order to provide a means of 'regenerating' the EGS reservoir working fluid lost during normal operations. As with other couplings of power plants with desalination plants, the desalination throughput rate could be increased when electrical load (demand) is low.
- Potential applications for geothermal desalination using low grade heat / power plant outlet water include treating wastewater streams such as cooling tower blowdown water, co-produced water from oil & gas production operations (which would also assist in addressing environmental issues including spills and earthquakes associated with the transport and disposal of oil & gas wastewater), or other water sources that would require treatment prior to use.

Secondary industrial heat use applications could optimize use of the resource for geothermal hybrid plants that can flexibly shift between power generation and use for process heat. Ideally, this secondary use could be applied during periods of off-peak electrical demand to enhance the load-following capabilities of the hybrid geothermal plant. Processes whose products could be stored more easily than electricity would lend themselves more readily to such uses.

- Using geothermal heat for a secondary application could decrease parasitic losses associated with time periods when power output is reduced, which results in increased reinjection brine temperatures, leading to lower density and increased reinjection pumping power. Ideally, dual-use systems would be able to vary the distribution of geothermal energy between power generation and secondary applications to offer flexibility in grid responsiveness.
- Desalination during off-peak load conditions is currently used in Hawaii to provide load-following power generation from geothermal resources. Further investigation and/or analysis is needed to develop an integrated design that would maximize the efficiency of both the power plant and the desalination plant at partial load conditions.
- Geothermal energy could also be utilized in a process for mineral recovery from geothermal brines. Although numerous technologies for mineral recovery could be utilized, most would benefit from a concentrated brine feed stream.
- Thermal- or membrane-based geothermal desalination could be incorporated into the mineral recovery process to preconcentrate the brine prior to processing, at which point the purified water stream could be reinjected into the reservoir or marketed as another product stream; this approach

would be expected to result in a thermal drawdown of the reservoir performance if there was not another known mechanism by which the reservoir fluid were being recharged.

- For power plants using geothermal heat to drive CO_2 capture systems, the ability to bypass capture during periods of peak electricity demand would allow the plant to generate more power when that is the highest-value use of the additional heat, and shift back to capturing mode at times when the demand (and price) for power drop.

Offsetting other sources of industrial process heat using geothermal resource may offer multiple benefits to industrial stakeholders as utilization of traditional heat sources becomes more complicated by market and regulatory uncertainties.

- While the hybrid systems studies reflected in the GeoVision study necessarily focus on the most monolithic targets for integrating geothermal heat—power generation, water desalination, and mineral recovery—myriad other industrial processes use heat across a wide range of temperatures where geothermal energy may be applicable.
- In many cases, because of the highly process- and site-specific nature of these applications, it's difficult to reflect them as case studies that generalize across a large number of potential facilities. However, finding creative ways to integrate geothermal resources to offset or augment the use of electricity or fuels could result incremental growth and increased familiarity with geothermal resource use in the U.S. and abroad.
- The market for such applications is likely to grow as small industrial facilities begin to upgrade existing coal- or oil-fired boilers for which permits may be difficult to obtain.
- Adding the possibility of renewable credits associated with a switch to geothermal energy could make these shifts more attractive, but only if the uncertainty of obtaining the geothermal resource can be mitigated to the industrial operator.

Driving down uncertainties and cost-based risks associated with switching to geothermal energy, as noted elsewhere in the GeoVision Study materials, is essential to wider-scale adoption of geothermal technologies.

- While subsurface exploration and development technologies advance to improve exploration risks, there may be near-term opportunities to leverage hybrid approaches to continue moving forward with development of geothermal energy in the U.S.
- Where known resources are of insufficient quality or quantity to attract commercial development for stand-alone, baseload geothermal power generation, there may be opportunities to integrate these resources for hybrid power generation or other industrial use.
- Capitalizing on these hybrid opportunities in the near-term could spur greater interest in such applications going forward, as well as deeper learning-by-doing within the geothermal energy sector.
- Early deployments of hybrid geothermal projects may also serve to establish an additional potential value stream to buy down risks associated with development of new resource potential, including EGS, by offering secondary (and perhaps tertiary) markets for resources that are determined to be unattractive on their own for commercial (stand-alone) power development.

12.0 References

[1] Y. Alvarenga, S. Handal, and M. Recinos, "Solar Steam Booster in the Ahuachapan Geothermal Field," in *GRC Transactions*, 2008, vol. 32, pp. 395-399.

[2] M. Astolfi, L. Xodo, M. C. Romano, and E. Macchi, "Technical and economical analysis of a solar–geothermal hybrid plant based on an Organic Rankine Cycle," *Geothermics,* vol. 40, no. 1, pp. 58-68, 2011.

[3] M. T. Balta, I. Dincer, and A. Hepbasli, "Potential methods for geothermal-based hydrogen production," *International Journal of Hydrogen Energy,* vol. 35, no. 10, pp. 4949-4961, 2010.

[4] N. Bezares, C. Augustine, and J. Tester, "Geothermal-Solar Hybrid for Continuous Steam Generation in Cerro Prieto, MX," in *American Institute of Chemical Engineers Annual Meeting*, 2008.

[5] J. G. Boghossian, "Dual-Temperature Kalina Cycle For Geothermal-Solar Hybrid Power Systems," Bachelor of Science, Department of Mechanical Engineering, Massachussetts Institute of Technology, 2011.

[6] G. DiMarzio, L. Angelini, W. Price, C. Chin, and S. Harris, "The Stillwater Triple Hybrid Power Plant: Integrating Geothermal, Solar Photovoltaic and Solar Thermal Power Generation," in *Proceedings World Geothermal Congress*, Melbourne, Australia, 2015.

[7] H. Ghasemi, E. Sheu, A. Tizzanini, M. Paci, and A. Mitsos, "Hybrid solar–geothermal power generation: Optimal retrofitting," *Applied Energy,* vol. 131, pp. 158-170, 2014.

[8] A. D. Greenhut, "Modeling And Analysis Of Hybrid Geothermal-Solar Thermal Energy Conversion Systems," Master of Science, Department of Mechanical Engineering, Massachussetts Institute of Technology, 2010.

[9] A. D. Greenhut *et al.*, "Solar-Geothermal Hybrid Cycle Analysis For Low Enthalpy Solar And Geothermal Resources," in *Proceedings World Geothermal Congress*, Bali, Indonesia, 2010.

[10] S. Handal, Y. Alvarenga, and M. Recinos, "Geothermal steam production by solar energy," in *GRC Transactions*, 2007, vol. 31, pp. 503-510.

[11] M. S. Jamel, A. Abd Rahman, and A. H. Shamsuddin, "Advances in the integration of solar thermal energy with conventional and non-conventional power plants," *Renewable and Sustainable Energy Reviews,* vol. 20, pp. 71-81, 2013.

[12] Á. Lentz and R. Almanza, "Parabolic troughs to increase the geothermal wells flow enthalpy," *Solar Energy,* vol. 80, no. 10, pp. 1290-1295, 2006.

[13] Á. Lentz and R. Almanza, "Solar–geothermal hybrid system," *Applied Thermal Engineering,* vol. 26, no. 14-15, pp. 1537-1544, 2006.

[14] G. Manente, "Analysis and Development of Innovative Binary Cycle Power Plants for Geothermal and Combined Geo-Solar Thermal Resources," Università degli Studi di Padova, 2011.

[15] G. Manente, R. Field, R. DiPippo, J. W. Tester, M. Paci, and N. Rossi, "Hybrid Solar-Geothermal Power Generation To Increase The Energy Production From A Binary Geothermal Plant," in *Proceedings of the ASME 2011 International Mechanical Engineering Congress & Exposition*, Denver, Colorado, 2011.

[16] P. N. Mathur, "Assessment of solar-geothermal hybrid system concepts," Aerospace Corp., El Segundo, CA (USA). Energy and Resources Div.SAN-1101-14/1, 1979.

[17] S. Meksvanh, "Solar Augmented Geothermal Energy," United States Patent US 7,472,548 B2, 2009.

[18] M. Paci, I. Fastelli, and N. Rossi, "Advanced Systems For Power Production From Geothermal Low Temperature Resources," 2009.

[19] D. Tempesti and D. Fiaschi, "Thermo-economic assessment of a micro CHP system fuelled by geothermal and solar energy," *Energy,* vol. 58, pp. 45-51, 2013.

[20] M. S. Todorovic, "Parametric Analysis And Thermodynamic Limits Of Solar Assisted Geothermal Co- And Tri-Generation Systems," *ASHRAE Transactions,* 2011.
[21] C. Turchi, G. Zhu, M. Wagner, T. Williams, and D. Wendt, "Geothermal / Solar Hybrid Designs: Use of Geothermal Energy for CSP Feedwater Heating," in *GRC Transactions*, Vol 38, 2014, vol. 38, pp. 817-823.
[22] D. Wendt, G. Mines, C. Turchi, and G. Zhu, "Geothermal Risk Reduction via Geothermal/Solar Hybrid Power Plants: Final Report," Idaho National LaboratoryINL/EXT-15-37307, November 2015.
[23] D. Wendt *et al.*, "Stillwater Hybrid Geo-Solar Power Plant Optimization Analysis," in *GRC Transactions*, Reno, NV, 2015, vol. 39, pp. 891-900.
[24] D. S. Wendt and G. L. Mines, "Use of a Geothermal-Solar Hybrid Power Plant to Mitigate Declines in Geothermal Resource Productivity," in *GRC Transactions*, Vol 38, 2014, vol. 38, pp. 825-832.
[25] C. Zhou, "Figure of merit analysis of a hybrid solar-geothermal power plant," *Engineering,* vol. 05, no. 01, pp. 26-31, 2013.
[26] C. Zhou, E. Doroodchi, and B. Moghtaderi, "An in-depth assessment of hybrid solar–geothermal power generation," *Energy Conversion and Management,* vol. 74, pp. 88-101, 2013.
[27] "System design verification of a hybrid geothermal/coal fired power plant," Parsons (Ralph M.) Co., Pasadena, CA (USA)1978.
[28] M. Becciani, C. De Maria, G. Manfrida, and D. Tempesti, "Thermo-Economic Comparison of Different Layouts of a Steam Power Plant Integrated with Geothermal Resource," *Chemical Engineering Transactions,* vol. 39, pp. 385-390, 2014.
[29] M. Bruhn, "Hybrid geothermal–fossil electricity generation from low enthalpy geothermal resources: geothermal feedwater preheating in conventional power plants," *Energy,* vol. 27, no. 4, pp. 329-346, 2002.
[30] J. Buchta, "Green power from conventional steam power plant combined with geothermal well," pp. 1-6, 2009.
[31] J. Buchta and A. Wawszczak, "Economical and ecological aspects of renewable energy generation in coal fired power plant supported with geothermal heat," pp. 1-6, 2010.
[32] R. DiPippo and E. M. Avelar, "Compound Hybrid Geothermal-Fossil Power Plants: Thermodynamic Analyses And Site-Specific Applications," Southeastern Massachusetts University1979.
[33] R. DiPippo, H. E. Khalifa, R. J. Correia, and J. Kestin, "Fossil superheating in geothermal steam power plants," Brown Univ., Providence, RI (USA). Div. of Engineering1978.
[34] R. L. Grijalva and S. K. Sanemitsu, "High geothermal energy utilization geothermal/fossil hybrid power cycle: a preliminary investigation," Burbank City Public Service Dept., CA (USA)1978.
[35] H. E. Khalifa, R. DiPippo, and J. Kestin, "Geothermal preheating in fossil-fired steam power plants," Brown Univ., Providence, RI (USA). Div. of Engineering1978.
[36] A. R. Mohan, U. Turaga, V. Subbaraman, V. Shembekar, D. Elsworth, and S. V. Pisupati, "Modeling the CO2-based enhanced geothermal system (EGS) paired with integrated gasification combined cycle (IGCC) for symbiotic integration of carbon dioxide sequestration with geothermal heat utilization," *International Journal of Greenhouse Gas Control,* vol. 32, pp. 197-212, 2015.
[37] J. Y. Qin, E. J. Hu, and G. Nathan, "A Modified Thermodynamic Model to Estimate the Performance of Geothermal Aided Power Generation Plant," *Advanced Materials Research,* vol. 347-353, pp. 2875-2878, 2011.
[38] D. H. White and L. A. Goldstone, "The Potential of Hybrid Geothermal / Coal Fired Power Plants in Arizona," Arizona Univ., Tucson (USA). Dept. of Chemical EngineeringDOE/RA/50076-12, 1982.

[39] C. Zhou, E. Doroodchi, and B. Moghtaderi, "Assessment of geothermal assisted coal-fired power generation using an Australian case study," *Energy Conversion and Management,* vol. 82, pp. 283-300, 2014.
[40] M. Bearden, C. L. Davidson, J. Horner, D. Heldebrant, and C. Freeman, "Techno-Economic Analysis of Integration of Low-Temperature Geothermal Resources for Coal-Fired Power Plants," Pacific Northwest National Laboratory30 October 2015 2015.
[41] F. Heberle and D. Bruggemann, "Thermoelectric analysis of hybrid power plant concepts for geothermal combined heat and power generation," *Energies,* vol. 7, p. 16, 14 July 2014 2014.
[42] D. Heldebrant, M. Bearden, C. L. Davidson, J. Horner, and C. Freeman, "Techno-Economic Analysis of Integration of Low-Temperature Geothermal Resources for Coal-Fired Power Plants," Pacific Northwest National Laboratory2014.
[43] G. Bidini, U. Desideri, and F. D. Maria, "A single flash integrated gas turbine-geothermalpower plant with non condensable gas combustion," *Geothermics,* vol. 28, no. 1, pp. 131-150, 1999.
[44] G. Bidini, U. Desideri, F. D. Maria, A. Baldacci, R. Papale, and F. Sabatelli, "Optimization of an integrated gas turbine–geothermal power plant," *Energy Conversion and Management,* vol. 39, no. 16-18, pp. 1945-1956, 1998.
[45] J. Brugman, M. Hattar, K. Nichols, and Y. Esaki, "Next Generation Geothermal Power Plants," CE Holt Company, Pasadena, California1995.
[46] J. Janes, "Evaluation of a superheater enhanced geothermal steam power plant in the Geysers area. Final report," California Energy Resources Conservation and Development Commission1984.
[47] GeoProducts Corporation, "Preconstruction of the Honey Lake Hybrid Power Plant: Final report," DOE/ID/12477-1, April 30 1988.
[48] A. Amoresano, P. D. Sio, G. Langella, and S. Meo, "Biomass and Solar Integration in Low Enthalpy Geothermal Plants," *International Review on Modelling & Simulations,* vol. 6, no. 3, p. 981, 2013.
[49] A. Borsukiewicz-Gozdur, "Dual-fluid-hybrid power plant co-powered by low-temperature geothermal water," *Geothermics,* vol. 39, no. 2, pp. 170-176, 2010.
[50] T. Lawford, "Geoproducts Hybrid Geothermal / Wood Fired Power Plant," in *Proceedings of the Geothermal Program Review*, Washington, DC, 1983.
[51] S. Srinivas, D. Eisenberg, N. Seifkar, P. Leoni, M. Paci, and R. P. Field, "Simulation-Based Study of a Novel Integration: Geothermal–Biomass Power Plant," *Energy & Fuels,* vol. 28, no. 12, pp. 7632-7642, 2014.
[52] C. L. Davidson, M. Bearden, J. Horner, J. E. Cabe, D. Appriou, and B. P. McGrail, "Geothermally Coupled Well-Based Compressed Air Energy Storage," Pacific Northwest National Laboratory, Richland, WAPNNL-25171, 2016.
[53] B. P. McGrail *et al.*, "Techno-economic Performance Evaluation of Compressed Air Energy Storage in the Pacific Northwest," Pacific Northwest National Laboratory, Richland, WAPNNL-22235, 2013, Available: http://caes.pnnl.gov/pdf/PNNL-22235.pdf.
[54] B. P. McGrail, C. L. Davidson, J. E. Cabe, M. Bearden, J. Horner, and M. Chamness, "Preliminary Siting and Feasibility Evaluation of Geothermal-Coupled Comrpessed Air Energy Storage," Pacific Northwest National Laboratory2015.
[55] K. Bourouni, J. C. Deronzier, and L. Tadrist, "Experimentation and modelling of an innovative geothermal desalination unit," *Desalination,* vol. 125, no. 1-3, pp. 147-153, 1999.
[56] K. Bourouni, R. Martin, and L. Tadrist, "Analysis of heat transfer and evaporation in geothermal desalination units," *Desalination,* vol. 122, no. 2-3, pp. 301-313, 1999.
[57] K. Bourouni, R. Martin, L. Tadrist, and M. T. Chaibi, "Heat transfer and evaporation in geothermal desalination units," *Applied Energy,* vol. 64, no. 1-4, pp. 129-147, 1999.
[58] J. Bundschuh, N. Ghaffour, H. Mahmoudi, M. Goosen, S. Mushtaq, and J. Hoinkis, "Low-cost low-enthalpy geothermal heat for freshwater production: Innovative applications using thermal

desalination processes," (in English), *Renewable & Sustainable Energy Reviews,* vol. 43, pp. 196-206, Mar 2015.
[59] A. Date, L. Gauci, R. Chan, and A. Date, "Performance review of a novel combined thermoelectric power generation and water desalination system," *Renewable Energy,* vol. 83, pp. 256-269, 2015.
[60] A. El Amali, S. Bouguecha, and M. Maalej, "Experimental study of air gap and direct contact membrane distillation configurations: application to geothermal and seawater desalination," *Desalination,* vol. 168, p. 357, 2004.
[61] M. Finster, C. Clark, J. Schroeder, and L. Martino, "Geothermal produced fluids: Characteristics, treatment technologies, and management options," *Renewable and Sustainable Energy Reviews,* vol. 50, pp. 952-966, 2015.
[62] L. Francis, N. Ghaffour, A. S. Alsaadi, S. P. Nunes, and G. L. Amy, "Performance evaluation of the DCMD desalination process under bench scale and large scale module operating conditions," *Journal of Membrane Science,* vol. 455, pp. 103-112, 2014.
[63] N. Ghaffour, J. Bundschuh, H. Mahmoudi, and M. F. A. Goosen, "Renewable energy-driven desalination technologies: A comprehensive review on challenges and potential applications of integrated systems," *Desalination,* vol. 356, pp. 94-114, 2015.
[64] N. Ghaffour, S. Lattemann, T. Missimer, K. C. Ng, S. Sinha, and G. Amy, "Renewable energy-driven innovative energy-efficient desalination technologies," *Applied Energy,* vol. 136, pp. 1155-1165, 2014.
[65] M. Goosen, H. Mahmoudi, and N. Ghaffour, "Water Desalination Using Geothermal Energy," *Energies,* vol. 3, no. 8, pp. 1423-1442, 2010.
[66] H. Gutierrez and S. Espindola, "Using Low Enthalpy Geothermal Resources to Desalinate Sea Water and Electricity Production on Desert Areas in Mexico," *GHC Bulletin,* vol. 29, pp. 19-24, August 2010.
[67] C. Karytsas, D. Mendrinos, and G. Radoglou, "The Current Geothermal Exploration and Development of the Geothermal Field of Milos Island in Greece," *GHC Bulletin,* vol. 25, pp. 17-21, June 2004.
[68] S. Loutatidou and H. A. Arafat, "Techno-economic analysis of MED and RO desalination powered by low-enthalpy geothermal energy," *Desalination,* vol. 365, pp. 277-292, 2015.
[69] F. Manenti, M. Masi, and G. Santucci, "Start-up operations of MED desalination plants," *Desalination,* vol. 329, pp. 57-61, 2013.
[70] F. Manenti, M. Masi, G. Santucci, and G. Manenti, "Parametric simulation and economic assessment of a heat integrated geothermal desalination plant," *Desalination,* vol. 317, pp. 193-205, 2013.
[71] H. M. Qiblawey and F. Banat, "Solar thermal desalination technologies," *Desalination,* vol. 220, no. 1-3, pp. 633-644, 2008.
[72] R. Sarbatly and C.-K. Chiam, "Evaluation of geothermal energy in desalination by vacuum membrane distillation," *Applied Energy,* vol. 112, pp. 737-746, 2013.
[73] B. Tomaszewska and M. Bodzek, "Desalination of geothermal waters using a hybrid UF-RO process. Part I: Boron removal in pilot-scale tests," *Desalination,* vol. 319, pp. 99-106, 2013.
[74] B. Tomaszewska and M. Bodzek, "Desalination of geothermal waters using a hybrid UF-RO process. Part II: Membrane scaling after pilot-scale tests," *Desalination,* vol. 319, pp. 107-114, 2013.
[75] J. Tonner, "Barriers to Thermal Desalination in the United States," Water Consultants InternationalDesalination and Water Purification Research and Development Program Report No. 144, March 2008.
[76] D. S. Wendt, G. L. Mines, C. J. Orme, and A. D. Wilson, "Produced Water Treatment Using Switchable Polarity Solvent Forward Osmosis (SPS FO) Technology," in *GRC Transactions*, Vol 39, 2015, vol. 39, pp. 671-674.

[77] D. S. Wendt, C. J. Orme, G. L. Mines, and A. D. Wilson, "Energy requirements of the switchable polarity solvent forward osmosis (SPS-FO) water purification process," *Desalination,* vol. 374, pp. 81-91, 2015.
[78] C. F. Austin, *Undersea geothermal deposits - their selection and potential use*. US Naval Ordnance Test Station, Pasadena,CA, 1966.
[79] W. C. Bauman and J. L. Burba, III, "Recovery of lithium values from brines," United States Patent 5599516, 1997.
[80] W. C. Bauman and J. L. Burba, III, "Composition for the recovery of lithium values from brine and process of making/using said composition," United States Patent 6280693, 2001.
[81] C. E. Berthold and D. H. Baker, "Lithium Resources and Requirements by the Year 2000," presented at the Geological Survey Professional Paper 1005, Golden, Colorado, January 22-24, 1976.
[82] R. L. Blake, "Extracting Minerals from Geothermal Brines: A Literature Study," Twin Cities Metallurgy Research Center, Twin Cities, MinnesotaInformation Circular 8638, 1974.
[83] W. Bourcier, C. Bruton, S. Roberts, B. Viani, S. Conley, and S. Martin, "Pilot-Scale Geothermal Silica Recovery at Mammoth Lakes. Public interest Energy Research (PIER) Program Final Project Report," Lawrence Livermore National Laboratory, Livermore, CaliforniaCEC-500-2009-077, May 2009.
[84] W. L. Bourcier, M. Lin, and G. Nix, "Recovery of minerals and metals from geothermal fluids," presented at the 2003 SME Annual Meeting, Cincinnati, Ohio, September 8, 2005.
[85] T. J. Clutter, "Mining economic benefits from geothermal brine," *Geo-Heat Center Quarterly Bulletin,* vol. 21, no. 2, pp. 1-3, 2000.
[86] S. R. Cosner and J. A. Apps, "A Compilation of Data on Fluids from Geothermal Resources in the United States," Lawrence Berkeley Laboratory, Berkeley, CaliforniaLBL-5936, 1978, Available: http://escholarship.org/uc/item/8jt1d9r3.
[87] W. P. C. Duyvesteyn, "Recovery of base metals from geothermal brines," *Geothermics,* vol. 21, no. 5-6, pp. 773-799, 1992.
[88] D. L. Gallup, "Geochemistry of geothermal fluids and well scales, and potential for mineral recovery," *Ore Geology Reviews,* vol. 12, no. 4, pp. 225-236, 1998.
[89] D. L. Gallup, J. L. Featherstone, J. P. Reverente, and P. H. Messer, "Recovery of precious metals from aqueous media," United States Patent 5082492, 1992.
[90] D. L. Gallup, J. L. Featherstone, J. P. Reverente, and P. H. Messer, "Line mine: A Process for Mitigating Injection Well Damage at the Salton Sea, California (USA) Geothermal Field," in *Proceedings World Geothermal Congress*, 1995.
[91] A. M. Kennedy, "The recovery of lithium and other minerals from geothermal water at Wairakei," in *Proceedings of the United Nations Conference on New Sources of Energy: Solar Energy, Wind Power and Geothermal Energy*, Rome G/56, 1961, pp. 502-511.
[92] K. Kimura, "On the utilization of hot springs in Japan," in *Proceeding of the Seventh Pacific Science Congress*, New Zealand, 1953, pp. 500-504.
[93] Y. C. Lo, C. L. Cheng, Y. L. Han, B. Y. Chen, and J. S. Chang, "Recovery of high-value metals from geothermal sites by biosorption and bioaccumulation," *Bioresour Technol,* vol. 160, pp. 182-90, May 2014.
[94] A. Maimoni, "Minerals Recovery from Salton-Sea Geothermal Brines - a Literature-Review and Proposed Cementation Process," (in English), *Geothermics,* vol. 11, no. 4, pp. 239-258, 1982.
[95] J. Mercado, A. Lopez, and R. Angulo, "Chemical recovery as alternative of environmental solution by geothermal brines in Cerro Prieto," in *GRC Transactions*, 1979, vol. 3.
[96] J. Park, H. Sato, S. Nishihama, and K. Yoshizuka, "Lithium Recovery from Geothermal Water by Combined Adsorption Methods," *Solvent Extraction and Ion Exchange,* vol. 30, no. 4, pp. 398-404, 2012.

[97] M. Petersková, C. Valderrama, O. Gibert, and J. L. Cortina, "Extraction of valuable metal ions (Cs, Rb, Li, U) from reverse osmosis concentrate using selective sorbents," *Desalination,* vol. 286, pp. 316-323, 2012.
[98] S. Roth, "Lithium plans in doubt as Simbol Materials fires dozens," *The Desert Sun,* Accessed on: February 4Available: http://www.desertsun.com/story/tech/science/energy/2015/02/03/lithium-plans-doubt-simbol-materials-fires-dozens/22828207/
[99] H. P. Rothbaum and K. Middendorf, "Lithium extraction from Wairakei geothermal waters," *New Zealand Journal of Technology,* vol. 2, no. 4, pp. 231-235, 1986.
[100] H. Thomas, T. P. Reinhardt, and B. Segneri, "Low Temperature Geothermal Mineral Recovery Program," in *Proceedings Fortieth Workshop on Geothermal Reservoir Engineering*, Stanford University, Stanford, California, 2015.
[101] H. H. Werner, "Contribution to the mineral extraction from supersaturated geothermal brines Salton Sea Area, California," *Geothermics,* vol. 2, pp. 1651-1655, 1970.
[102] J. Wisniak, "Borax, Boric acid, and Boron - From exotic to commodity," *Indian Journal of Chemical Technology,* vol. 12, pp. 488-500, July 2005.
[103] S. A. Wood, "Behavior of rare earth elements in geothermal systems: a new exploration/exploitation tool," University of Idaho, Moscow, IdahoDOE/ID-13575, 2002.
[104] National Renewable Energy Laboratory. (2017). *System Advisor Model, 2017.1.17 revision 1, 64 bit*. Available: https://sam.nrel.gov/
[105] National Renewable Energy Laboratory. (September 2016). *National Solar Radiation Database*. Available: https://nsrdb.nrel.gov/
[106] C. Turchi, "Parabolic Trough Reference Plant for Cost Modeling with the Solar Advisor Model (SAM)," National Renewable Energy LaboratoryNREL/TP-550-47605, July 2010.
[107] U.S. Department of Energy, "SunShot Vision Study," February 2012, Available: https://energy.gov/eere/sunshot/sunshot-vision-study.
[108] H. P. Loh, J. Lyons, and C. W. White, "Process Equipment Cost Estimation, Final Report," National Energy Technology LabDOE/NETL-2002/1169, 2002.
[109] National Renewable Energy Laboratory. *Solar Data: Summary spreadsheet of annual 10-kilometer solar data by state and zip code*. Available: http://www.nrel.gov/gis/docs/SolarSummaries.xlsx
[110] A. M. Patnode, "Simulation and Performance Evaluation of Parabolic Trough Solar Power Plants," Master of Science, Mechanical Engineering, University of Wisconsin-Madison, 2006.
[111] R. V. Padilla, "Simplified Methodology for Designing Parabolic Trough Solar Power Plants," Doctor of Philosophy, Department of Chemical and Biomedical Engineering, University of South Florida, 2011.
[112] A. Stodola and L. Loewenstein, *Steam and Gas Turbines*. New York: McGraw-Hill Book Company, 1945.
[113] R. Bartlett, *Steam turbine performance and economics*. McGraw-Hill, 1958.
[114] F. P. Incropera and D. P. DeWitt, *Fundamentals of Heat and Mass Transfer*, 5th ed. New York: John Wiley and Sons, Inc., 2002.
[115] M. J. Montes, A. Abánades, J. M. Martínez-Val, and M. Valdés, "Solar multiple optimization for a solar-only thermal power plant, using oil as heat transfer fluid in the parabolic trough collectors," *Solar Energy,* vol. 83, no. 12, pp. 2165-2176, 2009.
[116] A. Kostyuk and V. Frolov, *Steam and Gas Turbines*. Mir Publishers, 1988.
[117] P. Nag, *Power Plant Engineering*. Tata McGraw-Hill, 2002.
[118] M. J. Wagner and P. Gilman, "Technical Manual for the SAM Physical Trough Model," National Renewable Energy Laboratory, Golden, ColoradoNREL/TP-5500-51825, June 2011.
[119] L. Drbal, P. Boston, and K. Westra, *Power Plant Engineering*. Kluwer Academic Pub, 1996.
[120] National Energy Technology Laboratory, "Cost and Performance Baseline for Fossil Energy Plants Volume 1: Bituminous Coal and Natural Gas to Electricity (Revision 2, 2010)," National Energy Technology Laboratory, Pittsburgh, PA2010.

[121] Geothermal Technologies Office. (2016). *Geothermal Electricity Technology Evaluation Model, GeoVision 2016 version*.
[122] R. E. Athey and E. Spencer, "Deaerating condenser boosts combined-cycle plant efficiency," *Power Engineering,* July 1992.
[123] Black and Veatch, L. Drbal, K. Westra, and P. Boston, Eds. *Power Plant Engineering*. Norwell, MA: Kluwer Academic Publishers, 1996.
[124] T. Fout *et al.*, "Cost and Performance Baseline for Fossil Energy Plants Volume 1a: Bituminous Coal (PC) and Natural Gas to Electricity," National Energy Technology Laboratory, Pittsburgh, PADOE/NETL-2015/1723, Rev 3, 2015.
[125] W. E. Stewart, Jr., *Design Guide: Combustion Turbine Inlet Air Cooling Systems*. Atlanta, GA: ASHRAE.
[126] R. Zogg, M. Y. Feng, and D. Westphalen, "Guide to Developing Air-Cooled LiBr Absorption for Combined Heat and Power Applications," U.S. Department of Energy, Office of Energy Efficiency and Renewable Energy, Washington, D.C.2005.
[127] Geothermal Technologies Office. (2016). *Geothermal Electricity Technology Evaluation Model, 2016 version*. Available: https://energy.gov/eere/geothermal/geothermal-electricity-technology-evaluation-model
[128] S. B. Jones *et al.*, "Process Design and Economics for the Conversion of Algal Biomass to Hydrocarbons: Whole Algae Hydrothermal Liquefaction and Upgrading," Pacific Northwest National Laboratory, Richland, WAPNNL-23227, 2014.
[129] R. Slade and A. Bauen, "Micro-algae cultivation for biofuels: Cost, energy balance, environmental impacts and future prospects," *Biomass and Bioenergy,* June 2013 2013.
[130] R. H. Perry and D. Green, *Perry's Chemical Engineers Handbook*, 6th ed. New York: McGraw-Hill Book Company, Inc., 1984.
[131] B. P. McGrail, "Geothermal-Coupled Compressed Air Energy Storage," Pacific Northwest National Laboratory, Richland, WAPNNL-SA-109815, 2015.
[132] European Geothermal Energy Council. (2007). *Geothermal Desalination*. Available: http://egec.info/wp-content/uploads/2011/03/Brochure-DESALINATION1.pdf
[133] Sephton Water Technology, "VTE Geothermal Desalination Pilot/Demonstration Project," 2012, Available: http://www.sephtonwatertech.com/DocumentsPDF/VTE_Geothermal_Desalination_Project_Summary_2012_02_05.pdf.
[134] H. Mahmoudi, N. Spahis, M. F. Goosen, N. Ghaffour, N. Drouiche, and A. Ouagued, "Application of geothermal energy for heating and fresh water production in a brackish water greenhouse desalination unit: A case study from Algeria," *Renewable and Sustainable Energy Reviews,* vol. 14, no. 1, pp. 512-517, 2010.
[135] V. G. Gude, N. Nirmalakhandan, and S. Deng, "Renewable and sustainable approaches for desalination," *Renewable and Sustainable Energy Reviews,* vol. 14, no. 9, pp. 2641-2654, 2010.
[136] S. Akar and C. Turchi, "Low Temperature Geothermal Resource Assessment for Membrane Distillation Desalination in the United States," in *GRC Transactions*, Vol 40, 2016, vol. 40, pp. 129-140.
[137] NRC, Committee on Advancing Desalination Technology, Water Science and Technology Board, *Desalination: A National Perspective*. Washington, D.C.: National Research Council, 2008.
[138] G. P. Thiel, E. W. Tow, L. D. Banchik, H. W. Chung, and J. H. Lienhard, "Energy consumption in desalinating produced water from shale oil and gas extraction," *Desalination,* vol. 366, pp. 94-112, 2015.
[139] M. A. Darwish and H. K. Abdulrahim, "Feed water arrangements in a multi-effect desalting system," (in English), *Desalination,* vol. 228, no. 1-3, pp. 30-54, Aug 15 2008.
[140] M. A. Darwish, F. Al-Juwayhel, and H. K. Abdulraheim, "Multi-effect boiling systems from an energy viewpoint," *Desalination,* vol. 194, no. 1-3, pp. 22-39, 2006.

[141] H. El-Dessouky, I. Alatiqi, S. Bingulac, and H. Ettouney, "Steady-State Analysis of the Multiple Effect Evaporation Desalination Process," *Chem. Eng. Technol.,* vol. 21, no. 5, pp. 437-451, 1998.
[142] K. H. Mistry, M. A. Antar, and J. H. Lienhard V, "An improved model for multiple effect distillation," *Desalination and Water Treatment,* vol. 51, no. 4-6, pp. 807-821, 2013.
[143] M. Al-Sahali and H. Ettouney, "Developments in thermal desalination processes: Design, energy, and costing aspects," (in English), *Desalination,* vol. 214, no. 1-3, pp. 227-240, Aug 15 2007.
[144] J. E. Miller, "Review of Water Resources and Desalination Technologies," Sandia National LaboratorySAND 2003-0800, March 2003.
[145] H. M. Ettouney, H. T. El-Dessouky, R. S. Faibish, and P. J. Gowin, "Evaluating the Economics of Desalination," *Chemical Engineering Progress,* vol. 98, no. 12, pp. 32-40, December 2002.
[146] M. K. Wittholz, B. K. O'Neill, C. B. Colby, and D. Lewis, "Estimating the cost of desalination plants using a cost database," *Desalination,* vol. 229, no. 1-3, pp. 10-20, 2008.
[147] N. Ghaffour, T. M. Missimer, and G. L. Amy, "Technical review and evaluation of the economics of water desalination: Current and future challenges for better water supply sustainability," *Desalination,* vol. 309, pp. 197-207, 2013.
[148] U. K. Kesieme, N. Milne, H. Aral, C. Y. Cheng, and M. Duke, "Economic analysis of desalination technologies in the context of carbon pricing, and opportunities for membrane distillation," *Desalination,* vol. 323, pp. 66-74, 2013.
[149] A. Ophir and F. Lokiec, "Review of MED fundamentals and costing," in *Proceedings of the International Conference on Desalination Costing*, Limassol, Cyprus, 2004, pp. 69-78.
[150] K. V. Reddy and N. Ghaffour, "Overview of the cost of desalinated water and costing methodologies," *Desalination,* vol. 205, no. 1-3, pp. 340-353, 2007.
[151] N. M. Wade, "Distillation plant development and cost update," *Desalination,* vol. 136, no. 1-3, pp. 3-12, 2001.
[152] K. Mistry and J. Lienhard, "An Economics-Based Second Law Efficiency," *Entropy,* vol. 15, no. 7, pp. 2736-2765, 2013.
[153] San Diego County Water Authority. (2016). *Seawater Desalination: The Claude "Bud" Lewis Desalination Plant and Related Facilities*. Available: https://www.sdcwa.org/sites/default/files/desal-carlsbad-fs-single.pdf
[154] C. S. Turchi, S. Akar, T. Cath, J. Vanneste, and M. Geza, "Use of Low-Temperature Geothermal Energy for Desalination in the Western United States," National Renewable Energy Laboratory, Golden, CONREL/TP-5500-65277, November 2015.
[155] A. S. Nafey, H. E. S. Fath, and A. A. Mabrouk, "Thermo-economic investigation of multi effect evaporation (MEE) and hybrid multi effect evaporation—multi stage flash (MEE-MSF) systems," *Desalination,* vol. 201, no. 1-3, pp. 241-254, 2006.
[156] Veolia Water Solutions & Technologies. *Multiple Effect Distillation: Processes for Sea Water Desalination*. Available: http://www.veoliawatertech.com/nawatersytems/ressources/documents/1/20581,MultiEffectDistillation.pdf
[157] B. Rahimi, A. Christ, K. Regenauer-Lieb, and H. T. Chua, "A novel process for low grade heat driven desalination," *Desalination,* vol. 351, pp. 202-212, 2014.
[158] U.S. Department of Energy, "Energy Demands on Water Resources: Report to Congress on the Interdependency of Energy and Water," December 2006.
[159] T. Y. Cath, N. Walker, A. E. Childress, M. Hutton, and A. Weinberg, "Assessment of Traditional and Novel Membrane Processes for Recovery of Cooling Tower Water in Geothermal Power Plants," in *GRC Transactions*, 2008, vol. 32, pp. 401-406: Geothermal Resources Council.
[160] California Energy Commission, "Use of Degraded Water Sources as Cooling Water in Power Plants," P500-03-110, October 2003.
[161] C. E. Clark and J. A. Veil, "Produced water volumes and management practices in the United States," Argonne National LaboratoryANL/EVS/R-09/1, 2009.

[162] J. Veil, "U.S. Produced Water Volumes and Management Practices in 2012," Veil Environmental, LLCApril 2015, Available: http://www.gwpc.org/sites/default/files/Produced%20Water%20Report%202014-GWPC_0.pdf.
[163] M. G. Puder and J. A. Veil, "Offsite Commercial Disposal of Oil and Gas Exploration and Production Waste: Availability, Options, and Costs," Argonne National Laboratory2006.
[164] E. T. Igunnu and G. Z. Chen, "Produced water treatment technologies," *International Journal of Low-Carbon Technologies,* vol. 9, no. 3, pp. 157-177, 2014.
[165] Colorado School of Mines, "An Integrated Framework for Treatment and Management of Produced Water: Technical Assessment of Produced Water Treatment Technologies," Colorado School of Mines, RPSEA Project 07122-12November 2009 2009.
[166] D. S. Wendt, B. Adhikari, C. J. Orme, and A. D. Wilson, "Produced Water Treatment Using the Switchable Polarity Solvent Forward Osmosis (SPS FO) Desalination Process: Preliminary Engineering Design Basis," in *GRC Transactions*, Vol 40, 2016, vol. 40, pp. 147-159.
[167] C. Augustine and D. M. Falkenstern, "An Estimate of the Near-Term Electricity-Generation Potential of Coproduced Water From Active Oil and Gas Wells," *SPE Journal,* vol. 19, no. 03, pp. 530-541, 2014.
[168] B. J. Nelson, S. A. Wood, and J. L. Osiensky, "Rare earth element geochemistry of groundwater in the Palouse Basin, northern Idaho–eastern Washington," *Geochemistry: Exploration, Environment, Analysis,* vol. 4, no. 3, pp. 227-241, 2004.
[169] S. A. Wood and W. M. Shannon, "Rare-earth elements in geothermal waters from Oregon, Nevada, and California," *Journal of Solid State Chemistry,* vol. 171, no. 1-2, pp. 246-253, 2003.
[170] N. M. Fenneman, "Physiographic subdivision of the United States," *Proceedings of the National Academy of Sciences,* vol. 3, pp. 17-22, 1917.
[171] silverprice.org. Available: www.silverprice.org
[172] U. S. G. Survey, "Mineral commodity summaries 2015," p. 196 p., 2015.
[173] goldprice.org. Available: www.goldprice.org
[174] J. S. Dickson, "Rare earth elements: Global market overview," in *Symposium on Strategic and Critical Materials Proceedings, November 13-14, 2015*, G. J. Simandl and M. Neetz, Eds. Victoria, British Columbia: British Columbia Ministry of Energy and Mines, British Columbia Geological Survey Paper 2015-3, 2015, pp. 5-11.
[175] A. Norman, X. Zou, and J. Barnett, "Critical minerals: Rare earths and the US economy," National Center for Policy AnalysisBackgrounder No. 175, 2014.
[176] M. Humphries, "Rare earth elements: the global supply chain," Congressional Research Service7-5700, R41347, 2013.
[177] S. Harrison, "Technologies for extracting valuable metals and compounds from geothermal fluids," California Energy CommissionPublication Number: CEC-500-2015-023, 2014.
[178] H. Thomas, T. P. Reinhardt, A. Anderson, and B. Segneri, "Critical and strategic materials and potential importance for geothermal projects," in *Proceedings 41st Workshop on Geothermal Reservoir Engineering*, 2016.
[179] E. P. Farley, E. L. Watson, D. D. MacDonald, R. W. Bartlett, and G. N. Krishnan, "Recovery of heavy metals from high salinity geothermal brine," SRI International, U.S. Bureau of Mines, Reno, Nevadaopen file report, 1980.
[180] K. L. Brown and P. J. C. Roberts, "Extraction of gold and silver from geothermal fluid," in *Proceedings 10th New Zealand Geothermal Workshop*, 1988, pp. 161-163.
[181] K. L. Brown, "Gold Deposition from Geothermal Discharges in New-Zealand," (in English), *Economic Geology,* vol. 81, no. 4, pp. 979-983, Jun-Jul 1986.
[182] E. T. Premuzie, M. S. Lin, M. Bohnek, V. Bajsarowicz, and M. McCloud, "Advanced Biochemical Processes for Geothermal Brines Current Developments," in *GRC Transactions*, Vol 21, 1997, pp. 145-149.
[183] G. Allegrini, F. Luccioli, and A. Trivella, "Industrial uses of geothermal fluids at Larderello," *Geothermics,* vol. 21, no. 5-6, pp. 623-630, 1992.

[184] S. F. Hodgson, "Larderello to Las Vegas: 1818, 1944, 2013," GRC BulletinSeptember/October 2013.
[185] M. Badruk, N. Kabay, M. Demircioglu, H. Mordogan, and U. Ipekoglu, "Removal of boron from wastewater of geothermal power plant by selective ion-exchange resins. I. Batch sorption-elution studies," (in English), *Separation Science and Technology,* vol. 34, no. 13, pp. 2553-2569, 1999.
[186] O. Recepoğlu and ü. Beker, "A preliminary study on boron removal from Kizildere/Turkey geothermal waste water," *Geothermics,* vol. 20, no. 1-2, pp. 83-89, 1991.
[187] C. Yan, W. Yi, P. Ma, X. Deng, and F. Li, "Removal of boron from refined brine by using selective ion exchange resins," *J Hazard Mater,* vol. 154, no. 1-3, pp. 564-71, Jun 15 2008.
[188] L. Gilău and O. Stănăşel, "Experimental study of boron recovery from geothermal water on ion exchange," in *Proceedings World Geothermal Congress*, Bali, Indonesia, 2010.
[189] A. E. Yilmaz, R. Boncukcuoglu, M. M. Kocakerim, M. T. Yilmaz, and C. Paluluoglu, "Boron removal from geothermal waters by electrocoagulation," *J Hazard Mater,* vol. 153, no. 1-2, pp. 146-51, May 01 2008.
[190] D. H. Christopher, M. Stewart, and J. Rice, "The recovery and separation of mineral values from geothermal brines," Hazen Research, Inc., Golden, ColoradoResearch report, 1974--1975 (No. PB-245686), 1975.
[191] N. Zhang, D. L. Gao, M. M. Liu, and T. L. Deng, "Rubidium and Cesium Recovery from Brine Resources," *Advanced Materials Research,* vol. 1015, pp. 417-420, 2014.
[192] S. Harrison, C. K. Sharma, R. Bhakta, and P. Y. Lan, "Methods for Removing Potassium, Rubidium, and Cesium, Selectively or in Combination, From Brines and Resulting Compositions Thereof," United States Patent 14/188,293, 2014.
[193] L. E. Schultze and D. J. Bauer, "Recovering lithium chloride from a geothermal brine," Bureau of Mines, Reno Research Center, Reno, NV (USA)Report of investigations/1984 (No. PB-84-224500; BM-RI-8883), 1984.
[194] S. Harrison, "Technologies for extracting valuable metals and compounds from geothermal fluids," US Department of Energy, Energy Efficiency & Renewable Energy, Geothermal Technologies Program 2011 Peer ReviewJune 9 2011.
[195] R. Chitrakar, Y. Makita, K. Ooi, and A. Sonoda, "Synthesis of Iron-Doped Manganese Oxides with an Ion-Sieve Property: Lithium Adsorption from Bolivian Brine," (in English), *Industrial & Engineering Chemistry Research,* vol. 53, no. 9, pp. 3682-3688, Mar 5 2014.
[196] T. Iwanaga, E. Watanabe, E. Mroczek, and D. Graham, "Lithium extraction from geothermal brines using an adsorption method after removal is silica using electrocoagulation," in *Proceedings of the New Zealand Geothermal Workshop*, 2007.
[197] T. Matsushita, K. Yonezu, Y. Inoue, K. Watanabe, and T. Yokoyama, "Adsorption characteristics of lithium adsorbent aimed at recovery of lithium from geothermal fluid," in *Proceedings of 35th New Zealand Geothermal Workshop*, 2013.
[198] E. Mroczek, D. Graham, D. Dedual, and L. Bacon, "Lithium extraction from Wairakei geothermal fluid using electrodialysis," in *Proceedings World Geothermal Congress 2015*, Melbourne, Australia, 2015.
[199] S. Mercado and R. Hurtado, "Potash extraction from cerro prieto geothermal brine," *Geothermics,* vol. 21, no. 5-6, pp. 759-764, 1992.
[200] L. E. Schultze and D. J. Bauer, "Recovering zinc-lead sulfide from a geothermal brine," Bureau of Mines, Reno Research Center, Reno, NV (USA)Report of Investigations/1985 (No. PB-85-185254/XAB; BM-RI-8922), 1985.
[201] D. L. Gallup and G. T. Ririe, "Platinum recovery," United States Patent 5,290,339, 1994.
[202] K. Kato, A. Ueda, K. Mogi, H. Nakazawa, and K. Shimizu, "Silica recovery from Sumikawa and Ohnuma geothermal brines (Japan) by addition of CaO and cationic precipitants in a newly developed seed circulation device," *Geothermics,* vol. 32, no. 3, pp. 239-273, 2003.

[203] H. P. Rothbaum and B. H. Anderton, "Removal of silica and arsenic from geothermal discharge waters by precipitation of useful calcium silicates," in *United Nations 2nd Symposium on the development and use of geothermal resources*, San Francisco, 1975, vol. 2, pp. 1417-1425.
[204] W. T. Shannon, W. R. Owers, and H. P. Rothbaum, "Pilot scale solids/liquid separation in hot geothermal discharge waters using dissolved air flotation," *Geothermics,* vol. 11, no. 1, pp. 43-58, 1982.
[205] C. W. Noack, K. Perkins, N. Washburn, D. A. Dzombak, and A. K. Karamalidis, "Screening the effects of ligand chemistry and geometry on rare earth element partitioning from saline solutions to functionalized adsorbents," in *GRC Transactions*, vol 39, 2015, pp. 1023-1024.
[206] C. M. Ajo-Franklin, "Engineering thermophilic microorganisms to selectively extract strategic minerals," US Department of Energy, Energy Efficiency & Renewable Energy, Geothermal Technologies Office 2015 Peer ReviewMay 11-15 2015.
[207] B. P. McGrail, "Magnetic partitioning nanofluid for rare earth extraction from geothermal fluids," US Department of Energy, Energy Efficiency & Renewable Energy, Geothermal Technologies Office 2015 Peer ReviewMay 11-14 2015.
[208] D. P. Stull, "Environmentally friendly economical sequestration of rare earth metals from geothermal waters," US Department of Energy, Energy Efficiency & Renewable Energy, Geothermal Technologies Office 2015 Peer ReviewMay 11-14 2015.
[209] R. S. Addleman, "Recovery of rare earths, precious metals and other critical materials from geothermal waters with advanced sorbent structures," US Department of Energy, Energy Efficiency & Renewable Energy, Geothermal Technologies Office 2015 Peer ReviewMay 11-14 2015.
[210] T. B. O'Brien, "Recovery of elements from hydrothermal products," United States Patent 8,377,165B2, 2013.
[211] C. W. Nye, S. Quillinan, G. Neupane, and T. McLing, "Aqueous rare earth element patterns, concentrations, and stable isotopes in thermal brines associated with oil and gas production," in *Proceedings 42nd Workshop on Geothermal Reservoir Engineering*, Stanford University, Stanford, California, 2017, vol. SGP-TR-212.
[212] E. Mroczek, B. Carey, M. Climo, and Y. Li, "Technology review of mineral extraction from separated geothermal water," GNS Science Report2015, vol. 25.
[213] R. S. Addleman *et al.*, " Evaluation of advanced sorbent structures for recovery of rare earth, precious metals, and other critical materials from geothermal waters- preliminary results," Pacific Northwest National Laboratory, Richland, WA2016.
[214] D. P. Stull, "Environmentally friendly economical sequestration of rare earth metals from geothermal waters," Tussar Corp, Lafayette, COFinal Report, DE-EE006751, 2016.
[215] S. Ventura, S. Bhamidi, M. Hornbostel, A. Nagar, and E. Perea, "Selective recovery of metals from geothermal brines," SRI International, Menlo Park, CAFinal Report, 2016.
[216] I. Moch, "WTCOST II. Water Treatment and Cost Estimation Manual, Developed by I. Moch and Associates," Querns Engineering Services and Boulder Research Enterprises. With the US Bureau of Reclamation, Available through I. Moch &Associates2006.
[217] C. E. Clark, C. B. Harto, J. L. Sullivan, and M. Q. Wang, "Water Use in the Development and Operation of Geothermal Power Plants," Argonne National Laboratory, Argonne, ILANL/EVS/R-10/5, 2011.
[218] R. H. Mariner, J. B. Rapp, L. M. Willey, and T. S. Presser, "The chemical composition and estimated minimum thermal reservoir temperatures of selected hot springs in Oregon," USGS Open File Report 74-1067, 1974.
[219] C. F. Williams, M. J. Reed, R. H. Mariner, J. DeAngelo, and S. P. Galinis, Jr., "Assessment of Moderate- and High-Temperature Geothermal Resources of the United States," U.S. Geological SurveyFact Sheet 2008-3082, 2008.
[220] G. Neupane and D. Wendt, "Assessment of Mineral Resources in Geothermal Brines in the US," presented at the 42nd Workshop on Geothermal Reservoir Engineering, Stanford, California,

February 13-15, 2017, 2017. Available: https://pangea.stanford.edu/ERE/db/GeoConf/papers/SGW/2017/Neupane2.pdf
[221] J. K. Barrett and R. H. Pearl, "Hydrogeological data of thermal springs and wells in Colorado," Colorado Geological Survey Information Series 6, 1976.
[222] W. R. Benoit, "Preliminary Report on the Alvord Valley, Oregon, Geothermal Prospects," Phillips Petroleum Company, Geothermal Division1976.
[223] J. Berkstresser, C.F., "Data for springs in the southern coast, Transverse, and Peninsular Ranges of California," US Geological SurveyOpen-File Report 68-10, 1968.
[224] G. N. Breit, A. G. Hunt, R. E. Wolf, A. E. Koenig, R. Fifarek, and M. F. Coolbaugh, "Are modern geothermal waters in northwest Nevada forming epithermal gold deposits?," in *Geological Society of Nevada Symposium 2010, Great Basin Evolution and Metallogeny*, 2010, pp. 833-844.
[225] D. E. Brown, G. D. McLean, and G. L. Black, "Preliminary geology and geothermal resource potential of the western Snake River Plain, Oregon," Oregon Department of Geology and Mineral Industries1980.
[226] E. L. Culp *et al.*, "Surprise Valley Electrification Corp., Recovery Act: Rural cooperative geothermal development electric & agriculture," US Department of Energyfinal scientific report, 2015.
[227] M. R. Dolenc *et al.*, "Raft River geoscience case study," US Department of EnergyNo. EGG-2125(1), 1981.
[228] F. E. Goff, C. O. Grigsby, P. E. Trujillo, D. Counce, and A. Kron, "Geology, water geochemistry and geothermal potential of the Jemez Springs area, Canon de San Diego, New Mexico," *Journal of Volcanology and Geothermal Research,* vol. 10, pp. 227-244, 1981.
[229] R. B. Leonard, T. M. Brosten, and N. A. Midtlyng, "Selected data from thermal-spring areas, southwestern Montana," US Geological SurveyOpen-File Report 78-438, 1978.
[230] R. H. Mariner, S. J.R., G. J. Orris, T. S. Presser, and W. C. Evans, "Chemical and isotopic data for water from thermal springs and wells of Oregon," US Geological SurveyOpen File Report 80-737, 1980.
[231] R. H. Mariner, T. S. Presser, J. B. Rapp, and L. M. Willey, "Minor and trace elements, gas, and isotope compositions of the principal hot springs of Nevada and Oregon," US Geological SurveyOpen-File Report 75-0001, 1975.
[232] E. D. Mattson, M. E. Conrad, G. Neupane, T. R. Wood, and C. J. Cannon, "Geothermometry Mapping of Deep Hydrothermal Reservoirs in Southeastern Idaho," Idaho National LaboratoryINL/EXT-16-39154, 2016.
[233] J. C. Mitchell, "Geothermal Investigations in Idaho, Part 5, geochemistry and geologic setting of the thermal waters of the northern Cache Valley area, Franklin county, Idaho," Idaho Department of Water ResourcesWater Information Bulletin No 30, 1976.
[234] J. C. Mitchell, "Geothermal investigations in Idaho Part 7: Geochemistry and geologic setting of the thermal waters of the Camas Prairie Area, Blaine and Camas Counties, Idaho," Idaho Department of Water ResourcesWater Information Bulletin No. 30, 1976.
[235] J. C. Mitchell, L. L. Johnson, and J. E. Anderson, "Geothermal investigations in Idaho, part 9, potential for direct heat applications of geothermal resources," Idaho Department of Water ResourcesWater Information Bulletin No 30, 1980.
[236] J. C. Mundorff, "Major thermal springs of Utah," Utah Geol. and Mineralog. SurveyWater-Resources Bull. 13, 1970.
[237] N. L. Nehring and R. H. Mariner, "Sulfate-water isotopic equilibrium temperatures for thermal springs and wells of the Great Basin," in *Geothermal Resources Council Transactions*, Vol 3., 1979, vol. 3, pp. 485-488.
[238] N. L. Nehring *et al.*, "Sulfate geothermometry of thermal waters in the western United States," US Geological SurveyOpen-file Report 79-1135, 1979.

[239] G. Neupane *et al.*, "Potential hydrothermal resource areas and their reservoir temperatures in the eastern Snake River Plain, Idaho. Application of isotopic approaches for identifying hidden geothermal systems in southern Idaho," in *41st Workshop on Geothermal Reservoir Engineering*, Stanford University, Stanford, California, 2016, pp. SGP-TR-209.
[240] G. Neupane *et al.*, "Geochemical Evaluation of the Geothermal Resources of Camas Prairie, Idaho," in *42nd Workshop on Geothermal Reservoir Engineering*, Stanford University, Stanford, California, 2017, pp. SGP-TR-212.
[241] G. Neupane *et al.*, "Geothermometric evaluation of geothermal resources in southeastern Idaho," *Geothermal Energy Science,* vol. 4, no. 1, pp. 11-22, 2016.
[242] M. J. Reed, "Chemistry of thermal water in selected geothermal areas of California," California Div. of Oil and Gas, Sacramento, CaliforniaTR-15, 1975.
[243] J. W. Sanders and M. J. Miles, "Mineral content of selected geothermal waters," University of Nevada, Reno, Desert Research Institute, Center for Water ResourcesResearch Project Report 26, 1974.
[244] R. C. Scott and F. B. Barker, "Data on uranium and radium in ground water in the United States," U.S. Geological SurveyProf. Paper 426, 1962.
[245] C. A. Swanberg, P. Morgan, C. H. Stoyer, and J. C. Witcher, "An appraisal study of the geothermal resources of Arizona and adjacent areas in New Mexico and Utah and their value for desalination and other uses," New Mexico Energy InstituteReport. 006, 1977.
[246] D. T. Trexler, T. Flynn, B. A. Koenig, E. J. Bell, and G. Ghusn Jr, "Low-to moderate-temperature geothermal resource assessment for Nevada: area specific studies, Pumpernickel Valley, Carlin and Moana," University of Nevada, RenoFinal Report: DOE/NV/10220-1, 1982.
[247] D. E. White, J. D. Hem, and G. A. Waring, "Chemical composition of subsurface waters," US Geological Survey440-F, 1963.
[248] H. W. Young and J. C. Mitchell, "Geothermal investigations in Idaho. Part 1. Geochemistry and geologic setting of selected thermal waters," Idaho Department of Water AdministrationWater Information Bulletin No. 30, 1973.
[249] G. Mines, "Geothermal Electricity Technologies Evaluation Model DOE tool for assessing impact of research on cost of power," in *33rd Workshop on Geothermal Reservoir Engineering*, Stanford University, Stanford, California, 2008, pp. SGP-TR-185.
[250] DOE-GTO. (2017, July 6, 2017). *Geothermal*. Available: https://energy.gov/eere/geothermal/about
[251] J. Nordquist, T. Buchanan, and M. Kaleikini, "Automatic Generation Control and Ancillary Services," in *GRC Transactions*, Vol 37, 2013, vol. 37, pp. 761-766.
[252] J. McCall, J. Macknick, and D. Hillman, "Water-Related Power Plant Curtailments: An Overview of Incidents and Contributing Factors," National Renewable Energy LaboratoryNREL/TP-6A20-67084, December 2016, Available: http://www.nrel.gov/docs/fy17osti/67084.pdf.

Appendix A

Listing of GETEM Input Variable Changes to Improvement Scenarios Relative to Business-As-Usual Scenario

Table 37. Comparison of GETEM input parameters for scenarios evaluated. Highlighted cells designate values that differ from BAU Scenario values.

Geothermal Resource Type	Identified Hydrothermal			Undiscovered Hydrothermal			Near Field EGS			Deep EGS		
SCENARIO	BAU	Exploration De-Risk	Tech Transfer	BAU	Exploration De-Risk	Tech Transfer	BAU	Exploration De-Risk	Tech Transfer	BAU	Exploration De-Risk	Tech Transfer
ECONOMIC PARAMETERS												
Drilling Discount Rate	7%	7%	7%	7%	7%	7%	7%	7%	16%	7%	7%	16%
Duration of Exploration Phase (yr)	2.5	0.5	2.5	4	1	4	1.5	0.5	1.5	1.5	0.5	1.5
Duration of Drilling Phase (yr)	2.5	1	2.5	2.5	1	2.5	2	1	2	2	1.5	2
Duration of Field Gathering System (yr)	2.5	0.5	2.5	2.5	0.5	2.5	2	0.5	2	2	0.5	2
Duration of Plant Design & Finalizing PPA (yr)	1	0.5	1	1	1	1	1	0.5	1	1	1	1
Duration of Plant Construction (yr)	2	1	2	2	1.5	2	2	1	2	2	1.5	2
RESOURCE EXPLORATION												
Lump Sum Cost for Pre-Drilling Exploration Activities (per site)	$600,000	$300,000	$600,000	$900,000	$300,000	$900,000	$250,000	$125,000	$250,000	$250,000	$83,333	$550,000
Site Exploration Drilling Cost (includes all temperature gradient, slimhole, corehole wells drilled)	$3,300,000	$1,650,000	$3,300,000	$5,400,000	$1,800,000	$5,400,000	$1,500,000	$750,000	$1,500,000	$5,000,000	$1,666,667	$5,000,000
Number of full-size wells drilled at each unsuccessful site (per site)	0	0	0	2	0	2	1	0	1	1	0	1
Number of full-sized test wells drilled to get successful well	2	1	2	2	1	2	2	1	2	2	1	2
Multiplier for Test Well Costs (>= 1)	1.2	1.2	1.8	1.2	1.2	1.8	1.5	1.5	1.8	1.5	1.5	1.8
# successful full sized wells needed	2	2	2	3	3	3	9	3	3	9	3	3
Number of full-sized wells stimulated	0	0	1	0	0	2	9	3	3	9	3	3
DRILLING												
Are wells stimulated ?	No	No	Yes	No	No	Yes	Yes	Yes	Yes	Yes	Yes	Yes
Wells to be stimulated	0	0	Production	0	0	Production	Injection	Injection	Injection	Injection	Injection	Injection
Input Fixed Stimulation Cost per well ($/well)	$0	$0	$1,250,000	$0	$0	$1,250,000	$1,250,000	$1,250,000	$1,250,000	$1,250,000	$1,250,000	$1,250,000
Stimulation Success rate	0	0	90%	0	0	90%	75%	75%	90%	75%	75%	90%
RESERVOIR DEFINITION												
Production Well Flow Rate (kg/s)	110	110	110	110	110	110	40	110	110	40	110	110
Input Production Well Drawdown (psi-h/1000lb)	0.4	0.4	0.4	0.4	0.4	0.4	4	0.4	0.4	4	0.4	0.4
Flow into/out of multiple zones in production/injection interval?	No	No	Yes	No	No	Yes	Yes	Yes	Yes	Yes	Yes	Yes
HYBRIDIZATION COSTS												
Site Improvements ($/m²)	20	10	10	20	10	10	20	10	10	20	10	10
Solar Field ($/m²)	150	75	75	150	75	75	150	75	75	150	75	75
Storage ($/kWh$_t$)	25	15	15	25	15	15	25	15	15	25	15	15